ESBWR Design Control Document
Tier 2
Chapter 4
Reactor

(Conditional Release – pending closure of
design verifications)

Contents

List of Tables

List of Illustrations

Abbreviations And Acronyms

Term	Definition
10 CFR	Title 10, Code of Federal Regulations
A/D	Analog-to-Digital
AASHTO	American Association of Highway and Transportation Officials
AB	Auxiliary Boiler
ABS	Auxiliary Boiler System
ABWR	Advanced Boiling Water Reactor
ac / AC	Alternating Current
AC	Air Conditioning
ACF	Automatic Control Function
ACI	American Concrete Institute
ACS	Atmospheric Control System
AD	Administration Building
ADS	Automatic Depressurization System
AEC	Atomic Energy Commission
AFIP	Automated Fixed In-Core Probe
AGMA	American Gear Manufacturer's Association
AHS	Auxiliary Heat Sink
AISC	American Institute of Steel Construction
AISI	American Iron and Steel Institute
AL	Analytical Limit
ALARA	As Low As Reasonably Achievable
ALWR	Advanced Light Water Reactor
ANS	American Nuclear Society
ANSI	American National Standards Institute
AOO	Anticipated Operational Occurrence
AOV	Air Operated Valve
API	American Petroleum Institute
APLHGR	Average Planar Linear Head Generation Rate
APRM	Average Power Range Monitor
APR	Automatic Power Regulator
APRS	Automatic Power Regulator System
ARI	Alternate Rod Insertion
ARMS	Area Radiation Monitoring System
ASA	American Standards Association
ASD	Adjustable Speed Drive
ASHRAE	American Society of Heating, Refrigerating, and Air Conditioning Engineers
ASME	American Society of Mechanical Engineers
AST	Alternate Source Term

Term	**Definition**
ASTM	American Society of Testing Methods
AT	Unit Auxiliary Transformer
ATLM	Automated Thermal Limit Monitor
ATWS	Anticipated Transients Without Scram
AV	Allowable Value
AWS	American Welding Society
AWWA	American Water Works Association
B&PV	Boiler and Pressure Vessel
BAF	Bottom of Active Fuel
BHP	Brake Horse Power
BOC	Beginning of Cycle
BOP	Balance of Plant
BPU	Bypass Unit
BPWS	Banked Position Withdrawal Sequence
BRE	Battery Room Exhaust
BRL	Background Radiation Level
BTP	NRC Branch Technical Position
BTU	British Thermal Unit
BWR	Boiling Water Reactor
BWROG	Boiling Water Reactor Owners Group
CAV	Cumulative absolute velocity
C&FS	Condensate and Feedwater System
C&I	Control and Instrumentation
C/C	Cooling and Cleanup
CB	Control Building
CBHVAC	Control Building HVAC
CCI	Core-Concrete Interaction
CDF	Core Damage Frequency
CFR	Code of Federal Regulations
CIRC	Circulating Water System
CIS	Containment Inerting System
CIV	Combined Intermediate Valve
CLAVS	Clean Area Ventilation Subsystem of Reactor Building HVAC
CM	Cold Machine Shop
CMS	Containment Monitoring System
CMU	Control Room Multiplexing Unit
COL	Combined Operating License
COLR	Core Operating Limits Report
CONAVS	Controlled Area Ventilation Subsystem of Reactor Building HVAC
CPR	Critical Power Ratio

Term	**Definition**
CPS	Condensate Purification System
CPU	Central Processing Unit
CR	Control Rod
CRD	Control Rod Drive
CRDA	Control Rod Drop Accident
CRDH	Control Rod Drive Housing
CRDHS	Control Rod Drive Hydraulic System
CRGT	Control Rod Guide Tube
CRHA	Control Room Habitability Area
CRT	Cathode Ray Tube
CS&TS	Condensate Storage and Transfer System
CSDM	Cold Shutdown Margin
CS / CST	Condensate Storage Tank
CT	Main Cooling Tower
CTVCF	Constant Voltage Constant Frequency
CUF	Cumulative usage factor
CWS	Chilled Water System
D-RAP	Design Reliability Assurance Program
DAC	Design Acceptance Criteria
DAW	Dry Active Waste
DBA	Design Basis Accident
dc / DC	Direct Current
DCS	Drywell Cooling System
DCIS	Distributed Control and Information System
DEPSS	Drywell Equipment and Pipe Support Structure
DF	Decontamination Factor
D/F	Diaphragm Floor
DG	Diesel-Generator
DHR	Decay Heat Removal
DM&C	Digital Measurement and Control
DOF	Degree of freedom
DOI	Dedicated Operators Interface
DOT	Department of Transportation
dPT	Differential Pressure Transmitter
DPS	Diverse Protection System
DPV	Depressurization Valve
DR&T	Design Review and Testing
DS	Independent Spent Fuel Storage Installation
DTM	Digital Trip Module
DW	Drywell

Term	Definition
EB	Electrical Building
EBAS	Emergency Breathing Air System
EBHV	Electrical Building HVAC
ECCS	Emergency Core Cooling System
E-DCIS	Essential DCIS (Distributed Control and Information System)
EDO	Environmental Qualification Document
EFDS	Equipment and Floor Drainage System
EFPY	Effective full power years
EHC	Electrohydraulic Control (Pressure Regulator)
ENS	Emergency Notification System
EOC	Emergency Operations Center
EOC	End of Cycle
EOF	Emergency Operations Facility
EOP	Emergency Operating Procedures
EPDS	Electric Power Distribution System
EPG	Emergency Procedure Guidelines
EPRI	Electric Power Research Institute
EQ	Environmental Qualification
ERICP	Emergency Rod Insertion Control Panel
ERIP	Emergency Rod Insertion Panel
ESF	Engineered Safety Feature
ETS	Emergency Trip System
FAC	Flow-Accelerated Corrosion
FAPCS	Fuel and Auxiliary Pools Cooling System
FATT	Fracture Appearance Transition Temperature
FB	Fuel Building
FBHV	Fuel Building HVAC
FCI	Fuel-Coolant Interaction
FCISL	Fuel Cladding Integrity Safety Limit
FCM	File Control Module
FCS	Flammability Control System
FCU	Fan Cooling Unit
FDDI	Fiber Distributed Data Interface
FFT	Fast Fourier Transform
FFWTR	Final Feedwater Temperature Reduction
FHA	Fire Hazards Analysis
FIV	Flow-Induced Vibration
FMCRD	Fine Motion Control Rod Drive
FMEA	Failure Modes and Effects Analysis
FPS	Fire Protection System

Term	Definition
FO	Diesel Fuel Oil Storage Tank
FOAKE	First-of-a-Kind Engineering
FPE	Fire Pump Enclosure
FTDC	Fault-Tolerant Digital Controller
FTS	Fuel Transfer System
FW	Feedwater
FWCS	Feedwater Control System
FWS	Fire Water Storage Tank
GCS	Generator Cooling System
GDC	General Design Criteria
GDCS	Gravity-Driven Cooling System
GE	General Electric Company
GE-NE	GE Nuclear Energy
GEN	Main Generator System
GENE	General Electric Nuclear Energy
GETAB	General Electric Thermal Analysis Basis
GL	Generic Letter
GM	Geiger-Mueller Counter
GNF	Global Nuclear Fuel
GSIC	Gamma-Sensitive Ion Chamber
GSOS	Generator Sealing Oil System
GWSR	Ganged Withdrawal Sequence Restriction
HAZ	Heat-Affected Zone
HCU	Hydraulic Control Unit
HCW	High Conductivity Waste
HDVS	Heater Drain and Vent System
HEI	Heat Exchange Institute
HELB	High Energy Line Break
HEP	Human error probability
HEPA	High Efficiency Particulate Air/Absolute
HFE	Human Factors Engineering
HFF	Hollow Fiber Filter
HGCS	Hydrogen Gas Cooling System
HIC	High Integrity Container
HID	High Intensity Discharge
HIS	Hydraulic Institute Standards
HM	Hot Machine Shop & Storage
HP	High Pressure
HPNSS	High Pressure Nitrogen Supply System
HPT	High-pressure turbine

Term	**Definition**
HRA	Human Reliability Assessment
HSI	Human-System Interface
HSSS	Hardware/Software System Specification
HVAC	Heating, Ventilation and Air Conditioning
HVS	High Velocity Separator
HWCS	Hydrogen Water Chemistry System
HWS	Hot Water System
HX	Heat Exchanger
I&C	Instrumentation and Control
I/O	Input/Output
IAS	Instrument Air System
IASCC	Irradiation Assisted Stress Corrosion Cracking
IBC	International Building Code
IC	Ion Chamber
IC	Isolation Condenser
ICD	Interface Control Diagram
ICPR	Initial Critical Power Ratio
ICS	Isolation Condenser System
IE	Inspection and Enforcement
IEB	Inspection and Enforcement Bulletin
IED	Instrument and Electrical Diagram
IEEE	Institute of Electrical and Electronic Engineers
IGSCC	Intergranular Stress Corrosion Cracking
IIS	Iron Injection System
ILRT	Integrated Leak Rate Test
IOP	Integrated Operating Procedure
IMC	Induction Motor Controller
IMCC	Induction Motor Controller Cabinet
IRM	Intermediate Range Monitor
ISA	Instrument Society of America
ISI	In-Service Inspection
ISLT	In-Service Leak Test
ISM	Independent Support Motion
ISMA	Independent Support Motion Response Spectrum Analysis
ISO	International Standards Organization
ITA	Inspections, Tests or Analyses
ITAAC	Inspections, Tests, Analyses and Acceptance Criteria
ITA	Initial Test Program
LAPP	Loss of Alternate Preferred Power
LCO	Limiting Conditions for Operation

Term	**Definition**
LCW	Low Conductivity Waste
LD	Logic Diagram
LDA	Lay down Area
LD&IS	Leak Detection and Isolation System
LERF	Large early release frequency
LFCV	Low Flow Control Valve
LHGR	Linear Heat Generation Rate
LLRT	Local Leak Rate Test
LMU	Local Multiplexer Unit
LO	Dirty/Clean Lube Oil Storage Tank
LOCA	Loss-of-Coolant-Accident
LOFW	Loss-of-feedwater
LOOP	Loss of Offsite Power
LOPP	Loss of Preferred Power
LP	Low Pressure
LPCI	Low Pressure Coolant Injection
LPCRD	Locking Piston Control Rod Drive
LPMS	Loose Parts Monitoring System
LPRM	Local Power Range Monitor
LPSP	Low Power Setpoint
LUA	Lead Use Assembly
LWMS	Liquid Waste Management System
MAAP	Modular Accident Analysis Program
MAPLHGR	Maximum Average Planar Linear Head Generation Rate
MAPRAT	Maximum Average Planar Ratio
MBB	Motor Built-In Brake
MCC	Motor Control Center
MCES	Main Condenser Evacuation System
MCPR	Minimum Critical Power Ratio
MCR	Main Control Room
MCRP	Main Control Room Panel
MELB	Moderate Energy Line Break
MLHGR	Maximum Linear Heat Generation Rate
MMI	Man-Machine Interface
MMIS	Man-Machine Interface Systems
MOV	Motor-Operated Valve
MPC	Maximum Permissible Concentration
MPL	Master Parts List
MS	Main Steam
MSIV	Main Steam Isolation Valve

Term	**Definition**
MSL	Main Steamline
MSLB	Main Steamline Break
MSLBA	Main Steamline Break Accident
MSR	Moisture Separator Reheater
MSV	Mean Square Voltage
MT	Main Transformer
MTTR	Mean Time To Repair
MWS	Makeup Water System
NBR	Nuclear Boiler Rated
NBS	Nuclear Boiler System
NCIG	Nuclear Construction Issues Group
NDE	Nondestructive Examination
NE-DCIS	Non-Essential Distributed Control and Information System
NDRC	National Defense Research Committee
NDT	Nil Ductility Temperature
NFPA	National Fire Protection Association
NIST	National Institute of Standard Technology
NMS	Neutron Monitoring System
NOV	Nitrogen Operated Valve
NPHS	Normal Power Heat Sink
NPSH	Net Positive Suction Head
NRC	Nuclear Regulatory Commission
NRHX	Non-Regenerative Heat Exchanger
NS	Non-seismic (non-seismic Category I)
NSSS	Nuclear Steam Supply System
NT	Nitrogen Storage Tank
NTSP	Nominal Trip Setpoint
O&M	Operation and Maintenance
O-RAP	Operational Reliability Assurance Program
OBCV	Overboard Control Valve
OBE	Operating Basis Earthquake
OGS	Offgas System
OHLHS	Overhead Heavy Load Handling System
OIS	Oxygen Injection System
OLMCPR	Operating Limit Minimum Critical Power Ratio
OLU	Output Logic Unit
OOS	Out-of-service
ORNL	Oak Ridge National Laboratory
OSC	Operational Support Center
OSHA	Occupational Safety and Health Administration

<u>Term</u>	<u>Definition</u>
OSI	Open Systems Interconnect
P&ID	Piping and Instrumentation Diagram
PA/PL	Page/Party-Line
PABX	Private Automatic Branch (Telephone) Exchange
PAM	Post Accident Monitoring
PAR	Passive Autocatalytic Recombiner
PAS	Plant Automation System
PASS	Post Accident Sampling Subsystem of Containment Monitoring System
PCC	Passive Containment Cooling
PCCS	Passive Containment Cooling System
PCT	Peak cladding temperature
PCV	Primary Containment Vessel
PFD	Process Flow Diagram
PGA	Peak Ground Acceleration
PGCS	Power Generation and Control Subsystem of Plant Automation System
PH	Pump House
PL	Parking Lot
PM	Preventive Maintenance
PMCS	Performance Monitoring and Control Subsystem of NE-DCIS
PMF	Probable Maximum Flood
PMP	Probable Maximum Precipitation
PQCL	Product Quality Check List
PRA	Probabilistic Risk Assessment
PRMS	Process Radiation Monitoring System
PRNM	Power Range Neutron Monitoring
PS	Plant Stack
PSD	Power Spectra Density
PSS	Process Sampling System
PSWS	Plant Service Water System
PT	Pressure Transmitter
PWR	Pressurized Water Reactor
QA	Quality Assurance
RACS	Rod Action Control Subsystem
RAM	Reliability, Availability and Maintainability
RAPI	Rod Action and Position Information
RAT	Reserve Auxiliary Transformer
RB	Reactor Building
RBC	Rod Brake Controller
RBCC	Rod Brake Controller Cabinet
RBCWS	Reactor Building Chilled Water Subsystem

Term	**Definition**
RBHV	Reactor Building HVAC
RBS	Rod Block Setpoint
RBV	Reactor Building Vibration
RC&IS	Rod Control and Information System
RCC	Remote Communication Cabinet
RCCV	Reinforced Concrete Containment Vessel
RCCWS	Reactor Component Cooling Water System
RCPB	Reactor Coolant Pressure Boundary
RCS	Reactor Coolant System
RDA	Rod Drop Accident
RDC	Resolver-to-Digital Converter
REPAVS	Refueling and Pool Area Ventilation Subsystem of Fuel Building HVAC
RFP	Reactor Feed Pump
RG	Regulatory Guide
RHR	Residual heat removal (function)
RHX	Regenerative Heat Exchanger
RLP	Reference Loading Pattern
RMS	Root Mean Square
RMS	Radiation Monitoring Subsystem
RMU	Remote Multiplexer Unit
RO	Reverse Osmosis
ROM	Read-only Memory
RPS	Reactor Protection System
RPV	Reactor Pressure Vessel
RRPS	Reference Rod Pull Sequence
RSM	Rod Server Module
RSPC	Rod Server Processing Channel
RSS	Remote Shutdown System
RSSM	Reed Switch Sensor Module
RSW	Reactor Shield Wall
RTIF	Reactor Trip and Isolation Function(s)
RT_{NDT}	Reference Temperature of Nil-Ductility Transition
RTP	Reactor Thermal Power
RW	Radwaste Building
RWCU/SDC	Reactor Water Cleanup/Shutdown Cooling
RWE	Rod Withdrawal Error
RWM	Rod Worth Minimizer
SA	Severe Accident
SAR	Safety Analysis Report
SB	Service Building

<u>Term</u>	<u>Definition</u>
S/C	Digital Gamma-Sensitive GM Detector
SC	Suppression Chamber
S/D	Scintillation Detector
S/DRSRO	Single/Dual Rod Sequence Restriction Override
S/N	Signal-to-Noise
S/P	Suppression Pool
SAS	Service Air System
SB&PC	Steam Bypass and Pressure Control System
SBO	Station Blackout
SBWR	Simplified Boiling Water Reactor
SCEW	System Component Evaluation Work
SCRRI	Selected Control Rod Run-in
SDC	Shutdown Cooling
SDM	Shutdown Margin
SDS	System Design Specification
SEOA	Sealed Emergency Operating Area
SER	Safety Evaluation Report
SF	Service Water Building
SFP	Spent fuel pool
SIL	Service Information Letter
SIT	Structural Integrity Test
SIU	Signal Interface Unit
SJAE	Steam Jet Air Ejector
SLC	Standby Liquid Control
SLCS	Standby Liquid Control System
SLMCPR	Safety Limit Minimum Critical Power Ratio
SMU	SSLC Multiplexing Unit
SOV	Solenoid Operated Valve
SP	Setpoint
SPC	Suppression Pool Cooling
SPDS	Safety Parameter Display System
SPTMS	Suppression Pool Temperature Monitoring Subsystem of Containment Monitoring System
SR	Surveillance Requirement
SRM	Source Range Monitor
SRNM	Startup Range Neutron Monitor
SRO	Senior Reactor Operator
SRP	Standard Review Plan
SRS	Software Requirements Specification
SRSRO	Single Rod Sequence Restriction Override
SRSS	Sum of the squares

Term	Definition
SRV	Safety Relief Valve
SRVDL	Safety relief valve discharge line
SSAR	Standard Safety Analysis Report
SSC(s)	Structure, System and Component(s)
SSE	Safe Shutdown Earthquake
SSLC	Safety System Logic and Control
SSPC	Steel Structures Painting Council
ST	Spare Transformer
STP	Sewage Treatment Plant
STRAP	Scram Time Recording and Analysis Panel
STRP	Scram Time Recording Panel
SV	Safety Valve
SWH	Static water head
SWMS	Solid Waste Management System
SY	Switch Yard
TAF	Top of Active Fuel
TASS	Turbine Auxiliary Steam System
TB	Turbine Building
TBCE	Turbine Building Compartment Exhaust
TBE	Turbine Building Exhaust
TBLOE	Turbine Building Lube Oil Area Exhaust
TBS	Turbine Bypass System
TBHV	Turbine Building HVAC
TBV	Turbine Bypass Valve
TC	Training Center
TCCWS	Turbine Component Cooling Water System
TCS	Turbine Control System
TCV	Turbine Control Valve
TDH	Total Developed Head
TEMA	Tubular Exchanger Manufacturers' Association
TFSP	Turbine first stage pressure
TG	Turbine Generator
TGSS	Turbine Gland Seal System
THA	Time-history accelerograph
TLOS	Turbine Lubricating Oil System
TLU	Trip Logic Unit
TMI	Three Mile Island
TMSS	Turbine Main Steam System
TRAC	Transient Reactor Analysis Code
TRM	Technical Requirements Manual

Term	**Definition**
TS	Technical Specification(s)
TSC	Technical Support Center
TSI	Turbine Supervisory Instrument
TSV	Turbine Stop Valve
UBC	Uniform Building Code
UHS	ultimate heat sink
UL	Underwriter's Laboratories Inc.
UPS	Uninterruptible Power Supply
USE	Upper Shelf Energy
USM	Uniform Support Motion
USMA	Uniform support motion response spectrum analysis
USNRC	United States Nuclear Regulatory Commission
USS	United States Standard
UV	Ultraviolet
V&V	Verification and Validation
Vac / VAC	Volts Alternating Current
Vdc / VDC	Volts Direct Current
VDU	Video Display Unit
VW	Vent Wall
VWO	Valves Wide Open
WD	Wash Down Bays
WH	Warehouse
WS	Water Storage
WT	Water Treatment
WW	Wetwell
XMFR	Transformer
ZPA	Zero period acceleration

4. REACTOR

4.1 SUMMARY DESCRIPTION

The reactor assembly consists of the reactor pressure vessel, pressure-containing appurtenances including control rod drive (CRD) housings and in-core instrumentation housings. The reactor internal components are described in Subsection 4.1.2, Reactor Internal Components. Figure 5.3-3 (Reactor Pressure Vessel System Key Features) shows the arrangement of the reactor assembly components. A summary of the important design and performance characteristics of the reactor and plant is given in Table 1.3-1. Loading conditions for reactor assembly components are specified within Subsection 3.9.5.

Section 4.3 presents a typical fuel and control rod design and core loading pattern that is adapted for the ESBWR as the basis for the system response studies in Section 5.2, Section 6.3 and Chapter 15. The actual fuel and control rod designs and core loading pattern to be used at a plant must meet criteria approved by the NRC. The typical fuel and control rod design and core loading pattern are presented in this chapter; information to be provided by the utility referencing the ESBWR design is contained in the interface subsections.

4.1.1 Reactor Pressure Vessel

The reactor pressure vessel includes the shroud support brackets. Flow restrictors are included in the steam outlet nozzles and the GDCS/equalizing line nozzles. The reactor pressure vessel design and description are covered in Section 5.3.

4.1.2 Reactor Internal Components

The major reactor internal components described within Subsection 3.9.5 include:

- Core support structures (shroud, shroud support, top guide, core plate, control rod guide tubes and fuel supports),

- Chimney and partitions,

- Chimney head and steam separators assembly,

- Steam dryer assembly,

- Feedwater spargers,

- Standby liquid control header, sparger and piping assembly, and

- In-core guide tubes.

Except for the Zircaloy in the reactor core, these reactor internals are stress corrosion-resistant stainless steels or other high alloy steels. The fuel assemblies (including fuel rods and channels), control rods, chimney head and steam separator assembly, steam dryers and in-core instrumentation assemblies are removable when the reactor vessel is opened for refueling or maintenance.

4.1.2.1 Reactor Core

Important features of the reactor core are:

- The control rods are bottom-entry, cruciform shaped. Rods of this design were first introduced in the Dresden-1 reactor in April 1961 and have accumulated thousands of hours of service in BWRs around the world.

- Local power range monitors (LPRMs) are in-core fission chambers that are assembled and fixed inside enclosing tubes located in the core. These instrument assemblies provide signals for continuous local power range neutron flux monitoring. Fixed in-core gamma thermometer detectors, called automatic fixed in-core probe (AFIP) sensors, are also installed to provide axial local power information for LPRM calibration and core power calculation. The AFIP sensors are installed within the LPRM assembly with one sensor next to each LPRM detector. Startup range neutron monitors (SRNMs) are provided for monitoring core neutron flux at low power conditions. The SRNM sensors are fixed inside tubes that are located as shown in Figure 4.1-1. The LPRM cover tubes contain holes for the reactor coolant flow, whereas the SRNM tubes are pressure barrier dry tubes. All in-core instrument leads enter from the vessel bottom; this allows instrument assemblies to remain undisturbed in service through refueling. More information on in-core instrumentation is presented in Subsection 7.2.2. The instrument tubes are protected from water flow by in-core guide tubes in the bottom head plenum (Subsection 3.9.5).

- As shown by experience obtained at Dresden-1 and other BWR plants that utilize the in-core flux monitor system, the desired power distribution can be maintained within a large core by proper control rod scheduling.

- The fuel channels provide a flow path for the boiling coolant, serve as a guiding surface for the control rods, and protect the fuel during handling operations.

- The mechanical reactivity control permits criticality checks during refueling and provides maximum plant safety. The core is designed to be subcritical at any time in its operating history with any single control rod fully withdrawn and the other control rods fully inserted.

- The selected control rod pitch represents a practical value of individual control rod reactivity worth, and allows adequate clearance below the pressure vessel between CRD mechanisms for ease of maintenance and removal.

- The reactor core is arranged as an upright circular cylinder containing a large number of fuel cells and is located within the core shroud inside the reactor vessel.

4.1.2.1.1 Fuel Assembly Description

The fuel assembly description is provided in Section 4.2.

4.1.2.1.2 Fuel Assembly Support and Control Rod Location

A few peripheral fuel assemblies that are not adjacent to a control rod are supported by the core plate via single-assembly fuel supports. Otherwise, individual fuel assemblies in groups of four rest on orificed fuel supports that are mounted on top of the control rod guide tubes. Each guide tube, with its orificed fuel support, bears the weight of four assemblies and is supported on a

CRD penetration nozzle in the bottom head of the reactor vessel. The core plate provides lateral support and guidance at the top of each control rod guide tube and directs most of the reactor coolant flow into the fuel supports and the fuel assemblies. The top guide, mounted on top of the shroud, provides lateral support and guidance for the top of each fuel assembly.

The reactivity of the core is controlled by cruciform control rods and their associated electro-mechanical/hydraulic drive system (Section 4.6). The control rods occupy alternate spaces between fuel assemblies. Each independent CRD inserts a control rod into the core from the bottom, and accurately positions its associated control rod during normal operation with an electric motor-driven ball screw. Hydraulic pressure is applied on the hollow cylinder of a CRD to exert several times the force of gravity on the control rod for insertion during the scram mode of CRD operation. Bottom entry allows optimum power shaping in the core, ease of refueling and convenient drive maintenance.

4.1.2.1.3 Other Internals

Information on other major reactor internal components identified in Subsection Reactor Internal Components is presented in Subsection 3.9.5.

4.1.3 Reactivity Control Systems

4.1.3.1 Operation

The control rods perform dual functions of power distribution shaping and reactivity control. Power distribution in the core is controlled during operation of the reactor by manipulation of selected patterns of rods (Appendix 4A). These rods are positioned to counterbalance steam voids in the top of the core and effect significant power flattening. These groups of control elements, used for power flattening, experience a somewhat higher duty cycle and neutron exposure than the other rods in the control system.

The reactivity control function requires that all rods be available for either reactor "scram" (prompt shutdown) or reactivity control. Because of this, the control elements are mechanically designed to withstand the dynamic forces resulting from a scram. They are connected to bottom-mounted, electro-hydraulically actuated drive mechanisms that allow either electric motor controlled axial positioning for reactivity regulation or hydraulic scram insertion. The design of the rod-to-drive connection permits each rod to be attached or detached from its drive without disturbing the remainder of the control system. The bottom-mounted drives permit the entire control system to be left intact and remain operable for tests with the reactor vessel open.

4.1.3.2 Description of Control Rods

A description of the control rods is presented in Section 4.2 with a description of the CRD System in Section 4.6.

4.1.3.3 Supplementary Reactivity Control

The core control requirements are met by use of the combined effects of the movable control rods, supplementary burnable poison, and the reactor coolant natural flow. A description of the supplementary burnable poison is presented in Sections 4.2 and 4.3.

4.1.4 Analysis Techniques

4.1.4.1 Reactor Internal Components

Computer codes used for the analysis of the internal components are as follows:

- SAP4G07

- ANSYS

- SEISM03

4.1.4.1.1 SAP4G07

SAP4G07 is a general-purpose finite element computer program used to perform stress, dynamic, and seismic analyses of structural, mechanical and piping components. Dynamic analysis can be done using direct integration or mode superposition. Response spectrum analysis (a mode superposition method) can include multiple support excitation. SAP4G07 is a GENE in-house program based on similar programs developed by Professors E. L. Wilson and K. J. Bathe at UC Berkeley.

4.1.4.1.2 ANSYS

ANSYS is a general-purpose finite element computer program designed to solve a variety of problems in engineering analysis. The ANSYS program features the following capabilities:

- Structural analysis, including static elastic, plastic and creep, dynamic, seismic and dynamic plastic, and large deflection and stability analyses.

- One-dimensional fluid flow analysis.

- Transient heat transfer analyses, including conduction, convection, and radiation with direct input to thermal-stress analyses.

- An extensive finite element library, including gaps, friction interfaces, springs, cables (tension only), direct interfaces (compression only), curved elbows, etc. Many of the elements contain complete plastic, creep, and swelling capabilities.

- Plotting - Geometry plotting is available for all elements in the ANSYS library, including isometric and perspective views of three-dimensional structures.

- Restart Capability - The ANSYS program has restart capability for several analysis types. An option is also available for saving the stiffness matrix once it is calculated for the structure, and using it for other loading conditions.

ANSYS is used extensively in GENE for elastic and elastic-plastic analyses of the reactor pressure vessel, core support structures, reactor internals, fuel and fuel channel.

4.1.4.1.3 SEISM03

SEISM03 is a GENE proprietary computer program for non-linear dynamic analysis. It is based on the component element method developed by S. Levy and J.P. Wilkinson of GECR&D. The method uses basic mass, spring, damper, gap, and coupling elements in a direct integration

approach to solve non-linear dynamic analysis. This dynamic analysis engineering computer program (ECP) is used in conjunction with the following:

- **SEPRE:** This ECP is a preprocessor for SEISM. It takes the output from CRTFI and phases the input time histories of all loads with the basic load time histories. SEPRE also converts all input loads to the format required for input to SEISM.

- **SEPST:** This ECP is the SEISM post-processor. SEPST condenses the SEISM output data into a form that is more practical to interpret. It determines and prints the initial values, the maximum and minimum values for all components, and the times of their occurrence. In addition, it generates the response time history plots of selected components.

- **CRTFI:** This ECP uses, as input, the scaled or composite horizontal acceleration time histories at the mid-fuel and end-fuel positions to determine (1) the clamping forces to be applied to the analysis model friction elements, (2) the scram uplift forces on a bundle, (3) inertial forces of the fuel in order to obtain reaction forces on both ends of the fuel, and (4) fuel-center deflection and uplift forces due to scram.

4.1.4.2 Fuel Design Analysis

The fuel design analysis is discussed in Section 4.2.

4.1.4.3 Reactor Systems Dynamics

The analysis techniques and computer codes used in reactor systems dynamics are based on those approved or developed using NRC-approved criteria.

4.1.4.4 Nuclear Analysis

The analysis techniques are discussed in Section 4.3.

4.1.4.5 Neutron Fluence Calculations

Neutron vessel fluence calculations were carried out using a two-dimensional, discrete ordinates, Sn transport code with general anisotropic scattering.

This DORT code is the most widely used two-dimensional, discrete ordinates code that solves a wide variety of radiation transport problems. The program solves both fixed source and multiplication problems. Rectangular (X, Y), cylindrical (R, Z), or polar (R, θ) geometry is allowed with various boundary conditions. The fluence calculations incorporate, as an initial starting point, neutron fission distributions prepared from core physics data as a distributed source. Anisotropic scattering is considered for all regions. The cross sections are prepared with 1/E flux weighting using polynominal expansion matrices for anisotropic scattering but do not include the resonance self-shielding factors (Section 12.3).

4.1.4.6 Thermal-Hydraulic Calculations

The thermal-hydraulic models are discussed in Section 4.4.

4.1.5 COL Information

None.

4.1.6 References

None.

Figure 4.1-1. Core Configuration with Location of Instrumentation

4.2 FUEL SYSTEM DESIGN

The fuel system is defined as consisting of the fuel assembly and the reactivity control assembly. The fuel assembly is comprised of the fuel bundle, channel and channel fastener. The fuel bundle is comprised of fuel rods, water rods, and fuel rods containing burnable neutron absorber, spacers, springs and assembly fittings. The fuel to be loaded in an ESBWR is any fuel design that is approved by the USNRC or that meets the criteria documented in Appendix 4B. Using these designs assures that all fuel system design requirements are met.

To demonstrate the ESBWR system response in this DCD Tier 2, a reference core, based upon a current NRC-approved GE14 fuel design, is modified to account for the shorter active fuel length. The COL applicant provides the ESBWR fuel design for a specific application to the NRC. The latest GE14 information is provided in the most recent revision of the GE Fuel Bundle Designs Report and its supplements (Reference 4.2-1).

This section addresses the reactivity control elements that extend from the coupling interface of the control rod drive mechanism (per Regulatory Guide 1.70). The functional design of the reactivity control system is detailed in Section 4.6. The control rod design to be used in an ESBWR is any design that meets the criteria documented in Appendix 4C.

4.2.1 Design Bases

4.2.1.1 Fuel Assembly

The fuel assembly (comprised of the fuel bundle, channel and channel fastener) is designed to ensure that possible fuel damage would not result in the release of radioactive materials in excess of limits prescribed by 10 CFR 20, 10 CFR 50 and 10 CFR 100. The core nuclear and hydraulic characteristics, plant equipment characteristics, and instrumentation and protection systems are evaluated to assure that this requirement is met.

The thermal-mechanical design process emphasizes that:

- The fuel assembly provides substantial fission retention capability during all potential operational modes.

- The fuel assembly provides sufficient structural integrity to prevent operational impairment of any reactor safety equipment.

The fuel assembly and its components are designed to withstand:

- The predicted thermal, pressure and mechanical interaction loadings occurring during startup testing, normal operation, and anticipated operational occurrences, infrequent incidents and accidents.

- Loading predicted to occur during handling.

Operating limits are established to ensure that actual fuel operation is maintained within the fuel rod thermal-mechanical design bases. These operating limits define the maximum allowable fuel pellet operating power level as a function of fuel pellet exposure in terms of Maximum Linear Heat Generation Rate (MLHGR). Lattice local power and exposure distributions are applied in the determination of the MLHGR limits.

The detailed design bases for each of the fuel assembly damage, failure and cooling criteria are defined in Section II.A of Standard Review Plan 4.2 (except control rod reactivity; see Subsection 4.2.1.2) are provided in Section 4B.2 of Appendix 4B.

4.2.1.2 Control Rods

The control rod is designed to have:

- Sufficient mechanical strength to prevent displacement of its reactivity control material

- Sufficient strength to prevent deformation that could inhibit its motion

The detailed design bases for the control rod are provided in Appendix 4C.

The control rod patterns and associated power distribution for an ESBWR are provided in Appendix 4A.

4.2.2 Description and Design Drawings

4.2.2.1 Fuel Assembly

The components of the reference fuel assembly are shown in Figure 4.2-1, and consist of a fuel bundle and a channel that surrounds the fuel bundle. The fuel and water rods are spaced and supported by upper and lower tieplates and intermediate spacers. The lower tieplate has a nosepiece that has the function of supporting the fuel assembly in the reactor. The upper tieplate has a handle for transferring the fuel bundle from one location to another. The identifying fuel assembly serial number is engraved on the top of the handle; no two assemblies bear the same serial number. A boss projects from one side of the handle to ensure proper orientation of the assembly in the core. Finger springs, if used, are located between the lower tieplate and channel and are utilized to control the bypass flow through that flow path.

4.2.2.1.1 Fuel Rods

Three types of fuel rods are used in a fuel bundle; tie rods, standard rods, and partial length rods. The tie rods in each fuel bundle have lower end plugs that thread into the lower tieplate and threaded upper end plugs that extend through the upper tieplate. A nut and locking tab are installed on the upper end plug to hold the fuel bundle together. The tie rods support the weight of the assembly only during fuel handling operations. During operation, the assembly is supported by the lower tieplate.

The end plugs of the standard rods have shanks that fit into bosses in the tieplates. An expansion spring is located over the upper end plug shank of each rod in the bundle to keep the rods seated in the lower tieplate.

The partial length rods are installed to reduce the bundle pressure drop and have lower end plugs that thread into the lower tieplate, similar to the tie rods. The upper endplugs do not extend to the upper tieplate and are only used to seal the top end of the partial length rods.

Each fuel rod contains high-density ceramic uranium dioxide fuel pellets stacked within Zircaloy cladding. The fuel rod is evacuated, backfilled with helium, and sealed with end plugs welded into each end. U-235 enrichments may vary from fuel rod to fuel rod within a bundle to reduce

local peak-to-average fuel rod power ratios. Selected fuel rods within each bundle may include small amounts of gadolinium as a burnable poison.

Adequate free volume is provided within each fuel rod in the form of a pellet-to-cladding gap and a plenum region at the top of each fuel rod. A plenum spring, or retainer, is provided in the plenum space to minimize the movement of the column of fuel pellets inside the fuel rod during shipping and handling.

4.2.2.1.2 Water Rods

Water rods are hollow Zircaloy tubes with several holes around the circumference near each end to allow coolant to flow through. One water rod in each bundle axially positions the spacers.

4.2.2.1.3 Fuel Spacer

The primary function of the spacer is to provide lateral support and spacing of the fuel rods, with consideration of thermal-hydraulic performance, fretting wear, strength, neutron economy, and manufacturability.

4.2.2.1.4 Finger Springs

Finger springs can be employed to control the bypass flow through the channel-to-lower tieplate flow path for some fuel assemblies.

4.2.2.1.5 Channels

The fuel channel is composed of a Zirconium based material or equivalent, and performs the following functions:

- Forms the fuel bundle flow path outer periphery for bundle coolant flow

- Provides surfaces for control rod guidance in the reactor core

- Provides structural stiffness to the fuel bundle during lateral loadings applied from fuel rods through the fuel spacers

- Minimizes, in conjunction with the finger springs and bundle lower tieplate, coolant bypass flow at the channel/lower tieplate interface

- Transmits fuel assembly seismic loadings to the top guide and fuel support of the core internal structures

- Provides a heat sink during loss-of-coolant accident (LOCA)

- Provides a stagnation envelope for incore fuel sipping

The channel is open at the bottom and makes a sliding seal fit on the lower tieplate surface. The upper ends of the fuel assemblies in a four-bundle cell are positioned in the corners of the cell against the top guide beams by the channel fastener springs. At the top of the channel, two diagonally opposite corners have welded tabs which support the weight of the channel on the threaded raised posts of the upper tieplate. One of these raised posts has a threaded hole. The channel is attached to the fuel bundle using the threaded channel fastener assembly, which also includes the fuel assembly positioning spring. Channel-to-channel spacing is assured by to the

fuel bundle spacer buttons located on the upper portion of the channel adjacent to the control rod passage area.

4.2.2.2 Control Rods

The control rod assemblies (Figure 4.2-2) perform the functions of power shaping, reactivity control, and scram reactivity insertion for safety shutdown response. Power distribution in the core is controlled during operation of the reactor by manipulating selected patterns of control rods to counterbalance steam void effects at the top of the core.

The control rod main structure consists of a top handle, an absorber section, and a bottom connector assembled into a cruciform shape. The top handle contains a grapple opening for handling. The absorber section is an array of stainless steel tubes filled with boron carbide powder or a combination of boron carbide powder and hafnium rods. The connector is positioned on the bottom of the control rod for attachment to the control rod drive. While being inserted into the core, the control rod is restricted to the cruciform envelope created by the fuel bundles. The connector rollers guide the control rod within the guide tube as the control rod is inserted and withdrawn from the core.

4.2.3 Design Evaluation

4.2.3.1 Fuel Assembly

4.2.3.1.1 Evaluation Methods

The thermal-mechanical evaluations described in Section 4B.2 of Appendix 4B, with the exception of the stress/strain analyses are performed using the NRC-approved GESTR-MECHANICAL fuel rod thermal-mechanical performance model. The stress/strain methodology is described later in this subsection. Any change to this methodology requires prior NRC review and approval.

The GESTR-MECHANICAL fuel rod performance model performs best estimate coupled thermal and mechanical analyses of a fuel rod experiencing a variable operating history.

The model explicitly addresses the effects of:

- Fuel and cladding thermal expansion

- Fuel and cladding creep and plasticity

- Cladding irradiation growth

- Cladding irradiation hardening and thermal annealing of that irradiation hardening

- Fuel irradiation swelling

- Fuel irradiation-induced densification

- Fuel cracking and relocation

- Fuel hot pressing

- Fission gas generation and exposure-enhanced fission gas release including fission product helium release

- Differential axial expansion of the fuel and cladding reflecting axial slip or lockup of the fuel pellets with the cladding

- Fuel phase change volumetric expansion upon melting

The GESTR-MECHANICAL material properties and component models represent the latest experimental information available. NRC approval of the GESTR-MECHANICAL model and its application methodology is provided in Reference 4.2-2.

The fuel rod cladding stress analyses are performed using a Monte Carlo statistical method in conjunction with distortion energy theory. Fuel cladding plasticity analyses are also performed when required by the loading conditions. NRC approval of the stress/strain analyses methodology is provided in Reference 4.2-2.

4.2.3.1.2 Evaluation Results

The fuel rod thermal-mechanical evaluations described in Section 4B.2 of Appendix 4B have been completed for the reference fuel design using the methodologies described in Subsection 4.2.3.1.1. The evaluations demonstrate that the criteria of Appendix 4B are satisfied for the reference fuel design. The NRC previously reviewed and approved this in Reference 4.2-2.

The approval in Reference 4.2-2 contains the following conditions:

- The license/applicant must provide a plant-specific analysis of combined seismic and LOCA loading using NRC-approved methodology or another acceptable method to demonstrate conformance to the structural acceptance requirements described in Appendix A of Standard Review Plan Section 4.2.

- The license/applicant must provide an acceptable post-irradiation surveillance program or endorse the approved GE fuel surveillance program. For the reference fuel design, the second condition is satisfied by the fuel surveillance program described in Section 4B.2 of Appendix 4B (see also Reference 4.2-3).

4.2.3.2 Controls Rods

4.2.3.2.1 Evaluation Results

The control rod evaluation methods described in Section 4C.2 use established methodology for the control rod. The evaluation methodology history demonstrates that the criteria of Appendix 4C are satisfactory for the reference control rod.

4.2.4 Testing, Inspection, and Surveillance Plans

GE has an active program for the surveillance of both production and developmental fuel. The NRC has reviewed the GE program and approved it in Reference 4.2-3.

4.2.5 COL Information

Fuel Design: the COL applicant will provide the fuel bundle name (i.e., GE14 or other) and a reference to the fuel design documentation.

Control Rod Design: the COL applicant will provide the control rod model and a reference to the control rod design documentation.

4.2.6 References

4.2-1   GE Nuclear Energy, "GE Fuel Bundle Designs," NEDE-31152P, Revision 8, April 2001.

4.2-2   USNRC Letter, C. O. Thomas (NRC) to J. S. Charnley (GE), "Acceptance for referencing of Licensing Topical Report NEDE-24011-P Amendment 7 to Revision 6, General Electric Standard Application for Reactor Fuel", March 1, 1985.

4.2-3   USNRC Letter, L. S. Rubenstein (NRC) to R. L. Gridley (GE), "Acceptance of GE Proposed Fuel Surveillance Program", June 27, 1984.
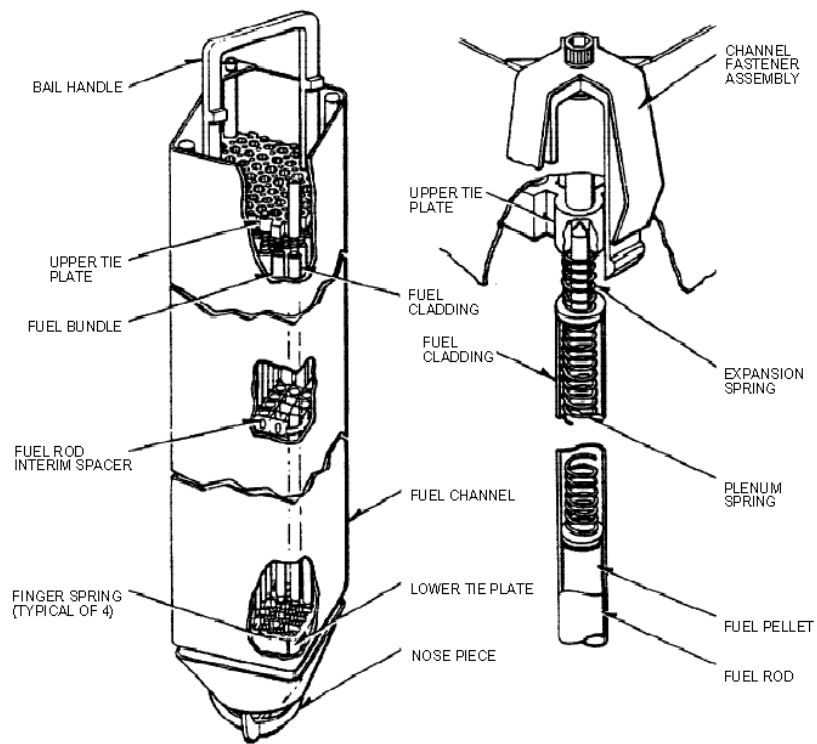
Figure 4.2-1. Fuel Assembly
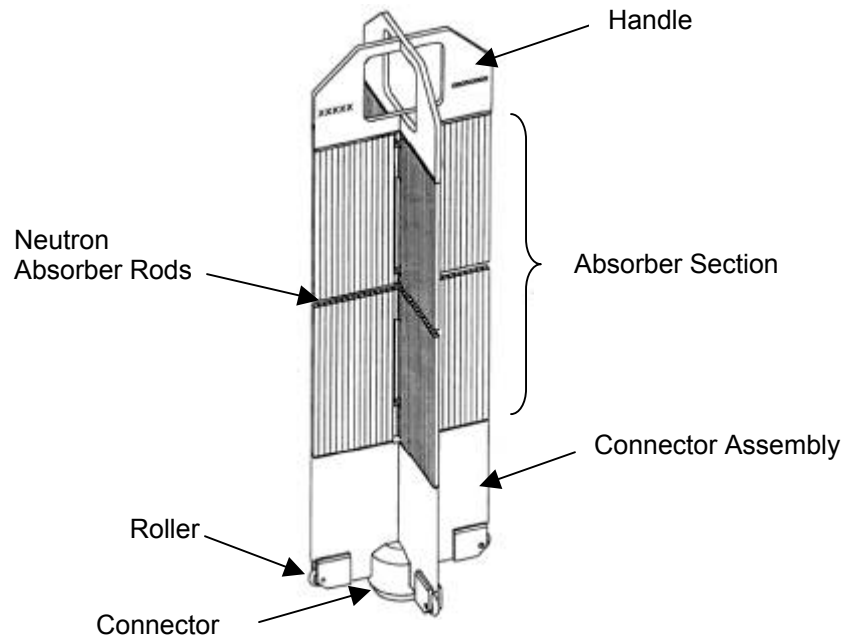
Figure 4.2-2. Control Rod Assembly

4.3 NUCLEAR DESIGN

4.3.1 Design Basis

The safety design bases that are required fall into two categories:

- The reactivity basis, which prevents an uncontrolled positive reactivity excursion, and

- The overpower bases, which prevent the core from operating beyond the fuel integrity limits.

4.3.1.1 Reactivity Basis

The core shall be capable of being made subcritical at any time or at any core condition with any control rod fully withdrawn.

4.3.1.2 Overpower Bases

The Minimum Critical Power Ratio (MCPR) and Maximum Linear Heat Generation Rate (MLHGR) are determined such that the fuel does not exceed required licensing limits during abnormal operational occurrences or accidents. The fuel design limits are defined as follows:

Maximum Linear Heat Generation Rate: The MLHGR is the maximum linear heat generation rate expressed in kW/ft for the fuel rod with the highest surface heat flux at a given nodal plane in the bundle. The MLHGR operating limit is bundle type dependent. The MLHGR can be monitored to assure that all mechanical design requirements are met.

Minimum Critical Power Ratio: The MCPR is the minimum CPR allowed for a given bundle type to avoid boiling transition. The CPR is a function of several parameters; the most important are bundle power, bundle flow, and bundle R-factor. The R-factor depends on the local power distribution and the details of the bundle mechanical design. The plant Operating Limit MCPR (OLMCPR) is established by considering the limiting anticipated operational occurrences (AOOs) for each operating cycle. The OLMCPR is determined such that 99.9% of the rods avoid boiling transition during the transient of the limiting analyzed AOO.

4.3.2 Description

The core design consists of a light-water moderated reactor, fueled with slightly enriched uranium-dioxide. The use of water as a moderator produces a neutron energy spectrum in which fissions are caused principally by thermal neutrons. At normal operating conditions, the moderator boils, producing a spatially variable distribution of steam voids in the core. The void reactivity feedback effect is an inherent safety feature of the ESBWR system. Any system change which increases reactor power, either in a local or core-wide sense, produces additional steam voids and thus reduces the power.

4.3.2.1 Nuclear Design Descriptions

The Reference Loading Pattern (RLP) is the nuclear design basis for fuel licensing. The core is designed to represent, as closely as possible, the actual core loading pattern. However, there may be occurrences where the number and/or types of bundles in the reference design and the actual core loading do not exactly agree. For the purpose of this report, the RLP is characterized

by Figure 4.3-1. This core is the basis for the system analyses in Subsection 5.2.2, Section 6.3 and Chapter 15.

4.3.2.2 Power Distribution

The core power distribution is a function of fuel bundle design, core loading, control rod pattern, core exposure distributions and core coolant flow rate. The thermal performance parameters, MLHGR and MCPR, limit the core power distribution. In the event the COL applicant chooses a different fuel design, the methodology for demonstrating stability shall be approved by the NRC. See Subsection 4.3.5.1 for COL information.

4.3.2.2.1 Power Distribution Measurements

The techniques for measurement of the power distribution within the reactor core, together with instrumentation correlations and operation limits, are discussed in Subsection 7A.3.2.

4.3.2.2.2 Power Distribution Accuracy

The accuracy of the calculated power distribution is discussed in Reference 4.3-1.

4.3.2.2.3 Power Distribution Anomalies

Stringent inspection procedures are utilized to ensure the correct arrangement of the core following fuel loading. A fuel loading error (a mislocated or a misoriented fuel bundle in the core) is a very improbable event, but calculations have been performed to determine the effects of such events. The fuel loading error is discussed further in Chapter 15.

The inherent design characteristics of the ESBWR are well suited to limit gross power tilting. The stabilizing nature of the large moderator void coefficient effectively reduces the effect of perturbations on the power distribution. In addition, the incore instrumentation system, together with the online computer, provide the operator with prompt information on the power distribution so that control rods or other means to limit the undesirable effects of power tilting can readily be used. Because of these design characteristics, it is not necessary to allocate a specific margin in the peaking factor to account for power tilt. If, for some reason, the power distribution cannot be maintained within normal limits using control rods, then the total core power can be reduced.

4.3.2.3 Reactivity Coefficients

Reactivity coefficients are a measure of the differential changes in reactivity produced by differential changes in core conditions. These coefficients are useful in understanding the response of the core to external disturbances. The Doppler reactivity coefficient and the moderator void reactivity coefficient are the two primary reactivity coefficients that characterize the dynamic behavior of boiling water reactors.

The safety analysis methods (described in Chapter 15) are based on system and core models that include a representation of the core space-time kinetics. Therefore, the reactivity coefficients are not directly used in the safety analysis methods, but are useful in the general understanding and discussion of the core response to perturbations.

4.3.2.3.1 Doppler Reactivity Coefficient

The Doppler coefficient is a measure of the reactivity change associated with an increase in the absorption of resonance-energy neutrons caused by a change in the temperature of the material in question. The Doppler reactivity coefficient provides instantaneous negative reactivity feedback to any rise in fuel temperature, on either a gross or local basis. The magnitude of the Doppler coefficient is inherent in the fuel design and does not vary significantly among BWR designs. For most structural and moderator materials, resonance absorption is not significant, but in U-238 and Pu-240 an increase in temperature produces a comparatively large increase in the effective absorption cross-section. The resulting parasitic absorption of neutrons causes an immediate loss in reactivity. The Doppler coefficient is determined using the theory and methods approved in Reference 4.3-2. In the event the COL applicant chooses a different fuel design, the methodology for demonstrating stability shall be that approved by the NRC.

The Doppler reactivity coefficient is determined by using an NRC-approved lattice physics code. The lattice physics code is used to calculate k∞ for any lattice at two temperatures. The first temperature is the standard hot operating temperature. The second temperature is set at 1773 K. The calculations are made at as a function of void fraction and at every standard hot uncontrolled exposure depletion point.

The Doppler Reactivity Coefficient (DRC) is characterized as follows:

$$DRC = \frac{1000(k_{T_1} - k_{T_0})}{k_{T_0}\left(\sqrt{T_1} - \sqrt{T_0}\right)}$$

where:

T_0 = normal hot operating temperature (Kelvin).

T_1 = elevated temperature (Kelvin).

k_{T1} = eigenvalue at elevated temperature.

k_{T0} = eigenvalue at normal operating temperature.

While the reactivity change caused by the Doppler effect is small compared to the moderator void reactivity changes during normal operation, it becomes very important during postulated rapid power excursions in which large fuel temperature changes occur (see Chapter 15).

Analyses were performed using the analytical models described above. For all cases evaluated, the calculated Doppler coefficient was found to be negative. The values are consistent with the analysis supporting compliance for GE14 found in Reference 4.3-3, which consisted of examination of the lattice level Doppler coefficients for several lattice configurations.

4.3.2.3.2 Moderator Void Coefficient

The moderator void coefficient should be large enough to prevent power oscillation due to spatial xenon changes yet small enough that pressurization transients do not unduly limit plant operation. In addition, the void coefficient has the ability to flatten the radial power distribution and to provide ease of reactor control due to the void feedback mechanism. The overall void coefficient is always negative over the complete operating range.

The lattice physics code is used to evaluate infinite lattice properties of each of the various lattices in the fuel bundle as a function of exposure, void history and temperature. Introducing the temperature specific nuclear libraries from the lattice physics code into the core simulator and performing a standard cold eigenvalue calculation then simulate a core temperature change. A detailed discussion of the methods used to calculate void reactivity coefficients, the accuracy and application to plant transient analyses, is presented in Reference 4.3-4.

Analyses were performed using the methodology described above. The results of the analyses at these conditions were that the moderator temperature coefficient is negative for all moderator temperatures in the operating temperature range. Therefore, the moderator temperature coefficient criteria are met.

4.3.2.4 Control Requirements

The ESBWR control rod system is designed to provide adequate control of the maximum excess reactivity anticipated during the plant operation.

4.3.2.4.1 Shutdown Reactivity

The core must be capable of being made subcritical, with margin, in the most reactive condition throughout the operating cycle with the most reactive control rod fully withdrawn and all other rods fully inserted. The shutdown margin is determined by using the BWR simulator code (see Section 4.3.3) to calculate the core multiplication at selected exposure points with the strongest rod fully withdrawn. For fuel cycles beyond the initial core, the shutdown margin is calculated based on the carryover of the expected exposure at the end of the previous cycle. The core is assumed to be in the cold, xenon-free condition in order to ensure that the calculated values are conservative. Further discussion of the uncertainty of these calculations is given in Reference 4.3-5.

As exposure accumulates and burnable poison depletes in the lower exposure fuel bundles, an increase in core reactivity may occur. The nature of the increase depends on specifics of fuel loading and control state.

The cold k_{eff} is calculated with the strongest control rod out at various exposures through the cycle. A value R is defined as the difference between the strongest rod out k_{eff} at beginning of cycle (BOC) and the maximum calculated strongest rod out k_{eff} at any exposure point.

The strongest rod out k_{eff} at any exposure point in the cycle is equal to or less than

$$k_{eff} = k_{eff}(Strongest\ rod\ withdrawn\ @\ BOC) + R.$$

Where R is always greater than or equal to 0. The value of R includes equilibrium Sm.

The calculated k_{eff} with the strongest rod withdrawn at BOC are reported in Table 4.3-1. The uncontrolled and fully controlled k_{eff} values are also reported in Table 4.3-1.

4.3.2.4.2 Reactivity Variations

The excess reactivity designed into the core is controlled by the control rod system supplemented by gadolinia-urania fuel rods. Control rods are used during the cycle to compensate for burnup and to control the power distribution.

4.3.2.4.3 Standby Liquid Control System

The Standby Liquid Control System (SLCS) is designed to provide the capability of bringing the reactor, at any time in a cycle, from full power with a minimum control rod inventory (which is defined to be at the peak of the xenon transient) to a subcritical condition with the reactor in the most reactive xenon-free state. The requirements of this system are dependent primarily on the reactor power level and on the reactivity effects of voids and temperature between full-power and cold, xenon-free condition. The SLCS is discussed in Subsection 9.3.5.

4.3.2.5 Criticality of Reactor During Refueling

The core is subcritical at all times.

4.3.2.6 Stability

4.3.2.6.1 Xenon Transients

Boiling water reactors do not have instability problems due to xenon. This has been demonstrated by:

- Never having observed xenon instabilities in operating BWRs;

- Special tests which have been conducted on operating BWRs in an attempt to force the reactor into xenon instability; and

- Calculations.

All of these indicators have proven that xenon transients are highly damped in a BWR due to the large negative moderator void feedback. Xenon stability analysis and experiments are reported in Reference 4.3-6.

4.3.2.6.2 Thermal Hydraulic Stability

The licensing basis for stability must comply with the requirements of 10 CFR 50, Appendix A, "General Design Criteria for Nuclear Power Plants". The Appendix A criteria related to stability is Criteria 10 and 12.

Criterion 10 (Reactor Design) requires that:

"The reactor core and associated coolant, control, and protection systems shall be designed with appropriate margin to assure that specified acceptable fuel design limits are not exceeded during any condition of normal operation, including the effects of anticipated operational occurrences."

Criterion 12 (Suppression of Reactor Power Oscillations) requires that:

"The reactor core and associated coolant, control, and protection systems shall be designed to assure that power oscillations which can result in conditions exceeding specified acceptable fuel design limits are not possible or can be reliably and readily detected and suppressed."

The ESBWR licensing basis for stability satisfies GDC 12 by designing the reactor system such that significant power oscillations are not possible. A high degree of confidence is established that oscillations will not occur by imposing conservative design criteria on the channel, core

wide and regional decay ratios under all conditions of normal operation and anticipated transients.

Because oscillations in power and flow are precluded by design, the requirements of GDC 10 are met through the analysis for AOOs, and are automatically satisfied with respect to stability.

In addition, the ESBWR will implement a Detect and Suppress solution as a defense-in-depth system as discussed in Appendix 4D.

A detailed discussion of the methods used to analyze ESBWR thermal hydraulic stability is presented in Reference 4.3-7.

4.3.3 Analytical Methods

The steady-state nuclear evaluations of GE designed cores are performed using the analytical tools and methods approved in Reference 4.3-2. Changes may be made to these techniques provided that NRC-approved methods, models, or criteria bound the changes.

The lattice analyses are performed during the bundle design process. The results of these single bundle calculations are reduced to "libraries" of lattice reactivities, relative rod powers, and few group cross-sections as a function of instantaneous void, exposure, exposure-void history, control state, and fuel and moderator temperature. The lattice analyses depend only on fuel lattice parameters and are valid for all plants and cycles for a specific bundle design. The ESBWR core is of the N-lattice type, which is identical to the ABWR, and the lattice physics methods have been qualified for this geometry including core tracking of operating ABWRs.

The core analysis is unique for each fuel cycle. It is performed in the months preceding the cycle loading to demonstrate that the core meets all applicable safety limits. The principal tool used in the core analysis is the three-dimensional BWR simulator code, which computes core reactivity, power distributions, exposure, and reactor thermal-hydraulic characteristics, with spatially varying voids, control rods, burnable poisons and other variables. The ESBWR core is not substantially different from operating BWRs from the viewpoint of steady-state nuclear simulations of core parameters.

4.3.4 Changes

Not applicable.

4.3.5 COL Information

4.3.5.1 Power Distribution

In the event the COL applicant chooses a fuel design different than that described herein, the methodology for characterizing the power distribution shall be approved by the NRC (Subsection 4.3.2.2).

4.3.5.2 Thermal Hydraulic Stability

In the event the COL applicant chooses a fuel design different than that described herein, the methodology for demonstrating stability compliance shall be approved by the NRC (Subsection 4.3.2.6.2).

4.3.6 References

4.3-1   Letter from R. J. Reda (GE) to R. C. Jones (NRC), MFN-098-96, "Implementation of Improved GE Steady-State Methods", July 2, 1996.

4.3-2   Letter from Stuart A. Richards to Glen A. Watford, "Amendment 26 to GE Licensing Topical Report NEDE–24011–P–A, GESTAR II – Implementing Improved GE Steady–State Methods (TAC No. MA6481)," November 10, 1999.

4.3-3   Global Nuclear Fuel, "GE14 Compliance With Amendment 22 of NEDE-24011-P-A (GESTAR II)," NEDC-32868P, Rev. 1, September 2000.

4.3-4   R. C. Stirn, "Generation of Void and Doppler Reactivity Feedback for Application to BWR Design," NEDO–20964, December 1975.

4.3-5   General Electric Company, "BWR/4,5,6 Standard Safety Analysis Report," Revision 2, Chapter 4, June 1977.

4.3-6   R. L. Crowther, "Xenon Considerations in Design of Boiling Water Reactors," APED–5640, June 1968.

4.3-7   General Electric Company, "TRACG Application for ESBWR Stability Analysis," NEDE-33083, Supplement 1, B. S. Shiralkar, et al., December 2004.

Table 4.3-1

Calculated Core Effective Multiplication and Control System Worth - No Voids, 20°C

Control Rod Pattern *	K-effective
Uncontrolled	1.1112
Fully Controlled	0.9508
Strongest Control Rod Out	0.9843

* For the Reference Core Loading Pattern at the limiting exposure of 0 GWd/MT.

	1	2	3	4	5	6	7	8	9	10	11	12	13	14	15	16	17	18	19	
1															33.4	32.3	35.3	32.6	33.8	76
2													39.0	34.1	33.3	17.4	16.0	15.3	0.0	74
3											35.7	33.4	17.9	0.0	19.6	20.5	18.0	0.0	30.5	72
4									35.6	33.7	16.1	0.0	0.0	0.0	20.5	18.6	0.0	0.0	13.4	70
5								37.3	13.5	0.0	0.0	0.0	17.0	0.0	0.0	0.0	29.4	0.0	20.5	68
6							34.7	14.8	0.0	0.0	0.0	19.4	0.0	20.7	0.0	21.1	0.0	20.9	0.0	66
7						34.7	35.3	0.0	16.7	0.0	29.2	18.2	0.0	0.0	24.7	18.9	20.0	0.0	21.4	64
8					37.3	14.8	0.0	0.0	0.0	20.1	15.7	28.6	0.0	12.2	14.0	14.6	0.0	19.9	20.9	62
9				35.6	13.5	0.0	16.7	0.0	16.9	0.0	0.0	0.0	19.1	0.0	19.9	0.0	20.0	0.0	19.9	60
10				33.7	0.0	0.0	0.0	20.1	0.0	21.0	0.0	19.8	0.0	20.5	0.0	0.0	0.0	20.0	0.0	58
11			35.8	16.1	0.0	0.0	29.2	15.7	0.0	0.0	27.8	19.9	19.7	0.0	28.0	19.9	20.3	0.0	21.2	56
12			33.4	0.0	0.0	19.4	18.2	28.6	0.0	19.8	19.9	20.8	0.0	0.0	19.8	20.3	0.0	0.0	20.1	54
13		39.0	17.9	0.0	16.9	0.0	0.0	0.0	19.1	0.0	19.7	0.0	21.0	0.0	20.1	0.0	20.5	0.0	20.4	52
14		34.1	0.0	0.0	0.0	20.7	0.0	12.2	0.0	20.5	0.0	0.0	0.0	20.8	0.0	20.1	0.0	20.0	0.0	50
15	33.4	33.3	19.6	20.5	0.0	0.0	24.7	14.0	19.9	0.0	28.0	19.8	20.1	0.0	27.8	20.7	0.0	0.0	26.4	48
16	32.3	17.4	20.5	18.6	0.0	21.1	18.9	14.6	0.0	0.0	19.9	20.3	0.0	20.1	20.6	20.8	0.0	19.5	20.6	46
17	35.3	16.0	18.0	0.0	29.4	0.0	19.9	0.0	20.0	0.0	20.3	0.0	20.5	0.0	0.0	0.0	20.9	0.0	20.5	44
18	32.6	15.3	0.0	0.0	0.0	20.8	0.0	19.9	0.0	20.0	0.0	0.0	0.0	20.0	0.0	19.5	0.0	21.0	0.0	42
19	33.8	0.0	30.5	13.4	20.5	0.0	21.4	20.9	19.9	0.0	21.2	20.1	20.4	0.0	26.4	20.6	20.5	0.0	21.0	40
	1	3	5	7	9	11	13	15	17	19	21	23	25	27	29	31	33	35	37	

Figure 4.3-1.   Core Loading Map – Reference Loading Pattern Exposures (GWD/ST)

4.4 THERMAL AND HYDRAULIC DESIGN

The thermal-hydraulic design meets the acceptance criteria documented in Appendix 4B. Typical thermal-hydraulic characteristics of the ESBWR core are compared with those of typical BWR-6 and ABWR cores in Table 4.4-1.

4.4.1 Design Basis

4.4.1.1 Safety Design Bases

Thermal-hydraulic design of the core shall establish the thermal-hydraulic safety limits for use in evaluating the safety margin relating the consequences of fuel cladding failure to public safety.

4.4.1.2 Requirements for Steady-State Conditions

Adequate safety margin during normal steady-state operation is maintained when the minimum critical power ratio (MCPR) is greater than the required MCPR operating limit (OLMCPR) and the linear heat generation rates (LHGRs) must be maintained below the maximum LHGR (MLHGR) limit(s). The steady-state OLMCPR and MLHGR limits are determined by analysis of the most severe anticipated operational occurrences (AOOs) to accommodate uncertainties and provide reasonable assurance that no fuel damage results during AOOs. These limits are provided in the Technical Specifications.

4.4.1.3 Requirements for Anticipated Operational Occurrences (AOOs)

The OLMCPR and MLHGR limits are established such that no safety limit is exceeded during the most severe AOO, as demonstrated in Chapter 15.

4.4.1.4 Summary of Design Bases

The steady-state operating limits have been established to assure that the design bases are satisfied for the most severe AOO. Demonstration that the steady-state MCPR and MLHGR limits are not exceeded is sufficient to conclude that the design bases are satisfied.

4.4.2 Description of the Thermal-Hydraulic Design of the Reactor Core

4.4.2.1 Summary Comparison

Typical thermal-hydraulic parameters for the ESBWR are compared to those for a typical BWR/6 plant and the ABWR in Table 4.4-1.

4.4.2.2 Critical Power Ratio

Criteria used to calculate the critical power operating limit are given in Appendix 4B.

4.4.2.3 Average Planar Linear Heat Generation Rate

Average Planar Linear Heat Generation Rate (APLHGR) limits are not needed for the ESBWR, because the most severe LOCA (see Subsection 6.3.3) does not result in the core being uncovered.

4.4.2.4 Void Fraction Distribution

The axial distribution of core void fractions for the average radial channel and the maximum radial channel for the core reference-loading pattern (Figure 4.3-1) are given in Table 4.4-2. The core average and maximum exit values are also provided. Similar distributions for steam quality are given in Table 4.4-3. The core average axial power distribution used to produce these tables is given in Table 4.4-4.

4.4.2.5 Core Coolant Flow Distribution and Orificing Pattern

The flow distribution to the fuel assemblies and bypass flow paths in steady state is calculated using the TRACG code. This code treats all fuel channels as one-dimensional (axial) components, but the vessel is modeled as a three-dimensional component. Hence, the pressure drop across two planes in the vessel is the same at all radial and azimuth locations if the geometry of the components in the vicinity of these planes has radial and azimuth symmetry. Otherwise, this pressure differential displays some (locally) radial and azimuth non-uniformity. Apart from this local non-uniformity, the pressure drop across the fuel assemblies and the bypass flows is essentially the same, and this is confirmed in References 4.4-1 - 4.4-3. The bundle pressure drop evaluation includes frictional, local, elevation, and acceleration losses (Sub-sections 4.4.2.6.1 - 4.4.2.6.4). Pressure drop measurements made in operating reactors confirm that the total measured core pressure drop and calculated core pressure drop are in good agreement. Therefore, there is reasonable assurance that the calculated and actual flow distributions through the core are in good agreement.

The total core flow less the control rod cooling flow enters the lower plenum. A fraction passes through various bypass flow paths. The remainder passes through the orifice in the fuel support plate (experiencing a pressure loss) where some of the flow exits into the bypass flow region through the fit-up between the fuel support and the lower tie plate and through the lower tie plate holes. All initial and reload core fuel bundles have lower tie plate holes. The majority of the flow continues through the lower tie plate (accompanied by a pressure loss), where some flow exits into the bypass flow region through the flow path defined by the fuel channel and the lower tie plate.

A heat balance on the active coolant is performed within each fuel assembly. Fluid properties are expressed as the bundle average at the particular node of interest, and are based on the 1967 International Standard Steam-Water Properties. An iteration is performed on flow through each flow path (fuel assemblies and bypass flow paths), which equates the total differential pressure (plenum to plenum) across each path and matches the sum of the flows through each flow path to the total core flow. When the equal pressure drop criterion described above is satisfied, the flow distributions are established.

4.4.2.6 Core Pressure Drop and Hydraulic Loads

4.4.2.6.1 Friction Pressure Drop

Friction pressure drop is calculated with a basic model as follows:

$$\Delta P_f = \frac{w^2}{2g_c\rho} \frac{fL}{D_H A_{ch}^2} \phi_{TPF}^2$$

where

ΔP_f = friction pressure drop, psi

w = mass flow rate

g_c = conversion factor

ρ = average nodal liquid density

D_H = channel hydraulic diameter

A_{ch} = channel flow area

L = incremental length

f = friction factor

ϕ_{TPF} = two–phase friction multiplier

The formulation for the two-phase multiplier is similar to that presented in References 4.4-4 and 4.4-5, and is based on data from prototypical BWR fuel bundles.

4.4.2.6.2 Local Pressure Drop

The local pressure drop is defined as the irreversible pressure loss associated with an area change, such as the orifice, lower tie plate, and spacers of a fuel assembly.

The general local pressure drop model is similar to the friction pressure drop and is

$$\Delta P_L = \frac{w^2}{2g_c\rho} \frac{K}{A_{ch}^2} \phi_{TPL}^2$$

where

ΔP_L = local pressure drop, psi

K = local pressure drop loss coefficient

A = reference area for local loss coefficient

ϕ_{TPL} = two–phase local multiplier

and w, g_c, and ρ are as previously defined. The formulation for the two-phase multiplier is similar to that reported in Reference 4.4-5. For advanced spacer designs a quality modifier has been incorporated in the two-phase multiplier to better fit the data. Empirical constants were added to fit the results to data taken for the specific designs of the BWR fuel assembly. These data were obtained from tests performed in single-phase water to calibrate the orifice, the lower tie plate, and the holes in the lower tie plate, and in both single and two-phase flow, to derive the best fit design values for spacer and upper tie plate pressure drop. The range of test variables was specified to include the range of interest for boiling water reactors. New test data are obtained whenever there is a significant design change to ensure the most applicable methods are used.

4.4.2.6.3 Elevation Pressure Drop

The elevation pressure drop is based on the relation:

$$\Delta P_E = \overline{\rho} \Delta L \frac{g}{g_c}$$

$$\overline{\rho} = \rho_f (1 - \alpha) + \rho_g \alpha$$

where

ΔP_E = elevation pressure drop

Δ_L = incremental length

$\overline{\rho}$ = average mixture density

g = acceleration of gravity

α = nodal average void fraction

ρ_f, ρ_g = saturated water and vapor density, respectively

Other terms are as previously defined. The TRACG code uses the drift-flux constitutive correlations to predict void fraction. These void fraction correlations are an extension of the Zuber-Findlay drift-flux model for prediction of void fraction (Reference 4.4-6).

4.4.2.6.4 Acceleration Pressure Drop

A reversible pressure change occurs when an area change is encountered, and an irreversible loss occurs when the fluid is accelerated through the boiling process. The basic formulation for the reversible pressure change resulting from a flow area change in the case of single–phase flow is given by:

$$\Delta P_{ACC} = \left(1 - \sigma_A^2\right) \frac{w^2}{2 g_c \rho_f A_2^2}$$

$$\sigma_A = \frac{A_2}{A_1} = \frac{final\ flow\ area}{initial\ flow\ area}$$

where:

ΔP_{ACC} = acceleration pressure drop

A_2 = final flow area

A_1 = initial flow area

In the case of two–phase flow, the liquid density is replaced by a density ratio so that the reversible pressure change is given by:

$$\Delta P_{ACC} = \left(1 - \sigma_A^2\right) \frac{w^2 \rho_H}{2 g_c \rho_{KE}^2 A_2^2}$$

where:

$$\frac{1}{\rho_H} = \frac{x}{\rho_g} + \frac{1-x}{\rho_f}\text{, homogeneous density,}$$

$$\frac{1}{\rho_{KE}^2} = \frac{x^3}{\rho_g^2 \alpha^2} + \frac{(1-x)^3}{\rho_f^2 (1-\alpha)^2}\text{, kinetic energy density,}$$

α = void fraction at A_2

x = steam quality at A_2

Other terms are as previously defined. The basic formulation for the acceleration pressure change due to density change is:

$$\Delta P_{ACC} = \frac{w^2}{g_c A_{ch}^2}\left[\frac{1}{\rho_{OUT}} - \frac{1}{\rho_{IN}}\right]$$

where ρ is either the homogeneous density, ρ_H, or the momentum density, ρ_M

$$\frac{1}{\rho_M} = \frac{x^2}{\rho_g \alpha} + \frac{(1-x)^2}{\rho_f (1-\alpha)}$$

ρ is evaluated at the inlet and outlet of each axial node. Other terms are as previously defined. The total acceleration pressure drop in boiling water reactors is on the order of a few percent of the total pressure drop.

4.4.2.7 Correlation and Physical Data

General Electric has substantial amounts of physical data in support of the pressure drop and thermal-hydraulic loads discussed in Subsection 4.4.2.6. Correlations have been developed to fit these data to the formulations discussed.

4.4.2.7.1 Pressure Drop Correlations

General Electric has taken significant amounts of friction pressure drop data in multi-rod geometries representative of BWR plant fuel bundles and correlated both the friction factor and two-phase multipliers on a best fit basis using the pressure drop formulations reported in Subsections 4.4.2.6.1 and 4.4.2.6.2. Tests are performed in single-phase water to calibrate the orifice and the lower tie-plate, and in both single and two-phase flow to arrive at best fit design values for spacer and upper tie plate pressure drop. The range of test variables is specified to include the range of interest to boiling water reactors. New data are taken whenever there is a significant design change to ensure the most applicable information is used.

Applicability of the single–phase and two–phase hydraulic models discussed in Subsections 4.4.2.6.1 and 4.4.2.6.2 for the fuel design described in Subsection 4.2.2, is confirmed by full scale prototype flow tests.

4.4.2.7.2 Void Fraction Correlation

The void fraction correlation includes effects of pressure, flow direction, mass velocity, quality, and sub-cooled boiling.

4.4.2.7.3 Heat Transfer Correlation

The Jens-Lottes (Reference 4.4-7) heat transfer correlation is used in fuel design to determine the cladding-to-coolant heat transfer coefficients for nucleate boiling.

4.4.2.8 Thermal Effects of Anticipated Operational Occurrences

The evaluation of the core's capability to withstand the thermal effects resulting from AOOs is covered in Section 15.2.

4.4.2.9 Uncertainties in Estimates

Uncertainties in thermal-hydraulic parameters are considered in the statistical analysis that is performed to establish the fuel cladding integrity safety limit documented in Subsection 4.4.5.5.1.

4.4.2.10 Flux Tilt Considerations

For flux tilt considerations, refer to Subsection 4.3.2.2.3.

4.4.3 Description of the Thermal–Hydraulic Design of the Reactor Coolant System

4.4.3.1 Plant Configuration Data

4.4.3.1.1 Reactor Coolant System Configuration

The Reactor Coolant System is described in Chapter 5. The ESBWR reactor coolant system is shown in Figure 5.1-1. The ESBWR design is similar to that of the operating BWRs, except that the recirculation pumps and associated piping are eliminated. Circulation of the reactor coolant through the ESBWR core is accomplished via natural circulation. The natural circulation flow rate depends on the difference in water density between the downcomer region and the core region. The core flow varies according to the power level, as the density difference changes with changes in power levels. Therefore, a core power-flow map is only a single line and there is no active control of the core flow at any given power level.

4.4.3.1.2 Reactor Coolant System Thermal–Hydraulic Data

The steady-state distribution of temperature, pressure and flow rate for each flow path in the Reactor Coolant System is shown in Figure 1.1-3.

4.4.3.1.3 Reactor Coolant System Geometric Data

Volumes of regions and components within the reactor vessel are shown in Figure 5.1-1. Table 4.4-5 provides the flow path length, height, liquid level, minimum elevations, and flow areas for each major flow path volume within the reactor vessel.

4.4.3.2 Operating Restrictions on Pumps

Not Applicable to the ESBWR. The ESBWR is a natural circulation design.

4.4.3.3 Power/Flow Operating Map

The core power-flow map is only a single line and there is no active control of the core flow at a given power level.

4.4.3.4 Temperature-Power Operating Map

Not Applicable to the ESBWR.

4.4.3.5 Load-Following Characteristics

Not Used.

4.4.3.6 Thermal-Hydraulic Characteristics Summary Tables

The thermal-hydraulic characteristics are provided in Table 4.4-1 and Table 4.4-5. The core axial power distributions for the average and hot channels are shown in Table 4.4-4. The axial distribution of core void fractions for the average power channel and the hot channel are given in Table 4.4-2. The core average and core maximum exit void fractions are also provided. Similar distributions for coolant flow quality are provided in Table 4.4-3.

4.4.3.7 Thermal-Hydraulic Stability Performance

Thermal- hydraulic stability performance and evaluation is provided in Appendix 4D.

4.4.4 Loose-Parts Monitoring System

The Loose Parts Monitoring System (LPMS) is designed to provide detection of loose metallic parts within the reactor pressure vessel. Detection of loose parts can provide early warning to the operator so that damage to or malfunctions of safety-related primary system components is avoided or mitigated. LPMS detects structure borne sound that can indicate the presence of loose parts impacting against the reactor pressure vessel internals. The system alarms when the signal amplitude exceeds preset limits. The LPMS can evaluate some aspects of selected signals. However, the system by itself does not diagnose the presence and location of a loose part. Review of LPMS data by an experienced LPM engineer is required to confirm the presence of a loose part.

4.4.4.1 Power Generation Design Bases

The LPMS is designed to provide detection and operator warning of loose parts in the reactor pressure vessel to avoid or mitigate damage to or malfunctions of safety-related primary system components. The LPMS is classified as a non-safety-related system. It is designed in conformance with Regulatory Guide 1.133.

Additional design considerations provide for the inclusion of electronic features to minimize operator-interfacing requirements during normal operation and to enhance the analysis function when operator action is required to investigate potential loose parts.

4.4.4.2 System Description

The LPMS continuously monitors the reactor pressure vessel and appurtenances for indications of loose parts. The LPMS consists of sensors, cables, signal conditioning equipment, alarming monitor, signal analysis and data acquisition equipment, and calibration equipment. The alarm setting after system installation is set low enough to meet the sensitivity requirements, yet is designed to discriminate between normal background noises and the loose part impact signal to minimize spurious alarms. Each sensor channel is isolated to reduce the possibility of signal ground loop problems and to minimize the background noise. Background noises are also minimized by use of tuned filters. A disable signal is provided during control rod movement and other plant maneuvers that may initiate a spurious alert-level alarm.

LPMS sensors are usually accelerometers. The array of LPMS sensors, typically twelve to twenty sensors, is strategically mounted on the external surface of the primary pressure boundary at various elevations and azimuths at natural collection regions for potential loose parts. General mounting locations are at (1) the main steam outlet nozzle, (2) feedwater inlet nozzle, (3) standby liquid control nozzle, and (4) CRD housings. The sensors are mounted in such a fashion as to provide high frequency response and sensitivity.

The online system sensitivity is such that the system meets the calibration requirements of Subsection 4.4.4.5, Test and Inspection. The LPMS frequency range of interest is typically from 1 to 10 kHz. Frequencies lower than 1 kHz are generally associated with flow induced vibration signals or flow noise.

Physical separation is maintained from the sensors at each natural collection region to an area where they are combined and routed through the cable penetration to a termination point. The termination point is selected in the plant where it is accessible for maintenance during full power operation.

The LPMS includes provisions for both automatic and manual start-up of data acquisition equipment with automatic activation in the event the preset alert level is reached or exceeded. The system also initiates an alarm to the control room personnel when an alert condition is reached. The data acquisition system automatically selects the alarmed channel plus additional channels for simultaneous recording. The signal analysis equipment allows immediate visual and audio monitoring of all signals.

Provisions exist for periodic online channel check and functional test and for offline channel calibration during periods of cold shutdown or refueling. The LPMS electronics is designed to facilitate the recognition, location, replacement, repair, and adjustment of malfunctioning LPMS components. The LPMS components located inside the containment have been designed and installed to perform their function following all seismic events that do not require plant shutdown. The LPMS components selected for this application are rated to meet the normal operating radiation, vibration, temperature, and humidity environments in which the components are installed.

All LPMS components within the containment are designed for a 60-year design life. In those instances where a 60-year design life is not practicable, a replacement program is established for those parts that are anticipated to have limited service life.

4.4.4.3 Normal System Operation

The LPMS are set to alarm for detected signals having characteristics of metal-to-metal impacts.

After installation of the sensor array, the LPMS overall and individual channels can be characterized at plant start-up before operation monitoring. Each accelerometer channel exhibits its own particular and unique frequency spectrum. This frequency signature, or background noise, results from a combination of both internal and external sources due to normal and transient conditions.

Calibration is an important part of LPMS operation. The LPMS is calibrated to requirements identified in Subsection 4.4.4.5, Test and Inspection. Alarm level set-point is determined by using a manual calibration device to simulate the presence of a loose part impact near each sensor. The set-point is typically based on a percentage of the calibration signal magnitude, and is a function of actual background noise. Additionally, calibrated impacts at various locations near the sensors assist in diagnosing the source of the signal.

Discrimination logic is typically incorporated in the LPMS to avoid spurious alarms. Discrimination logic rejects events that do not have the characteristics of an impact signal of a loose part. Typical discrimination functions are based on the length of time the signal is above the set-point, the number of channels alarming, the time between alarms, the repetition of the signal, and the waveform and frequency content. False alert signals due to plant maneuvers are avoided by the use of administrative procedures by control room personnel.

Once the loose parts monitor detects an unusual signal characteristic of a metal-to-metal impact, it is essential to determine the source or cause of the alarm. An alarm does not necessarily indicate the presence of a loose part in the reactor. Electrical noises, system malfunctions, limitations in alarm logic, or non-impact noises could cause the alarm. The LPMS detection system is designed to incorporate the discrimination logic to distinguish between an actual loose parts signal and a non-loose parts signal before signaling the control room operator.

Usually the plant operator makes the preliminary evaluation based on the available information. If the presence of unusual metal impact sound is indicated, then the station engineers perform additional evaluation. LPMS experts are required to correctly diagnose the presence and location of a loose part. In order to reach proper conclusions, various factors must be considered such as: plant operating conditions; location of the channels that alarmed; and comparison of the amplitude and frequency contents of the signals with known normal operation data.

4.4.4.4 Safety Evaluation

The LPMS is for use by the plant operator and only for information purposes. The plant operators do not rely on the information provided by the LPMS for the performance of any safety-related action; the LPMS is classified as a non-safety-related system. The LPMS is designed to meet the seismic and environmental operability recommendations of Regulatory Guide 1.133.

4.4.4.5 Test and Inspection

The LPMS is calibrated to detect a metallic loose part that impacts on the inside surface of the reactor pressure vessel within the maximum proximity of a sensor. Provision is made to verify the calibration of the LPMS at each refueling. The system is recalibrated as necessary when

found to be out of calibration. A test and reset capability is included for functional test capability.

The manufacturer provides services of qualified personnel to provide technical guidance for installation, start-up, and acceptance testing of the system. In addition, the manufacturer provides the necessary training of plant personnel for proper system operation and maintenance and planned operating and record-keeping procedures.

4.4.4.6 Instrumentation Application

The LPMS consists of sensors, cables, signal conditioning equipment, alarming monitor, signal analysis and data acquisition equipment, and calibration equipment.

4.4.5 Evaluation

4.4.5.1 Critical Power

The objective for normal operation and AOOs is to maintain nucleate boiling and thus avoid a transition to film boiling. Limits are specified to maintain adequate margin to the onset of the boiling transition. The figure of merit utilized for plant operation is the critical power ratio (CPR). The CPR is the ratio of the bundle power at which some point within the assembly experiences onset of boiling transition to the operating bundle power. Thermal margin is stated in terms of the minimum value of the critical power ratio (MCPR) that corresponds to the most limiting fuel assembly in the core. The design requirement is based on a statistical analysis such that for AOOs at least 99.9% of the fuel rods would be expected to avoid boiling transition (Reference 4.4-8).

4.4.5.2 Core Hydraulics

Core hydraulics models and correlations are discussed in Subsection 4.4.2.

4.4.5.3 Influence of Power Distributions

The influence of power distributions on the thermal-hydraulic design is discussed in Reference 4.4-8.

4.4.5.4 Core Thermal Response

The thermal response of the core for postulated accidents and AOOs is given Section 15.2.

4.4.5.5 Analytical Methods

4.4.5.5.1 Fuel Cladding Integrity Safety Limit

GDC 10 requires, and safety limits ensure, that specified acceptable fuel design limits are not exceeded during steady state operation, normal operational transients, and anticipated operational occurrences (AOOs). Since the parameters that result in fuel damage are not directly observable during reactor operation, the thermal and hydraulic conditions that result in the onset of transition boiling have been used to mark the beginning of the region in which fuel damage could occur. The Fuel Cladding Integrity Safety Limit (FCISL) is set such that no significant fuel damage is calculated to occur during normal operation and AOOs. Although it is recognized that

the onset of transition boiling would not result in damage to BWR fuel rods, a calculated fraction of rods expected to avoid boiling transition has been adopted as a convenient limit. The FCISL is defined as the fraction (%) of total fueled rods that are expected to avoid boiling transition during normal operation and AOOs[1]. A value of 99.9% provides assurance that specified acceptable fuel design limits are met.

4.4.5.5.2 MCPR Operating Limit Calculation

A plant-unique MCPR operating limit is established to provide adequate assurance that the FCISL for that plant is not exceeded for any AOO[1]. This operating requirement is obtained by statistically combining the maximum $\Delta CPR/ICPR$ (delta CPR divided by the initial CPR) value for the most limiting AOO[1] (including any imposed adjustment factors) from conditions postulated to occur at the plant with the uncertainties associated with plant initial conditions and modeling of the transient ΔCPR.

4.4.5.5.2.1 Statistical Model

The statistical analysis utilizes a model of the core that simulates the process computer function. The code produces a critical power ratio (CPR) map of the core based on inputs of power distribution, flow and heat balance information. Details of the procedure are documented in Appendix IV of Reference 4.4-8. Random Monte Carlo selections of all operating parameters based on the uncertainty ranges of manufacturing tolerances, uncertainties in measurement of core operating parameters, calculation uncertainties, the uncertainty in the calculation of the transient ΔCPR and statistical uncertainty associated with the critical power correlations are imposed on the analytical representation of the core and the resulting bundle critical power ratios are calculated.

The minimum allowable operating critical power ratio is set to correspond to the FCISL (99.9% of the rods are expected to avoid boiling transition) by interpolation among the means of the distributions formed by all the trials.

4.4.5.5.2.2 Bounding BWR Statistical Analysis

Statistical analyses have been performed which provide operating limit MCPRs applicable to the GE fuel design in the ESBWR initial core. The results of the analyses show that at least 99.9% of the fuel rods in the core are expected to avoid boiling transition for the most severe AOO[1], if the MCPR is equal to or greater than the calculated OLMCPR for the initial core.

4.4.5.5.3 Calculation Procedure for AOO Events

All ESBWR AOO events are analyzed using the TRACG computer code, described in Reference 4.4-9.

4.4.6 Testing and Verification

The testing and verification techniques to be used to assure that the planned thermal and hydraulic design characteristics of the core have been provided, and remain within required limits throughout core lifetime, are discussed in Chapter 14.

---

[1] AOOs that are not in combination with (i.e., without [w/o] assuming) an additional single active component failure (SACF) or single operator error (SOE)

4.4.7 COL Information

4.4.7.1 Thermal Limits

The COL applicant will provide the thermal limits for the specific core loading at a plant to the NRC for information. (See Appendix 4B.)

4.4.8 References

4.4-1 General Electric Company, "Core Flow Distribution in a Modern Boiling Water Reactor as Measured in Monticello," NEDO-10299A, October 1976.

4.4-2 General Electric Company, "Core Flow Distribution in a General Electric Boiling Water Reactor as Measured in Quad Cities Unit 1," NEDO-10722A, August 1976.

4.4-3 General Electric Company, "Brunswick Steam Electric Plant Unit 1 Safety Analysis Report for Plant Modifications to Eliminate Significant In-Core Vibrations," NEDO-21215, March 1976.

4.4-4 R. C. Martinelli and D.E. Nelson, "Prediction of Pressure Drops During Forced Convection Boiling of Water," ASME Trans., 70, 695-702, 1948.

4.4-5 C. J. Baroczy, "A Systematic Correlation for Two-Phase Pressure Drop," Heat Transfer Conference (Los Angeles), AICLE, Preprint No. 37, 1966.

4.4-6 N. Zuber and J. A. Findlay, "Average Volumetric Concentration in Two-Phase Flow Systems," Transactions of the ASME Journal of Heat Transfer, November 1965.

4.4-7 USAEC, W. H. Jens and P. A. Lottes, "Analysis of Heat Transfer, Burnout, Pressure Drop and Density Data for High Pressure Water," USAEC Report- 4627, 1972.

4.4-8 General Electric Company, "General Electric BWR Thermal Analysis Basis (GETAB): Data Correlation and Design Application," NEDO-10958-A, January 1977.

4.4-9 GE Nuclear Energy, "TRACG Application for Anticipated Operational Occurrences Transient Analysis," NEDO-32906-A, Class I (non-proprietary), June 2003.

Table 4.4-1a

Typical Thermal–Hydraulic Design Characteristics of the Reactor Core (SI Units)

General Operating Conditions	BWR/6	ABWR	ESBWR
Reference design thermal output (MWt)	3579	3926	4500
Power level for engineered safety features (MWt)	3730	4005	4590
Steam flow rate, at 420°F final feedwater temperature (kg/s)	1940	2122	2433
Core coolant flow rate (kg/s)	13104	14502	9034-10584
Feedwater flow rate (kg/s)	1936	2118	2451
System pressure, nominal in steam dome (kPa)	7171	7171	7171
System pressure, nominal core design (kPa)	7274	7274	7240
Coolant saturation temperature at core design pressure (°C)	288	288	288
Average power density (kW/L)	54.1	50.6	54.3
Core total heat transfer area (m2)	6810	7727	9976
Core inlet enthalpy (kJ/kg)	1227	1227	1183-1197
Core inlet temperature (°C)	278	278	270-272
Core maximum exit voids within assemblies (%)	79.0	75.1	91.6
Core average void fraction, active coolant	0.414	0.408	0.320
Active coolant flow area per assembly (m^2)	0.0098	0.0101	0.0093
Core average inlet velocity (m/s)	2.13	1.96	1.12
Maximum inlet velocity (m/s)	2.60	26.7	1.15
Total core pressure drop (kPa)	182.0	168.2	70.0
Core support plate pressure drop (kPa)	151.7	137.9	41.3
Average orifice pressure drop, central region (kPa)	39.4	60.3	20.3
Average orifice pressure drop, peripheral region (kPa)	129	122	37.1
Maximum channel pressure loading (kPa)	106	75.2	24.4
Average-power assembly channel pressure loading (bottom) (kPa)	97.2	65.5	21.5
Shroud support ring and lower shroud pressure loading (kPa)	177	165	7.4
Upper shroud pressure loading (kPa)	25.5	24.1	17.4

Table 4.4-1b

Typical Thermal–Hydraulic Design Characteristics of the Reactor Core (English Units)

General Operating Conditions	BWR/6	ABWR	ESBWR
Reference design thermal output (MWt)	3579	3926	4500
Power level for engineered safety features (MWt)	3730	4005	4590
Steam flow rate, at 420°F final feedwater temperature (Mlb/hr)	15.40	16.84	19.31
Core coolant flow rate (Mlb/hr)	104.0	115.1	71.7-84.0
Feedwater flow rate (Mlb/hr)	15.4	16.8	19.5
System pressure, nominal in steam dome (psia)	1040	1040	1040
System pressure, nominal core design (psia)	1055	1055	1050
Coolant saturation temperature at core design pressure (°F)	551	551	550.6
Average power density (kW/L)	54.1	50.6	54.3
Core total heat transfer area (ft2)	73,303	83,176	107,376
Core inlet enthalpy (Btu/lb)	527.7	527.6	508.7-514.7
Core inlet temperature (°F)	533	533	517.5-522.4
Core maximum exit voids within assemblies (%)	79.0	75.1	91.6
Core average void fraction, active coolant	0.41	0.41	0.32
Active coolant flow area per assembly (in.^{2})	15.2	15.7	14.4
Core average inlet velocity (ft/sec)	7.0	6.4	3.7
Maximum inlet velocity (ft/sec)	8.5	7.5	3.8
Total core pressure drop (psi)	26.4	24.4	10.2
Core support plate pressure drop (psi)	22	20	6.0
Average orifice pressure drop, central region (psi)	5.7	8.8	2.9
Average orifice pressure drop, peripheral region (psi)	18.7	17.7	5.4
Maximum channel pressure loading (psi)	15.40	10.9	3.5
Average-power assembly channel pressure loading (bottom) (psi)	14.1	9.5	3.1
Shroud support ring and lower shroud pressure loading	25.7	23.9	1.1
Upper shroud pressure loading (psi)	3.7	3.5	2.5

Table 4.4-2a

Void Distribution for Analyzed Core - Average Channel

Core Average Value = 0.32

Maximum Core Exit Value = 0.92

Active Fuel Length = 3.048 m / 120.00 inches

Node	Average Node Value	Node	Average Node Value
1 (Bottom of Core)	0.00	19	0.40
2	0.00	20	0.49
3	0.00	21	0.57
4	0.00	22	0.63
5	0.00	23	0.68
6	0.00	24	0.71
7	0.01	25	0.73
8	0.02	26	0.74
9	0.04	27	0.75
10	0.07	28	0.77
11	0.10	29	0.79
12	0.12	30	0.80
13	0.15	31	0.82
14	0.18	32	0.83
15	0.21	33	0.83
16	0.23	34	0.83
17	0.26	35 (Top of Core)	0.83
18	0.29		

Table 4.4-2b

Void Distribution for Analyzed Core - Hot Channel

Core Average Value = 0.32
Maximum Core Exit Value = 0.92
Active Fuel Length = 3.048 m / 120.00 inches

Node	Average Node Value	Node	Average Node Value
1 (Bottom of Core)	0.00	19	0.59
2	0.00	20	0.67
3	0.00	21	0.72
4	0.00	22	0.74
5	0.00	23	0.75
6	0.02	24	0.78
7	0.04	25	0.81
8	0.07	26	0.84
9	0.11	27	0.86
10	0.15	28	0.88
11	0.19	29	0.89
12	0.23	30	0.90
13	0.27	31	0.91
14	0.31	32	0.92
15	0.35	33	0.91
16	0.39	34	0.92
17	0.43	35 (Top of Core)	0.92
18	0.46		

Table 4.4-3a

Flow Quality Distribution for Analyzed Core - Average Channel

Core Average Value = 0.10
Maximum Core Exit Value = 0.44
Active Fuel Length = 3.048 m / 120.00 inches

Node	Average Node Value	Node	Average Node Value
1 (Bottom of Core)	0.0	19	0.05
2	0.0	20	0.07
3	0.0	21	0.09
4	0.0	22	0.11
5	0.00	23	0.13
6	0.00	24	0.16
7	0.00	25	0.18
8	0.00	26	0.20
9	0.00	27	0.22
10	0.00	28	0.23
11	0.01	29	0.25
12	0.01	30	0.27
13	0.01	31	0.28
14	0.01	32	0.29
15	0.02	33	0.29
16	0.02	34	0.29
17	0.02	35 (Top of Core)	0.29
18	0.03		

Table 4.4-3b

Flow Quality Distribution for Analyzed Core - Hot Channel

Core Average Value = 0.10

Maximum Core Exit Value = 0.44

Active Fuel Length = 3.048 m / 120.00 inches

Node	Average Node Value	Node	Average Node Value
1 (Bottom of Core)	0.00	19	0.10
2	0.00	20	0.13
3	0.00	21	0.16
4	0.00	22	0.20
5	0.00	23	0.23
6	0.00	24	0.26
7	0.00	25	0.29
8	0.00	26	0.32
9	0.01	27	0.35
10	0.01	28	0.37
11	0.01	29	0.40
12	0.02	30	0.42
13	0.02	31	0.44
14	0.03	32	0.45
15	0.04	33	0.44
16	0.05	34	0.44
17	0.05	35 (Top of Core)	0.44
18	0.06		

Table 4.4-4a

Axial Power Distribution Used to Generate Void and Quality for Analyzed Core

- Average Channel

Node	Axial Power Factor	Node	Axial Power Factor
1 (Bottom of Core)	0.18	17	0.43
2	0.18	18	0.42
3	0.18	19	0.41
4	0.30	20	0.40
5	0.33	21	0.39
6	0.33	22	0.39
7	0.37	23	0.39
8	0.40	24	0.38
9	0.40	25	0.35
10	0.42	26	0.33
11	0.43	27	0.31
12	0.43	28	0.29
13	0.44	29	0.25
14	0.44	30	0.20
15	0.44	31	0.14
16	0.44	32 (Top of Core)	0.07

Table 4.4-4b

Axial Power Distribution Used to Generate Void and Quality for Analyzed Core

- Hot Channel

Node	Axial Power Factor	Node	Axial Power Factor
1 (Bottom of Core)	0.17	17	0.45
2	0.17	18	0.43
3	0.17	19	0.42
4	0.30	20	0.41
5	0.33	21	0.40
6	0.33	22	0.39
7	0.38	23	0.38
8	0.42	24	0.37
9	0.42	25	0.34
10	0.44	26	0.32
11	0.46	27	0.30
12	0.46	28	0.27
13	0.46	29	0.23
14	0.46	30	0.18
15	0.46	31	0.13
16	0.46	32 (Top of Core)	0.07

Table 4.4-5

ESBWR Reactor Coolant System Geometric Data

	Flow Path Length (m)	**Height and Liquid Level (m)**	**Elevation of Bottom of Volume (m³)**	**Average Flow Area (m²)**
Lower Plenum	4.13 (Axial)) 1.78 (Radial)	4.13/4.13	0.000	16.83
Core	3.79	3.77/2-Phase	4.13	20.22
Chimney	6.61	6.61/2-Phase	7.90	29.27
Upper Plenum	2.75	2.75/2-Phase	14.51	29.53
Dome	1.78 (Radial) 2.79 (Axial)	2.79/Steam	24.77	28.67
Downcomer	14.53	14.53/14.53	2.74	8.40

4.5 REACTOR MATERIALS

4.5.1 Control Rod Drive System Structural Materials

4.5.1.1 Material Specifications

Materials

The metallic structural components of the control rod drive (CRD) mechanism are made from four types of materials: 300 series stainless steel, Nickel-Chrome-Iron alloy X-750, XM-19 and 17-4 PH materials. The only primary pressure boundary components are the lower housing of the spool piece assembly, and flange of the Outer tube assembly. These components are made with 300 series stainless steel materials in accordance with the ASME Code, Section III.

The properties of the non-primary pressure retaining materials selected for the CRD mechanism are equivalent to those given in Parts A, B and D of Section II of the ASME Code, or are included in Regulatory Guide 1.85. Cold worked 300 series austenitic stainless steels are not used except that minor forming and straightening are controlled by limiting the material hardness, bend radius, or the amount of strain induced by a process.

Special Materials

The bayonet coupling, latch and latch spring, and separation spring are fabricated from Alloy X-750 in the annealed condition, and aged 20 hours at 704 degrees Celsius (1300 degrees Fahrenheit). The ball spindle and ball nut are 17-4 PH in condition H-1075 [aged 4 hours at 580 degrees Celsius (1075 degrees Fahrenheit)]. These are widely used materials, whose properties are well known. The parts are readily accessible for inspection and replaceable if necessary.

All materials for use in this system are selected for their compatibility with the reactor coolant as described in Articles NB-2160 and NB-3120 of the ASME Code.

XM-19 is used for the bayonet coupling on the buffer assembly, the hollow piston tube, and the outer tube. This material has been successfully used for many years in similar drive mechanisms. Extensive laboratory tests have demonstrated that XM-19 is a suitable material and that it is resistant to stress corrosion in a BWR environment.

No austenitic stainless steels strengthened by cold working are employed in the CRD system. For incidental cold working introduced during fabrication and installation, special controls are used to limit the induced strain and hardness, and the bend radii are kept above a minimum value.

4.5.1.2 Austenitic Stainless Steel Components

4.5.1.2.1 Processes, Inspections and Tests

All austenitic stainless steels are used in the solution heat-treated condition. In all welded components that are exposed to service temperature exceeding 93°C, the carbon content is limited not to exceed 0.020%. On qualification, there is a special process employed which subjects selected 300 Series stainless steel components to temperatures in the sensitization range. The drive shaft and buffer sleeve are examples of hard surfaced parts with Colmonoy and Stellite (or their equivalent). Colmonoy and Stellite (or its equivalent) hard surfaced components have

performed successfully for many years in drive mechanisms. It is normal practice to remove some CRDs at each refueling outage. At this time, the CRD bolting and hard-surfaced parts are accessible for visual examination. This inspection program is adequate to detect any incipient defects before they could become serious enough to cause operating problems (see Subsection 4.5.3.1 for COL license information). The CRD penetration and bolting are included in the reactor coolant pressure boundary inservice inspection program (Subsection 5.2.4). The degree of conformance to Regulatory Guide 1.44 is presented in Subsection 4.5.2.4.

4.5.1.2.2 Control of Delta Ferrite Content

Discussion of this subject and the degree of conformance to Regulatory Guide 1.31 is presented in Subsection 4.5.2.4.

4.5.1.3 Other Materials

Stellite 3/Haynes 25 are used for rollers/pins at latch (outside), and Haynes 25 for the latch joint pin. A Stellite 6 equivalent is used in the guide shaft at the top of the ball spindle. Stellite 12 is used for the bushing at the top of the ball spindle and the bushing on the drive shaft. Stellite Star J-metal is used for the ball check valve.

Non-cobalt hard alloys are used in guide rollers and guide pins. These components are located above and below the labyrinth seal, on the stop piston, ball screw stationary guide, piston head and ball nut.

4.5.1.4 Cleaning and Cleanliness Control

All the CRD parts are fabricated under a process specification that limits contaminants in cutting, grinding and tapping coolants and lubricants. It also restricts all other processing materials (marking inks, tape, etc.) to those that are completely removable by the applied cleaning process. All contaminants are then required to be removed by the appropriate cleaning process prior to any of the following:

- Any processing which increases part temperature above 93°C
- Assembly which results in decrease of accessibility for cleaning
- Release of parts for shipment

The specification for packaging and shipping the control rod drive provides the following:

The CRD is rinsed in hot de-ionized water and dried in preparation for shipment. The ends of the drive are then covered with a vapor-tight barrier with desiccant. Packaging is designed to protect the drive and prevent damage to the vapor barrier. Audits have indicated satisfactory protection.

Semiannual examination of 10% of the units humidity indicators is performed to verify that the units are dry and in satisfactory condition. The position indicator probes are not subject to this inspection.

Site or warehouse storage specifications require inside heated storage comparable to Level B of NQA-1, Part 2.2.

The degree of surface cleanliness obtained by these procedures meets the requirements of Regulatory Guide 1.37.

4.5.2 Reactor Internal Materials

4.5.2.1 Material Specifications

Reactor internal material specifications are provided in Table 4.5-1. All core support structures are fabricated from ASME specified materials, and designed in accordance with requirements of ASME Code Section III, Subsection NG. The other reactor internals are non-coded, and they may be fabricated from ASTM or ASME specification materials or other equivalent specifications.

4.5.2.2 Controls on Welding

Core support structures are fabricated in accordance with requirements of ASME Code Section III, Subsection NG-4000, and the examination and acceptance criteria shown in NG-5000. The internals, other than the core support structures meet the requirements of the industry standards, e.g., ASME or AWS, as applicable. ASME B&PV Code Section IX qualification requirements are followed in fabrication of core support structures. All welds are made with controlled weld heat input.

4.5.2.3 Non-Destructive Examination of Wrought Seamless Tubular Products

The stainless steel CRD housings (CRDHs), which are partially core support structures (inside the reactor vessel), serve as the reactor coolant boundary outside the reactor vessel. The CRD housing material is supplied in accordance with ASME Code Section III Class 1 requirements. The CRDHs are examined and hydrostatically tested to the ASME Code Section III Class 1 requirements as well as Class CS requirements.

The peripheral fuel supports are supplied in accordance with ASME Section III, Class CS requirements. The material is procured and examined by ultrasonic methods according to Paragraph NG-2540.

Wrought seamless tubular products for other internals are supplied in accordance with the applicable ASTM or ASME material specifications. These specifications require a hydrostatic test on each length of tubing or pipe.

4.5.2.4 Fabrication and Processing of Austenitic Stainless Steel—Regulatory Guide Conformance

Significantly cold-worked stainless steels are not used in the reactor internals except for vanes in the steam dryers. Applying limits on hardness controls cold work, bend radii and surface finish on ground surfaces. Furnace sensitized material are not allowed. Electroslag welding is not applied for structural welds. The delta ferrite content for weld materials used in welding austenitic stainless steel assemblies is verified on undiluted weld deposits for each heat or lot of filler metal and electrodes. The delta ferrite content is defined for weld materials as 5.0 Ferrite Number (FN) minimum, 8.0FN average and 20FN maximum. This ferrite content is considered adequate to prevent any micro-fissuring (Hot Cracking) in austenitic stainless steel welds. This procedure complies with the requirements of Regulatory Guide 1.31.

The limitation placed upon the delta ferrite in austenitic stainless steel castings is 8% minimum and a maximum value of 20%. The maximum limit is used for those castings designed for a 60-year life such as the fuel support pieces, in order to limit the effects of thermal aging degradation.

Proper solution annealing of the 300 series austenitic stainless steel is verified by testing per ASTM-A262, "Recommended Practices for Detecting Susceptibility to Intergranular Attack in Stainless Steels." Welding of austenitic stainless steel parts is performed in accordance with Section IX (Welding and Brazing Qualification) and Section II Part C (Welding Rod Electrode and Filler Metals) of the ASME B&PV Code. Welded austenitic stainless steel assemblies require solution annealing to minimize the possibility of the sensitizing. However, welded assemblies are dispensed from this requirement when the assemblies are of material of low carbon content (less than 0.020%). These controls are employed in order to comply with the intent of Regulatory Guide 1.44.

Careful control of all cleaning materials and process materials that contact stainless steel during manufacture and construction prevent exposure to contaminants. Any inadvertent surface contamination is removed to avoid potential detrimental effects.

Special care is exercised to insure removal of surface contaminants prior to any heating operation. Water quality for rinsing, flushing, and testing is controlled and monitored.

The degree of cleanliness obtained by these procedures meets the requirements of Regulatory Guide 1.37.

4.5.2.5 Other Materials

Hardenable martensitic stainless steel and precipitation hardening stainless steels are not used in the reactor internals.

Materials, other than Type-300 stainless steel, employed in reactor internals are:

- Type or Grade XM-19 stainless steel

- Niobium modified Alloy 600 per ASME Code Case No. N-580-1

- N07750 (Alloy X-750) or equivalent

All Niobium modified Alloy 600 material is used in the solution annealed condition.

Alloy X-750 components are fabricated in the annealed and aged condition. Where maximum resistance to stress corrosion is required, the material is used in the high temperature (1093°C) annealed plus single aged condition.

Hard chromium plating surface is applied to austenitic stainless steel couplings.

All materials used for reactor internals shall be selected for their compatibility with the reactor coolant as shown in ASME Code Section III, NG-2160 and NG-3120. The fabrication and cleaning controls preclude contamination of nickel-based alloys by chloride ions, fluoride ions, sulfur, or lead.

All materials referenced in this subsection have been successfully used for many years in BWR applications.

4.5.3 COL Information

4.5.3.1 CRD Inspection Program

The COL applicant shall provide a CRD inspection program that shall include provisions to detect incipient defects of hard-surfaced parts.

4.5.4 References

None

Table 4.5-1

Reactor Internals Material Specifications

Materials Used for the Core Support Structure:

- Shroud Support—Niobium modified Nickel-Chromium-Iron-Alloy 600 per ASME Code Case No. N-580-1

- Shroud, Core Plate, and Top Guide—ASME material of Type or Grade 304 / 304L / 316 / 316L

- Peripheral Fuel Supports—ASME material of Type or Grade 304 / 304L / 316 / 316L

- Core Plate and Top Guide Studs, Nuts, and Sleeves—ASME material of Type or Grade 304 / 304L / 316 / 316L, and XM-19

- Control Rod Drive Housing—ASME material of Type or Grade 304 / 304L / 316 / 316L

- Control Rod Guide Tube— ASME material of Type or Grade 304 / 304L / 316 / 316L, and XM-19

- Orificed Fuel Support— ASME material Grade CF3 / CF3M

Materials Employed in Chimney, Chimney Partitions, Chimney Head and Separator Assembly and Steam Dryer Assembly:

- All materials are 304/304L or 316/316L stainless steel in various product forms except castings and some Steam Dryer components. Steam Dryer seismic blocks are Type XM-19.

  − Plate, Sheet—ASTM or ASME Type 304/304L or 316/316L

  − Forgings—ASTM or ASME Grade 304/304L or 316/316L

  − Bars—ASTM or ASME Type 304/304L or 316/316L

  − Pipe—ASTM or ASME Grade TP 304/304L or TP 316/316L

  − Tube—ASTM or ASME Grade TP 304/304L or TP 316/316L

  − Castings—ASTM or ASME Grade CF3/CF3M

4.6 FUNCTIONAL DESIGN OF REACTIVITY CONTROL SYSTEM

The Reactivity Control System consists of:

- Control rods and Control Rod Drive (CRD) system;

- Supplementary reactivity control in the form of gadolinia-urania fuel rods (Section 4.2); and

- The Standby Liquid Control System (Subsection 9.3.5).

Conformance of these reactivity control systems to General Design Criteria (GDC) 23, 25, 26, 27, 28 and 29 is addressed in Section 3.1.

4.6.1 Information for Control Rod Drive System

4.6.1.1 Design Bases

4.6.1.1.1 Safety (10 CFR 50.2) Design Bases

The CRD system meets the following safety design bases:

- The design shall provide for rapid control rod insertion (scram) so that no fuel damage results from any Anticipated Operational Occurrence (Chapter 15).

- The design shall include positioning devices, each of which individually supports and positions a control rod.

- Each positioning device shall be capable of holding the control rod in position and preventing it from inadvertently withdrawing outward during any non-accident, accident, post-accident and seismic condition.

- Each positioning device shall be capable of detecting the separation of the control rod from the drive mechanism to prevent a rod drop accident.

- Each positioning device shall provide a means to prevent or limit the rate of control rod ejection from the core due to a break in the drive mechanism pressure boundary. This is to prevent fuel damage resulting from rapid insertion of reactivity.

4.6.1.1.2 Power Generation (Non-safety) Design Basis

The CRD system design meets the following power generation design bases:

- The design shall provide for controlling changes in core reactivity by positioning neutron-absorbing control rods within the core.

- The design shall provide for movement and positioning of control rods in increments to enable optimized power control and core power shaping.

- The design shall provide for the supply of high-pressure makeup water to the reactor when the normal makeup supply system (feedwater) is unable to maintain water level.

4.6.1.2 Description

The CRD system is composed of three major elements:

- Electro-hydraulic fine motion control rod drive (FMCRD) mechanisms;

- Hydraulic control units (HCU); and

- Control rod drive hydraulic subsystem (CRDHS).

The FMCRDs provide electric-motor-driven positioning for normal insertion and withdrawal of the control rods and hydraulic-powered rapid insertion (scram) of control rods during abnormal operating conditions.

The hydraulic power required for scram is provided by high-pressure water stored in the individual HCUs. Each HCU contains a nitrogen-water accumulator charged to high pressure and the necessary valves and components to scram two FMCRDs. Additionally, during normal operation, the HCUs provide a flow path for purge water to the associated FMCRDs.

The CRDHS supplies clean, demineralized water that is regulated and distributed to provide charging of the HCU scram accumulators and purge water flow to the FMCRDs during normal operation. The CRDHS is also the source of pressurized water for purging the Reactor Water Cleanup/Shutdown Cooling (RWCU/SDC) system pumps and the Nuclear Boiler System (NBS) reactor water level reference leg instrument lines. Additionally, the CRDHS provides high pressure makeup water to the reactor during events in which the feedwater system is unable to maintain reactor water level. This makeup water is supplied to the reactor via a bypass line off the CRD pump discharge header that connects to the feedwater inlet piping via the RWCU/SDC return piping.

The CRD system performs the following functions:

- Controls changes in core reactivity by positioning neutron-absorbing control rods within the core in response to control signals from the Rod Control and Information System (RC&IS).

- Provides movement and positioning of control rods in increments to enable optimized power control and core power shape in response to control signals from the RC&IS.

- Provides the ability to position large groups of rods simultaneously in response to control signals from the RC&IS.

- Provides rapid control rod insertion (scram) in response to manual or automatic signals from the Reactor Protection System (RPS) so that no fuel damage results from any plant anticipated operational occurrence (AOO).

- In conjunction with the RC&IS, provides automatic electric motor-driven insertion of the control rods simultaneously with hydraulic scram initiation. This provides an additional, diverse means of fully inserting a control rod.

- Supplies rod status and rod position data for rod pattern control, performance monitoring, operator display and scram time testing by the RC&IS.

- In conjunction with the RC&IS, prevents undesirable rod pattern or rod motions by imposing rod motion blocks in order to protect the fuel.

- In conjunction with the RC&IS, prevents the rod drop accident by detecting rod separation and imposing rod motion block.

- Provides rapid control rod insertion (scram) in response to signals from the Diverse Protection System (DPS). Also in response to signals from the DPS, provides alternate rod insertion (ARI), an alternate means of actuating hydraulic scram, should an anticipated transient without scram (ATWS) occur.

- In conjunction with the RC&IS, provides for selected control rod run-in (SCRRI).

- Prevents rod ejection from the core due to a break in the drive mechanism pressure boundary or a failure of the attached scram line by means of a passive brake mechanism for the FMCRD motor and a scram line inlet check valve.

- Supplies high-pressure makeup water to the reactor when the normal makeup supply system (feedwater) is unable to prevent reactor water level from falling below the normal water level range.

- Supplies purge water for the RWCU/SDC System pumps.

- Provides a continuous flow of water to the NBS to keep the reactor water level reference leg instrument lines filled.

The design bases and further discussion of both the RC&IS and RPS, and their control interfaces with the CRD system, are presented in Chapter 7.

4.6.1.2.1 Fine Motion Control Rod Drive Mechanism

The FMCRD used for positioning the control rod in the reactor core is a mechanical/hydraulic actuated mechanism (Figures 4.6-1 and 4.6-2). An electric motor-driven ball-nut and ball screw assembly is capable of positioning the drive at a minimum of 36.5 mm (1.44 in.) increments. Hydraulic pressure is used for scrams. The FMCRD penetrates the bottom head of the reactor pressure vessel. The FMCRD does not interfere with refueling and is operative even when the head is removed from the reactor vessel.

The fine motion capability is achieved with a ball-nut and ball screw arrangement driven by an electric motor. The ball-nut is keyed to the guide tube (roller key) to prevent its rotation and traverses axially as the ball screw rotates. A hollow piston rests on the ball-nut, and upward motion of the ball-nut drives this piston and the control rod into the core. The weight of the control rod keeps the hollow piston and ball-nut in contact during withdrawal.

A single HCU powers the scram action of two FMCRDs. Upon scram valve initiation, high pressure nitrogen from the HCU raises the piston within the accumulator forcing water through the scram piping. This water is directed to each FMCRD connected to the HCU. Inside each FMCRD, high-pressure water lifts the hollow piston off the ball-nut and drives the control rod into the core. A spring washer buffer assembly stops the hollow piston at the end of its stroke. Departure from the ball-nut releases spring-loaded latches in the hollow piston that engage slots in the guide tube. These latches support the control rod and hollow piston in the inserted position. The control rod cannot be withdrawn until the ball-nut is driven up and engaged with the hollow piston. Stationary fingers on the ball-nut then cam the latches out of the slots and hold them in the retracted position. A scram action is complete when every FMCRD has reached its fully inserted position.

The use of the FMCRD mechanisms in the CRD system provides several features that enhance both the system reliability and plant operations. Some of these features are listed and discussed briefly as follows:

Diverse Means of Rod Insertion — The FMCRDs can be inserted either hydraulically or electrically. In response to a scram signal, the FMCRD is inserted hydraulically via the stored energy in the scram accumulators. A signal is also given simultaneously to insert the FMCRD electrically via its motor drive. This diversity provides a high degree of assurance of rod insertion on demand.

Absence of FMCRD Piston Seals — The FMCRD pistons have no seals and, thus, do not require maintenance.

FMCRD Discharge — The water that scrams the control rod discharges into the reactor vessel and does not require a scram discharge volume, thus eliminating a potential source for common mode scram failure.

Plant Maneuverability — The fine motion capability of the FMCRD allows rod pattern optimization in response to fuel burnup or load-following demands.

Plant Automation — The relatively simple logic of the FMCRD permits plant automation. This feature is utilized for automatic reactor startup and shutdown and for automatic load following.

Reactor Startup Time — The FMCRDs can be moved in large groups. Movements of large groups of control rods (called gangs) are utilized to reduce the time for reactor startup.

Rod Drop Accident Prevention — The control rod separation detection feature of the FMCRD virtually eliminates the possibility of a rod drop accident by preventing rod withdrawal when control rod separation is detected. Additionally, movement of rods in large groups during reactor startup greatly reduces the maximum relative rod worth to levels lower than current rod pattern controls. Rod pattern controls provide verification of proper automatic rod movements and to mitigate the consequences of a rod withdrawal error.

The drives are readily accessible for inspection and servicing. The bottom location makes maximum utilization of the water in the reactor as a neutron shield and gives the least possible neutron exposure to the drive components. Using water from the condensate treatment system, and/or condensate storage tanks as the operating fluid eliminates the need for special hydraulic fluid.

4.6.1.2.2 FMCRD Components

Figure 4.6-1 provides a simplified schematic of the FMCRD operating principles. Figure 4.6-2 illustrates the drive in more detail.

The basic elements of the FMCRD are as follows:

- Components of the FMCRD required for electrical rod positioning or fine motion control (including the motor, brake release, associated connector, ball screw shaft, ball-nut and hollow piston).

- Components of the FMCRD required for hydraulic scram (including hollow piston and buffer).

- Components of the FMCRD required for pressure integrity (including the outer tube, middle flange, installation bolts and spool piece).

- Rod position indication (position signal detectors).

- Reed position switches for scram surveillance.

- Control rod separation detection devices (dual Class 1E CRD separation switches).

- Bayonet coupling between the hollow piston and control rod.

- Brake mechanism to prevent rod ejection in the event of a break in the FMCRD primary pressure boundary and ball check valve to prevent rod ejection in the event of a failure of the scram insert line.

- Integral internal blowout support (to prevent CRD blowout).

- Magnetic coupling.

These features and functions of the FMCRD are described below.

Components for Fine Motion Control

The fine motion capability is achieved with a ball-nut and ball screw arrangement driven by an electric motor. The ball-nut is keyed to the guide tube (roller key) to prevent its rotation as it traverses axially as the ball screw rotates. A hollow piston rests on the ball-nut and upward motion of the ball-nut drives the control rod into the core. The weight of the control rod keeps the hollow piston and ball-nut in contact during withdrawal.

The drive motor, located outside the pressure boundary, is magnetically coupled to the drive shaft located inside the pressure boundary. A splined coupling connects the drive shaft to the ball screw. The lower half of the splined coupling is keyed to the drive shaft and the upper half keyed to the ball screw. The tapered end of the drive shaft fits into a conical seat on the end of the ball screw to keep the two axially aligned. A drive shaft thrust bearing carries the entire weight of the control rod and drive internals.

The axially moving parts are centered and guided by radial rollers. The ball-nut and bottom of the hollow piston include radial rollers bearing against the guide tube. Radially adjustable rollers at both ends of the labyrinth seal keep the hollow piston precisely centered in this region.

A stationary guide supports the top of the ball screw against the inside of the hollow piston. A hardened bushing provides the circumferential bearing between the rotating ball screw and stationary guide. Rollers of the guide run in axial grooves in the hollow piston to prevent the guide from rotating with the ball screw.

Components for Scram

The scram action is initiated by the HCU. High pressure water lifts the hollow piston off the ball-nut and drives the control rod into the core. A spring washer buffer assembly stops the hollow piston at the end of its stroke. Departure from the ball-nut releases spring-loaded latches in the hollow piston that engage slots in the guide tube. These latches support the control rod in the inserted position.

The control rod cannot be withdrawn until the ball-nut is driven up and engaged with the hollow piston. Stationary fingers on the ball-nut cam the latches in the hollow piston out of the slots in

the guide tube and hold them in the retracted position when the ball-nut and hollow piston are re-engaged.

Re-engagement of the ball-nut with the hollow piston following scram is automatic. Simultaneous with the initiation of the hydraulic scram each FMCRD motor is signaled to start in order to cause movement of the ball-nut upward until it is in contact with the hollow piston. This action completes the rod full-in insertion and leaves the drives in a condition ready for restarting the reactor. With the latches in the hollow piston retracted, and the motor and brake de-energized, the control rods are kept fully inserted by the passive holding torque from the brake and the magnetic coupling between the motor and drive shaft.

The automatic run-in of the ball-nut using the electric motor drive following the hydraulic scram provides a diverse means of rod insertion as a backup to the accumulator scram.

FMCRD Pressure Boundary

The CRD housing (attached to the RPV) and the CRD middle flange and lower housing (spool piece) which enclose the lower part of the drive are a part of the reactor pressure boundary (Figure 4.6-1). The middle housing is attached to the CRD housing by four threaded bolts. The lower housing (spool piece) is, in turn, held to the middle housing and secured to the CRD housing by a separate set of eight main mounting bolts that become a part of the reactor pressure boundary. This arrangement permits removing the lower housing, drive shaft and seal assembly without disturbing the rest of the drive. Removing the lower housing transfers the weight of the driveline from the drive shaft to the seat in the middle housing. Both the ball screw and drive shaft are locked to prevent rotation while the two are separated.

The part of the drive inserted into the CRD housing is contained within the outer tube. The outer tube is the drive hydraulic scram pressure boundary, eliminating the need for designing the CRD housing for the scram pressure. The outer tube is welded to the middle flange at the bottom and is attached at the top with the CRD blowout support, which bears against the CRD housing. The blowout support and outer tube are attached by a slip type connection that accounts for any slight variation in length between the drive and the drive housing.

Purge water continually flows through the drive. The water enters through the ball check valve in the middle housing and flows around the hollow piston into the reactor. O-rings seal the lower housing. A labyrinth seal near the top of the drive restricts the flow into the reactor. During a scram, the labyrinth seals the high-pressure scram water from the reactor vessel without adversely affecting the movement of the hollow piston.

Rod Position Indication

Control rod position indication is provided by the FMCRDs to the control system by a position detection system, which consists of position detectors and position signal converters.

Each FMCRD provides two position detectors, one for each control system channel, in the form of signal detectors directly coupled to the motor shaft through gearing. The output signals from these detectors are analog. The analog signals are converted to digital signals by position signal converters. This configuration provides continuous detection of rod position during normal operation.

Scram Position Indication

Scram position indication is provided by a series of magnetic reed switches to allow for measurement of adequate drive performance during scram. The magnetic switches are located at intermediate intervals over 60% of the drive stroke. They are mounted in a position indicator probe exterior to the drive housing. A magnet in the hollow piston trips each reed switch, in turn, as it passes by.

As the bottom of the hollow piston contacts and enters the buffer, a magnet is lifted that operates a reed switch, indicating scram completion. This continuous full-in indicating switch is shown conceptually in Figure 4.6-3. It provides indication whenever the drive is at the full-in latched position or above.

Control Rod Separation Detection

Two redundant and separate Class 1E switches are provided to detect the separation of the hollow piston from the ball-nut. This means two sets of reed switches physically separated from one another with their cabling run through separate conduits. The separation switch is classified Class 1E, because its function detects a detached control rod and causes a rod block, thereby preventing a rod drop accident. Actuation of either switch also initiates an alarm in the control room.

The principle of operation of the control rod separation mechanism is illustrated in Figure 4.6-4. During normal operation, the weight of the control rod and hollow piston resting on the ball-nut causes the ball screw assembly to compress a spring on which the lower half of the splined coupling between the drive shaft and ball screw assembly rests (the lower half of the splined coupling is also known as the "weighing table"). When the hollow piston separates from the ball-nut, or when the control rod separates from the hollow piston, the spring is unloaded and pushes the weighing table and ball screw assembly upward. This action causes a magnet in the weighing table to operate the Class 1E reed switches located in probes outside the lower housing.

Bayonet Couplings

There are two bayonet couplings associated with the FMCRD. The first is at the FMCRD/control rod guide tube/housing interface as illustrated in Figure 4.6-1. This bayonet locks the FMCRD and the base of the control rod guide tube to the CRD housing and functions to retain the control rod guide tube during normal operation and dynamic loading events. The bayonet also holds the FMCRD against ejection in the event of a hypothetical failure of the CRD housing weld. The locating pin on the core plate that engages the flange of the control rod guide tube and the bolt pattern on the FMCRD/housing flange assure proper orientation between the control rod guide tube and the FMCRD to assure that the bayonet is properly engaged.

The second bayonet is located between the control rod and FMCRD as shown on Figure 4.6-5. The coupling spud at the top end of the FMCRD hollow piston engages and locks into a mating socket at the base of the control rod. The coupling requires a 45° rotation for engaging or disengaging. Once locked, the drive and rod form an integral unit that can only be unlocked manually by specific procedures before the components can be separated.

The FMCRD design allows the coupling integrity of this second bayonet to be checked by driving the ball nut down into an overtravel-out position. After the weighing spring has raised the ball screw assembly to the limit of its travel, further rotation of the ball screw in the withdraw

direction drives the ball-nut down away from the hollow piston (assuming the coupling is engaged). If the hollow piston is not properly coupled to the control rod, the hollow piston will remain in contact with the ball nut and move with it to the overtravel position. A reed switch at the overtravel position will detect this movement of the hollow piston.

FMCRD Brake and Ball Check Valve

The FMCRD design incorporates an electro-mechanical brake (Figure 4.6-6) keyed to the motor shaft. The brake is normally engaged by passive spring force when the FMCRD is stationary. It is disengaged for normal rod movements by signals from the RC&IS. Disengagement is caused by the energized magnetic force overcoming the spring load force. The braking torque of 49 N·m (minimum) and the magnetic coupling torque between the motor and the drive shaft are sufficient to prevent control rod ejection in the event of failure in the pressure retaining parts of the drive mechanism. The brake is designed so that its failure does not prevent the control rod from rapid insertion (scram).

The electromechanical brake is located between the motor and the position signal detectors. The stationary spring-loaded disk and coil assembly is contained within the brake mounting bolted to the bottom of the motor. The rotating disk is keyed to the motor shaft and synchro shaft.

The brake is classified as passive safety related because it performs its holding function when it is in its normally de-energized condition.

A ball check valve is located in the middle flange of the drive at the scram inlet port. The check valve is classified as safety related because it actuates to close the scram inlet port by reverse flow under system pressure, fluid flow and temperature conditions caused by a break of the scram line. This prevents the loss of pressure to the underside of the hollow piston and the generation of loads on the drive that could cause a rod ejection.

Integral Internal Blowout Support

An internal CRD blowout support replaces the support structure of beams, hanger rods, grids and support bars used in BWR/6 and product lines before that. The internal support concept is illustrated schematically in Figure 4.6-7. This system utilizes the CRD outer tube integral with the internal support to provide the anti-ejection support. The outer tube is locked at top via the internal support to the control rod guide tube (CRGT) base by a bayonet coupling, which is described above. The outer tube is bolted to the CRD housing flange via the middle flange welded to it at the bottom, as described above in a discussion on FMCRD pressure boundary.

The CRD blowout support is designed to prevent ejection of the CRD and the attached control rod considering failures of two types at the weld (Point A in Figure 4.6-7) between the CRD housing and the stub tube penetration of the RPV bottom head: (1) a failure through the housing along the fusion line just below the weld with the weld and the housing extension inside the vessel remaining intact, or (2) a failure of the weld itself with the entire housing remaining intact but without support at the penetration.

With a housing failure, the weight plus pressure load acting on the drive and housing would tend to eject the drive. In this event, the CRGT base remains supported by the intact housing extension inside the vessel and the CRD remains supported in turn by its positive lock to the CRGT base. Coolant leakage is restricted to the small annular area between the CRD outer tube and the inside of the CRD housing. In the event of total failure of the weld itself, with the entire

housing intact, the housing would tend to be driven downward by the total weight plus vessel pressure. However, after the interconnected assembly of the housing, CRD and CRGT moves down a short distance, the flange at the top of the CRGT contacts the core plate, stopping further movement of the assembly. Because the CRD is positively locked to the CRGT base, it cannot eject. In this case, the housing, which bears on top of the blowout support, is also prevented from leaving the penetration. Coolant leakage for this condition is restricted to the small annular area between the outside of CRD housing and the inside of the penetration stub tube.

An orderly shutdown would result if any of the two failures were to occur, because the restricted coolant leakage would be less than the supply from the normal make up systems. The components that provide the anti-ejection function are:

- internal CRD blowout support,

- CRD outer tube,

- entire CRD housing,

- CRGT, and

- core plate.

The materials of these components are specified to meet quality requirements consistent with that function.

If a total failure of all the flange bolts attaching the spool piece flange and also the middle flange with the CRD housing flange (Point B on Figure 4.6-7) were to occur, the drive would be prevented from moving downward by the middle flange seat provided for the ball screw adapter as part of the anti-rotation gear (see Subsection 4.6.2.3.3).

Magnetic Coupling

The magnetic coupling is located in the spool piece. It is employed to achieve seal-less, leak-free operation of the control rod drive mechanism. The magnetic coupling consists of an inner and an outer rotor. The inner rotor is located inside the spool piece pressure boundary. The outer rotor is located outside the spool piece pressure boundary. Each rotor has permanent magnets mounted on it. As a result, the inner and outer rotors are locked together by the magnetic forces acting through the pressure boundary and work as a synchronous coupling. The outer rotor is coupled with the motor unit and driven by the motor and the inner rotor follows the rotation of the outer rotor.

The magnetic coupling is designed so that its maximum coupling torque exceeds the maximum torque of the motor unit to prevent decoupling or slippage due to motor torque.

Materials of Construction

The materials of construction for the FMCRD are discussed in Subsection 4.5.1.

4.6.1.2.3 Hydraulic Control Units

Each hydraulic control unit (HCU) furnishes pressurized water for hydraulic scram, on signal from the RPS, to two drive units. Additionally, each HCU provides the capability to adjust purge flow to the two drives. A test port is provided on the HCU for connection to a portable test station to allow controlled venting of the scram insert line to test the FMCRD ball check

valve during plant shutdown. Operation of the electrical system that supplies scram signals to the HCU is described in Chapter 7.

The basic components of each HCU are described in the following paragraphs. The HCU configuration is shown on Figure 4.6-8.

The check valves shown inside the HCU boundary on Figure 4.6-8 have an active safety-related function to close under system pressure, fluid flow and temperature conditions during scram. This ensures that the water stored in the HCU accumulator is delivered to the FMCRDs to accomplish the scram function.

Scram Pilot Valve Assembly

The scram pilot valve assembly is operated from the RPS. The scram pilot valve assembly, with two solenoids, controls the scram inlet valve. The scram pilot valve assembly is solenoid-operated and is normally energized. Upon loss of electrical signal (such as the loss of external AC power) to the solenoids, the inlet port closes and the exhaust port opens. The pilot valve assembly (Figure 4.6-8) is designed so that the trip system signal must be removed from both solenoids before air pressure can be discharged from the scram valve operators. This prevents the inadvertent scram of both drives associated with a given HCU in the event of a failure of one of the pilot valve solenoids.

Scram Inlet Valve

The scram inlet valve opens to supply pressurized water to the bottom of the drive piston. This quick opening globe valve is operated by an internal spring and system pressure. It is closed by air pressure applied to the top of its diaphragm operator. A position indicator switch on this valve energizes a light in the control room as soon as the valve starts to open.

Scram Accumulator

The scram accumulator stores sufficient energy to fully insert two control rods at any reactor pressure. The accumulator is a hydraulic cylinder with a free-floating piston. The piston separates the water on top from the nitrogen below. A check valve in the accumulator charging line prevents loss of water pressure in the event that supply pressure is lost.

During normal plant operation, the accumulator piston is seated at the bottom of its cylinder. Loss of nitrogen decreases the nitrogen pressure, which actuates a pressure switch and sounds an alarm in the control room.

To ensure that the accumulator is always able to produce a scram, it is continuously monitored for water leakage. A float type level switch actuates an alarm if water leaks past the piston barrier and collects in the accumulator instrumentation block.

Purge Water Orifice and Makeup Valve

Each HCU has a restricting orifice in the purge water line to control the purge flow rate to the two associated FMCRDs. This orifice maintains the flow at a constant value while the drives are stationary. A bypass line containing a solenoid-operated valve is provided around this orifice. The valve is signaled to open and increase the purge water flow whenever either of the two associated FMCRDs is commanded to insert by the Rod Control and Information System (RC&IS). During FMCRD insertion cycles, the hollow piston moves upward, leaving an increased volume for water within the drive. Opening of the purge water makeup valve increases

the purge flow to offset this volumetric increase and precludes the backflow of reactor water into the drive, thereby preventing long-term drive contamination.

Test Connection for FMCRD Ball Check Valve Testing and Friction Testing

Contained within the HCU is a test port to allow connection of temporary test equipment for the conduct of FMCRD ball check valve testing and drive friction testing. This test port, which has a quick-connect type coupling, is located downstream of the restricting orifice and check valve in the purge water line.

Performance of FMCRD ball check valve testing is accomplished by attaching the check valve test fixture to the HCU test port. The test fixture exercises the check valve by generating a controlled backflow through the check valve housing, causing the valve to backseat. The backflow is contained within a controlled volume inside the test fixture.

During plant shutdown, the friction of each control rod and its drive mechanism is measured to confirm that there is no abnormal driveline resistance that would adversely affect drive operation. Friction testing is performed after FMCRD maintenance or fuel reshuffling. Connecting a portable friction test cart between the CRD hydraulic system and the HCU test port using flexible hoses performs this test. The test cart contains all the necessary hydraulic, electrical and pneumatic equipment, controls and instrumentation to apply hydraulic pressure to the bottom surface of the FMCRD hollow piston that is resting on the ball nut. When the pressure under the hollow piston is high enough to overcome both the combined hollow piston and control rod weight and the driveline friction, the hollow piston will separate from the ball nut and drift the control rod into the core. The pressure acting on the bottom surface of the hollow piston is a direct indication of the driveline friction and is measured and recorded while the piston is being inserted. The recorded pressure trace for each rod is then compared against a reference trace. Any fluctuation in the peak-to-peak reading that exceeds acceptable limits is considered abnormal and indicates further maintenance is required. Only one rod is tested at a time. Since one HCU drives two rods, the rod not under test is isolated. Discharge water during testing is directed back to the RPV via the FMCRD labyrinth seal.

4.6.1.2.4 Control Rod Drive Hydraulic Subsystem

The CRDHS supplies water under high pressure to charge the accumulators, purge the FMCRDs and Reactor Water Cleanup/Shutdown Cooling (RWCU/SDC) system pumps, provide makeup water to the Nuclear Boiler System (NBS) reactor water level reference leg instrument lines and provide makeup water to the reactor vessel following the loss of the normal makeup supply (feedwater). The CRDHS provides the required functions with the pumps, valves, filters, piping, instrumentation and controls shown on Figure 4.6-8. Duplicate components are included where necessary to assure continuous system operation if an inservice component should require maintenance. For system and component classification, see Section 3.2.

The CRDHS hydraulic requirements and components are described in the following paragraphs.

Hydraulic Requirements

The CRDHS process conditions are shown in Figure 4.6-9. The hydraulic requirements, identified by the function they perform, are:

- The required purge water to the drives is shown in Table 4.6-1.

- The approximate purge flow provided to the RWCU/SDC a pump is shown in Table 4.6-1. This flow is provided at approximately CRD pump discharge pressure. The RWCU/SDC system provides its own pressure breakdown equipment to satisfy its individual hydraulic requirements.

- The approximate purge flow provided to the NBS reference leg instrument lines are shown in Table 4.6-1. The purge flow maintains the RPV water level reference leg instrument lines filled to address the effects of noncondensible gases in the instrument lines to prevent erroneous reference information after a rapid RPV depressurization event.

- The approximate flow provided to the Process Sampling System (PSS) is shown in Table 4.6-1. The PSS monitors this flow for CRD water conductivity and dissolved oxygen level.

- The minimum flow supplied to the reactor in the high-pressure makeup mode of operation is shown in Table 4.6-1. This flow is based on a reactor gauge pressure less than or equal to the reference pressure shown in Table 4.6-1.

CRD Supply Pump

One supply pump pressurizes the system with water from the condensate treatment system and/or condensate storage tanks. One spare pump is provided for standby. A discharge check valve prevents backflow through the non-operating pump. A portion of the pump discharge flow is diverted through a minimum flow bypass line to the condensate storage tank. This flow is controlled by an orifice and is sufficient to prevent pump damage if the pump discharge is inadvertently closed.

Redundant filters in both the pump suction and discharge lines process the system water. A differential pressure indicator and control room alarm monitor each filter element as they collect foreign materials.

For the high-pressure makeup mode of operation, the CRDHS operates with both pumps running simultaneously. The standby pump is initiated automatically by low reactor water level so that the combined flow from both pumps can provide the required high-pressure makeup flow to the reactor vessel. The standby pump also starts automatically if loss of discharge header pressure is sensed during normal operation, indicating a failure of the operating pump. This prevents a scram due to low charging water header pressure from occurring as result of an inadvertent pump trip.

The pump suction filters are bypassed automatically during two-pump operation to assure that adequate NPSH is available for the pumps. Two bypass lines are provided around the suction filters, each line containing a normally closed motor-operated valve. These valves are signaled to open when the high-pressure makeup mode of operation is initiated.

Accumulator Charging Water Header

Accumulator charging pressure is established by pre-charging the nitrogen accumulator to a precisely controlled pressure at known temperature. During scram, the scram valves open and permit the stored energy in the accumulators to discharge into the drives. The resulting pressure decrease in the charging water header allows the CRD supply pump to "run out" (i.e., flow rate

to increase substantially) into the control rod drives via the charging water header. The flow element upstream of the charging water header senses high flow and provides a signal to the manual/auto flow control station which in turn closes the system flow control valve. This action effectively blocks the flow to the purge water header so that the runout flow is confined to the charging water header.

Pressure instrumentation is provided in the charging water header to monitor header performance. The pressure signal from this instrumentation is provided to both the RC&IS and RPS. If charging water header pressure degrades, the RC&IS initiates a rod block and alarm at a predetermined low-pressure setpoint. If pressure degrades even further, the RPS initiates a scram at a predetermined low-low pressure setpoint. This ensures the capability to scram and reactor shutdown before the HCU accumulator pressure can degrade to the level where scram performance is adversely affected following the loss of charging header pressure.

The charging water header contains a check valve and a bladder type accumulator. The accumulator is located downstream of the check valve in the vicinity of the low header pressure instrumentation. It is sized to maintain the header pressure downstream of the check valve above the scram setpoint until the standby CRD pump starts automatically, following a trip or failure of the operating CRD pump. Pressure instrumentation installed on the pump discharge header downstream of the CRD pump drive water filters monitors system pressure and generates the actuation signals for startup of the standby pump if the pressure drops below a predetermined value that indicates a failure of the operating pump.

An air-operated isolation valve is also provided in the charging water header. It closes automatically when the system is initiated into the high-pressure makeup mode of operation. It blocks the flow through the header to allow all CRDHS flow in this mode to be directed to the reactor via the feedwater system. The valve is designed to preferentially fail closed upon loss of control power or instrument air.

Purge Water Header

The purge water header is located downstream from the flow control valve. The flow control valve adjusts automatically to maintain constant flow to the FMCRDs as reactor vessel pressure changes. Because flow is constant, the differential pressure between the reactor vessel and CRDHS is maintained constant independent of reactor vessel pressure. A flow indicator in the control room monitors system flow. A differential pressure indicator is provided at a local panel to indicate the difference between reactor vessel pressure and purge water pressure.

An air-operated isolation valve is also provided in the purge water header. It closes automatically when the system is initiated into the high-pressure makeup mode of operation. It blocks the flow through the header to allow all CRDHS flow in this mode to be directed to the reactor via the feedwater system. The valve is designed to preferentially fail closed upon loss of control power or instrument air.

High Pressure Makeup Line

The CRDHS supplies high-pressure makeup water to the reactor vessel through piping connecting the discharge lines of the CRD pumps to the RWCU/SDC. The flow is then routed through RWCU/SDC piping to the feedwater system for delivery to the reactor via the feedwater sparger.

Each pump provides half the flow capacity for the high-pressure makeup mode of operation. Located downstream of each pump is a flow control station containing the flow instrumentation and control valve for regulating the pump flow during high-pressure makeup. The piping from the two flow control stations is then combined together into a single line to deliver the combined pump flow to the RWCU/SDC. This line contains a check valve and a normally open motor-operated isolation valve. The check valve is provided to prevent backflow from the RWCU/SDC system. The isolation valve is provided for system testing. During testing, it isolates the line and diverts the flow to the system test line.

System Test Line

A system test line is provided to allow testing of the high-pressure makeup mode during normal plant operation without injecting the relatively cold CRDHS water into the reactor. It connects with the high pressure makeup line at a point downstream of the two pump flow control stations and is routed back to the condensate storage tank (CST). The line contains a variable position valve, which is used to throttle the test flow so that the upstream pressure in the line can be varied to simulate operation over the full range of reactor pressure.

4.6.1.2.5 Control Rod Drive System Operation

The operating modes of the CRD system are described in this subsection.

Normal Operation

Normal operation is defined as those periods of time when no control rod drives are in motion. Under this condition, the CRD system provides charging pressure to the HCUs and supplies purge water to the control rod drives, the RWCU/SDC pumps and reactor water level reference leg instrument lines.

One of the two multi-stage centrifugal pumps supplies the system with water from the condensate and feedwater system and/or CST. The other pump is shutdown and on standby. A constant portion of the pump discharge is continuously bypassed back to the CST in order to maintain a minimum flow through the pump. This prevents overheating of the pump if the discharge line is blocked. The total pump flow during normal operation is the sum of the bypass flow, the FMCRD purge water flow through the flow control valve, the RWCU/SDC pump purge flow, the flow to the reactor water level reference leg instrument lines and the CRDHS water sample flow. The standby pump provides a full capacity backup capability to the operating pump. It starts automatically if failure of the operating pump is detected by pressure instrumentation located in the common discharge piping downstream of the drive water filters.

Redundant filters in both the pump suction and discharge lines process the system water. One suction filter and one drive water filter are normally in operation, while the backup filters are on standby and valved out of service. Differential pressure instrumentation and control room alarms monitor the filter elements as they collect foreign material.

The purge water header provides the purge water for each drive. The purge water flow control valve automatically regulates the purge water flow to the drive mechanisms. The purge water flow rate is indicated in the control room.

In order to maintain the ability to scram, the charging water header maintains the accumulators at a high pressure. The scram valves remain closed except during and after scram, so during

normal operation no flow passes through the charging water header. Pressure in the charging water header is monitored continuously. A significant degradation in the charging header pressure causes a low-pressure warning alarm and rod withdrawal block by the RC&IS. Further degradation, if occurring, causes a reactor scram by the RPS.

Pressure in the pump discharge header downstream of the drive water filters is also monitored continuously. Low pressure in this line is used to indicate that the operating pump has failed or tripped. If it should occur, automatic startup of the standby pump is initiated and the system is quickly re-pressurized. A bladder-type accumulator located in the charging water header maintains the pressure in the header above the scram setpoint during the time delay associated with startup of the standby pump. These features protect against a loss of charging water header pressure which may occur as a result of a malfunction of the operating pump, and which could cause the reactor to scram due to a low charging water header pressure.

Control Rod Insertion and Withdrawal

The FMCRD design provides the capability to move a control rod in fine steps. Normal control rod movement is under the control of the RC&IS. The RC&IS controls the input of actuation power to the FMCRD motor from the electrical power supply in order to complete a rod motion command. The FMCRD motor rotates a ball screw that, in turn, causes the vertical translation of a ball-nut on the ball screw. This motion is transferred to the control rod via a hollow piston that rests on the ball-nut. Thus, the piston with the control rod is raised or lowered, depending on the direction of rotation of the FMCRD motor and ball screw.

During a control rod insertion, opening the solenoid-operated purge water makeup valve within the associated HCU increases the purge water flow to the drive. The increased flow offsets the volumetric displacement within the drive as the hollow piston is inserted into the core and prevents reactor water from being drawn back into the drive.

Scram

Upon loss of electric power to both scram solenoid pilot valve (SSPV) coils, the scram valve in the associated HCU opens to apply the hydraulic insert forces to its respective FMCRDs using high pressure water stored within the precharged accumulator (the nitrogen-water accumulator having previously been pressurized with charging water from the CRDHS). Once the hydraulic force is applied, the hollow piston disengages from the ball-nut and inserts the control rod rapidly. The water displaced from the FMCRD is discharged into the reactor vessel. Indication that the scram has been successfully completed (all rods full-in position) is displayed to the operator.

Table 4.6-2 shows the scram performance provided by the CRD system at full power operation, in terms of the average maximum elapsed time to attain the listed scram position (percent insertion) after loss of signal to the scram solenoid pilot valves (time zero).

The start of motion is the time delay between loss of signal to the scram solenoid pilot valve and actuation of the 0% reed switch.

Simultaneous with the hydraulic scram, each FMCRD motor is started in order to cause electric-driven run-up of the ball-nut until it reengages with the hollow piston at the full-in position. This action is known as the scram follow function. It completes the rod full-in insertion and prepares the drives for subsequent withdrawal to restart the reactor.

After reset of the RPS logic, each scram valve re-closes and allows the CRDHS to recharge the accumulators.

Alternate Rod Insertion

The alternate rod insertion (ARI) function of the CRD system provides an alternate means for actuating hydraulic scram that is diverse and independent from the RPS. The signals to initiate the ARI are high reactor dome pressure or low reactor vessel water Level 2 or manual operator action. Following receipt of any of these signals, solenoid-operated valves on the scram air header actuate to depressurize the header, allowing the HCU scram valves to open. The FMCRDs then insert the control rods hydraulically in the same manner as the RPS initiated scram. The same signals that initiate ARI simultaneously actuate the FMCRD motors to insert the control rods electrically.

High Pressure Makeup

The high-pressure makeup mode of operation initiates on receipt of a low reactor water Level 2 signal. When this occurs, the following actions take place automatically:

- The CRD pump suction filter bypass valves open.

- The standby CRD pump is actuated. Both CRD pumps are operated in parallel in order to deliver the required makeup flow capacity to the reactor.

- The flow control valves in the high-pressure makeup lines open to regulate the makeup water flow rate to the reactor. The test valve in the high pressure makeup line to the RWCU/SDC System opens, if it is closed at the start of the event, and the test valve in the return line to the CST closes, if it is open at the start of the event. The pump minimum flow bypass isolation valve closes.

- The isolation valves in the purge water header and charging water header close so that all makeup flow is delivered to the reactor through the high-pressure makeup lines.

At high reactor water Level 8, the high-pressure makeup flow control valves close to stop flow to the reactor in order to prevent flooding of the main steam lines. The pump minimum flow bypass valve reopens and both pumps continue to operate in a low flow condition by directing their flow back to the CST through the pump minimum flow lines. Alternately, the operator may choose at this time to manually realign the system into its normal operation mode by shutting down one pump and reopening the charging water header and purge water header isolation valves so that HCU accumulator charging and FMCRD purge water flow can be reestablished. In either case, the system is reset for an automatic restart of high-pressure makeup if a subsequent Level 2 should occur.

During testing of this mode of operation, the high-pressure makeup line isolation valve is closed and pump flow is directed back to the CST through the test line. The backpressure in the line is varied by positioning of the throttle valve in the test line to simulate system operation over the full range of reactor pressure.

4.6.1.2.6 Instrumentation and Control

Instrumentation

The instrumentation for the CRD system includes the following:

- Differential pressure sensors monitor pressure drop across the pump suction filters and drive water filters. High filter differential pressure is alarmed in the control room.

- A pressure sensor is located in the inlet piping to each CRD pump to monitor the suction pressure. A low-pressure condition trips the associated pump and is alarmed in the control room.

- Two pressure sensors are located in the common pump discharge line downstream of the drive water filters to monitor system pressure. A low-pressure condition indicates a failure of the operating pump. A low-pressure signal from either sensor actuates the standby pump.

- Four safety-related pressure sensors are located in the HCU accumulator charging water header. The output signals from these sensors are provided to the RC&IS logic and RPS logic. A low-pressure condition from two-out-of-four sensors causes the RC&IS to generate an all-rod-withdrawal block. A low-low pressure condition causes the RPS to generate a reactor scram.

- A flow sensor is provided in the common pump discharge line downstream of the drive water filters and upstream of the charging water and purge water headers. The flow signal from this sensor provides the control input signal to the purge water flow control valves.

- Each of the two high-pressure makeup lines downstream of the CRD pumps contains a flow sensor. The flow control signal from these sensors provides the control input signals to the high-pressure makeup flow control valves.

- A pressure sensor is provided in the scram air header piping at a location downstream of the air header dump valves and ARI valves and upstream of the scram valves. Both high and low-pressure conditions in the header are alarmed in the control room.

- Status indication for the scram valve position is provided in the control room.

Controls and Interlocks

The controls and interlocks for the CRD system include the following:

- The high-pressure makeup mode of operation is initiated by a low reactor water Level 2 signal. On receipt of this signal, the following automatic actions occur:

  – The standby CRD pump is started. Both pumps operate in parallel to deliver the required makeup flow capacity to the reactor.

  – The two pump suction filter bypass valves are opened.

  – The charging water header isolation valve and purge water header isolation valve are closed.

  – The pump minimum flow bypass line isolation valve closes.

- The flow control valves in the high pressure makeup lines open to regulate the makeup water flow rate to the reactor.

- The test valve in the high-pressure makeup line to the RWCU/SDC system opens if it is closed at the start of the event and the test valve in the return line to the CST closes if it is open at the start of the event.

- The high-pressure makeup flow control valves close to stop flow to the reactor at high reactor water Level 8. The pump minimum flow bypass line isolation valve opens and both pumps continue to operate in a low flow condition by directing their flow back to the CST through the pump minimum flow lines. The control valves reopen and the pump minimum flow bypass isolation valve closes to restart high-pressure makeup flow if a subsequent Level 2 signal should occur.

- The standby CRD pump is started if a low system pressure condition occurs.

- The CRD pump trips upon receipt of a low suction pressure condition. An adjustable time delay is provided in the pump trip logic to protect against transient conditions.

- The CRD pumps are prevented from being started, or are tripped if running, if the pump lube oil pressure is low.

- The RC&IS and the RPS sense the CRD charging header pressure. The following actions occur based on the level of pressure degradation. The actions are based on 2-out-of-4 logic. A time delay is provided in the RPS to avoid spurious or inadvertent trips.

  - Alarm and all rod withdrawal block due to low charging header pressure.

  - Reactor trip due to low low charging header pressure.

- Control rod separation detection for any FMCRD causes both annunciation in the control room and a rod withdrawal block.

- The following signals in the CRD system initiate a rod withdrawal block by the RC&IS:

  - Rod separation detection (individual rod block).

  - Scram charging header pressure low (all rods block).

  - Rod gang misalignment (all rods in gang block).

- The high-pressure makeup flow control valves are prevented from opening when the inboard feedwater maintenance valve on the feedwater line through which the CRD system delivers flow to the reactor is closed.

- When in the high-pressure makeup mode of operation, the CRD pumps are tripped to terminate CRD system flow on receipt of low water level signals from two of the three Gravity Driven Cooling System (GDCS) pools.

4.6.1.2.7 Power Supplies

Each of the four divisional HCU charging header pressure sensors is powered from their respective divisional Class 1E power supply. Independence is provided between the Class 1E divisions for these sensors and between the Class 1E and non-Class 1E equipment.

For the FMCRD separation switches, independence is provided between the Class 1E divisions and between the Class 1E divisions and the non-Class 1E equipment.

The Medium Voltage Distribution System (MVD) provides the normal and standby electrical power to the nonsafety-related FMCRD motors.

4.6.1.2.8 Environmental Qualification

The following CRD system safety-related electrical equipment are located in either the Reactor Building or primary containment and are qualified for harsh environment: the HCU charging header pressure instrumentation, the scram solenoid pilot valves, and the FMCRD separation switches.

4.6.2 Evaluations of the CRD System

4.6.2.1 Safety Evaluation

The safety evaluation of the control rod drives is given below.

4.6.2.1.1 Evaluation of Scram Time

The rod scram function of the CRD system provides the negative reactivity insertion required by the Safety Design Bases in subsection 4.6.1.1.1. The scram time shown in the description is reflected in Chapter 15 safety analyses.

4.6.2.1.2 Scram Reliability

High scram reliability is the result of a number of features of the CRD system. For example:

- Each accumulator provides sufficient stored energy to scram two CRDs at any reactor pressure.

- Each pair of drive mechanisms has its own scram valve and dual solenoid scram pilot valve; therefore, only a single scram valve needs to open for scram to be initiated. Both pilot valve solenoids must be de-energized to initiate a scram.

- The RPS and the HCUs are designed so that the scram signal and mode of operation override all others.

- The FMCRD hollow piston and guide tube are designed so they do not restrain or prevent control rod insertion during scram.

- Each FMCRD mechanism initiates electric motor-driven insertion of its control rod simultaneous with the initiation of hydraulic scram. This provides a diverse means to assure control rod insertion.

4.6.2.1.3 Precluding Excessive Rate of Reactivity Addition

Excessive rates of reactivity addition are precluded in the design of the FMCRD. Prevention of rod ejection due to FMCRD pressure boundary failure and prevention of control rod drop are described below.

Control Rod Ejection Prevention

A failure of the CRD system pressure boundary generates differential pressure forces across the drive, which tends to eject the CRD and its attached control rod. The design of the FMCRD includes features that preclude rod ejection from occurring in these hypothetical circumstances. The following subsections describe how these features function for pressure boundary failures at various locations.

Failures at Drive Housing Weld - The bottom head of the reactor vessel has a penetration for each CRD location. A drive housing is raised into position inside each penetration and fastened by welding. The drive is raised into the drive housing and bolted to a flange at the bottom of the housing. In the event of a failure of the housing just below the housing-to-penetration weld, or a failure of weld itself with housing remaining intact, ejection of the CRD and attached control rod is prevented by the integral internal CRD blowout support. The details of this internal blowout support are contained in Subsection 4.6.1.2.2.

Rupture of Hydraulic Line to Drive Housing Flange

For the case of a scram insert line break, a partial or complete circumferential opening is postulated at or near the point where the line enters the housing flange. This failure, if not mitigated by special design features, could result in rod ejection at speeds exceeding maximum allowable limits. Failure of the scram insert line would cause loss of pressure to the underside of the hollow piston. The force resulting from full reactor pressure acting on the cross-sectional area of the hollow piston, plus the weights of the control rod and hollow piston, is imposed on the ball-nut. The ball-nut, in turn, translates this resultant force into a torque acting on the ball screw. When this torque exceeds the motor residual torque and seal friction, reverse rotation of the ball screw occurs permitting rod withdrawal.

The FMCRD design provides two diverse means of protection against the results of a postulated scram insert line failure. The first means of protection is a ball check valve located in the middle flange of the drive at the scram port. Reverse flow during a line break causes the ball to move to the closed position. This prevents loss of pressure to the underside of the hollow piston, which, in turn, prevents the generation of loads on the drive that could cause rod ejection.

The second means of protection is the FMCRD brake described in Subsection 4.6.1.2.2. In the event of the failure of the check valve, the passive brake prevents the ball screw rotation and rod ejection.

Total Failure of All Drive Flange Bolts - The FMCRD design provides an anti-rotation device which engages when the lower housing (spool piece) is removed for maintenance. This device prevents rotation of the ball screw and hence control rod motion when the spool piece is removed. The two components of the anti-rotation device are (1) the upper half of the coupling between the lower housing drive shaft and ball screw, and (2) the back seat of the middle flange (Figure 4.6-1). The coupling of the lower housing drive shaft to the ball screw is splined to permit removal of the lower housing. The underside of the upper coupling piece has a circumferentially splined surface that engages with a mating surface on the middle flange back seat when the ball screw is lowered during spool piece removal. When engaged, ball screw rotation is prevented. In addition to preventing rotation, this device also provides sealing of leakage from the drive while the spool piece is removed.

In the unlikely event of total failure of all the drive flange bolts attaching the spool piece flange and the middle flange of the drive to the housing flange, the anti-rotation device is engaged when the spool piece falls and the middle flange/outer tube/CRD blowout support is restrained by the control rod guide tube base bayonet coupling, thus preventing rod ejection (see Subsection 4.6.1.2.2).

Control Rod Drop Prevention

The following features prevent control rod drop:

- Two redundant Class 1E switches in the FMCRD sense separation of the hollow piston, which positions the control rod, from the ball-nut. These switches sense either separation of the piston from the nut or separation of the control rod from the piston, and block further lowering of the nut thereby preventing drop of either the control rod or the control rod and hollow piston as an assembly (see Subsection 4.6.1.2.2 for further details).

- Two redundant spring-loaded latches on the hollow piston open to engage in openings in the guide tube within the FMCRD to support the hollow piston if separation from the nut were to occur. These latches open to support the hollow piston (and control rod) following every scram until the ball-nut is run in to provide the normal support for the hollow piston (and control rod).

- The control rod to hollow piston coupling is a bayonet type coupling. Coupling is verified by pull test for the control rod upon initial coupling at refueling and again each time an attempt is made to drive beyond the "full out" position during reactor operation. The control rod can only be uncoupled from the FMCRD by relative rotation that is not possible during operation. The control rod cannot rotate, because it is always constrained between four fuel assemblies, and the hollow piston/CRD spud coupling cannot rotate, because the hollow piston has rollers that operate in a track within the FMCRD. Only structural failure would permit or result in control rod to FMCRD uncoupling, which, in turn, could only result in rod drop if the redundant switches failed to sense separation. In such failure scenarios, the rate of rod drop may exceed acceptable reactivity addition rates; however, the sequence of failures assumed involve so numerous a failure that the probability of occurrence would be low enough for the event to be categorized as an incredible event.

4.6.2.1.4 CRD Maintenance

The procedure for removal of the FMCRD for maintenance or replacement is similar to previous BWR product lines. The control rod is first withdrawn to the full-out position. During removal of the lower housing (spool piece) following removal of the position indicator probes and motor unit, the control rod backseats onto the control rod guide tube. This metal-to-metal contact provides the seal that prevents draining of reactor water when the FMCRD is subsequently lowered out of the CRD housing. The control rod normally remains in this backseated condition at all times with the FMCRD out; however, in the unlikely event it also has to be removed, a temporary blind flange is first installed on the end of the CRD housing to prevent draining of reactor water.

If the operator inadvertently removes the control rod after FMCRD is out without first installing the temporary blind flange, or conversely, inadvertently removes the FMCRD after first

removing the control rod, an un-isolable opening in the bottom of the reactor is created, resulting in drainage of reactor water. The possibility of inadvertent reactor drain-down by this means is considered remote for the following reasons:

- Procedural controls similar to those of current BWRs provide the primary means for prevention. Current BWR operating experience demonstrates this to be an acceptable approach. There has been no instance of an inadvertent drain-down of reactor water due to simultaneous CRD and control rod removal.

- During drive removal operations, personnel are required to monitor under the RPV for water leakage out of the CRD housing. Abnormal or excessive leakage occurring after only a partial lowering of the FMCRD within its housing indicates the absence of the full metal-to-metal seal between the control rod and control rod guide tube required for full drive removal. In this event, the FMCRD can then be raised back into its installed position to stop the leakage and allow corrective action.

See Subsection 4.6.6.1 for COL applicant license information.

The FMCRD design also allows for separate removal of the motor unit, position indicator probe (PIP), separation indicator probe (SIP) and spool piece for maintenance during plant outages without disturbing the upper assembly of the drive. While these FMCRD components are removed for servicing, the associated control rod is maintained in the fully inserted position by one of two mechanical locking devices that prevent rotation of the ball screw and drive shaft.

The first anti-rotation device (Detail A in Figure 4.6-10) is engaged when the motor unit consisting of the induction motor, reduction gear, brake and position signal detector is removed. It is a spring-actuated locking cam located on the bottom of the spool piece. When the motor unit is lowered away from the spool piece, the locking cam is released from its normally retracted position and engaged by spring force with gear teeth on the bottom of the magnetic coupling outer rotor, thereby locking the shaft in place.

With the motor unit removed, the locking cam can be visually checked from below the drive to verify that it is properly engaged. When the vessel head is removed, another means of verification of proper locking is for the operator to view the top of the control rod from over the reactor vessel. If the top of the control rod is visible at its normal full in position, it provides both direct indication that the control rod remains fully inserted and additional assurance that the ball screw is restrained from reverse rotation. The drive shaft remains locked in this manner until the motor unit is reattached to the spool piece. During motor installation, a release pin on the motor unit pushes up a plunger linked to the locking cam as the motor unit is raised into contact with the spool piece. The release pin forces the locking cam away from the teeth on the bottom of the magnetic coupling outer rotor and into the normally retracted, unlocked position.

The second anti-rotation device (Detail B in Figure 4.6-10) is engaged when the spool piece is removed from the FMCRD. As described in Subsection 4.6.2.1.3, this device is a spline arrangement between the ball screw lower coupling and the middle flange backseat. When removing and lowering the spool piece, the weight of the ball screw, hollow piston and control rod provides a vertical force in the downward direction that brings the two splines together. This locks the ball screw into the backseat and prevents reverse rotation. As with the first anti-rotation device, proper engagement of this device can be visually checked from below the drive. If the splines do not completely lock together, there is indication of this because the ball screw

does not seat against the backseat and there is a small gap for leakage of water. If this should occur, removal of the spool piece can be discontinued and corrective action taken. If there is no leakage, it confirms that the splines are properly locked together. Also as in the case of the first anti-rotation device, visual observation of the top of the control rod from over the reactor vessel provides another means for verifying proper locking of the ball screw. The ball screw remains locked in this position until the spool piece is reattached to the FMCRD. During spool piece installation, the end of the drive shaft fits into a seat on the end of the ball screw. As the ball screw piece is raised off the middle flange backseat, the anti-rotation splines disengage and the weight of the ball screw, hollow piston and control rod is transferred to the spool piece assembly.

4.6.3 Testing and Verification of the CRDs

4.6.3.1 Factory Quality Control Tests

The quality control specifications and procedures follow the general pattern established for such specifications and procedures in BWRs presently in operation.

Quality control of welding, heat treatment, dimensional tolerances, material verification and similar factors are maintained throughout the manufacturing process to assure reliable performance of the mechanical reactivity control components.

Some of the quality control tests performed on the CRD mechanisms and HCUs are listed below:

- CRD Mechanism Tests

  - Pressure welds on the drives are hydrostatically tested in accordance with ASME codes.

  - Electrical components are checked for electrical continuity and resistance to ground.

  - Drive parts that cannot be visually inspected for dirt are flushed with filtered water at high velocity. No significant foreign material is permitted in effluent water.

  - Each drive is tested for shim (drive-in and -out) motion and control rod position indication.

  - Each drive is subjected to cold scram tests at various reactor pressures to verify correct scram performance.

- HCU Tests

  - Hydraulic systems are hydrostatically tested in accordance with the applicable code.

  - Electrical components and systems are tested for electrical continuity and resistance to ground.

  - Correct operation of the accumulator pressure and level switches is verified.

  - Each HCU's ability to perform as part of a scram is demonstrated.

4.6.3.2 Functional Tests

These tests evaluate drive performance under conditions of crud/contamination, seismic misalignment, channel bulge, failed buffer, rod drop (to test hollow piston latch functionality), and rod ejection (to test FMCRD brake functionality).

4.6.3.3 Operational Tests

After installation, all rods and drive mechanisms can be tested through their full stroke for operability.

The switches that detect separation provide indication and automatic rod withdrawal block should a control rod separate from the drive mechanism during rod withdrawal. Additionally, the operator can observe the incore monitor indications to verify that the control rod is following the drive mechanism. All control rods that are partially withdrawn from the core can be tested for rod-following by inserting or withdrawing the rod one or two steps and returning it to its original position, while the operator observes the incore monitor indications.

To make a positive test of control rod to CRD coupling integrity, the operator can withdraw a control rod to the end of its travel and then attempt to withdraw the drive to the overtravel position. Failure of the hollow piston to overtravel-out demonstrates the integrity of the rod-to-drive coupling.

CRDHS pressures can be observed from instrumentation in the control room. Scram accumulator pressures can be observed on the nitrogen pressure gauges.

4.6.3.4 Acceptance Tests

Criteria for acceptance of the individual CRD mechanisms and the associated control and protection systems is incorporated in specifications and test procedures covering three distinct phases:

- Pre-installation
- After installation prior to startup
- During startup testing

The pre-installation specification defines criteria and acceptable ranges of such characteristics as seal leakage, friction and scram performance under fixed test conditions that must be met before the component can be shipped.

The after-installation, pre-startup tests (Chapter 14) include normal and scram motion and are primarily intended to verify that piping, valves, electrical components and instrumentation are properly installed. The test specifications include criteria and acceptable ranges for drive speed, scram valve response times, and control pressures. These are tests intended more to document system condition rather than tests of performance.

As fuel is placed in the reactor, the startup test procedure (Chapter 14) is followed. The tests in this procedure are intended to demonstrate that the initial operational characteristics meet the limits of the specifications over the range of primary coolant temperatures and pressures from ambient to operating. The detailed specifications and procedures are similar to those in BWRs presently in operation.

4.6.3.5 Surveillance Tests

The surveillance requirements for the CRD system are described below. While these requirements have not yet been formalized, the intent is to follow the general pattern established for surveillance testing in BWRs presently in operation.

- Sufficient control rods shall be withdrawn, following a refueling outage when core alterations are performed, to demonstrate with adequate shutdown margin that the core can be made subcritical at any time in the subsequent fuel cycle with the maximum worth control rod pair having the same HCU or the single rod attached to the unpaired HCU, if of greater worth, withdrawn and all other operable rods fully inserted.

- Each fully withdrawn control rod is exercised at least once each week. Each partially withdrawn control rod is exercised at least once each month.

- The coupling integrity shall be verified for each withdrawn control rod as follows:

  − When the rod is first withdrawn, observe the control rod separation switch response and discernible response of the nuclear instrumentation.

  − When the rod is fully withdrawn the first time, observe that the drive does not go to the overtravel-out position. Observation of the separation switches provides direct indication that the control rod is following the drive during withdrawal, but does not provide a direct check on coupling integrity. Additionally, observation of a response from the nuclear instrumentation during an attempt to withdraw a control rod provides another indirect indication that the rod and drive are coupled. The overtravel-out position feature provides a positive check on the coupling integrity, for only an uncoupled drive can reach the overtravel-out position.

- During operation, accumulator pressure and level at the normal operating value are verified. Experience with CRD systems of the same type indicates that weekly verification of accumulator pressure and level is sufficient to assure operability of the accumulator portion of the CRD system.

- At the time of each major refueling outage, each operable control rod is subjected to scram time tests from the fully withdrawn position. Experience indicates that the scram times of the control rods do not significantly change over the time interval between refueling outages. A test of the scram times at each refueling outage is sufficient to identify any significant lengthening of the scram times.

- The high-pressure makeup mode of operation is tested to verify the automatic response of the system to a simulated or actual initiation signal. The CRD pumps are tested to verify they can develop the required flow rate for high-pressure makeup against a system head corresponding to the required reactor pressure. This test uses the system test return line to the CST.

4.6.4 Information for Combined Performance of Reactivity Control Systems

4.6.4.1 Vulnerability to Common Mode Failures

The Reactivity Control System is located such that it is protected from common mode failures due to missiles, failures of moderate and high energy piping, and fire. Sections 3.5, 3.6 and 3.7,

and Subsection 9.5.1 discuss protection of essential systems against missiles, pipe breaks, seismic and fire, respectively.

4.6.4.2 Accidents Taking Credit for Multiple Reactivity Systems

There are no postulated accidents documented in Chapter 15 that take credit for two or more reactivity control systems preventing or mitigating an accident.

4.6.5 Evaluation of Combined Performance

As indicated in Subsection 4.6.4.2, credit is not taken for multiple reactivity control systems for any postulated accidents documented in Chapter 15.

4.6.6 COL Information

4.6.6.1 CRD and FMCRD Maintenance Procedures

The COL applicant shall develop maintenance procedures with provisions to prohibit coincident removal of the CRD blade and drive of the same assembly. In addition, the COL applicant shall develop contingency procedures to provide core and spent fuel cooling capability and mitigative actions during CRD replacement with fuel in the vessel.

4.6.7 References

None

Table 4.6-1

Hydraulic Requirements

Parameter	Value
Required purge water flow to control rod drives, l/min (gpm)	1.3 (0.34)
Approximate purge water flow to RWCU/SDC pumps, l/min (gpm)	20 (5.3)
Approximate makeup flow to NBS instrument lines, l/min (gpm)	4 (1)
Minimum flow to reactor in high pressure makeup mode with both pumps running, l/min (gpm)	3920 (1036)
Minimum flow to reactor in high pressure makeup mode with one pump running, l/min (gpm)	1960 (518)
Reference pressure for high pressure makeup mode, MPa (psig)	8.62 (1250)
Design pressure for the piping and components of the CRD pump suction supply, which extends from the CRD system interfaces with the Condensate and Feedwater System (C&FS) and Condensate Storage and Transfer System (CS&TS) to the inlet connections of the CRD pumps, MPa (psig)	2.82 (409)

Table 4.6-2

CRD System Scram Performance

Insertion	Time (sec)
Start of Motion	≤ 0.20
10%	≤ 0.34
40%	≤ 0.80
60%	≤ 1.15
100%	≤ 2.23

BAYONET COUPLING TYPE
COUPLING SPUD
(TO CONTROL ROD
SOCKET COUPLING)

BAYONET COUPLING TYPE
INTERNAL CRD BLOWOUT SUPPORT
(TO CONTROL ROD
GUIDE TUBE BASE COUPLING)

CRD HOUSING

BUFFER

LABYRINTH SEAL

STOP PISTON

HOLLOW PISTON

OUTER TUBE

BALL SCREW

POSITION INDICATOR
PROBE (PIP)

GUIDE TUBE

SCRAM POSITION
SENSING MAGNET

BALL NUT

SCRAM INSERT LINE

FULL-IN MAGNET

MIDDLE FLANGE

BALL CHECK VALVE

MAGNET (FOR SEPARATION
DETECTION)

BACKSEAT

SPRING (FOR SEPARATION DETECTION)

LOWER HOUSING
(SPOOL PIECE)

SEPARATION INDICATOR PROBE

DRIVE SHAFT

MAGNETIC COUPLING

MOTOR UNIT
(WITH BRAKE,
POSITION DETECTOR
AND GEAR UNIT)

Figure 4.6-1. Fine Motion Control Rod Drive Schematic

No.	MAIN PART NAME
1	DRAIVE SHAFT
2	BEARING
3	MAGNET (INNER ROTOR)
4	MAGNET (OUTER ROTOR)
5	LOWER HOUSING (SPOOL PIECE)
6	BALL SCREW
7	BALL NUT AND BALL
8	GUIDE ROLLER AND PIN (FOR NUT)
9	GUIDE SHAFT
10	BUSHING (STATIONARY GUIDE)
11	SPRING (FOR SEPARATION DETECTION)
12	MAGNET (FOR SEPARATION DETECTION)
13	BUFFER SPRING
14	BUFFER SLEEVE (LABYRINTH SEAL)
15	GUIDE ROLLER, PIN
16	STOP PISTON
17	HOLLOW PISTON
18	DRIVE PISTON
19	LATCH
20	LATCH SPRING
21	SPUD (BAYONET COUPLING)
22	COMPRESSION ROD
23	GUIDE TUBE
24	OUTER TUBE
25	MIDDLE FLANGE
26	BALL CHECK VALVE
27	O RING SEAL (BETWEEN CRD HOUSING AND CRD)
28	CRD MOUNTING BOLT
29	BLOWOUT SUPPORT
30	FULL IN MAGNET
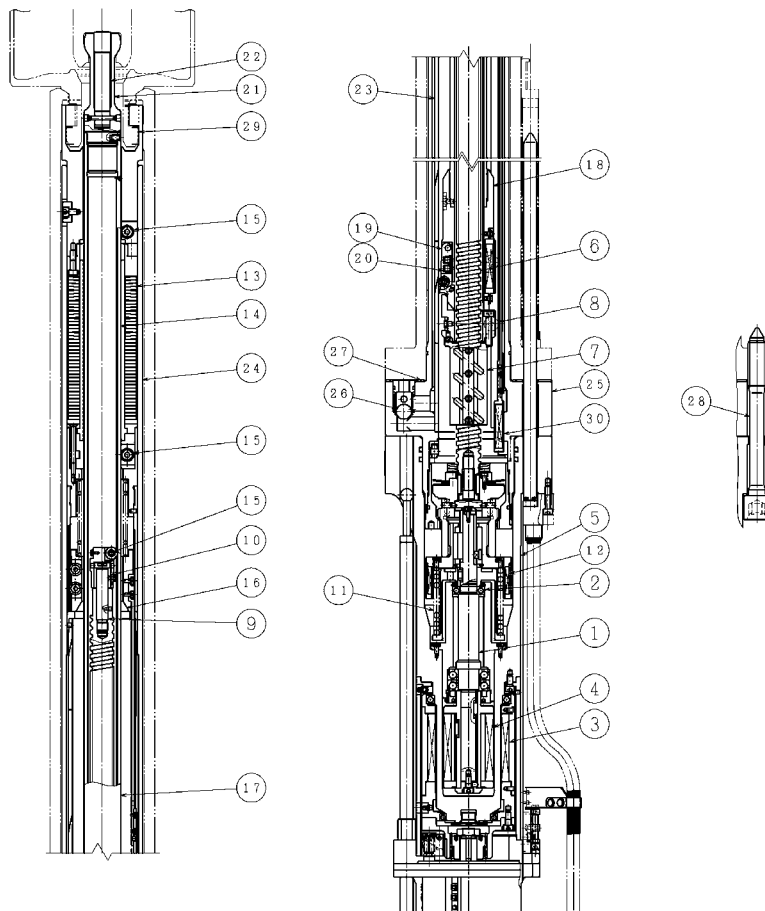
Figure 4.6-2. Fine Motion Control Rod Drive Unit (Cutaway)
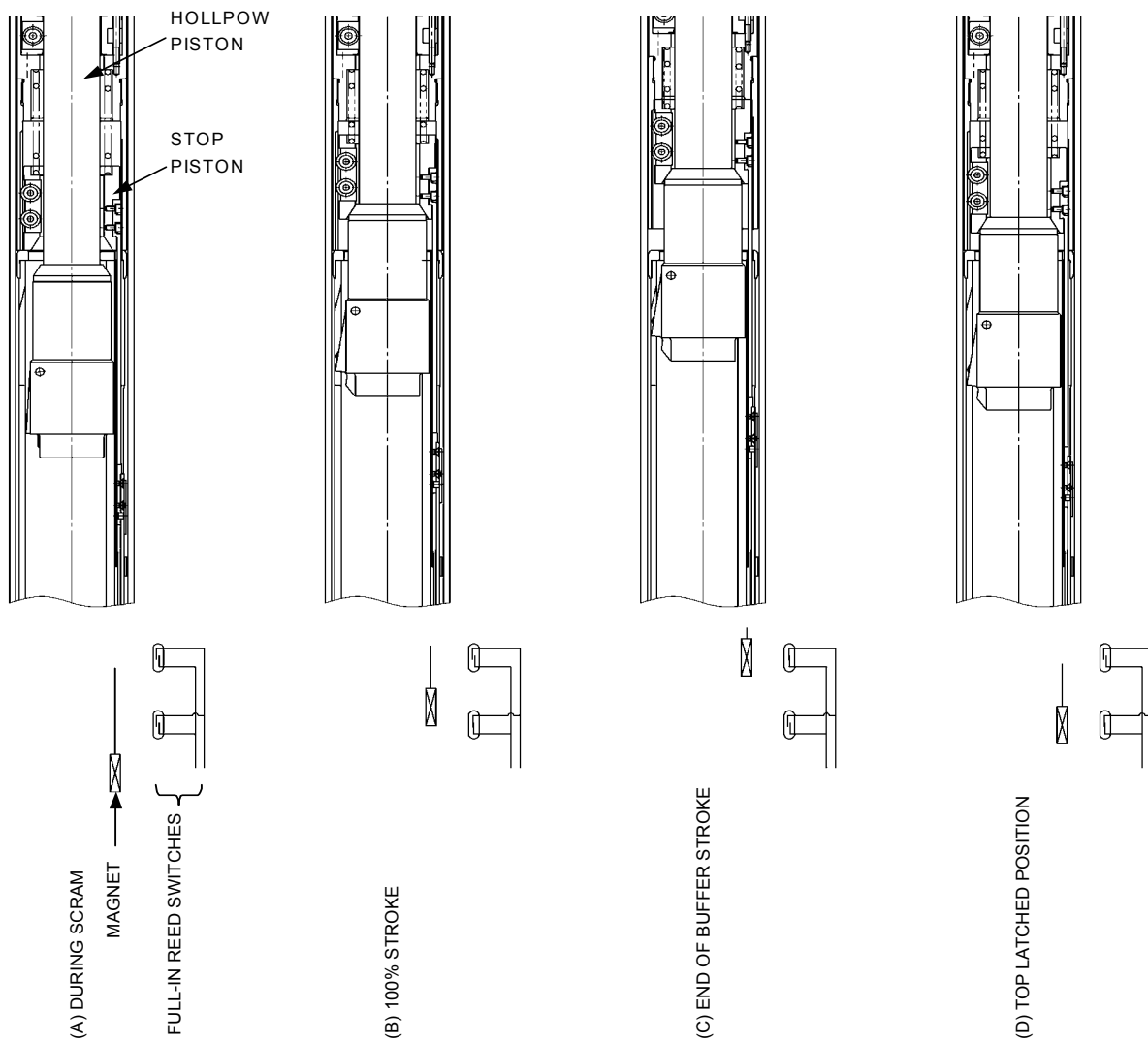
Figure 4.6-3. Continuous Full-in Indicating Device
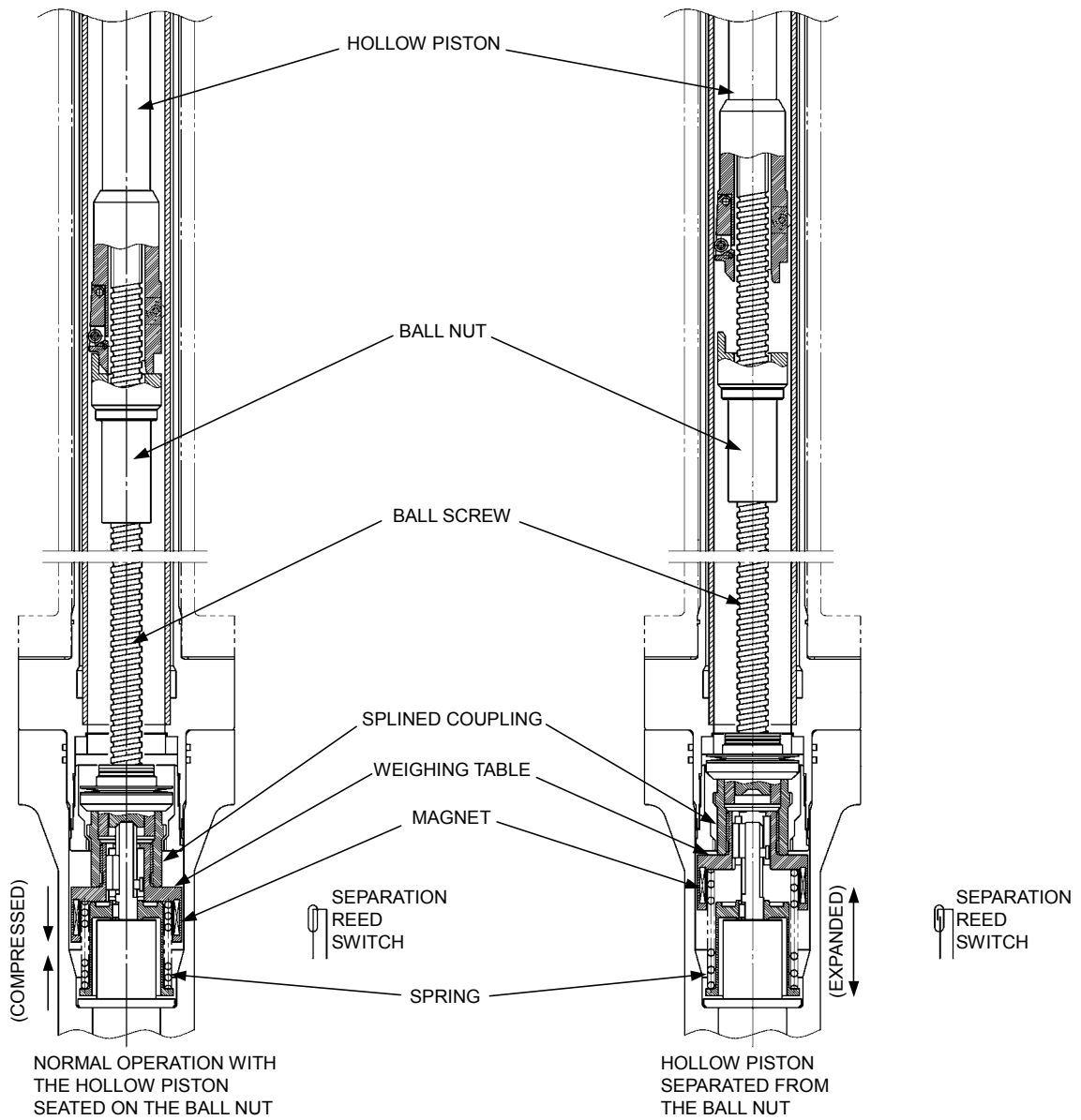
Figure 4.6-4. Control Rod Separation Detection

1   CONTROL ROD COUPLING SOCKET

CRD COUPLING SPUD

2

3

4   CONTROL ROD COUPLED WITH CRD

(INSERT)

(ROTATE 45 DEGREES)
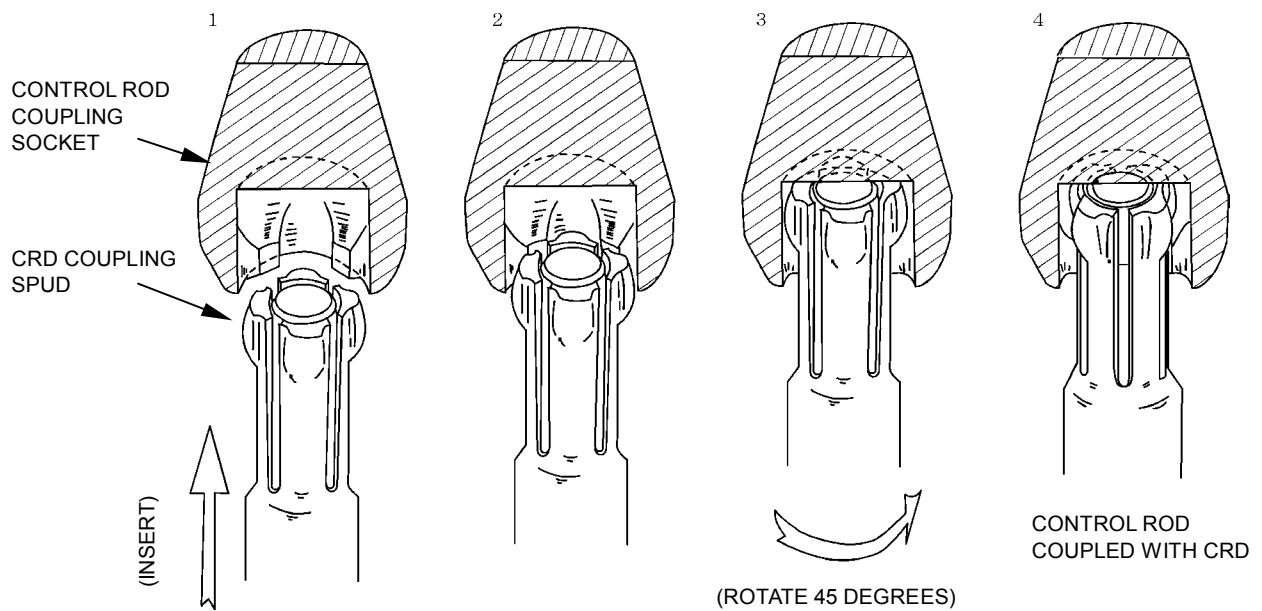
Figure 4.6-5. Control Rod to Control Rod Drive Coupling
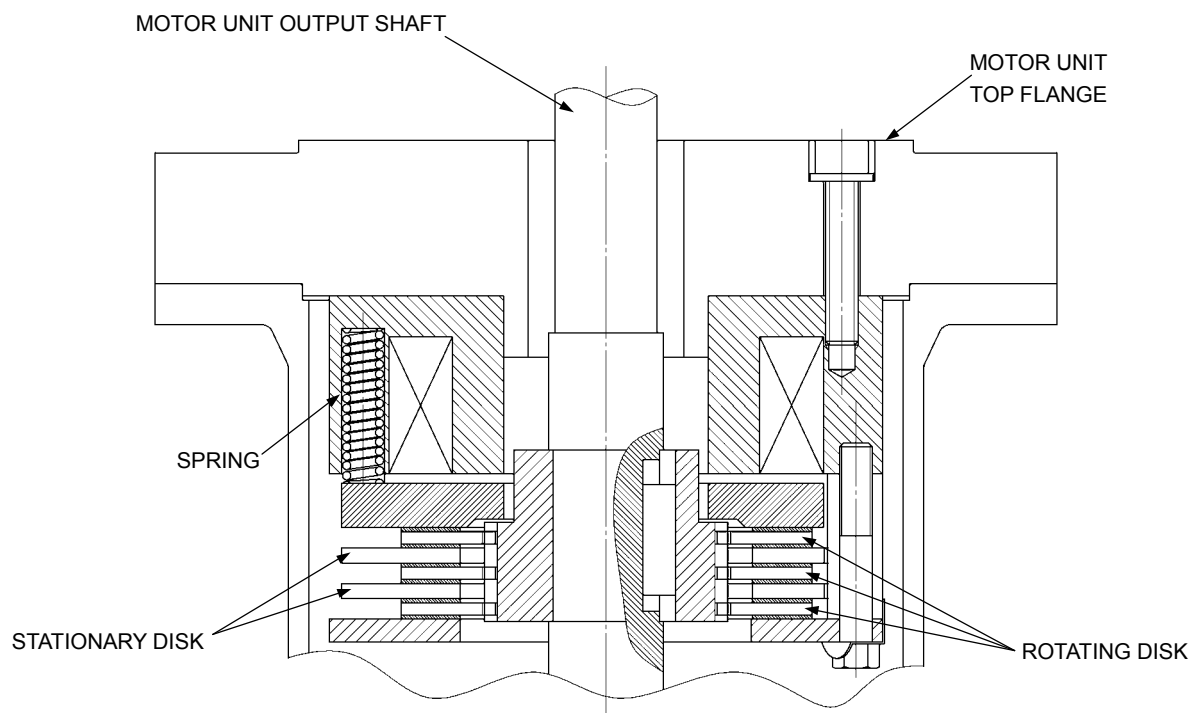
Figure 4.6-6. FMCRD Electro-mechanical Brake

FLANGE OF CONTROL ROD
GUIDE TUBE

CORE PLATE

CR GUIDE TUBE BASE

CONTROL ROD GUIDE TUBE
BASE COUPLING
(BAYONET TYPE)

INTERNAL CRD BLOWOUT
SUPPORT (BAYONET TYPE)

STUB TUBE

"A"

FMCRD OUTER TUBE

CRD HOUSING

"B"

SPOOL PIECE
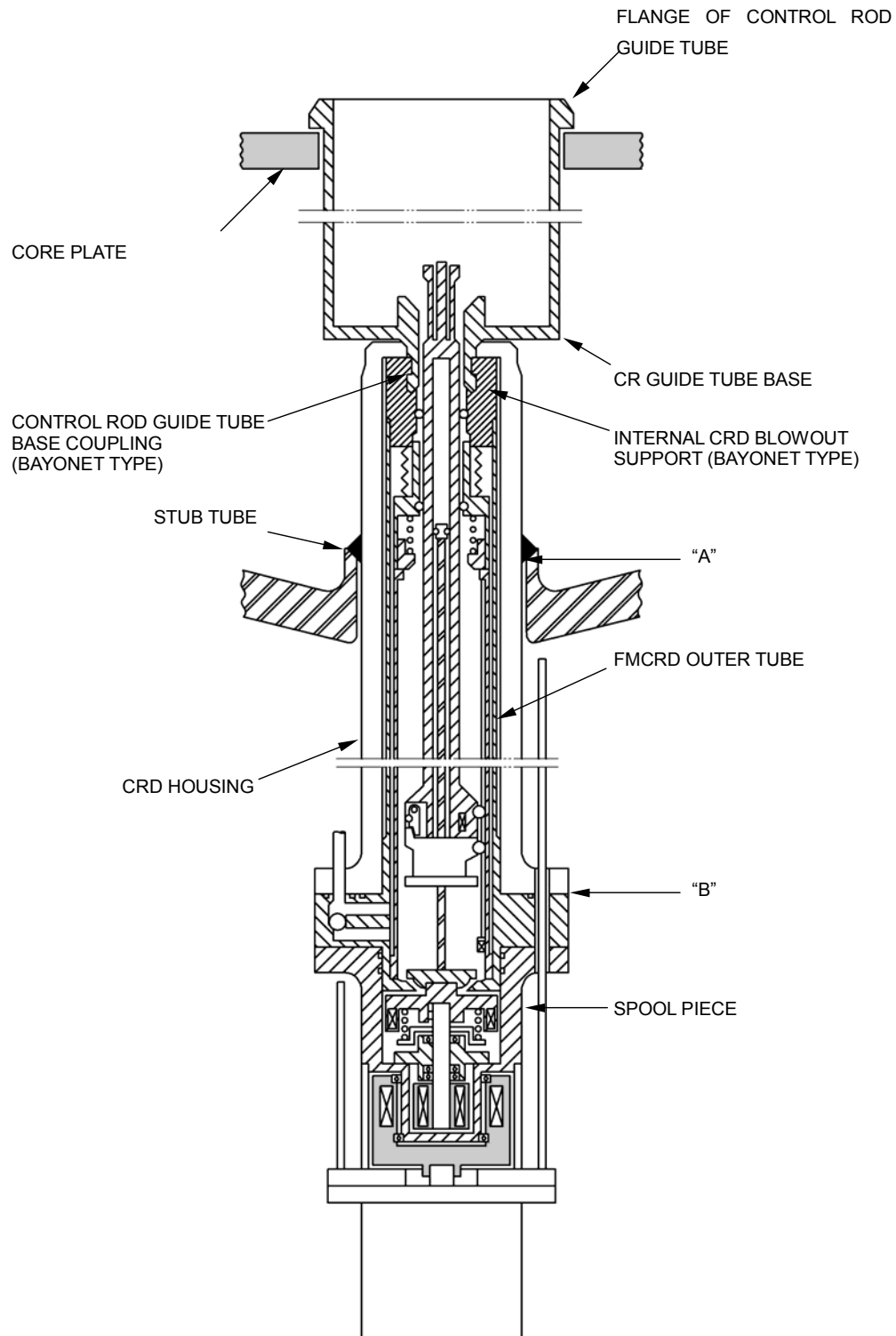
Figure 4.6-7. Internal CRD Blowout Support Schematic

Figure 4.6-8. Control Rod Drive System Simplified Process and Instrumentation Diagram

1. ALL EQUIPMENT NUMBERS SHOWN ON THIS DIAGRAM ARE PREFIXED BY C12- UNLESS OTHERWISE INDICATED.

2. LINE SIZES ARE SPECIFIED ON THE PIPING AND INSTRUMENTATION DIAGRAM (MPL NO. C12-1010).

3. ALL VALUES ARE NOMINAL UNLESS NOTED OTHERWISE.

4. THE TERM PR DENOTES REACTOR PRESSURE IMMEDIATELY ABOVE THE CORE PLATE.

5. THE CST WILL PROVIDE AN ALTERNATE SOURCE OF WATER FOR THE CRD SYSTEM IF THE CONDENSATE AND FEEDWATER SYSTEM IS NOT AVAILABLE.

6. ONE PUMP IS RUNNING AND ONE IS ON STANDBY DURING OPERATING MODES A, B, AND C. THE OPERATOR WILL SELECT WHICH PUMP IS TO RUN. PUMP A IS USED TO DEFINE THE PROCESS CONDITIONS FOR THE OPERATING PUMP. BOTH PUMPS RUN DURING OPERATING MODES D AND E. FOR THESE MODES, THE PROCESS CONDITIONS OF PUMP B ARE IDENTICAL TO THOSE OF PUMP A.

7. DURING NORMAL MOTOR-DRIVEN ROD INSERTIONS (SINGLE ROD OR GANGED MOVEMENTS) IN MODE A, THE PURGE WATER FLOW AT LOCATION 8 IS INCREASED TO A MINIMUM OF 8.2 L/MIN (2.2 GPM) TO EACH HCU ASSOCIATED WITH A MOVING DRIVE. THIS IS ACCOMPLISHED BY AUTOMATIC OPENING OF THE PURGE WATER MAKE-UP VALVE IN THE HCU. THE FLOW FROM EACH HCU THEN DIVIDES EVENLY BETWEEN THE TWO DRIVES SUCH THAT THE FLOW AT LOCATIONS 9 AND 10 IS A MINIMUM OF 4.1 L/MIN (1.1 GPM). THE PURGE WATER FLOW TO THE STATIONARY DRIVES CORRESPONDINGLY DECREASES SINCE THE TOTAL PURGE WATER HEADER FLOW RATE AT LOCATION 7 REMAINS CONSTANT.

8. IN MODE A, THE MINIMUM DRIVE PURGE FLOW RATE AT LOCATIONS 9 AND 10 SHALL NOT BE LESS THAN 0.7 L/MIN (0.18 GPM) TO ANY DRIVE WHILE ALL DRIVES ARE STATIONARY. THE PURGE FLOW RATE TO THE STATIONARY DRIVES IN MODE A MAY BE LESS THAN THIS LIMIT FOR BRIEF PERIODS OF TIME DURING GANG ROD MOVEMENTS AS DESCRIBED IN NOTE 7.

9. SYSTEM OPERATION IS POSSIBLE WITH INTERMEDIATE PRESSURES IN THE REACTOR VESSEL. HOWEVER, THESE CONDITIONS DO NOT CONTROL PIPE OR VALVE SIZING OR SPECIFICATION, AND NO DATA IS SHOWN.

10. PUMP FLOW OF 767 L/MIN (203 GPM) SHALL NOT BE EXCEEDED. ORIFICE D009 REDUCES THE PRESSURE AT THE INSERT LINE SO THAT NO GREATER THAN A TOTAL OF 455 L/MIN (120 GPM) WILL LEAK THROUGH ALL THE DRIVES WHEN PR = 0 MPa GAUGE (0 PSIG). FLOW AT LOCATIONS 9 AND 10 IS EQUAL TO 455 L/MIN (120 GPM) DIVIDED BY 269 (THE NUMBER OF DRIVES).

11. RESTRICTING ORIFICES D006 AND D009 ARE COMPOSED OF MULTIPLE ORIFICES CONNECTED IN SERIES.

12. THE SPECIFIED LINE LOSSES ARE FOR SCRAM LINE ONLY. TOTAL COMBINED LOSSES FOR THE HCU PLUS SCRAM LINE ARE 1.68 MPa (243 PSI) MINIMUM AND 2.12 MPa (307 PSI) MAXIMUM AT THE SPECIFIED FLOW RATE.

13. FCV-F020 LIMITS FLOW TO THE REACTOR IN THE VESSEL INJECTION MODE TO 1960 L/MIN (518 GPM) SO THAT PUMP RUNOUT CAPACITY OF 1973 L/MIN (521 GPM) SHALL NOT BE EXCEEDED.

14. THE PRESSURE CONDITIONS IDENTIFIED IN THIS DRAWING ARE BASED ON PREVIOUS BWR SYSTEM DESIGN OF SIMILAR CONFIGURATION AND ARE REPRESENTATIVE OF TYPICAL EXPECTED VALUES. THE CONDITIONS SPECIFIC FOR ESBWR WILL BE ESTABLISHED DURING THE COMBINED LICENSE (COL) DESIGN PHASE OF THE PROJECT.

Figure 4.6-9. Control Rod Drive System Process Flow Diagram
(Sheet 1 of 2)

MODE A NORMAL OPERATION - SIZES PURGE WATER HEADER

LOCATION ⬡	1	2	3	4	5	6	7	8	9	10	11	12	13	14	15	16	17	18	19	20	21
FLOW L/MIN (GPM)	662 (175)	662 (175)	662 (175)	662 (175)	375 (99)	350 (92.5)	350 (92.5)	2.6 (0.68)	1.3 (0.34) MAX	1.3 (0.34) MAX	---	0	0	287 (76)	287 (76)	0	0	0	0	0	287 (76)
PRESSURE MPa GAUGE (PSIG)			*	*	*	*	PR+0.25 (PR+36) MIN	PR+0.25 (PR+36) MIN	PR+0.20 (PR+29) MIN	PR+0.20 (PR+29) MIN	PR			*							

SEE NOTE 7

CONDITIONS: 1. NORMAL DRIVE OPERATION
2. MAXIMUM PURGE FLOW TO DRIVES (SEE NOTE 8)
3. REACTOR PRESSURE PR = 7.067 MPa GAUGE (1025 PSIG)(SEE NOTE 9)

MODE B SCRAM - SIZES SCRAM INSERT LINE

LOCATION ⬡	1	2	3	4	5	6	7	8	9	10	11	12	13	14	15	16	17	18	19	20	21
FLOW L/MIN (GPM)	312 (82)	312 (82)	312 (82)	312 (82)	25 (6.6)	0	0	0	473 (125)	473 (125)	---	0	0	287 (76)	287 (76)	0	0	0	0	0	287 (76)
PRESSURE MPa GAUGE (PSIG)									*	*	PR			*							

CONDITIONS: 1. DRIVES SCRAMMING
2. SCRAM INSERT LINE LOSSES AT SPECIFIED LIMITS
3. REACTOR PRESSURE PR = 7.067 MPa GAUGE (1025 PSIG) (SEE NOTE 9)

MODE C SCRAM COMPLETED - SIZES THE PUMP SUCTION FILTER LINES AND CHARGING THE WATER HEADER

LOCATION ⬡	1	2	3	4	5	6	7	8	9	10	11	12	13	14	15	16	17	18	19	20	21
FLOW L/MIN (GPM)	767 (203)	767 (203)	767 (203)	767 (203)	480 (127)	455 (120)	0	0	SEE NOTES 10 AND 11		---	455 (120) MAX	3.4 (0.9) MAX	287 (76)	287 (76)	0	0	0	0	0	287 (76)
PRESSURE MPa GAUGE (PSIG)			*	*							PR			*							

CONDITIONS: 1. SCRAMMING OF DRIVES COMPLETED
2. MAXIMUM CRD SUPPLY PUMP FLOW THROUGH PUMP SUCTION FILTER
3. REACTOR PRESSURE PR = 0 MPa GAUGE (0 PSIG) (SEE NOTE 9)

MODE D REACTOR VESSEL INJECTION - SIZES THE PUMP SUCTION AND VESSEL INJECTION LINES

LOCATION ⬡	1	2	3	4	5	6	7	8	9	10	11	12	13	14	15	16	17	18	19	20	21
FLOW L/MIN (GPM)	3945 (1042)	3945 (1042)	1973 (521)	1973 (521)	25 (6.6)	0	0	0	0	0	---	0	0	0	0	1960 (518)	3920 (1036)	3920 (1036)	3920 (1036)	0	0
PRESSURE MPa GAUGE (PSIG)			*	*							PR			*		SEE NOTE 13					

CONDITIONS: 1. SCRAMMING OF DRIVES COMPLETED
2. MAXIMUM CRD SUPPLY PUMP FLOW (PUMP RUNOUT)
3. REACTOR PRESSURE PR = 8.619 MPa GAUGE (1250 PSIG) (SEE NOTE 9)

MODE E TEST MODE

LOCATION ⬡	1	2	3	4	5	6	7	8	9	10	11	12	13	14	15	16	17	18	19	20	21
FLOW L/MIN (GPM)	3945 (1042)	3945 (1042)	1973 (521)	1973 (521)	25 (6.6)	0	0	0	0	0	---	0	0	0	0	1960 (518)	3920 (1036)	0	0	3920 (1036)	3920 (1036)
PRESSURE MPa GAUGE (PSIG)			*	*							PR			*						*	*

CONDITIONS: 1. PURGE FLOW TO DRIVES INTERRUPTED
2. DISCHARGE TO CONDENSATE STORAGE
3. NORMAL REACTOR OPERATION

DESIGN PRESSURE / TEMPERATURE
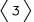
LOCATION ⬡	1-2	2-3	4-5	5-6	6-7	7-8	9-10	6-12	12-13	4A-14	14-15	15-21	4B-16	16-17	17-18	17A-20	20-21	21-21A
PRESSURE MPa GAUGE (PSIG)	2.82 (409)	2.82 (409)	18.6 (2700)	18.6 (2700)	18.6 (2700)	18.6 (2700)	23.54 (3410)	18.6 (2700)	18.6 (2700)	18.6 (2700)	18.6 (2700)	18.6 (2700)	18.6 (2700)	18.6 (2700)	18.6 (2700)	18.6 (2700)	18.6 (2700)	18.6 (2700)
TEMPERATURE °C (°F)	66 (150)	66 (150)	66 (150)	66 (150)	66 (150)	66 (150)	66 (150)	66 (150)	66 (150)	66 (150)	66 (150)	66 (150)	66 (150)	302 (575)	302 (575)	302 (575)	66 (150)	66 (150)

EQUIPMENT OPERATIONAL CONDITIONS
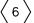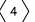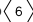
EQUIPMENT IDENTIFICATION	EQUIPMENT DESCRIPTION	MODE A	MODE B	MODE C	MODE D	MODE E
C001A, B	CRD PUMP (NO. RUNNING)	1	1	1	2	2
F010	FCV	0	0	C	0	0
F012	AO VALVE	0	0	0	C	C
F014A, B	MO VALVE	C	C	C	0	0
F020A, B	FCV	C	C	C	0	0
F023	MO VALVE	0	0	0	0	C
F024	MO VALVE	C	C	C	C	0
F030	AO VALVE	0	0	0	C	C
F062	MO VALVE	0	0	0	C	C
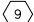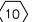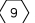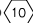
∗ THE PRESSURE AT THIS LOCATION DEPENDS ON PIPING ARRANGEMENT, AND MAY BE VARIED WITHIN THE FOLLOWING LIMITS. SEE NOTE 14.

LOCATION:

③ MINIMUM NPSH AT PUMP SUCTION = 11 METER (36 FEET) AT 1973 L/MIN (521 GPM)

   MAXIMUM SUCTION PRESSURE 0.34 MPa (50 PSIG)

④ MINIMUM PUMP TOTAL DYNAMIC HEAD (TDH):

   1560 METER (5120 FEET) FOR MODES A AND B
   1200 METER (3940 FEET) FOR MODE C
   1000 METER (3280 FEET) FOR MODES D AND E

⑥ MAXIMUM PRESSURE DROP BETWEEN LOCATIONS

   ④ AND ⑥ = 0.50 MPa (72 PSIG) FOR MODE A

⑨ ⑩ LINE LOSS BETWEEN LOCATIONS

   ⑨ AND ⑩ FOR MODE B

   0.72 MPa (104 PSI) MINIMUM
   1.16 MPa (168 PSI) MAXIMUM

   AT THE SPECIFIED FLOW RATE (SEE NOTE 12).

⑭ SUFFICIENT PRESSURE TO RETURN FLOW TO CONDENSATE STORAGE.

⑳ ㉑ SUFFICIENT PRESSURE TO RETURN FLOW TO CONDENSATE STORAGE.

Figure 4.6-9. Control Rod Drive System Process Flow Diagram
(Sheet 2 of 2)

PART OF
BALL SCREW

BACK SEAT

ANTI-ROTATING
DEVICE SPLINE

DETAIL B

B

SPOOL PIECE

A

MOTOR UNIT

OUTER ROTOR
COUPLING GEAR

LOCKING CAM

SPRING

PLUNGER

RELEASE PIN

DETAIL A
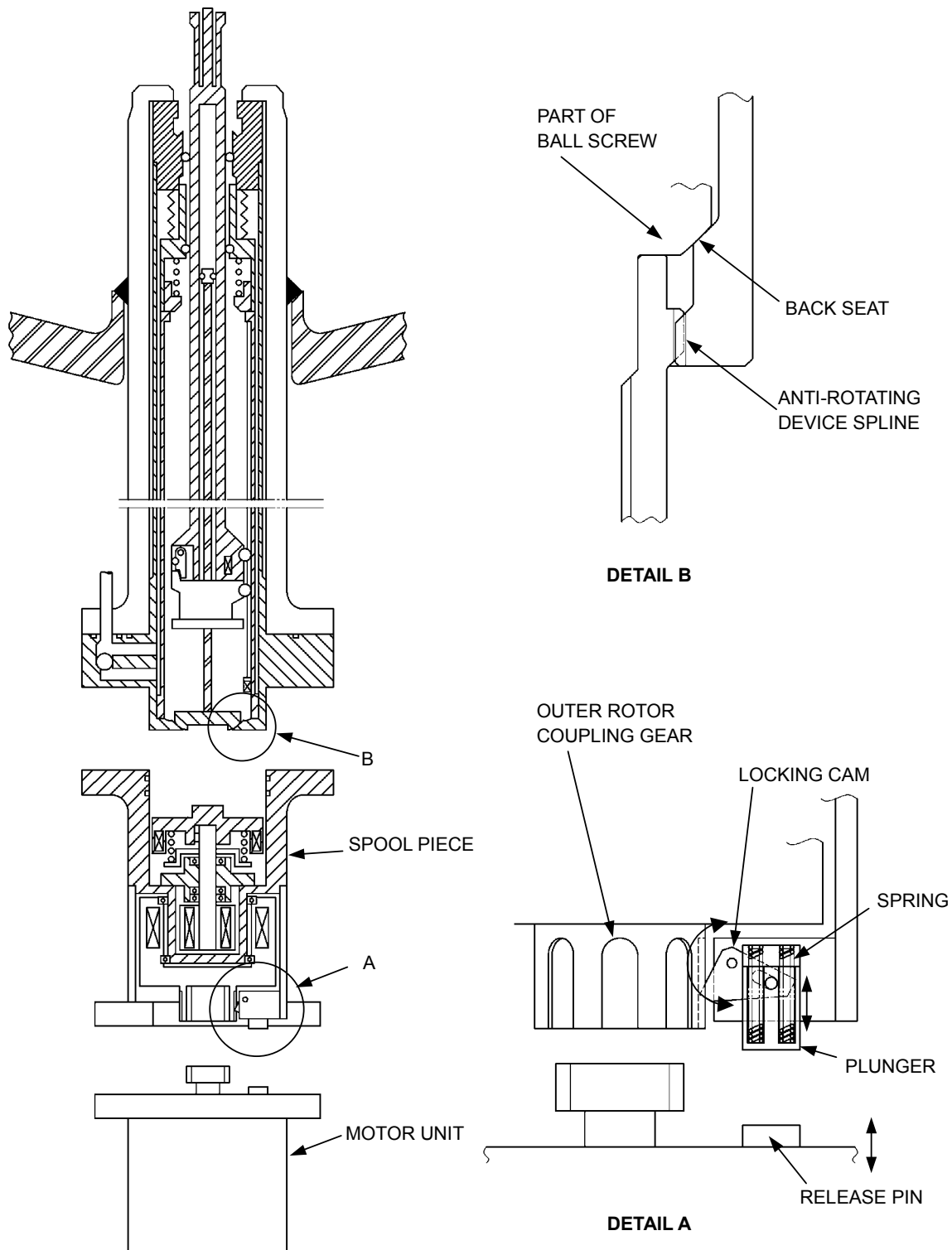
Figure 4.6-10. Control Rod Drive System Separation Mechanism

4A. TYPICAL CONTROL ROD PATTERNS AND ASSOCIATED POWER DISTRIBUTION FOR ESBWR

4A.1 INTRODUCTION

This appendix contains a typical simulation of an equilibrium cycle. The control rod patterns used are just one example of a set of control rod patterns which could be used to provide the radial and axial power shaping needed to meet the Technical Specifications.

The basic control rod strategy for this case consists of control rod patterns used only to compensate for excess reactivity and to aid in shaping the axial power profile.

4A.2 RESULTS OF CORE SIMULATION STUDIES

Table 4A-1 itemizes the stepwise rod pattern for exposure steps and their related figure numbers. Control rod patterns, relative axial power, axial exposure, relative integrated power per bundle, and average bundle exposure for a range of exposure are shown on Figures 4A-1 through 4A-18. The detailed data presented demonstrate that this design can be operated throughout this cycle with adequate margins to allow for operating flexibility. The variation of the minimum critical power ratio (MCPR) with cycle exposure is shown in Figure 4A-19. Similarly, a large margin is indicated with respect to the expected MCPR operating limit.

4A.3 COL INFORMATION

Results within this section identify the example rod patterns, loading pattern, bundle description, and mechanical design of a fuel bundle assembly that demonstrates certification of the ESBWR plant description. In the event the COL applicant chooses a fuel design different than that described herein, the rod patterns and associated power distribution consistent with the chosen loading patterns, bundle descriptions, and the mechanical design of the fuel bundle assembly shall satisfy the criteria identified in this Section 4B.

Table 4A-1

Incremental Exposure Steps and Related Figure Numbers

Incremental Exposure (GWd/MT)	Figure Numbers
0.0	4A-1a through 4A-1e
1.1	4A-2a through 4A-2e
2.2	4A-3a through 4A-3e
3.3	4A-4a through 4A-4e
4.4	4A-5a through 4A-5e
5.5	4A-6a through 4A-6e
6.6	4A-7a through 4A-7e
7.7	4A-8a through 4A-8e
8.8	4A-9a through 4A-9e
9.9	4A-10a through 4A-10e
11.0	4A-11a through 4A-11e
12.1	4A-12a through 4A-12e
13.2	4A-13a through 4A-13e
14.3	4A-14a through 4A-14e
15.4	4A-15a through 4A-15e
16.5	4A-16a through 4A-16e
17.6	4A-17a through 4A-17e
18.5	4A-18a through 4A-18e

Figure 4A-1a. Control Rod Pattern Summary at 0.0 GWd/MT Exposure

```
( ROD PATTERN DEPLETION

NITER    0  POWER        IMAX  19  POWER(MWT)          4.5000E+03  ( 100.0 %)
IBOUN    1  1/4          JMAX  19  PRESSURE(PSIA)      1.0550E+03
IRN      1  MIRROR       KMAX  25  FLOW(*10E-6LB/HR)   7.8508E+01  ( 100.0 %)           CONTROL ROD CONFIGURATION
ILPA     0               NSMAX 10  BYPASS(LB/HR)       1.1742E+07  (  15.0 %)              IN NOTCHES WITHDRAWN
IFLW     2  DETAIL       LMAX  20  ENTHALPY(BTU/LB)        512.30
RSTART   0  NEW          LVDCT  8  INLET TEMP(DEG F)       520.47
NEWPHY   2               IPFTL  0  BEGINNING EXPOSURE    13105.1    1  3  5  7  9 11 13 15 17 19 21 23 25 27 29 31 33 35 75
NEXO     3  CALC.                  DELTA EXPOS.(DELTE)       0.0
RBOCA    0               IALPRM 0  DELBRN                    0.0                                                         71
IACF     0               IFAST  0  TOTAL NOTCHES            1394
            IPDOME  1  IAHB  0  CORE FUEL MASS     MTU:162.928      1                      40                           67
                                  CORE FUEL MASS     STU:179.596
ENERGY (MWD) (DELTE)         0.  ENERGY (MWD) (DELBRN)       0.     3                                                   63
CYCLE ENERGY (MWD)           0.  CYCLE EXPOSURE            0.0
CORE AVG. POWER DENSITY   54.328033                                5                59                                 59
NEUTRON MULTIPLICATION    1.00738454 FINAL AVG. EXPOSURE   13105.1
DIFP   (EPS5 = 0.00200)  0.00133967 CORE AVG. NEUTRON FLUX 1.424E+14 7                                                 55
AVERAGE VOID FRACTION     0.547267 CORE AVG. GD WORTH        0.000
CORE PRESSURE DROP,PSI    8.192806 CORE AVG. GD RESIDUAL WORTH 0.000 9          47          16                         51
EXP RATIO INDEX (INER-II)   0.0000 CORE AVERAGE XENON WORTH -0.0216
                                                                  11                                                  47
CORE HISTORY MAX. VALUES:     LOCATION: I  J  K
  NODAL EXPOSURE, MWD/T   47824.      7  7  5   METRIC   52716.    13     59          50                               43
  BUNDLE EXPOSURE, MWD/T  39032.     13  2      METRIC   43025.
  EXPOSURE RATIO, NEXRAT  0.0000      0  0  0                      15                                                  39
  AXIAL POWER PEAK        1.4253            5
                                                                  17 40          16          22                       35

                                                                  19                                                  31

                                                                  21                                                  27

                                                                  23                                                  23

                                                                  25                                                  19

                                                                  27                                                  15

                                                                  29                                                  11

                                                                  31                                                   7

                                                                  33                                                   3
```

Figure 4A-1b. Relative Axial Power at 0.0 GWd/MT Exposure

0.0GWD/MT

Node	Axial Power
25	0.124
24	0.246
23	0.365
22	0.484
21	0.597
20	0.692
19	0.778
18	0.848
17	0.904
16	0.999
15	1.156
14	1.227
13	1.285
12	1.321
11	1.347
10	1.361
9	1.356
8	1.367
7	1.388
6	1.411
5	1.425
4	1.408
3	1.308
2	1.056
1	0.546
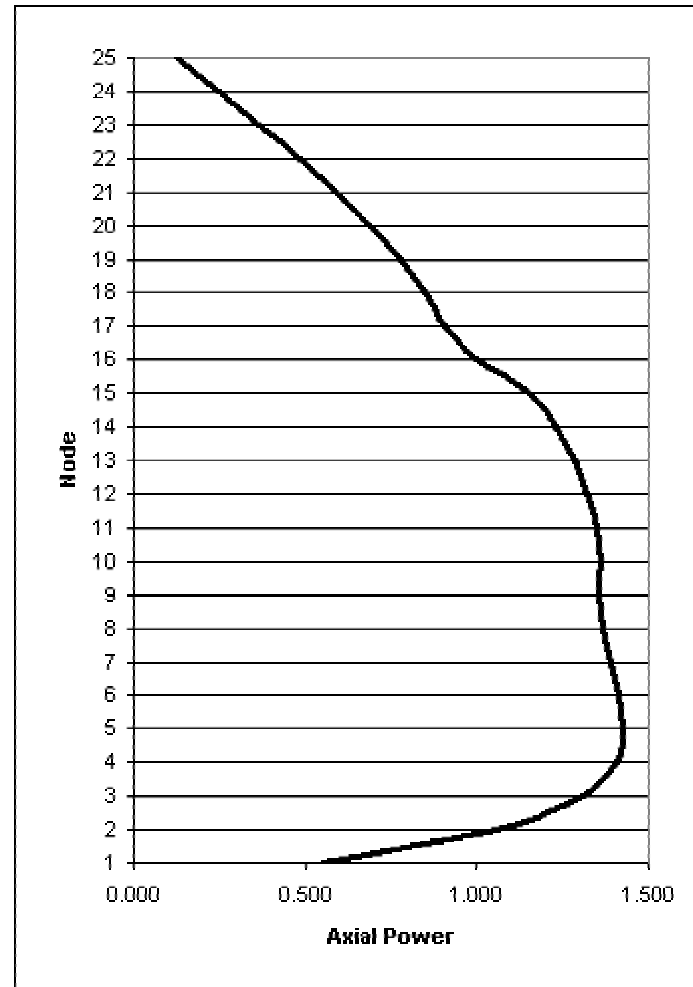
Figure 4A-1c. Axial Exposure at 0.0 GWd/MT Exposure

0.0GWD/MT

Node	Axial Exposure (MWD/MT)
25	3064.4
24	5314.1
23	7426.4
22	9532.7
21	11406.6
20	12957.8
19	14216.4
18	15117.2
17	15652.8
16	15999.9
15	15447.7
14	16013.1
13	16500.0
12	16865.0
11	17193.6
10	17465.8
9	17613.4
8	17804.7
7	18064.1
6	18307.6
5	18383.4
4	17976.8
3	16406.0
2	12947.7
1	6569.7

4A-5
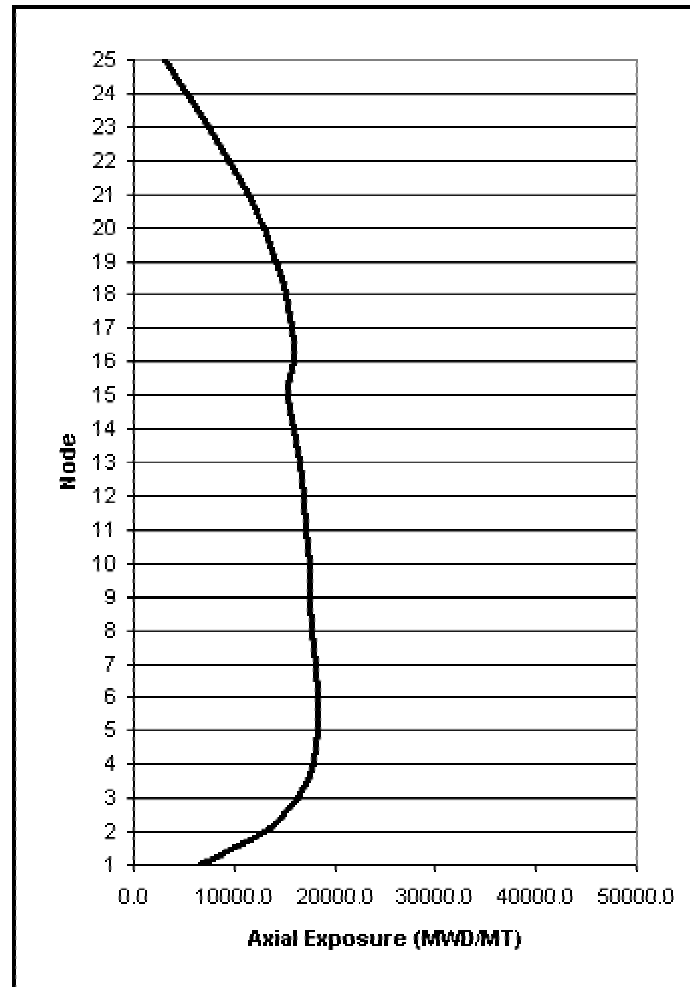
Figure 4A-1d. Relative Integrated Power Per Bundle at 0.0 GWd/MT Exposure

	1	2	3	4	5	6	7	8	9	10	11	12	13	14	15	16	17	18	19
1															0.37	0.42	0.44	0.43	0.40
2													0.37	0.49	0.58	0.76	0.78	0.72	0.62
3											0.40	0.49	0.67	0.76	0.88	0.92	0.94	0.85	0.63
4									0.36	0.47	0.66	0.75	0.85	0.91	0.97	1.04	1.02	0.95	0.84
5								0.43	0.62	0.71	0.82	0.92	0.99	1.02	1.05	1.09	0.98	1.09	1.06
6							0.42	0.65	0.78	0.86	0.96	1.04	1.08	1.07	1.09	1.11	1.15	1.14	1.16
7						0.42	0.54	0.79	0.92	1.00	0.97	1.14	1.09	1.12	1.02	1.12	1.19	1.22	1.23
8					0.43	0.65	0.79	0.89	1.01	1.05	1.16	1.06	1.15	1.21	1.15	1.14	1.21	1.25	1.29
9				0.36	0.62	0.78	0.92	1.01	1.07	1.08	1.09	1.14	1.20	1.21	1.20	1.20	1.22	1.24	1.25
10				0.47	0.71	0.86	1.00	1.05	1.08	1.09	1.10	1.14	1.19	1.20	1.21	1.20	1.21	1.18	1.14
11			0.40	0.66	0.82	0.96	0.97	1.16	1.09	1.10	0.94	1.03	1.19	1.20	1.17	1.26	1.20	1.12	0.85
12			0.49	0.75	0.92	1.04	1.14	1.06	1.14	1.14	1.03	1.02	1.16	1.19	1.26	1.25	1.19	1.09	0.86
13		0.37	0.67	0.85	0.99	1.08	1.09	1.15	1.20	1.19	1.19	1.16	1.18	1.21	1.23	1.23	1.19	1.16	1.13
14		0.49	0.76	0.91	1.02	1.07	1.12	1.21	1.21	1.20	1.20	1.19	1.21	1.19	1.19	1.19	1.18	1.18	1.18
15	0.37	0.58	0.88	0.98	1.05	1.09	1.02	1.15	1.20	1.21	1.17	1.26	1.23	1.19	1.00	1.05	1.15	1.20	1.17
16	0.42	0.76	0.92	1.04	1.09	1.11	1.12	1.14	1.20	1.20	1.26	1.25	1.23	1.19	1.05	1.05	1.18	1.24	1.28
17	0.44	0.78	0.94	1.02	0.98	1.15	1.19	1.21	1.22	1.21	1.20	1.19	1.19	1.19	1.15	1.18	1.20	1.23	1.24
18	0.43	0.72	0.85	0.95	1.09	1.14	1.22	1.25	1.24	1.18	1.12	1.09	1.16	1.18	1.20	1.24	1.23	1.18	1.15
19	0.40	0.62	0.63	0.84	1.06	1.16	1.23	1.29	1.25	1.14	0.85	0.86	1.13	1.18	1.17	1.28	1.24	1.15	0.89

Figure 4A-1e. Average Bundle Exposure at 0.0 GWd/MT Exposure

	1	2	3	4	5	6	7	8	9	10	11	12	13	14	15	16	17	18	19
1															36.82	35.60	38.91	35.94	37.26
2													42.99	37.59	36.71	19.18	17.64	16.87	0.00
3											39.35	36.82	19.73	0.00	21.61	22.60	19.84	0.00	33.62
4									39.24	37.15	17.75	0.00	0.00	0.00	22.60	20.50	0.00	0.00	14.77
5								41.12	14.88	0.00	0.00	0.00	18.74	0.00	0.00	0.00	32.41	0.00	22.60
6							38.25	16.31	0.00	0.00	0.00	21.38	0.00	22.82	0.00	23.26	0.00	23.04	0.00
7						38.25	38.91	0.00	18.41	0.00	32.19	20.06	0.00	0.00	27.23	20.83	22.05	0.00	23.59
8					41.12	16.31	0.00	0.00	0.00	22.16	17.31	31.53	0.00	13.45	15.43	16.09	0.00	21.94	23.04
9				39.24	14.88	0.00	18.41	0.00	18.63	0.00	0.00	0.00	21.05	0.00	21.94	0.00	22.05	0.00	21.94
10				37.15	0.00	0.00	0.00	22.16	0.00	23.15	0.00	21.83	0.00	22.60	0.00	0.00	0.00	22.05	0.00
11			39.46	17.75	0.00	0.00	32.19	17.31	0.00	0.00	30.64	21.94	21.72	0.00	30.86	21.94	22.38	0.00	23.37
12			36.82	0.00	0.00	21.38	20.06	31.53	0.00	21.83	21.94	22.93	0.00	0.00	21.83	22.38	0.00	0.00	22.16
13		42.99	19.73	0.00	18.63	0.00	0.00	0.00	21.05	0.00	21.72	0.00	23.15	0.00	22.16	0.00	22.60	0.00	22.49
14		37.59	0.00	0.00	0.00	22.82	0.00	13.45	0.00	22.60	0.00	0.00	0.00	22.93	0.00	22.16	0.00	22.05	0.00
15	36.82	36.71	21.61	22.60	0.00	0.00	27.23	15.43	21.94	0.00	30.86	21.83	22.16	0.00	30.64	22.82	0.00	0.00	29.10
16	35.60	19.18	22.60	20.50	0.00	23.26	20.83	16.09	0.00	0.00	21.94	22.38	0.00	22.16	22.71	22.93	0.00	21.50	22.71
17	38.91	17.64	19.84	0.00	32.41	0.00	21.94	0.00	22.05	0.00	22.38	0.00	22.60	0.00	0.00	0.00	23.04	0.00	22.60
18	35.94	16.87	0.00	0.00	0.00	22.93	0.00	21.94	0.00	22.05	0.00	0.00	0.00	22.05	0.00	21.50	0.00	23.15	0.00
19	37.26	0.00	33.62	14.77	22.60	0.00	23.59	23.04	21.94	0.00	23.37	22.16	22.49	0.00	29.10	22.71	22.60	0.00	23.15

Figure 4A-2a. Control Rod Pattern Summary at 1.1 GWd/MT Exposure

```
( ROD PATTERN DEPLETION

NITER    0  POWER         IMAX  19  POWER(MWT)           4.5000E+03  ( 100.0 %)
IBOUN    1  1/4           JMAX  19  PRESSURE(PSIA)       1.0550E+03
IRN      1  MIRROR        KMAX  25  FLOW(*10E-6LB/HR)    7.8508E+01  ( 100.0 %)
ILPA     0                NSMAX 10  BYPASS(LB/HR)        1.1742E+07  (  15.0 %)      CONTROL ROD CONFIGURATION
IFLW     2  DETAIL        LMAX  20  ENTHALPY(BTU/LB)        512.30                     IN NOTCHES WITHDRAWN
RSTART   0  NEW           LVDCT  6  INLET TEMP(DEG F)       520.47
NEWPHY   2                IPFTL  0  BEGINNING EXPOSURE    13105.1      1  3  5  7  9 11 13 15 17 19 21 23 25 27 29 31 33 35 75
NEXO     3  CALC.                   DELTA EXPOS.(DELTE)      0.0
RBOCA    1                IALPRM 0  DELBRN                1000.0                                                         71
IACF     0                IFAST  0  TOTAL NOTCHES           1394
            IPDOME   1    IAHB   0  CORE FUEL MASS    MTU:162.928    1                         40                       67
                                    CORE FUEL MASS    STU:179.596
ENERGY (MWD) (DELTE)           0.  ENERGY (MWD) (DELBRN)   179596.    3                                                  63
CYCLE ENERGY (MWD)        179598.  CYCLE EXPOSURE          1000.0
CORE AVG. POWER DENSITY  54.328033                                   5                    59                            59
NEUTRON MULTIPLICATION  1.00571275 FINAL AVG. EXPOSURE     14105.1
DIFP   (EPS5 = 0.00200)  0.00151962 CORE AVG. NEUTRON FLUX 1.430E+14  7                                                  55
AVERAGE VOID FRACTION     0.538595 CORE AVG. GD WORTH        0.000
CORE PRESSURE DROP,PSI    8.128465 CORE AVG. GD RESIDUAL WORTH 0.000  9              47         16                       51
EXP RATIO INDEX (INER-II)   0.0000 CORE AVERAGE XENON WORTH  -0.0216
                                                                    11                                                  47
CORE HISTORY MAX. VALUES:      LOCATION: I   J   K
  NODAL EXPOSURE, MWD/T  48513.        7   7   5   METRIC    53476.  13        59         50                            43
  BUNDLE EXPOSURE, MWD/T 39404.       13   2       METRIC    43435.
  EXPOSURE RATIO, NEXRAT 0.0000        0   0   0                     15                                                  39
  AXIAL POWER PEAK        1.3669               6
                                                                    17 40         16         22                         35

                                                                    19                                                  31

                                                                    21                                                  27

                                                                    23                                                  23

                                                                    25                                                  19

                                                                    27                                                  15

                                                                    29                                                  11

                                                                    31                                                   7

                                                                    33                                                   3
```

Figure 4A-2b. Relative Axial Power at 1.1 GWd/MT Exposure

1.1GWD/MT

Node	Axial Power
25	0.133
24	0.264
23	0.392
22	0.517
21	0.633
20	0.730
19	0.816
18	0.885
17	0.941
16	1.035
15	1.191
14	1.257
13	1.310
12	1.340
11	1.359
10	1.365
9	1.352
8	1.353
7	1.360
6	1.367
5	1.364
4	1.328
3	1.218
2	0.979
1	0.510
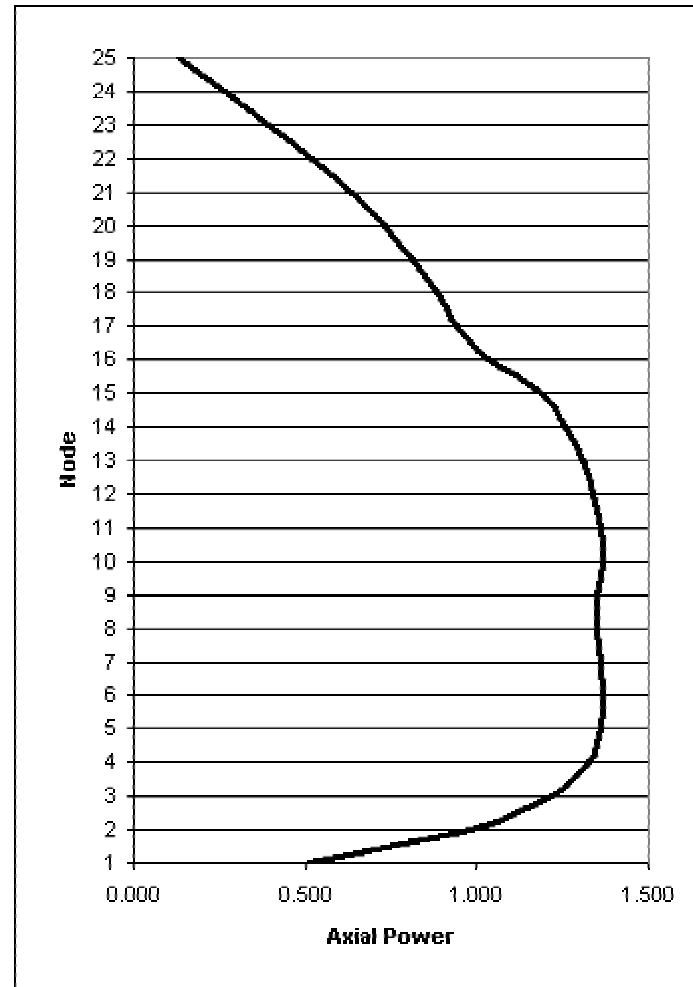
Figure 4A-2c. Axial Exposure at 1.1 GWd/MT Exposure

1.1GWD/MT

Node	Axial Exposure (MWD/MT)
25	3243.8
24	5625.9
23	7870.8
22	10121.7
21	12132.7
20	13800.0
19	15162.5
18	16148.4
17	16752.4
16	17170.4
15	16637.1
14	17275.5
13	17822.1
12	18224.4
11	18579.8
10	18866.4
9	19010.0
8	19213.0
7	19493.8
6	19760.7
5	19851.5
4	19426.8
3	17753.3
2	14035.8
1	7120.2
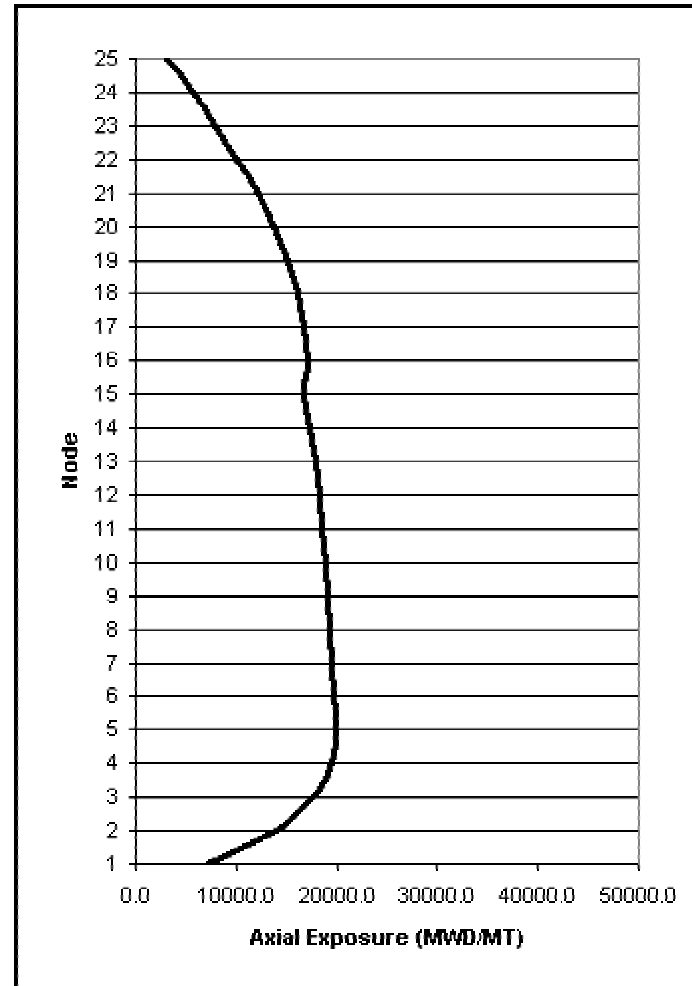
Figure 4A-2d. Relative Integrated Power Per Bundle at 1.1 GWd/MT Exposure

														0.37	0.41	0.44	0.43	0.4
												0.37	0.48	0.58	0.75	0.78	0.72	0.62
										0.39	0.49	0.67	0.76	0.87	0.91	0.93	0.85	0.64
								0.36	0.47	0.66	0.74	0.84	0.91	0.97	1.03	1.01	0.96	0.85
							0.43	0.62	0.71	0.82	0.92	0.99	1.02	1.05	1.09	0.98	1.09	1.06
						0.42	0.65	0.78	0.86	0.96	1.04	1.08	1.07	1.09	1.11	1.15	1.13	1.16
					0.42	0.54	0.79	0.92	1	0.96	1.14	1.1	1.13	1.03	1.13	1.18	1.22	1.22
				0.43	0.65	0.79	0.89	1.01	1.05	1.16	1.06	1.16	1.23	1.17	1.16	1.22	1.24	1.27
			0.36	0.62	0.78	0.92	1.01	1.08	1.09	1.1	1.15	1.21	1.22	1.21	1.21	1.22	1.24	1.24
			0.47	0.71	0.86	1	1.05	1.09	1.09	1.1	1.14	1.2	1.2	1.22	1.21	1.21	1.18	1.14
		0.39	0.66	0.82	0.96	0.96	1.16	1.1	1.1	0.94	1.03	1.2	1.21	1.17	1.25	1.2	1.12	0.85
		0.49	0.75	0.92	1.04	1.14	1.06	1.15	1.14	1.03	1.02	1.17	1.2	1.25	1.24	1.2	1.1	0.86
	0.37	0.67	0.84	0.99	1.08	1.1	1.16	1.21	1.2	1.2	1.17	1.18	1.21	1.22	1.23	1.18	1.16	1.12
	0.48	0.76	0.91	1.02	1.07	1.13	1.23	1.22	1.2	1.21	1.2	1.21	1.19	1.19	1.19	1.19	1.18	1.18
0.37	0.58	0.87	0.97	1.05	1.09	1.03	1.17	1.21	1.22	1.17	1.25	1.22	1.19	1.01	1.05	1.15	1.2	1.16
0.41	0.75	0.91	1.03	1.09	1.11	1.13	1.16	1.21	1.21	1.25	1.24	1.23	1.19	1.05	1.05	1.18	1.23	1.26
0.44	0.78	0.93	1.01	0.98	1.15	1.18	1.22	1.22	1.21	1.2	1.2	1.18	1.19	1.15	1.18	1.19	1.23	1.22
0.43	0.72	0.85	0.96	1.09	1.13	1.22	1.24	1.24	1.18	1.12	1.1	1.16	1.18	1.2	1.23	1.23	1.17	1.14
0.4	0.62	0.64	0.85	1.06	1.16	1.22	1.27	1.24	1.14	0.85	0.86	1.12	1.18	1.16	1.26	1.22	1.14	0.89

Figure 4A-2e. Average Bundle Exposure at 1.1 GWd/MT Exposure

	1	2	3	4	5	6	7	8	9	10	11	12	13	14	15	16	17	18	19
1															37.26	36.05	39.35	36.38	37.70
2													43.43	38.14	37.37	19.95	18.52	17.75	0.66
3											39.79	37.37	20.50	0.88	22.60	23.59	20.94	0.99	34.28
4									39.57	37.70	18.41	0.77	0.88	0.99	23.59	21.61	1.10	1.10	15.65
5								41.56	15.54	0.77	0.88	0.99	19.73	1.10	1.21	1.21	33.51	1.21	23.81
6							38.69	17.09	0.88	0.99	1.10	22.49	1.21	24.03	1.21	24.47	1.21	24.25	1.32
7						38.69	39.46	0.88	19.40	1.10	33.18	21.27	1.21	1.21	28.33	22.05	23.26	1.32	24.91
8					41.56	17.09	0.88	0.99	1.10	23.26	18.52	32.63	1.21	14.77	16.64	17.42	1.32	23.26	24.47
9				39.57	15.54	0.88	19.40	1.10	19.73	1.21	1.21	1.21	22.38	1.32	23.26	1.32	23.37	1.32	23.37
10				37.70	0.77	0.99	1.10	23.26	1.21	24.36	1.21	23.15	1.32	23.92	1.32	1.32	1.32	23.37	1.21
11			39.90	18.41	0.88	1.10	33.18	18.52	1.21	1.21	31.64	23.04	23.04	1.32	32.08	23.37	23.70	1.21	24.25
12			37.37	0.77	0.99	22.49	21.27	32.74	1.21	23.15	23.04	24.14	1.32	1.32	23.15	23.81	1.32	1.21	23.15
13		43.43	20.50	0.88	19.73	1.21	1.21	1.21	22.38	1.32	23.04	1.32	24.36	1.32	23.59	1.32	23.92	1.32	23.70
14		38.14	0.88	0.99	1.10	23.92	1.21	14.77	1.32	23.81	1.32	1.32	1.32	24.25	1.32	23.48	1.32	23.37	1.32
15	37.26	37.37	22.49	23.59	1.21	1.21	28.33	16.64	23.26	1.32	32.08	23.15	23.59	1.32	31.75	23.92	1.21	1.32	30.42
16	36.05	19.95	23.59	21.61	1.21	24.47	22.05	17.42	1.32	1.32	23.37	23.81	1.32	23.48	23.92	24.14	1.32	22.82	24.14
17	39.35	18.52	20.94	1.10	33.51	1.21	23.26	1.32	23.37	1.32	23.70	1.32	23.92	1.32	1.21	1.32	24.36	1.32	23.92
18	36.38	17.75	0.99	1.10	1.21	24.25	1.32	23.26	1.32	23.37	1.21	1.21	1.32	23.37	1.32	22.82	1.32	24.36	1.21
19	37.70	0.66	34.28	15.65	23.81	1.32	24.91	24.47	23.37	1.21	24.25	23.15	23.70	1.32	30.42	24.14	23.92	1.21	24.03

Figure 4A-3a. Control Rod Pattern Summary at 2.2 GWd/MT Exposure

```
( ROD PATTERN DEPLETION

NITER    0  POWER          IMAX  19  POWER(MWT)          4.5000E+03  ( 100.0 %)
IBOUN    1  1/4            JMAX  19  PRESSURE(PSIA)      1.0550E+03
IRN      1  MIRROR         KMAX  25  FLOW(*10E-6LB/HR)   7.8508E+01  ( 100.0 %)
ILPA     0                 NSMAX 10  BYPASS(LB/HR)       1.1742E+07  (  15.0 %)      CONTROL ROD CONFIGURATION
IFLW     2  DETAIL         LMAX  20  ENTHALPY(BTU/LB)        512.30                   IN NOTCHES WITHDRAWN
RSTART   0  NEW            LVDCT  7  INLET TEMP(DEG F)       520.47
NEWPHY   2                 IPFTL  0  BEGINNING EXPOSURE    14105.1    1  3  5  7  9 11 13 15 17 19 21 23 25 27 29 31 33 35 75
NEXO     3  CALC.                    DELTA EXPOS.(DELTE)       0.0
RBOCA    1                 IALPRM 0  DELBRN                 1000.0                                                          71
IACF     0                 IFAST  0  TOTAL NOTCHES             1393
            IPDOME   1     IAHB   0  CORE FUEL MASS    MTU:162.928    1                              46                     67
                                     CORE FUEL MASS    STU:179.596
ENERGY (MWD) (DELTE)              0. ENERGY (MWD) (DELBRN)   179596.   3                                                    63
CYCLE ENERGY (MWD)          359195. CYCLE EXPOSURE            2000.0
CORE AVG. POWER DENSITY   54.328033                                   5                    65                              59
NEUTRON MULTIPLICATION    1.00590420 FINAL AVG. EXPOSURE     15105.1
DIFP   (EPS5 = 0.00200)    0.00114238 CORE AVG. NEUTRON FLUX 1.434E+14 7                                                   55
AVERAGE VOID FRACTION      0.539310 CORE AVG. GD WORTH         0.000
CORE PRESSURE DROP,PSI     8.113264 CORE AVG. GD RESIDUAL WORTH 0.000  9               21          12                      51
EXP RATIO INDEX (INER-II)    0.0000 CORE AVERAGE XENON WORTH  -0.0217
                                                                     11                                                    47
CORE HISTORY MAX. VALUES:      LOCATION: I   J   K
  NODAL EXPOSURE, MWD/T  49163.        7   7   5    METRIC   54192.  13          65           67                           43
  BUNDLE EXPOSURE, MWD/T 39773.       13   2        METRIC   43842.
  EXPOSURE RATIO, NEXRAT 0.0000        0   0   0                     15                                                    39
  AXIAL POWER PEAK       1.4242                    9
                                                                     17 46           12             3                      35

                                                                     19                                                    31

                                                                     21                                                    27

                                                                     23                                                    23

                                                                     25                                                    19

                                                                     27                                                    15

                                                                     29                                                    11

                                                                     31                                                     7

                                                                     33                                                     3
```

Figure 4A-3b. Relative Axial Power at 2.2 GWd/MT Exposure

2.2 GWD/MT

Node	Axial Power
25	0.132
24	0.260
23	0.385
22	0.506
21	0.613
20	0.706
19	0.785
18	0.852
17	0.908
16	1.003
15	1.162
14	1.241
13	1.307
12	1.358
11	1.397
10	1.423
9	1.424
8	1.407
7	1.392
6	1.382
5	1.365
4	1.318
3	1.202
2	0.964
1	0.507
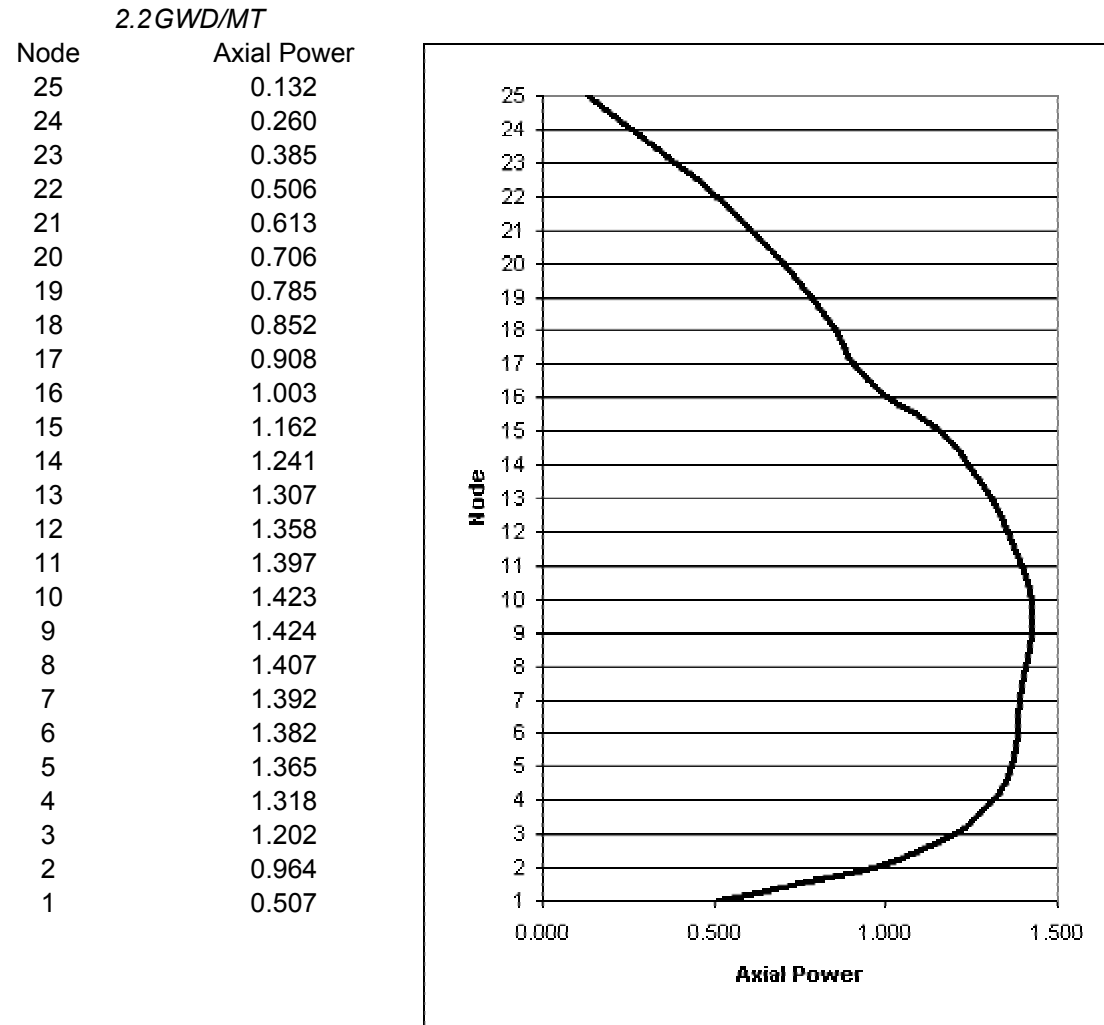
Figure 4A-3c. Axial Exposure at 2.2 GWd/MT Exposure

2.2GWD/MT

Node	Axial Exposure (MWD/MT)
25	3436.3
24	5960.2
23	8347.5
22	10751.4
21	12903.3
20	14688.4
19	16154.8
18	17225.7
17	17897.2
16	18382.9
15	17862.3
14	18568.9
13	19169.9
12	19602.9
11	19978.2
10	20271.2
9	20402.3
8	20606.0
7	20894.5
6	21168.4
5	21255.8
4	20794.9
3	19007.9
2	15043.7
1	7635.3
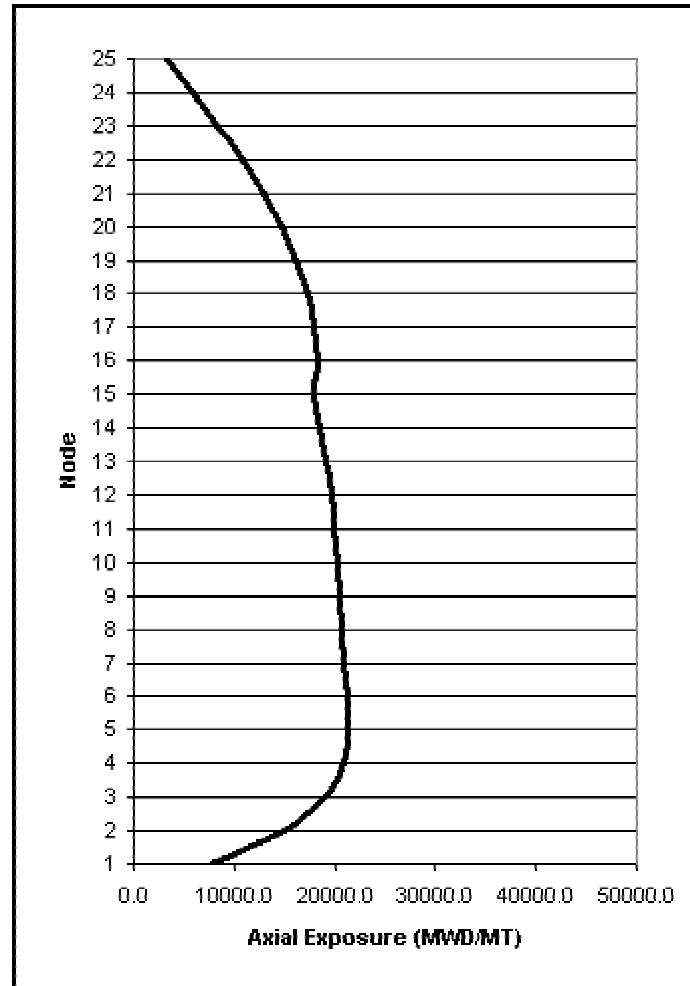
Figure 4A-3d. Relative Integrated Power Per Bundle at 2.2 GWd/MT Exposure

	1	2	3	4	5	6	7	8	9	10	11	12	13	14	15	16	17	18	19
1															0.37	0.41	0.44	0.44	0.41
2													0.37	0.48	0.57	0.75	0.78	0.74	0.65
3											0.39	0.49	0.67	0.76	0.87	0.91	0.94	0.88	0.67
4									0.36	0.47	0.66	0.75	0.85	0.92	0.97	1.04	1.03	0.99	0.90
5								0.43	0.62	0.71	0.82	0.92	0.99	1.04	1.07	1.11	0.99	1.11	1.07
6							0.41	0.64	0.78	0.86	0.96	1.03	1.10	1.07	1.12	1.12	1.17	1.14	1.18
7						0.41	0.53	0.78	0.90	0.99	0.94	1.12	1.11	1.16	1.06	1.16	1.19	1.24	1.21
8					0.43	0.64	0.78	0.89	1.00	1.02	1.13	1.03	1.17	1.24	1.21	1.20	1.25	1.23	1.25
9				0.36	0.62	0.78	0.90	1.00	1.05	1.06	1.07	1.12	1.18	1.23	1.20	1.24	1.22	1.25	1.22
10				0.47	0.71	0.86	0.99	1.02	1.06	1.03	1.04	1.06	1.16	1.17	1.23	1.22	1.23	1.17	1.15
11			0.39	0.66	0.82	0.96	0.94	1.13	1.07	1.04	0.77	0.84	1.12	1.19	1.14	1.23	1.19	1.13	0.83
12			0.49	0.75	0.92	1.03	1.12	1.03	1.12	1.06	0.84	0.84	1.12	1.18	1.23	1.22	1.21	1.11	0.84
13		0.37	0.67	0.85	0.99	1.10	1.11	1.17	1.18	1.16	1.12	1.12	1.14	1.21	1.22	1.25	1.19	1.18	1.12
14		0.48	0.76	0.92	1.04	1.07	1.16	1.24	1.23	1.17	1.19	1.18	1.21	1.19	1.23	1.21	1.23	1.19	1.20
15	0.37	0.57	0.87	0.97	1.07	1.12	1.06	1.21	1.20	1.23	1.14	1.23	1.22	1.23	1.09	1.15	1.21	1.23	1.16
16	0.41	0.75	0.91	1.04	1.11	1.12	1.16	1.20	1.24	1.22	1.23	1.22	1.25	1.21	1.15	1.15	1.23	1.23	1.25
17	0.44	0.78	0.94	1.03	0.99	1.17	1.19	1.25	1.22	1.23	1.19	1.21	1.19	1.23	1.21	1.23	1.21	1.25	1.21
18	0.44	0.74	0.88	0.99	1.11	1.14	1.24	1.23	1.25	1.17	1.13	1.11	1.18	1.19	1.23	1.23	1.25	1.16	1.14
19	0.41	0.65	0.67	0.90	1.07	1.18	1.21	1.25	1.22	1.15	0.83	0.84	1.12	1.20	1.16	1.25	1.21	1.14	0.81

Figure 4A-3e. Average Bundle Exposure at 2.2 GWd/MT Exposure

	1	2	3	4	5	6	7	8	9	10	11	12	13	14	15	16	17	18	19
1															37.70	36.49	39.90	36.93	38.14
2													43.87	38.58	38.03	20.83	19.40	18.52	1.32
3											40.23	37.81	21.27	1.65	23.48	24.58	21.94	1.87	34.94
4									40.01	38.25	19.18	1.65	1.87	1.98	24.69	22.82	2.20	2.09	16.64
5								42.00	16.20	1.54	1.76	1.98	20.83	2.20	2.31	2.43	34.61	2.43	24.91
6							39.24	17.75	1.76	1.87	2.09	23.70	2.43	25.13	2.43	25.68	2.54	25.46	2.54
7						39.24	40.12	1.76	20.39	2.20	34.28	22.60	2.43	2.43	29.54	23.37	24.58	2.65	26.35
8					42.00	17.75	1.76	1.98	2.20	24.47	19.84	33.84	2.54	16.09	17.97	18.63	2.65	24.58	25.90
9				40.01	16.20	1.76	20.39	2.20	20.94	2.43	2.43	2.54	23.70	2.65	24.58	2.65	24.69	2.76	24.69
10				38.25	1.54	1.87	2.20	24.47	2.43	25.46	2.43	24.36	2.65	25.24	2.65	2.65	2.65	24.69	2.54
11			40.23	19.18	1.76	2.09	34.28	19.84	2.43	2.43	32.74	24.25	24.36	2.65	33.40	24.69	25.02	2.43	25.24
12			37.92	1.65	1.98	23.70	22.60	33.84	2.54	24.36	24.25	25.24	2.54	2.65	24.58	25.13	2.65	2.43	24.03
13		43.76	21.27	1.87	20.83	2.43	2.43	2.54	23.70	2.65	24.36	2.54	25.68	2.65	24.91	2.76	25.24	2.54	24.91
14		38.58	1.65	1.98	2.20	25.13	2.43	16.09	2.65	25.13	2.65	2.65	2.65	25.57	2.65	24.80	2.65	24.69	2.65
15	37.70	38.03	23.48	24.69	2.31	2.43	29.54	17.97	24.58	2.65	33.40	24.58	24.91	2.65	32.85	25.13	2.54	2.65	31.64
16	36.49	20.83	24.58	22.82	2.43	25.68	23.37	18.63	2.65	2.65	24.69	25.13	2.76	24.80	25.13	25.24	2.65	24.25	25.46
17	39.90	19.40	21.94	2.20	34.61	2.54	24.58	2.65	24.69	2.65	25.02	2.65	25.24	2.65	2.54	2.65	25.57	2.76	25.35
18	36.93	18.52	1.87	2.09	2.43	25.46	2.65	24.58	2.76	24.69	2.43	2.43	2.54	24.69	2.65	24.25	2.76	25.68	2.54
19	38.14	1.32	34.94	16.64	24.91	2.54	26.35	25.90	24.69	2.54	25.24	24.03	24.91	2.65	31.64	25.46	25.35	2.54	25.02

Figure 4A-4a. Control Rod Pattern Summary at 3.3 GWd/MT Exposure

```
( ROD PATTERN DEPLETION

NITER  0  POWER        IMAX 19  POWER(MWT)          4.5000E+03  ( 100.0 %)
IBOUN  1  1/4          JMAX 19  PRESSURE(PSIA)      1.0550E+03
IRN    1  MIRROR       KMAX 25  FLOW(*10E-6LB/HR)   7.8508E+01  ( 100.0 %)          CONTROL ROD CONFIGURATION
ILPA   0               NSMAX 10 BYPASS(LB/HR)       1.1742E+07  (  15.0 %)            IN NOTCHES WITHDRAWN
IFLW   2  DETAIL       LMAX 20  ENTHALPY(BTU/LB)       512.30
RSTART 0  NEW          LVDCT 6  INLET TEMP(DEG F)      520.47
NEWPHY 2               IPFTL 0  BEGINNING EXPOSURE   15105.1    1  3  5  7  9 11 13 15 17 19 21 23 25 27 29 31 33 35 75
NEXO   3  CALC.                 DELTA EXPOS.(DELTE)      0.0
RBOCA  1               IALPRM 0 DELBRN               1000.0                                                       71
IACF   0               IFAST 0  TOTAL NOTCHES           1393
        IPDOME  1  IAHB  0  CORE FUEL MASS  MTU:162.928   1                    46                                 67
                            CORE FUEL MASS  STU:179.596
ENERGY (MWD) (DELTE)        0. ENERGY (MWD) (DELBRN)   179596.   3                                                63
CYCLE ENERGY (MWD)      538793. CYCLE EXPOSURE          3000.0
CORE AVG. POWER DENSITY  54.328033                            5              65                                   59
NEUTRON MULTIPLICATION  1.00554371 FINAL AVG. EXPOSURE   16105.1
DIFP  (EPS5 = 0.00200)  0.00116009 CORE AVG. NEUTRON FLUX 1.438E+14  7                                            55
AVERAGE VOID FRACTION    0.534038 CORE AVG. GD WORTH       0.000
CORE PRESSURE DROP,PSI   8.093859 CORE AVG. GD RESIDUAL WORTH 0.000  9        21          12                      51
EXP RATIO INDEX (INER-II)  0.0000 CORE AVERAGE XENON WORTH  -0.0218
                                                              11                                                 47
CORE HISTORY MAX. VALUES:     LOCATION: I  J  K
  NODAL EXPOSURE, MWD/T  49804.        7  7  5  METRIC  54899.  13     65          67                             43
  BUNDLE EXPOSURE, MWD/T 40142.       13  2     METRIC  44248.
  EXPOSURE RATIO, NEXRAT 0.0000        0  0  0                 15                                                 39
  AXIAL POWER PEAK       1.4071             10
                                                              17 46           12             3                   35

                                                              19                                                 31

                                                              21                                                 27

                                                              23                                                 23

                                                              25                                                 19

                                                              27                                                 15

                                                              29                                                 11

                                                              31                                                  7

                                                              33                                                  3
```

Figure 4A-4b. Relative Axial Power at 3.3 GWd/MT Exposure

3.3GWD/MT

Node	Axial Power
25	0.142
24	0.279
23	0.412
22	0.538
21	0.647
20	0.741
19	0.819
18	0.883
17	0.936
16	1.026
15	1.180
14	1.251
13	1.310
12	1.354
11	1.387
10	1.407
9	1.405
8	1.385
7	1.365
6	1.350
5	1.327
4	1.276
3	1.159
2	0.929
1	0.493
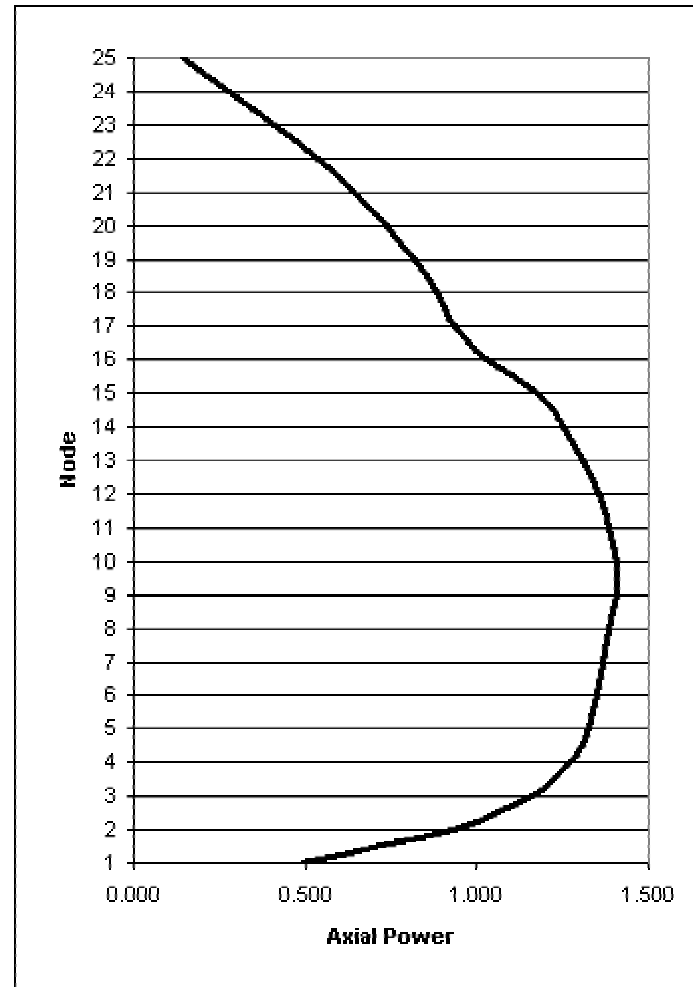
Figure 4A-4c. Axial Exposure at 3.3 GWd/MT Exposure

3.3GWD/MT

Node	Axial Exposure (MWD/MT)
25	3626.9
24	6289.9
23	8816.4
22	11366.8
21	13648.8
20	15547.1
19	17109.9
18	18262.4
17	19002.2
16	19558.5
15	19057.9
14	19845.9
13	20514.7
12	21000.0
11	21415.6
10	21734.6
9	21868.7
8	22055.6
7	22328.2
6	22592.1
5	22661.6
4	22152.5
3	20245.5
2	16036.4
1	8147.0

ESBWR Design Control Document/Tier 2
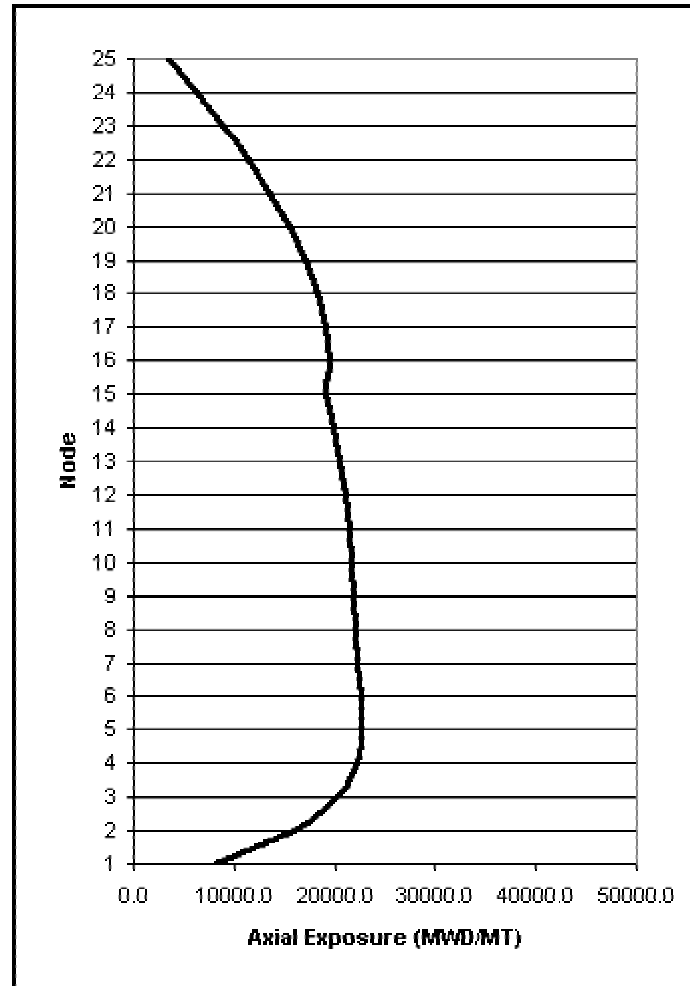
Figure 4A-4d. Relative Integrated Power Per Bundle at 3.3 GWd/MT Exposure

	1	2	3	4	5	6	7	8	9	10	11	12	13	14	15	16	17	18	19
1															0.36	0.40	0.44	0.44	0.40
2													0.37	0.48	0.57	0.74	0.77	0.73	0.65
3											0.40	0.49	0.67	0.77	0.86	0.90	0.93	0.88	0.67
4									0.36	0.47	0.66	0.76	0.86	0.93	0.96	1.03	1.04	0.99	0.91
5								0.43	0.63	0.73	0.83	0.93	1.00	1.05	1.08	1.11	0.98	1.12	1.06
6							0.42	0.65	0.79	0.87	0.97	1.03	1.11	1.07	1.13	1.11	1.18	1.12	1.18
7						0.42	0.53	0.80	0.91	1.00	0.94	1.12	1.13	1.17	1.06	1.15	1.18	1.24	1.19
8					0.43	0.65	0.80	0.90	1.01	1.02	1.13	1.03	1.18	1.24	1.21	1.20	1.25	1.22	1.23
9				0.36	0.63	0.79	0.91	1.01	1.05	1.08	1.08	1.14	1.18	1.24	1.20	1.25	1.20	1.25	1.20
10				0.47	0.73	0.87	1.00	1.02	1.08	1.03	1.06	1.06	1.18	1.17	1.24	1.23	1.24	1.16	1.15
11			0.40	0.66	0.83	0.97	0.94	1.13	1.08	1.06	0.77	0.85	1.12	1.20	1.13	1.22	1.18	1.14	0.83
12			0.49	0.76	0.93	1.03	1.12	1.03	1.14	1.06	0.85	0.84	1.13	1.19	1.22	1.21	1.22	1.12	0.84
13		0.37	0.67	0.86	1.00	1.11	1.13	1.18	1.18	1.18	1.12	1.13	1.13	1.22	1.20	1.26	1.18	1.19	1.11
14		0.48	0.77	0.93	1.05	1.07	1.17	1.24	1.24	1.17	1.20	1.19	1.22	1.18	1.24	1.20	1.24	1.18	1.20
15	0.36	0.57	0.86	0.96	1.08	1.13	1.06	1.21	1.20	1.24	1.13	1.22	1.20	1.24	1.08	1.14	1.21	1.23	1.14
16	0.40	0.74	0.90	1.03	1.11	1.11	1.15	1.20	1.25	1.23	1.22	1.21	1.26	1.20	1.14	1.13	1.24	1.21	1.22
17	0.44	0.77	0.93	1.04	0.98	1.18	1.18	1.25	1.20	1.24	1.18	1.22	1.18	1.24	1.21	1.24	1.19	1.24	1.18
18	0.44	0.73	0.88	0.99	1.12	1.12	1.24	1.22	1.25	1.16	1.14	1.12	1.19	1.18	1.23	1.21	1.24	1.14	1.13
19	0.40	0.65	0.67	0.91	1.06	1.18	1.19	1.23	1.20	1.15	0.83	0.84	1.11	1.20	1.14	1.22	1.18	1.13	0.80

Figure 4A-4e. Average Bundle Exposure at 3.3 GWd/MT Exposure

	1	2	3	4	5	6	7	8	9	10	11	12	13	14	15	16	17	18	19
1															38.03	36.93	40.34	37.37	38.58
2													44.20	39.13	38.58	21.61	20.28	19.29	2.09
3											40.68	38.36	21.94	2.54	24.47	25.57	22.93	2.87	35.71
4									40.45	38.69	19.84	2.43	2.76	3.09	25.79	23.92	3.42	3.20	17.64
5								42.55	16.98	2.31	2.76	3.09	21.94	3.42	3.53	3.64	35.71	3.64	26.12
6							39.68	18.52	2.54	2.87	3.20	24.80	3.64	26.35	3.64	26.90	3.86	26.79	3.86
7						39.68	40.68	2.65	21.38	3.31	35.27	23.81	3.64	3.75	30.64	24.58	25.90	4.08	27.67
8					42.55	18.52	2.65	2.98	3.31	25.57	21.05	34.94	3.86	17.42	19.29	19.95	4.08	26.01	27.23
9				40.45	16.98	2.54	21.38	3.31	22.16	3.53	3.64	3.75	25.02	3.97	25.90	3.97	26.01	4.08	26.01
10				38.69	2.31	2.87	3.31	25.57	3.53	26.68	3.53	25.57	3.86	26.46	4.08	3.97	3.97	25.90	3.75
11			40.68	19.84	2.76	3.20	35.27	21.05	3.64	3.53	33.62	25.13	25.57	3.97	34.61	26.12	26.35	3.75	26.12
12			38.36	2.43	3.09	24.80	23.81	34.94	3.75	25.57	25.13	26.12	3.75	3.97	25.90	26.46	3.97	3.64	25.02
13		44.20	21.94	2.76	21.94	3.64	3.64	3.86	25.02	3.86	25.57	3.75	27.01	3.97	26.23	4.08	26.46	3.86	26.12
14		39.13	2.54	3.09	3.42	26.35	3.75	17.42	3.97	26.46	3.97	3.97	3.97	26.90	3.97	26.12	3.97	26.01	3.97
15	38.03	38.58	24.47	25.79	3.53	3.64	30.64	19.29	25.90	4.08	34.61	25.90	26.23	3.97	34.06	26.35	3.86	3.97	32.96
16	36.93	21.61	25.57	23.92	3.64	26.90	24.58	19.95	3.97	3.97	26.12	26.46	4.08	26.12	26.35	26.57	3.97	25.57	26.90
17	40.34	20.28	22.93	3.42	35.71	3.86	25.90	4.08	26.01	3.97	26.35	3.97	26.46	3.97	3.86	3.97	26.90	4.08	26.68
18	37.37	19.29	2.87	3.20	3.64	26.79	4.08	26.01	4.08	25.90	3.75	3.64	3.86	26.01	3.97	25.57	4.08	27.01	3.75
19	38.58	2.09	35.71	17.64	26.12	3.86	27.67	27.23	26.01	3.75	26.12	25.02	26.12	3.97	32.96	26.90	26.68	3.75	25.90

Figure 4A-5a. Control Rod Pattern Summary at 4.4 GWd/MT Exposure

```
( ROD PATTERN DEPLETION

NITER   0  POWER         IMAX  19  POWER(MWT)          4.5000E+03  ( 100.0 %)
IBOUN   1  1/4           JMAX  19  PRESSURE(PSIA)      1.0550E+03
IRN     1  MIRROR        KMAX  25  FLOW(*10E-6LB/HR)   7.8508E+01  ( 100.0 %)
ILPA    0                NSMAX 10  BYPASS(LB/HR)       1.1742E+07  (  15.0 %)        CONTROL ROD CONFIGURATION
IFLW    2  DETAIL        LMAX  20  ENTHALPY(BTU/LB)        512.30                      IN NOTCHES WITHDRAWN
RSTART  0  NEW           LVDCT  7  INLET TEMP(DEG F)       520.47
NEWPHY  2                IPFTL  0  BEGINNING EXPOSURE     16105.1    1  3  5  7  9 11 13 15 17 19 21 23 25 27 29 31 33 35 75
NEXO    3  CALC.                   DELTA EXPOS.(DELTE)        0.0
RBOCA   1                IALPRM 0  DELBRN                  1000.0                                                        71
IACF    0                IFAST  0  TOTAL NOTCHES             1506
           IPDOME  1     IAHB   0  CORE FUEL MASS    MTU:162.928    1                        76                         67
                                   CORE FUEL MASS    STU:179.596
ENERGY (MWD) (DELTE)            0. ENERGY (MWD) (DELBRN)   179596.   3                                                   63
CYCLE ENERGY (MWD)        718391. CYCLE EXPOSURE           4000.0
CORE AVG. POWER DENSITY  54.328033                                  5                        48                         59
NEUTRON MULTIPLICATION   1.00330782 FINAL AVG. EXPOSURE    17105.1
DIFP   (EPS5 = 0.00200)  0.00131279 CORE AVG. NEUTRON FLUX 1.439E+14 7                                                  55
AVERAGE VOID FRACTION     0.532918 CORE AVG. GD WORTH        0.000
CORE PRESSURE DROP,PSI    8.081793 CORE AVG. GD RESIDUAL WORTH 0.000 9          52              9                        51
EXP RATIO INDEX (INER-II)   0.0000 CORE AVERAGE XENON WORTH  -0.0219
                                                                   11                                                   47
CORE HISTORY MAX. VALUES:      LOCATION: I   J   K
  NODAL EXPOSURE, MWD/T  50435.         7   7   5   METRIC    55595. 13      48              12                          43
  BUNDLE EXPOSURE, MWD/T 40509.        13   2       METRIC    44653.
  EXPOSURE RATIO, NEXRAT  0.0000        0   0   0                  15                                                   39
  AXIAL POWER PEAK        1.3389                7
                                                                   17 76              9              14                 35

                                                                   19                                                   31

                                                                   21                                                   27

                                                                   23                                                   23

                                                                   25                                                   19

                                                                   27                                                   15

                                                                   29                                                   11

                                                                   31                                                    7

                                                                   33                                                    3
```

Figure 4A-5b. Relative Axial Power at 4.4 GWd/MT Exposure

4.4 GWD/MT

Node	Axial Power
25	0.156
24	0.304
23	0.449
22	0.579
21	0.689
20	0.784
19	0.866
18	0.930
17	0.978
16	1.060
15	1.202
14	1.257
13	1.297
12	1.310
11	1.317
10	1.327
9	1.329
8	1.334
7	1.339
6	1.336
5	1.315
4	1.267
3	1.152
2	0.926
1	0.496
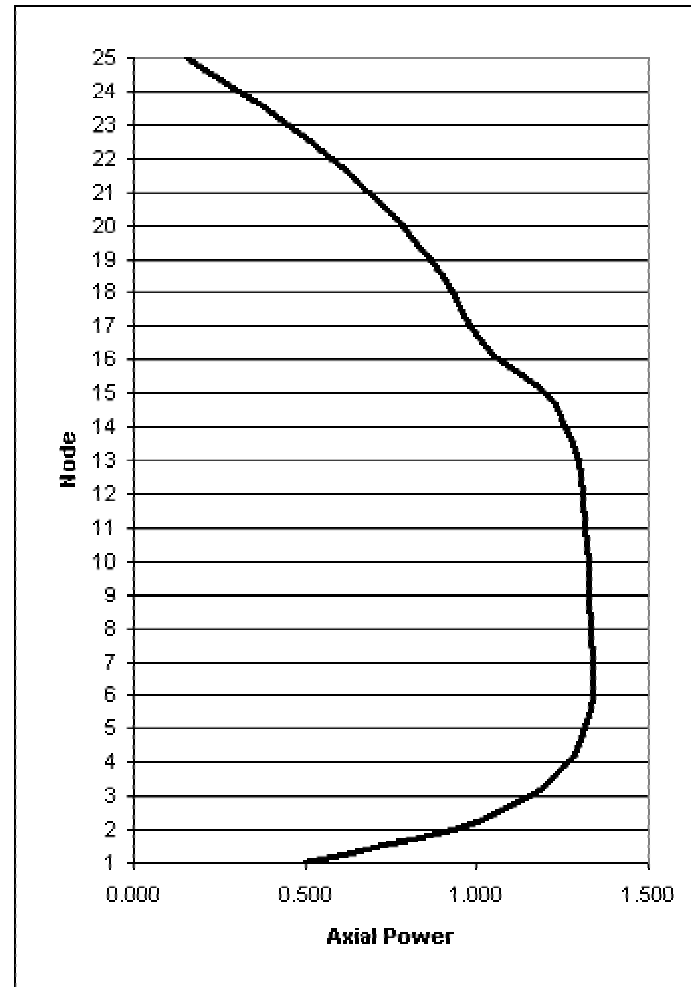
Figure 4A-5c. Axial Exposure at 4.4 GWd/MT Exposure

4.4GWD/MT

Node	Axial Exposure (MWD/MT)
25	3832.1
24	6643.2
23	9318.0
22	12021.9
21	14436.5
20	16448.1
19	18105.9
18	19337.1
17	20141.2
16	20761.3
15	20271.5
14	21132.9
13	21862.0
12	22392.8
11	22842.5
10	23182.2
9	23315.3
8	23481.6
7	23733.9
6	23982.7
5	24028.7
4	23466.6
3	21438.7
2	16993.1
1	8644.2
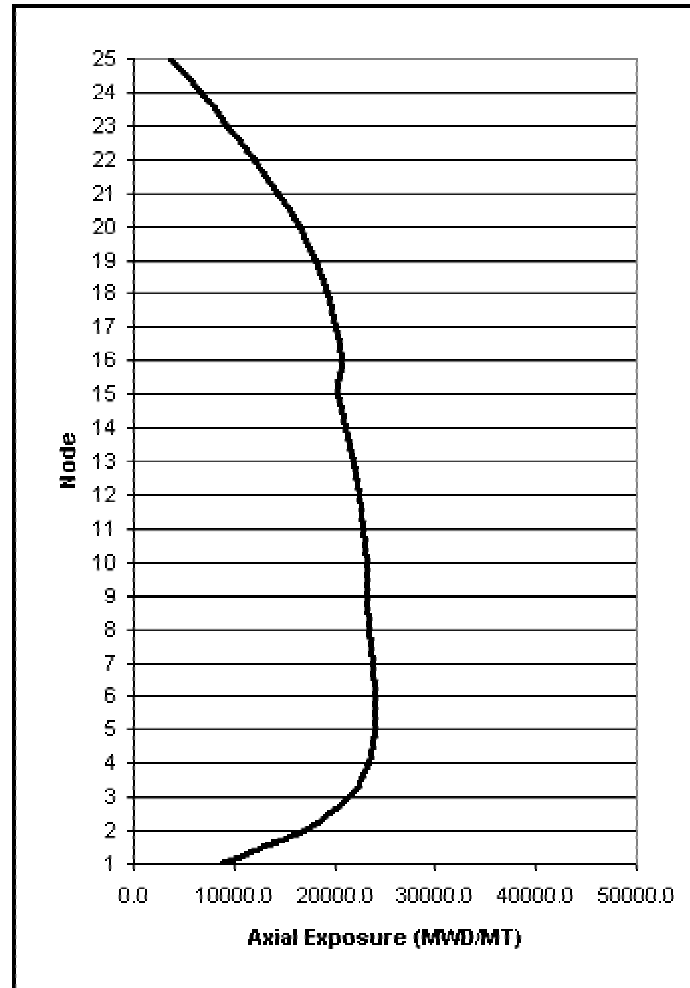
Figure 4A-5d. Relative Integrated Power Per Bundle at 4.4 GWd/MT Exposure

	1	2	3	4	5	6	7	8	9	10	11	12	13	14	15	16	17	18	19
1															0.37	0.42	0.46	0.48	0.45
2													0.38	0.49	0.58	0.76	0.81	0.80	0.75
3											0.41	0.51	0.69	0.79	0.88	0.92	0.97	0.97	0.83
4									0.38	0.50	0.69	0.79	0.89	0.96	0.97	1.05	1.09	1.08	1.10
5								0.46	0.66	0.77	0.87	0.97	1.02	1.07	1.10	1.13	1.00	1.18	1.13
6							0.45	0.68	0.84	0.92	1.01	1.05	1.14	1.07	1.13	1.09	1.19	1.14	1.22
7						0.45	0.57	0.85	0.96	1.06	0.98	1.15	1.16	1.17	0.98	1.06	1.15	1.24	1.18
8					0.46	0.68	0.85	0.96	1.08	1.07	1.18	1.07	1.22	1.23	1.12	1.10	1.23	1.19	1.20
9				0.38	0.66	0.84	0.96	1.08	1.12	1.17	1.18	1.22	1.22	1.26	1.18	1.23	1.18	1.24	1.18
10				0.50	0.77	0.92	1.06	1.07	1.17	1.12	1.18	1.16	1.25	1.19	1.25	1.23	1.23	1.13	1.13
11			0.41	0.69	0.87	1.01	0.98	1.18	1.18	1.18	1.00	1.07	1.20	1.24	1.12	1.19	1.14	1.12	0.80
12			0.51	0.79	0.97	1.05	1.15	1.07	1.22	1.16	1.07	1.06	1.21	1.22	1.18	1.16	1.18	1.08	0.79
13		0.38	0.69	0.89	1.02	1.14	1.16	1.22	1.22	1.25	1.20	1.21	1.15	1.21	1.13	1.18	1.10	1.13	1.04
14		0.49	0.79	0.96	1.08	1.07	1.17	1.23	1.26	1.19	1.24	1.22	1.21	1.10	1.11	1.04	1.12	1.07	1.12
15	0.37	0.58	0.88	0.97	1.10	1.13	0.98	1.12	1.18	1.25	1.12	1.18	1.13	1.11	0.74	0.77	1.05	1.12	1.03
16	0.42	0.76	0.92	1.05	1.13	1.09	1.06	1.10	1.23	1.23	1.19	1.16	1.18	1.04	0.77	0.76	1.05	1.07	1.09
17	0.46	0.81	0.97	1.09	1.00	1.19	1.15	1.23	1.18	1.23	1.14	1.18	1.10	1.12	1.05	1.05	1.04	1.12	1.07
18	0.48	0.80	0.97	1.08	1.18	1.14	1.24	1.19	1.24	1.13	1.12	1.08	1.13	1.07	1.12	1.07	1.12	1.03	1.05
19	0.45	0.75	0.83	1.10	1.13	1.22	1.18	1.20	1.18	1.14	0.80	0.79	1.04	1.12	1.03	1.09	1.07	1.05	0.76

Figure 4A-5e. Average Bundle Exposure at 4.4 GWd/MT Exposure

	1	2	3	4	5	6	7	8	9	10	11	12	13	14	15	16	17	18	19
1															38.47	37.37	40.90	37.92	39.02
2													44.64	39.68	39.24	22.49	21.05	20.17	2.76
3											41.12	38.91	22.71	3.42	25.46	26.57	24.03	3.86	36.49
4									40.79	39.24	20.61	3.31	3.75	4.08	26.79	25.02	4.52	4.30	18.63
5								42.99	17.64	3.20	3.64	4.08	23.04	4.52	4.74	4.85	36.82	4.85	27.23
6							40.12	19.18	3.42	3.75	4.19	25.90	4.85	27.56	4.85	28.22	5.07	28.00	5.18
7						40.12	41.23	3.53	22.38	4.41	36.38	25.02	4.85	5.07	31.86	25.90	27.23	5.40	28.99
8					42.99	19.18	3.53	3.97	4.41	26.68	22.38	36.16	5.18	18.85	20.61	21.27	5.40	27.34	28.66
9				40.79	17.64	3.42	22.38	4.41	23.26	4.74	4.74	4.96	26.35	5.40	27.23	5.40	27.34	5.51	27.34
10				39.24	3.20	3.75	4.41	26.68	4.74	27.78	4.74	26.68	5.18	27.78	5.40	5.40	5.40	27.23	5.07
11			41.12	20.61	3.64	4.19	36.38	22.38	4.74	4.74	34.39	26.12	26.79	5.29	35.94	27.45	27.56	4.96	27.01
12			38.91	3.31	4.08	25.90	25.02	36.16	4.96	26.68	26.01	27.12	5.07	5.18	27.23	27.78	5.29	4.85	25.90
13		44.64	22.71	3.75	23.04	4.85	4.85	5.18	26.35	5.18	26.79	5.07	28.22	5.40	27.56	5.51	27.78	5.18	27.34
14		39.68	3.42	4.08	4.52	27.56	5.07	18.85	5.40	27.78	5.29	5.18	5.40	28.22	5.40	27.45	5.29	27.23	5.29
15	38.47	39.24	25.46	26.79	4.74	4.85	31.86	20.61	27.23	5.40	35.94	27.23	27.56	5.40	35.27	27.67	5.18	5.40	34.17
16	37.37	22.49	26.57	25.02	4.85	28.11	25.90	21.27	5.40	5.40	27.45	27.78	5.51	27.45	27.56	27.78	5.29	26.90	28.22
17	40.90	21.05	24.03	4.52	36.82	5.07	27.23	5.40	27.34	5.40	27.56	5.29	27.78	5.29	5.18	5.29	28.22	5.40	28.00
18	37.92	20.06	3.86	4.30	4.85	28.00	5.40	27.34	5.51	27.23	4.96	4.85	5.18	27.23	5.40	26.90	5.40	28.22	5.07
19	39.02	2.76	36.49	18.63	27.23	5.18	28.99	28.66	27.34	5.07	27.01	25.90	27.34	5.29	34.17	28.22	27.89	5.07	26.79

Figure 4A-6a. Control Rod Pattern Summary at 5.5 GWd/MT Exposure

```
( ROD PATTERN DEPLETION

NITER   0  POWER           IMAX  19  POWER(MWT)          4.5000E+03  ( 100.0 %)
IBOUN   1  1/4             JMAX  19  PRESSURE(PSIA)      1.0550E+03
IRN     1  MIRROR          KMAX  25  FLOW(*10E-6LB/HR)   7.8508E+01  ( 100.0 %)
ILPA    0                  NSMAX 10  BYPASS(LB/HR)       1.1742E+07  (  15.0 %)     CONTROL ROD CONFIGURATION
IFLW    2  DETAIL          LMAX  20  ENTHALPY(BTU/LB)       512.30              IN NOTCHES WITHDRAWN
RSTART  0  NEW             LVDCT  5  INLET TEMP(DEG F)      520.47
NEWPHY  2                  IPFTL  0  BEGINNING EXPOSURE    17105.2     1  3  5  7  9 11 13 15 17 19 21 23 25 27 29 31 33 35 75
NEXO    3  CALC.                     DELTA EXPOS.(DELTE)       0.0
RBOCA   1                  IALPRM 0  DELBRN               1000.0                                                      71
IACF    0                  IFAST  0  TOTAL NOTCHES          1506
           IPDOME  1       IAHB   0  CORE FUEL MASS     MTU:162.928   1                          76                   67
                                     CORE FUEL MASS     STU:179.596
ENERGY (MWD) (DELTE)            0.  ENERGY (MWD) (DELBRN)   179596.    3                                               63
CYCLE ENERGY (MWD)        897988.  CYCLE EXPOSURE           5000.0
CORE AVG. POWER DENSITY   54.328033                                   5                    48                         59
NEUTRON MULTIPLICATION    1.00301790 FINAL AVG. EXPOSURE   18105.2
DIFP   (EPS5 = 0.00200)   0.00165278 CORE AVG. NEUTRON FLUX 1.442E+14  7                                               55
AVERAGE VOID FRACTION      0.529502 CORE AVG. GD WORTH        0.000
CORE PRESSURE DROP,PSI     8.086357 CORE AVG. GD RESIDUAL WORTH 0.000  9            52             9                   51
EXP RATIO INDEX (INER-II)    0.0000 CORE AVERAGE XENON WORTH -0.0220
                                                                     11                                               47
CORE HISTORY MAX. VALUES:      LOCATION: I   J   K
  NODAL EXPOSURE, MWD/T   51081.        7   7   5   METRIC    56306.  13       48         12                           43
  BUNDLE EXPOSURE, MWD/T  40886.       13   2       METRIC    45069.
  EXPOSURE RATIO, NEXRAT  0.0000        0   0   0                     15                                               39
  AXIAL POWER PEAK        1.3231                7
                                                                     17 76          9          14                     35

                                                                     19                                               31

                                                                     21                                               27

                                                                     23                                               23

                                                                     25                                               19

                                                                     27                                               15

                                                                     29                                               11

                                                                     31                                                7

                                                                     33                                                3
```

Figure 4A-6b. Relative Axial Power at 5.5 GWd/MT Exposure

5.5GWD/MT

Node	Axial Power
25	0.165
24	0.321
23	0.473
22	0.605
21	0.716
20	0.809
19	0.888
18	0.949
17	0.993
16	1.070
15	1.204
14	1.253
13	1.289
12	1.299
11	1.304
10	1.312
9	1.314
8	1.319
7	1.323
6	1.320
5	1.298
4	1.248
3	1.132
2	0.909
1	0.489
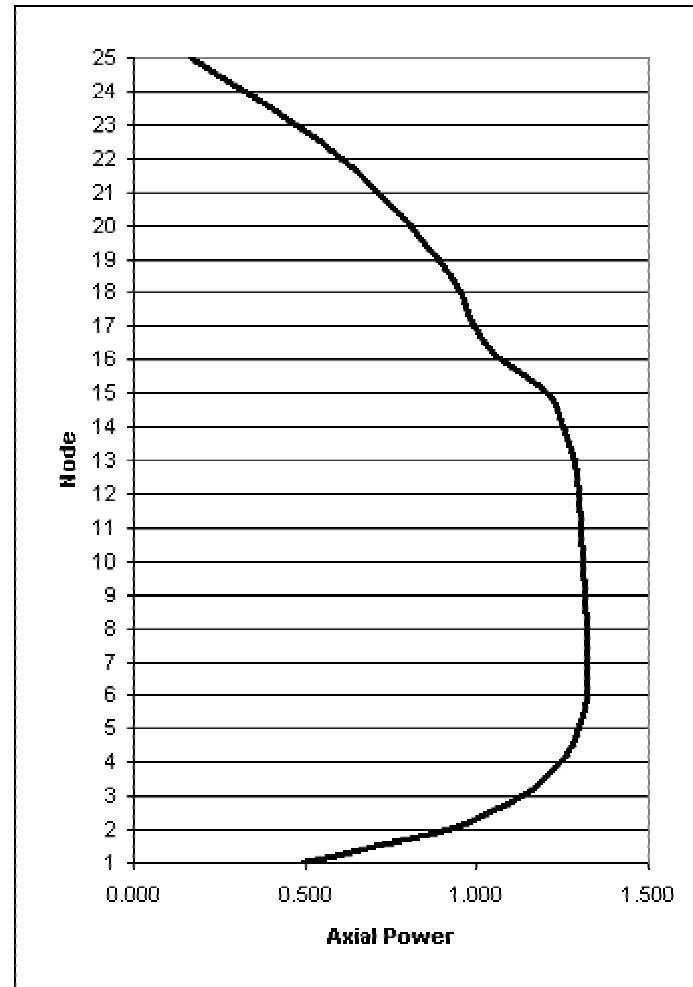
Figure 4A-6c. Axial Exposure at 5.5 GWd/MT Exposure

5.5GWD/MT

Node	Axial Exposure (MWD/MT)
25	4056.6
24	7028.8
23	9864.0
22	12726.2
21	15275.3
20	17402.4
19	19159.6
18	20468.9
17	21331.4
16	22004.2
15	21507.7
14	22426.3
13	23196.6
12	23740.1
11	24197.7
10	24547.0
9	24683.7
8	24855.5
7	25112.9
6	25359.1
5	25383.6
4	24771.4
3	22625.6
2	17947.2
1	9144.2
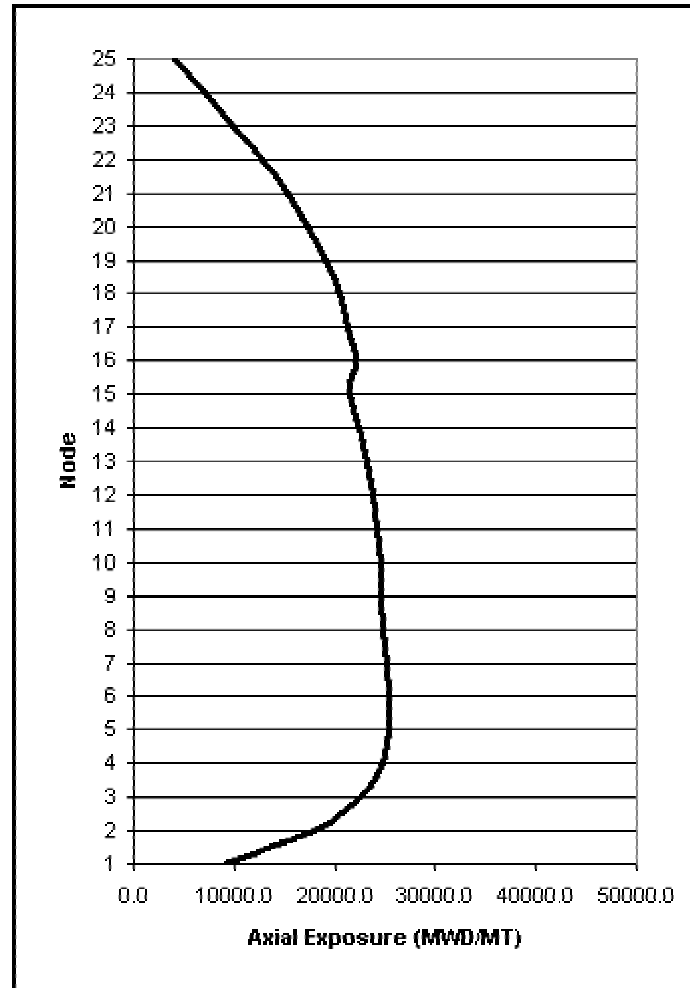
Figure 4A-6d. Relative Integrated Power Per Bundle at 5.5 GWd/MT Exposure

	1	2	3	4	5	6	7	8	9	10	11	12	13	14	15	16	17	18	19
1															0.36	0.41	0.45	0.47	0.45
2													0.37	0.49	0.57	0.75	0.80	0.79	0.74
3											0.41	0.51	0.68	0.79	0.86	0.90	0.96	0.97	0.82
4									0.39	0.50	0.69	0.80	0.90	0.96	0.97	1.04	1.09	1.08	1.09
5								0.46	0.66	0.78	0.88	0.98	1.02	1.09	1.10	1.14	1.00	1.18	1.11
6							0.45	0.69	0.85	0.93	1.02	1.05	1.15	1.07	1.14	1.08	1.19	1.13	1.22
7						0.45	0.57	0.86	0.96	1.07	0.97	1.14	1.17	1.19	0.98	1.05	1.14	1.24	1.16
8					0.46	0.69	0.86	0.98	1.09	1.07	1.18	1.07	1.23	1.23	1.11	1.09	1.23	1.18	1.18
9				0.39	0.66	0.85	0.96	1.09	1.12	1.19	1.19	1.23	1.21	1.28	1.17	1.24	1.17	1.25	1.16
10				0.50	0.78	0.93	1.07	1.07	1.19	1.12	1.20	1.16	1.26	1.19	1.26	1.24	1.24	1.13	1.14
11			0.41	0.69	0.88	1.02	0.97	1.18	1.19	1.20	0.99	1.07	1.20	1.25	1.11	1.18	1.14	1.13	0.79
12			0.51	0.80	0.98	1.05	1.14	1.07	1.23	1.16	1.07	1.05	1.23	1.23	1.17	1.15	1.19	1.10	0.79
13		0.37	0.68	0.90	1.02	1.15	1.17	1.23	1.21	1.26	1.20	1.23	1.15	1.22	1.13	1.19	1.09	1.14	1.03
14		0.49	0.79	0.96	1.09	1.07	1.19	1.23	1.28	1.19	1.25	1.23	1.22	1.10	1.12	1.03	1.13	1.07	1.13
15	0.36	0.57	0.86	0.97	1.10	1.14	0.98	1.11	1.17	1.26	1.11	1.17	1.13	1.12	0.74	0.77	1.06	1.12	1.02
16	0.41	0.75	0.90	1.04	1.14	1.08	1.05	1.09	1.24	1.24	1.18	1.15	1.19	1.04	0.77	0.76	1.06	1.06	1.08
17	0.45	0.80	0.96	1.09	1.00	1.19	1.14	1.23	1.17	1.24	1.14	1.19	1.09	1.13	1.06	1.06	1.03	1.12	1.05
18	0.47	0.79	0.97	1.08	1.18	1.13	1.24	1.18	1.25	1.13	1.13	1.10	1.14	1.07	1.12	1.06	1.12	1.02	1.05
19	0.45	0.74	0.82	1.09	1.11	1.22	1.16	1.18	1.16	1.14	0.79	0.79	1.03	1.13	1.02	1.08	1.05	1.05	0.76

Figure 4A-6e. Average Bundle Exposure at 5.5 GWd/MT Exposure

	1	2	3	4	5	6	7	8	9	10	11	12	13	14	15	16	17	18	19
1															38.91	37.92	41.34	38.36	39.46
2													45.08	40.23	39.90	23.26	21.94	20.94	3.64
3											41.56	39.46	23.48	4.19	26.35	27.56	25.02	4.85	37.37
4									41.23	39.79	21.38	4.19	4.74	5.07	27.89	26.23	5.73	5.51	19.84
5								43.43	18.30	3.97	4.63	5.18	24.14	5.73	5.95	6.06	37.92	6.17	28.55
6							40.57	19.95	4.41	4.85	5.40	27.12	6.06	28.66	6.17	29.32	6.39	29.21	6.50
7						40.57	41.89	4.41	23.48	5.51	37.48	26.35	6.17	6.28	32.96	27.01	28.44	6.83	30.20
8					43.43	19.95	4.41	4.96	5.62	27.89	23.59	37.26	6.50	20.17	21.83	22.49	6.83	28.66	29.98
9				41.23	18.30	4.41	23.48	5.62	24.47	6.06	6.06	6.39	27.67	6.72	28.55	6.72	28.66	6.83	28.66
10				39.79	3.97	4.85	5.51	27.89	6.06	28.99	6.06	28.00	6.61	29.10	6.72	6.72	6.72	28.44	6.28
11			41.56	21.38	4.63	5.40	37.48	23.59	6.06	6.06	35.49	27.23	28.11	6.61	37.15	28.77	28.88	6.17	27.89
12			39.57	4.19	5.18	27.12	26.35	37.37	6.39	28.00	27.23	28.22	6.39	6.61	28.55	29.10	6.61	6.06	26.79
13		45.08	23.48	4.74	24.14	6.06	6.17	6.50	27.67	6.61	28.11	6.39	29.43	6.72	28.77	6.72	28.99	6.39	28.55
14		40.23	4.19	5.07	5.73	28.66	6.28	20.17	6.72	29.10	6.61	6.61	6.72	29.43	6.61	28.66	6.61	28.44	6.50
15	38.91	39.90	26.35	27.89	5.95	6.17	32.96	21.83	28.55	6.72	37.15	28.55	28.77	6.61	36.05	28.44	6.39	6.61	35.38
16	37.92	23.26	27.56	26.23	6.06	29.32	27.01	22.49	6.72	6.72	28.77	29.10	6.72	28.66	28.44	28.66	6.50	28.11	29.43
17	41.34	21.94	25.02	5.73	37.92	6.39	28.44	6.83	28.66	6.72	28.88	6.61	28.99	6.61	6.39	6.50	29.43	6.72	29.10
18	38.36	20.94	4.85	5.51	6.17	29.21	6.83	28.66	6.83	28.44	6.17	6.06	6.39	28.44	6.61	28.11	6.72	29.32	6.17
19	39.46	3.64	37.37	19.84	28.55	6.50	30.20	29.98	28.66	6.28	27.89	26.79	28.55	6.50	35.38	29.43	29.10	6.17	27.67

Figure 4A-7a. Control Rod Pattern Summary at 6.6 GWd/MT Exposure

```
( ROD PATTERN DEPLETION

NITER   0  POWER          IMAX  19  POWER(MWT)          4.5000E+03  ( 100.0 %)
IBOUN   1  1/4            JMAX  19  PRESSURE(PSIA)      1.0550E+03
IRN     1  MIRROR         KMAX  25  FLOW(*10E-6LB/HR)   7.8508E+01  ( 100.0 %)
ILPA    0                 NSMAX 10  BYPASS(LB/HR)       1.1742E+07  (  15.0 %)       CONTROL ROD CONFIGURATION
IFLW    2  DETAIL         LMAX  20  ENTHALPY(BTU/LB)       512.30                    IN NOTCHES WITHDRAWN
RSTART  0  NEW            LVDCT  5  INLET TEMP(DEG F)      520.47
NEWPHY  2                 IPFTL  0  BEGINNING EXPOSURE   18105.1     1  3  5  7  9 11 13 15 17 19 21 23 25 27 29 31 33 35 75
NEXO    3  CALC.                    DELTA EXPOS.(DELTE)      0.0
RBOCA   1                 IALPRM 0  DELBRN                1000.0                                                        71
IACF    0                 IFAST  0  TOTAL NOTCHES           1506
           IPDOME   1     IAHB   0  CORE FUEL MASS    MTU:162.928    1                         76                      67
                                    CORE FUEL MASS    STU:179.596
ENERGY (MWD) (DELTE)          0.  ENERGY (MWD) (DELBRN)    179596.   3                                                 63
CYCLE ENERGY (MWD)       1077586. CYCLE EXPOSURE            6000.0
CORE AVG. POWER DENSITY   54.328033                                 5                48                               59
NEUTRON MULTIPLICATION   1.00301909 FINAL AVG. EXPOSURE    19105.1
DIFP   (EPS5 = 0.00200)  0.00133359 CORE AVG. NEUTRON FLUX 1.445E+14 7                                                 55
AVERAGE VOID FRACTION     0.526597 CORE AVG. GD WORTH        0.000
CORE PRESSURE DROP,PSI    8.082487 CORE AVG. GD RESIDUAL WORTH 0.000 9         52               9                      51
EXP RATIO INDEX (INER-II)   0.0000 CORE AVERAGE XENON WORTH  -0.0222
                                                                   11                                                 47
CORE HISTORY MAX. VALUES:      LOCATION: I   J   K
  NODAL EXPOSURE, MWD/T  51720.       7   7   5   METRIC    57011.  13      48           12                            43
  BUNDLE EXPOSURE, MWD/T 41261.      13   2       METRIC    45482.
  EXPOSURE RATIO, NEXRAT 0.0000       0   0   0                     15                                                 39
  AXIAL POWER PEAK        1.3100              7
                                                                   17 76          9           14                      35

                                                                   19                                                 31

                                                                   21                                                 27

                                                                   23                                                 23

                                                                   25                                                 19

                                                                   27                                                 15

                                                                   29                                                 11

                                                                   31                                                  7

                                                                   33                                                  3
```

Figure 4A-7b. Relative Axial Power at 6.6 GWd/MT Exposure

6.6GWD/MT

Node	Axial Power
25	0.173
24	0.337
23	0.495
22	0.629
21	0.739
20	0.831
19	0.907
18	0.965
17	1.004
16	1.076
15	1.202
14	1.245
13	1.277
12	1.285
11	1.290
10	1.297
9	1.300
8	1.305
7	1.310
6	1.308
5	1.287
4	1.237
3	1.120
2	0.898
1	0.485
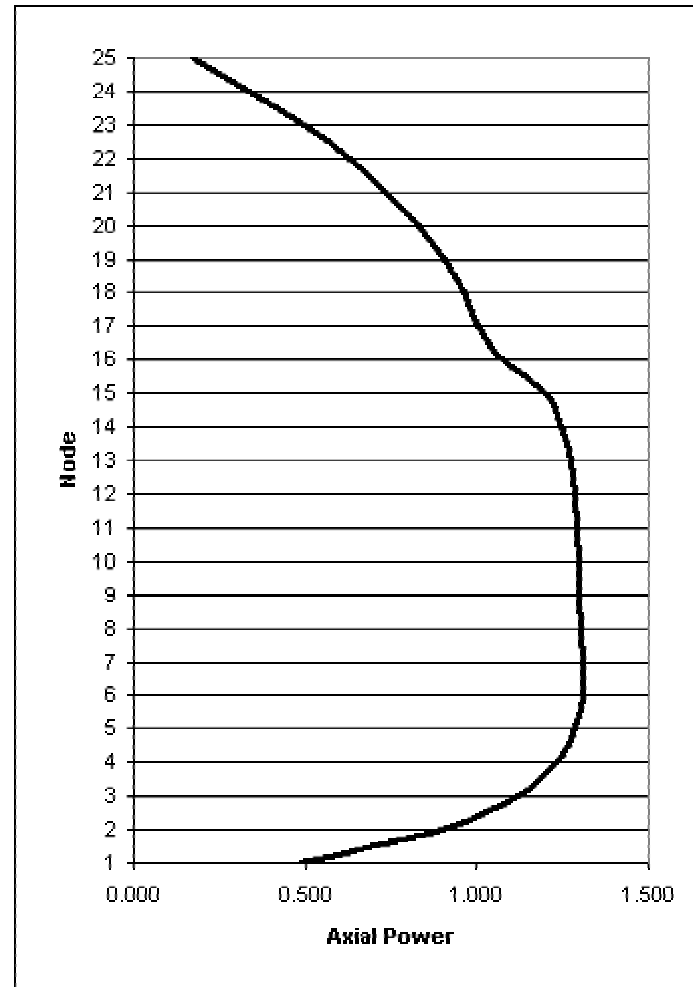
Figure 4A-7c. Axial Exposure at 6.6 GWd/MT Exposure

6.6GWD/MT

Node	Axial Exposure (MWD/MT)
25	4294.4
24	7435.5
23	10439.1
22	13462.6
21	16146.2
20	18387.0
19	20240.2
18	21624.0
17	22539.5
16	23258.1
15	22746.1
14	23715.2
13	24522.2
12	25076.0
11	25539.5
10	25897.1
9	26037.1
8	26213.8
7	26475.6
6	26718.3
5	26720.1
4	26056.4
3	23791.4
2	18883.3
1	9637.3
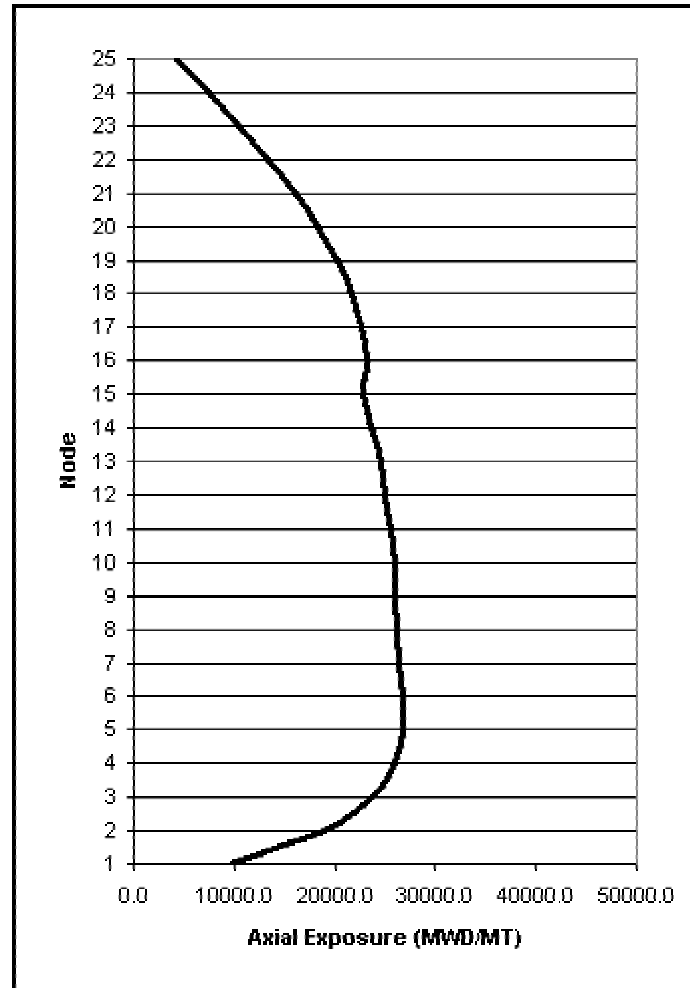
Figure 4A-7d. Relative Integrated Power Per Bundle at 6.6 GWd/MT Exposure

	1	2	3	4	5	6	7	8	9	10	11	12	13	14	15	16	17	18	19
1															0.35	0.40	0.44	0.46	0.44
2													0.37	0.48	0.56	0.73	0.78	0.78	0.74
3											0.41	0.51	0.68	0.79	0.85	0.88	0.94	0.97	0.81
4									0.39	0.50	0.70	0.81	0.91	0.97	0.95	1.02	1.09	1.08	1.08
5								0.46	0.67	0.79	0.89	0.99	1.02	1.10	1.11	1.14	0.99	1.18	1.10
6							0.45	0.69	0.86	0.94	1.03	1.05	1.16	1.07	1.15	1.07	1.19	1.11	1.22
7						0.45	0.57	0.87	0.96	1.08	0.97	1.14	1.19	1.20	0.97	1.04	1.12	1.24	1.14
8					0.46	0.69	0.87	0.99	1.11	1.07	1.17	1.06	1.25	1.22	1.11	1.09	1.24	1.16	1.16
9				0.39	0.67	0.86	0.96	1.11	1.13	1.20	1.21	1.25	1.21	1.29	1.17	1.25	1.16	1.25	1.14
10				0.50	0.79	0.94	1.08	1.07	1.20	1.12	1.21	1.15	1.28	1.18	1.28	1.25	1.25	1.12	1.15
11			0.41	0.70	0.89	1.03	0.97	1.17	1.21	1.21	0.99	1.06	1.19	1.27	1.11	1.17	1.13	1.14	0.79
12			0.51	0.81	0.99	1.05	1.14	1.06	1.25	1.15	1.06	1.05	1.24	1.25	1.17	1.14	1.20	1.11	0.79
13		0.37	0.68	0.91	1.02	1.16	1.19	1.25	1.21	1.28	1.19	1.24	1.15	1.24	1.12	1.20	1.09	1.15	1.02
14		0.48	0.79	0.97	1.10	1.07	1.20	1.22	1.29	1.18	1.27	1.25	1.24	1.10	1.13	1.03	1.15	1.07	1.14
15	0.35	0.56	0.85	0.95	1.11	1.15	0.97	1.11	1.17	1.28	1.11	1.17	1.12	1.13	0.74	0.77	1.07	1.13	1.01
16	0.40	0.73	0.88	1.02	1.14	1.07	1.04	1.09	1.25	1.25	1.17	1.14	1.20	1.03	0.77	0.76	1.07	1.05	1.06
17	0.44	0.78	0.94	1.09	0.99	1.19	1.12	1.24	1.16	1.25	1.13	1.20	1.09	1.15	1.07	1.07	1.03	1.13	1.04
18	0.46	0.78	0.97	1.08	1.18	1.11	1.24	1.16	1.25	1.12	1.14	1.11	1.15	1.07	1.13	1.05	1.13	1.02	1.05
19	0.44	0.74	0.81	1.08	1.10	1.22	1.14	1.16	1.14	1.15	0.79	0.79	1.03	1.14	1.01	1.06	1.04	1.05	0.76

Figure 4A-7e. Average Bundle Exposure at 6.6 GWd/MT Exposure

	1	2	3	4	5	6	7	8	9	10	11	12	13	14	15	16	17	18	19
1															39.24	38.36	41.89	38.91	40.01
2													45.53	40.79	40.45	24.14	22.82	21.83	4.41
3											42.11	40.12	24.25	5.07	27.34	28.55	26.12	5.95	38.25
4									41.67	40.34	22.16	5.07	5.73	6.17	28.99	27.34	6.94	6.72	21.05
5								43.98	19.07	4.85	5.51	6.17	25.35	6.94	7.17	7.39	39.02	7.50	29.76
6							41.12	20.72	5.29	5.84	6.50	28.22	7.39	29.87	7.39	30.53	7.72	30.42	7.83
7						41.12	42.55	5.40	24.58	6.72	38.47	27.56	7.50	7.61	33.95	28.22	29.76	8.16	31.53
8					43.98	20.72	5.40	6.06	6.83	28.99	24.91	38.47	7.83	21.50	23.04	23.70	8.16	29.98	31.20
9				41.67	19.07	5.29	24.58	6.83	25.79	7.39	7.39	7.72	28.99	8.16	29.87	8.05	29.98	8.27	29.87
10				40.34	4.85	5.84	6.72	28.99	7.39	30.20	7.39	29.32	7.94	30.42	8.16	8.05	8.05	29.76	7.50
11			42.11	22.16	5.51	6.50	38.47	24.91	7.39	7.39	36.60	28.44	29.43	8.05	38.36	30.09	30.09	7.50	28.77
12			40.12	5.07	6.17	28.22	27.56	38.47	7.72	29.32	28.44	29.43	7.72	7.94	29.87	30.31	7.94	7.28	27.67
13		45.42	24.25	5.73	25.35	7.39	7.50	7.83	28.99	7.94	29.43	7.72	30.75	8.05	30.09	8.05	30.20	7.72	29.65
14		40.79	5.07	6.17	6.94	29.87	7.61	21.50	8.16	30.42	8.05	7.94	8.05	30.64	7.83	29.76	7.83	29.65	7.72
15	39.24	40.57	27.34	28.99	7.17	7.39	33.95	23.04	29.87	8.16	38.36	29.87	30.09	7.83	36.93	29.32	7.50	7.83	36.49
16	38.36	24.14	28.55	27.34	7.39	30.53	28.22	23.70	8.05	8.05	30.09	30.31	8.05	29.76	29.32	29.43	7.61	29.21	30.64
17	41.89	22.82	26.12	6.94	39.02	7.72	29.76	8.16	29.98	8.05	30.09	7.94	30.20	7.83	7.50	7.61	30.53	7.94	30.31
18	38.91	21.83	5.95	6.72	7.50	30.42	8.16	29.98	8.27	29.76	7.50	7.28	7.72	29.65	7.83	29.21	7.94	30.53	7.39
19	40.01	4.41	38.25	21.05	29.76	7.83	31.53	31.20	29.87	7.50	28.77	27.67	29.65	7.72	36.49	30.64	30.31	7.39	28.55

Figure 4A-8a. Control Rod Pattern Summary at 7.7 GWd/MT Exposure

```
( ROD PATTERN DEPLETION

NITER    0  POWER            IMAX  19  POWER(MWT)           4.5000E+03  ( 100.0 %)
IBOUN    1  1/4              JMAX  19  PRESSURE(PSIA)       1.0550E+03
IRN      1  MIRROR           KMAX  25  FLOW(*10E-6LB/HR)    7.8508E+01  ( 100.0 %)
ILPA     0                   NSMAX 10  BYPASS(LB/HR)        1.1742E+07  ( 15.0 %)      CONTROL ROD CONFIGURATION
IFLW     2  DETAIL           LMAX  20  ENTHALPY(BTU/LB)       512.30               IN NOTCHES WITHDRAWN
RSTART   0  NEW              LVDCT  7  INLET TEMP(DEG F)      520.47
NEWPHY   2                   IPFTL  0  BEGINNING EXPOSURE   19105.1     1  3  5  7  9 11 13 15 17 19 21 23 25 27 29 31 33 35 75
NEXO     3  CALC.                      DELTA EXPOS.(DELTE)      0.0
RBOCA    1                   IALPRM 0  DELBRN               1000.0                                                         71
IACF     0                   IFAST  0  TOTAL NOTCHES          1515
            IPDOME   1  IAHB  0  CORE FUEL MASS      MTU:162.928     1                                                    67
                                       CORE FUEL MASS      STU:179.596
ENERGY (MWD) (DELTE)            0. ENERGY (MWD) (DELBRN)    179596.    3                                                    63
CYCLE ENERGY (MWD)        1257184. CYCLE EXPOSURE            7000.0
CORE AVG. POWER DENSITY   54.328033                                   5                45                                   59
NEUTRON MULTIPLICATION    1.00171828 FINAL AVG. EXPOSURE     20105.1
DIFP   (EPS5 = 0.00200)   0.00138599 CORE AVG. NEUTRON FLUX 1.449E+14  7                                                    55
AVERAGE VOID FRACTION     0.531062 CORE AVG. GD WORTH          0.000
CORE PRESSURE DROP,PSI    8.079894 CORE AVG. GD RESIDUAL WORTH 0.000   9             19              4                      51
EXP RATIO INDEX (INER-II)   0.0000 CORE AVERAGE XENON WORTH  -0.0224
                                                                     11                                                    47
CORE HISTORY MAX. VALUES:       LOCATION: I   J   K
  NODAL EXPOSURE, MWD/T   52358.        7   7   5   METRIC   57714.   13       45              26                           43
  BUNDLE EXPOSURE, MWD/T  41633.       13   2       METRIC   45892.
  EXPOSURE RATIO, NEXRAT  0.0000        0   0   0                     15                                                    39
  AXIAL POWER PEAK         1.3294               5
                                                                     17             4               29                     35

                                                                     19                                                    31

                                                                     21                                                    27

                                                                     23                                                    23

                                                                     25                                                    19

                                                                     27                                                    15

                                                                     29                                                    11

                                                                     31                                                     7

                                                                     33                                                     3
```

Figure 4A-8b. Relative Axial Power at 7.7 GWd/MT Exposure

7.7GWD/MT

Node	Axial Power
25	0.185
24	0.357
23	0.522
22	0.661
21	0.775
20	0.860
19	0.923
18	0.964
17	0.985
16	1.040
15	1.146
14	1.176
13	1.195
12	1.214
11	1.235
10	1.254
9	1.269
8	1.287
7	1.307
6	1.324
5	1.329
4	1.301
3	1.196
2	0.970
1	0.528
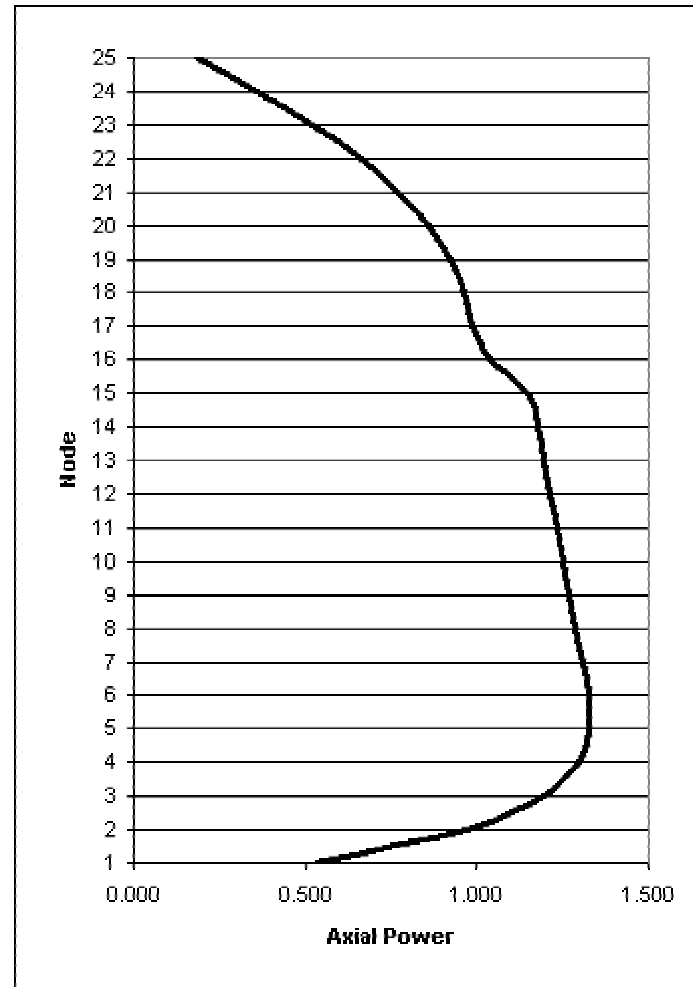
Figure 4A-8c. Axial Exposure at 7.7 GWd/MT Exposure

7.7 GWD/MT

Node	Axial Exposure (MWD/MT)
25	4544.6
24	7862.4
23	11041.6
22	14228.5
21	17045.6
20	19397.7
19	21343.7
18	22797.8
17	23761.6
16	24518.7
15	23982.4
14	24996.1
13	25835.7
12	26397.7
11	26866.1
10	27231.5
9	27375.3
8	27557.9
7	27824.7
6	28065.0
5	28045.2
4	27329.9
3	24944.9
2	19808.5
1	10126.7
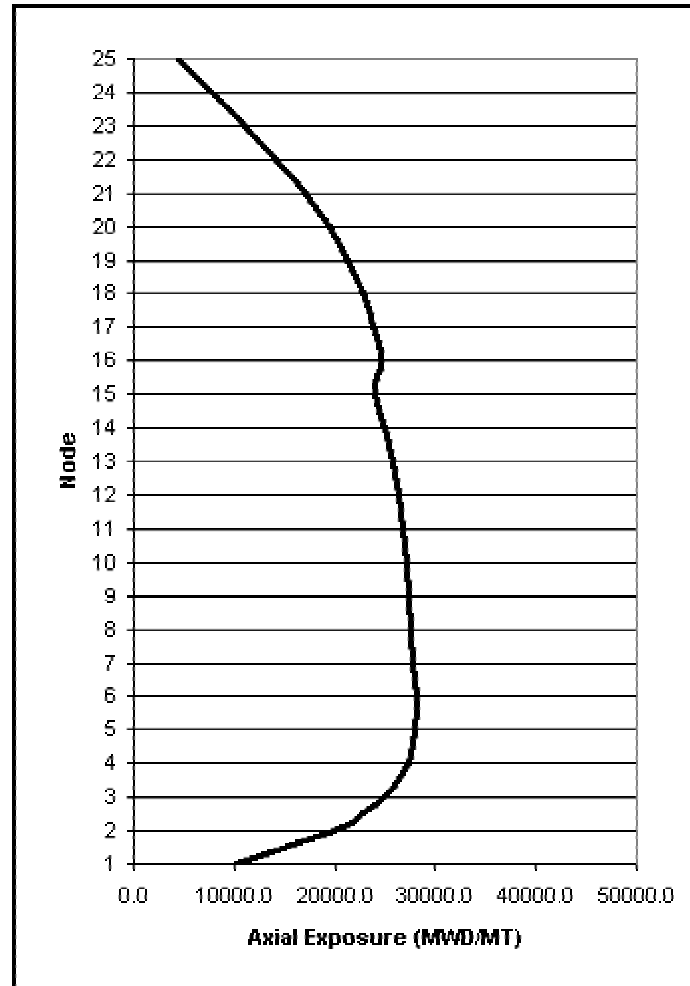
Figure 4A-8d. Relative Integrated Power Per Bundle at 7.7 GWd/MT Exposure

	1	2	3	4	5	6	7	8	9	10	11	12	13	14	15	16	17	18	19
1															0.35	0.39	0.44	0.46	0.45
2													0.37	0.47	0.55	0.72	0.78	0.78	0.76
3											0.41	0.51	0.68	0.79	0.84	0.87	0.94	0.98	0.84
4									0.38	0.50	0.69	0.81	0.91	0.97	0.94	1.01	1.10	1.10	1.12
5								0.45	0.66	0.79	0.90	0.99	1.01	1.10	1.11	1.14	0.98	1.19	1.10
6							0.44	0.68	0.86	0.94	1.03	1.03	1.16	1.06	1.14	1.05	1.20	1.10	1.23
7						0.44	0.56	0.86	0.95	1.07	0.95	1.11	1.18	1.19	0.94	1.01	1.10	1.24	1.13
8					0.45	0.68	0.86	0.98	1.10	1.03	1.13	1.03	1.23	1.19	1.07	1.05	1.23	1.14	1.14
9				0.38	0.66	0.86	0.95	1.10	1.09	1.18	1.17	1.21	1.17	1.27	1.14	1.25	1.15	1.26	1.13
10				0.50	0.79	0.94	1.07	1.03	1.18	1.06	1.14	1.06	1.23	1.14	1.27	1.26	1.27	1.12	1.16
11			0.41	0.69	0.90	1.03	0.95	1.13	1.17	1.14	0.78	0.84	1.10	1.24	1.09	1.16	1.13	1.17	0.79
12			0.51	0.81	0.99	1.03	1.11	1.02	1.21	1.06	0.84	0.84	1.18	1.23	1.15	1.14	1.23	1.15	0.79
13		0.37	0.68	0.91	1.01	1.16	1.18	1.23	1.17	1.23	1.10	1.18	1.11	1.24	1.13	1.24	1.12	1.20	1.05
14		0.47	0.79	0.97	1.10	1.06	1.19	1.19	1.27	1.14	1.24	1.23	1.24	1.11	1.18	1.08	1.21	1.11	1.20
15	0.35	0.55	0.84	0.94	1.11	1.14	0.94	1.07	1.14	1.27	1.09	1.15	1.13	1.18	0.84	0.88	1.16	1.21	1.06
16	0.39	0.72	0.87	1.01	1.14	1.05	1.01	1.05	1.25	1.26	1.16	1.14	1.24	1.08	0.88	0.87	1.17	1.12	1.12
17	0.44	0.78	0.94	1.10	0.98	1.20	1.10	1.23	1.15	1.27	1.13	1.23	1.12	1.21	1.16	1.17	1.10	1.22	1.11
18	0.46	0.78	0.98	1.10	1.19	1.10	1.25	1.14	1.26	1.12	1.17	1.15	1.20	1.12	1.21	1.12	1.22	1.10	1.17
19	0.45	0.76	0.84	1.12	1.10	1.23	1.13	1.14	1.13	1.16	0.79	0.79	1.05	1.20	1.07	1.12	1.11	1.17	0.90

Figure 4A-8e. Average Bundle Exposure at 7.7 GWd/MT Exposure

	1	2	3	4	5	6	7	8	9	10	11	12	13	14	15	16	17	18	19
1															39.68	38.80	42.33	39.46	40.45
2													45.86	41.34	41.12	24.91	23.70	22.71	5.29
3											42.55	40.68	25.02	5.95	28.33	29.54	27.12	7.05	39.13
4									42.11	40.90	22.93	5.95	6.72	7.28	29.98	28.44	8.16	7.83	22.27
5								44.53	19.84	5.73	6.50	7.28	26.46	8.16	8.38	8.60	40.01	8.71	30.97
6							41.56	21.50	6.28	6.83	7.61	29.43	8.60	31.09	8.60	31.75	9.04	31.75	9.15
7						41.56	43.10	6.28	25.57	7.94	39.57	28.77	8.71	8.93	35.05	29.32	30.97	9.48	32.74
8					44.53	21.50	6.28	7.17	8.05	30.20	26.23	39.68	9.26	22.93	24.25	24.91	9.48	31.20	32.52
9				42.11	19.84	6.28	25.57	8.05	27.01	8.71	8.71	9.04	30.42	9.59	31.09	9.48	31.20	9.59	31.20
10				40.90	5.73	6.83	7.94	30.20	8.71	31.53	8.71	30.53	9.37	31.64	9.59	9.48	9.48	30.97	8.82
11			42.55	22.93	6.50	7.61	39.57	26.23	8.71	8.71	37.70	29.54	30.75	9.48	39.57	31.31	31.42	8.71	29.65
12			40.68	5.95	7.28	29.43	28.77	39.68	9.04	30.53	29.54	30.53	9.15	9.26	31.09	31.64	9.26	8.49	28.55
13		45.86	24.91	6.72	26.46	8.60	8.71	9.26	30.31	9.37	30.75	9.15	31.97	9.37	31.31	9.37	31.42	8.93	30.75
14		41.34	5.95	7.28	8.16	31.09	8.93	22.93	9.59	31.64	9.48	9.26	9.37	31.86	9.04	30.86	9.04	30.86	8.93
15	39.68	41.12	28.33	29.98	8.38	8.60	35.05	24.25	31.09	9.59	39.57	31.09	31.31	9.04	37.70	30.20	8.71	9.04	37.59
16	38.80	24.91	29.54	28.44	8.60	31.75	29.32	24.91	9.48	9.48	31.31	31.64	9.37	30.86	30.20	30.31	8.82	30.42	31.75
17	42.33	23.70	27.12	8.16	40.01	9.04	30.97	9.48	31.20	9.48	31.31	9.26	31.42	9.04	8.71	8.82	31.64	9.15	31.42
18	39.46	22.71	7.05	7.83	8.82	31.75	9.48	31.20	9.59	30.97	8.71	8.49	8.93	30.86	9.04	30.42	9.15	31.64	8.49
19	40.45	5.29	39.13	22.27	30.97	9.15	32.74	32.52	31.20	8.82	29.65	28.55	30.75	8.93	37.59	31.75	31.42	8.49	29.32

Figure 4A-9a. Control Rod Pattern Summary at 8.8 GWd/MT Exposure

```
         ( ROD PATTERN DEPLETION

NITER   0  POWER        IMAX  19  POWER(MWT)         4.5000E+03  ( 100.0 %)
IBOUN   1  1/4          JMAX  19  PRESSURE(PSIA)     1.0550E+03
IRN     1  MIRROR       KMAX  25  FLOW(*10E-6LB/HR)  7.8508E+01  ( 100.0 %)
ILPA    0               NSMAX 10  BYPASS(LB/HR)      1.1742E+07  ( 15.0 %)    CONTROL ROD CONFIGURATION
IFLW    2  DETAIL       LMAX  20  ENTHALPY(BTU/LB)      512.30                   IN NOTCHES WITHDRAWN
RSTART  0  NEW          LVDCT  5  INLET TEMP(DEG F)     520.47
NEWPHY  2               IPFTL  0  BEGINNING EXPOSURE   20105.1     1  3  5  7  9 11 13 15 17 19 21 23 25 27 29 31 33 35 75
NEXO    3  CALC.                  DELTA EXPOS.(DELTE)      0.0
RBOCA   1               IALPRM 0  DELBRN               1000.0                                                       71
IACF    0               IFAST  0  TOTAL NOTCHES           1515
           IPDOME   1   IAHB   0  CORE FUEL MASS    MTU:162.928    1                                                67
                                  CORE FUEL MASS    STU:179.596
ENERGY (MWD) (DELTE)           0. ENERGY (MWD) (DELBRN)   179596.   3                                                63
CYCLE ENERGY (MWD)       1436781. CYCLE EXPOSURE          8000.0
CORE AVG. POWER DENSITY  54.328033                                 5               45                               59
NEUTRON MULTIPLICATION   1.00232923 FINAL AVG. EXPOSURE   21105.1
DIFP   (EPS5 = 0.00200)  0.00136071 CORE AVG. NEUTRON FLUX 1.451E+14  7                                             55
AVERAGE VOID FRACTION    0.530853 CORE AVG. GD WORTH        0.000
CORE PRESSURE DROP,PSI   8.099077 CORE AVG. GD RESIDUAL WORTH  0.000  9           19             4                  51
EXP RATIO INDEX (INER-II)  0.0000 CORE AVERAGE XENON WORTH   -0.0226
                                                                  11                                                47
CORE HISTORY MAX. VALUES:       LOCATION: I   J   K
  NODAL EXPOSURE, MWD/T  53011.         7   7   5   METRIC    58434.  13    45             26                       43
  BUNDLE EXPOSURE, MWD/T 42000.        13   2       METRIC    46297.
  EXPOSURE RATIO, NEXRAT 0.0000         0   0   0                     15                                            39
  AXIAL POWER PEAK       1.3400                 5
                                                                    17         4             29                     35

                                                                    19                                             31

                                                                    21                                             27

                                                                    23                                             23

                                                                    25                                             19

                                                                    27                                             15

                                                                    29                                             11

                                                                    31                                              7

                                                                    33                                              3
```

Figure 4A-9b. Relative Axial Power at 8.8 GWd/MT Exposure

8.8GWD/MT

Node	Axial Power
25	0.189
24	0.366
23	0.533
22	0.672
21	0.783
20	0.867
19	0.927
18	0.966
17	0.986
16	1.035
15	1.135
14	1.160
13	1.178
12	1.196
11	1.217
10	1.238
9	1.257
8	1.279
7	1.305
6	1.329
5	1.340
4	1.316
3	1.211
2	0.981
1	0.535
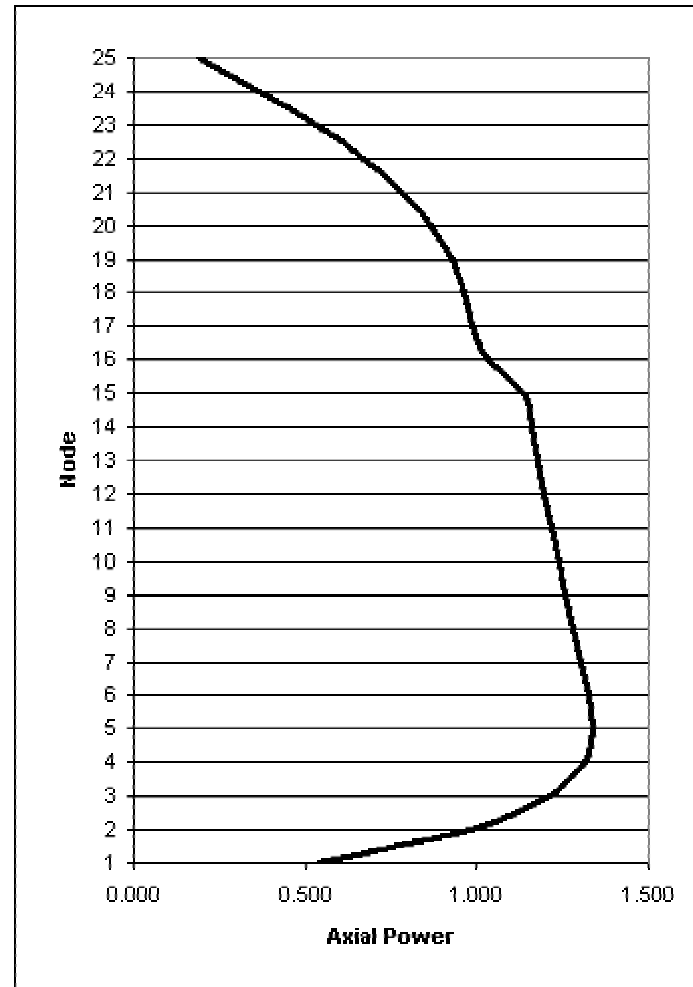
Figure 4A-9c. Axial Exposure at 8.8 GWd/MT Exposure

8.8GWD/MT

Node	Axial Exposure (MWD/MT)
25	4811.0
24	8314.8
23	11676.2
22	15033.0
21	17988.3
20	20444.3
19	22466.4
18	23970.3
17	24960.5
16	25737.2
15	25161.3
14	26205.7
13	27065.2
12	27647.0
11	28136.1
10	28521.3
9	28681.4
8	28883.1
7	29170.8
6	29428.9
5	29414.5
4	28669.3
3	26177.0
2	20807.1
1	10659.4
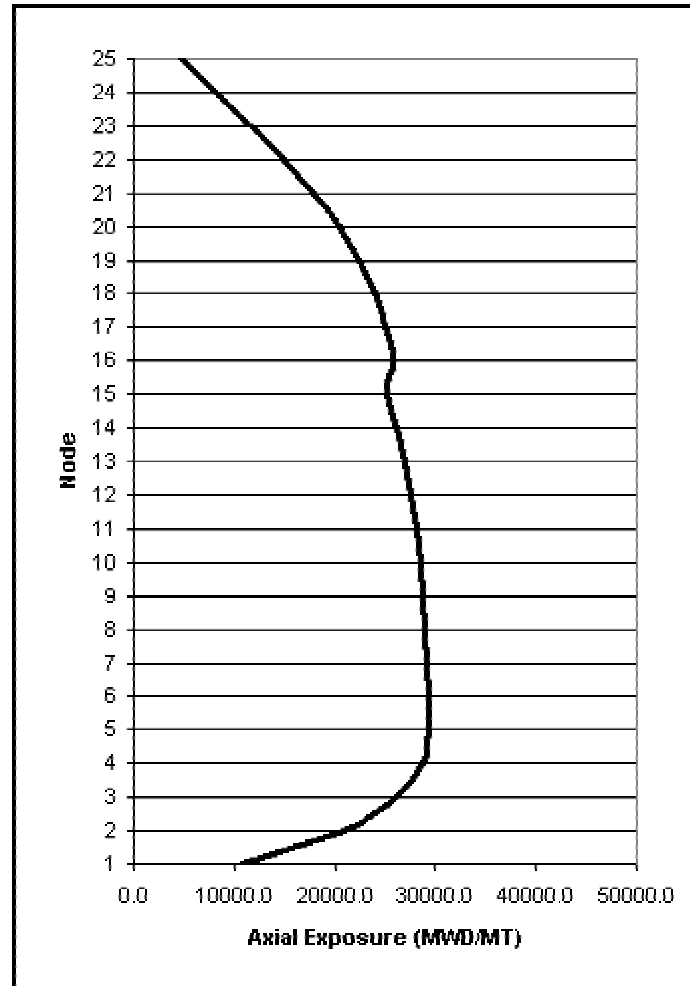
Figure 4A-9d. Relative Integrated Power Per Bundle at 8.8 GWd/MT Exposure

	1	2	3	4	5	6	7	8	9	10	11	12	13	14	15	16	17	18	19
1															0.34	0.38	0.42	0.45	0.44
2													0.36	0.47	0.54	0.70	0.76	0.77	0.75
3											0.41	0.51	0.67	0.79	0.82	0.85	0.92	0.98	0.83
4									0.38	0.50	0.69	0.82	0.92	0.98	0.93	1.00	1.09	1.10	1.10
5								0.45	0.67	0.80	0.91	1.00	1.01	1.11	1.12	1.14	0.97	1.19	1.08
6							0.44	0.68	0.87	0.96	1.04	1.03	1.17	1.05	1.15	1.04	1.20	1.09	1.23
7						0.44	0.56	0.87	0.95	1.08	0.94	1.10	1.20	1.21	0.93	0.99	1.09	1.25	1.11
8					0.45	0.68	0.87	1.00	1.11	1.03	1.13	1.02	1.25	1.19	1.06	1.05	1.24	1.13	1.12
9				0.38	0.67	0.87	0.95	1.11	1.09	1.19	1.19	1.22	1.16	1.29	1.13	1.26	1.14	1.27	1.11
10				0.50	0.80	0.96	1.08	1.03	1.19	1.06	1.15	1.06	1.25	1.14	1.29	1.28	1.28	1.11	1.17
11			0.41	0.69	0.91	1.04	0.94	1.13	1.19	1.15	0.78	0.84	1.10	1.26	1.08	1.15	1.13	1.18	0.79
12			0.51	0.82	1.00	1.03	1.10	1.02	1.22	1.06	0.84	0.84	1.20	1.25	1.14	1.13	1.25	1.16	0.79
13		0.36	0.67	0.92	1.01	1.17	1.20	1.25	1.16	1.25	1.10	1.20	1.11	1.26	1.12	1.25	1.12	1.22	1.05
14		0.47	0.79	0.98	1.11	1.05	1.21	1.19	1.29	1.14	1.26	1.25	1.26	1.11	1.19	1.08	1.23	1.11	1.21
15	0.34	0.54	0.82	0.93	1.12	1.15	0.93	1.06	1.13	1.29	1.08	1.14	1.12	1.19	0.84	0.88	1.17	1.22	1.05
16	0.38	0.70	0.85	1.00	1.14	1.04	0.99	1.05	1.26	1.28	1.15	1.13	1.25	1.08	0.88	0.87	1.18	1.11	1.10
17	0.42	0.76	0.92	1.09	0.97	1.20	1.09	1.24	1.14	1.28	1.13	1.25	1.12	1.23	1.17	1.18	1.10	1.23	1.10
18	0.45	0.77	0.98	1.10	1.19	1.09	1.25	1.13	1.27	1.11	1.18	1.16	1.22	1.11	1.22	1.11	1.23	1.09	1.17
19	0.44	0.75	0.83	1.10	1.08	1.23	1.11	1.12	1.11	1.17	0.79	0.79	1.05	1.21	1.05	1.10	1.10	1.17	0.90

Figure 4A-9e. Average Bundle Exposure at 8.8 GWd/MT Exposure

	1	2	3	4	5	6	7	8	9	10	11	12	13	14	15	16	17	18	19
1															40.01	39.24	42.77	39.90	41.01
2													46.30	41.78	41.78	25.68	24.58	23.59	6.06
3											42.99	41.23	25.68	6.83	29.21	30.53	28.22	8.16	40.12
4									42.55	41.45	23.70	6.83	7.72	8.27	31.09	29.65	9.37	9.04	23.48
5								44.97	20.50	6.61	7.50	8.38	27.56	9.37	9.59	9.92	41.12	10.03	32.19
6							42.11	22.27	7.17	7.94	8.82	30.53	9.92	32.19	9.92	32.85	10.36	32.96	10.58
7						42.11	43.76	7.28	26.68	9.15	40.68	30.09	10.03	10.25	36.16	30.42	32.19	10.91	34.06
8					44.97	22.27	7.28	8.27	9.26	31.31	27.45	40.79	10.58	24.14	25.46	26.12	10.91	32.52	33.73
9				42.55	20.50	7.17	26.68	9.26	28.22	9.92	10.03	10.36	31.64	11.02	32.41	10.80	32.52	11.02	32.41
10				41.45	6.61	7.94	9.15	31.31	9.92	32.63	9.92	31.75	10.69	32.96	11.02	10.80	10.91	32.19	10.03
11			42.99	23.70	7.50	8.82	40.68	27.45	10.03	9.92	38.58	30.53	31.97	10.80	40.79	32.63	32.63	10.03	30.53
12			41.23	6.83	8.38	30.53	30.09	40.79	10.36	31.75	30.53	31.42	10.36	10.69	32.41	32.85	10.58	9.81	29.43
13		46.30	25.68	7.72	27.56	9.92	10.03	10.58	31.64	10.69	31.97	10.36	33.18	10.80	32.52	10.80	32.63	10.25	31.97
14		41.78	6.83	8.27	9.37	32.19	10.25	24.25	11.02	32.96	10.80	10.69	10.80	33.07	10.36	32.08	10.36	32.08	10.25
15	40.01	41.78	29.21	31.09	9.59	9.92	36.16	25.46	32.41	11.02	40.79	32.41	32.52	10.36	38.58	31.09	9.92	10.36	38.80
16	39.24	25.68	30.53	29.65	9.92	32.85	30.42	26.12	10.80	10.80	32.63	32.85	10.80	32.08	31.09	31.31	10.14	31.64	32.96
17	42.77	24.58	28.22	9.37	41.12	10.36	32.19	10.91	32.52	10.91	32.63	10.58	32.63	10.36	9.92	10.14	32.85	10.47	32.63
18	39.90	23.59	8.16	9.04	10.03	32.96	10.91	32.52	11.02	32.19	10.03	9.81	10.25	32.08	10.36	31.64	10.47	32.85	9.81
19	41.01	6.06	40.12	23.48	32.19	10.58	34.06	33.73	32.41	10.03	30.53	29.43	31.97	10.25	38.80	32.96	32.63	9.81	30.31

Figure 4A-10a. Control Rod Pattern Summary at 9.9 GWd/MT Exposure

```
( ROD PATTERN DEPLETION

NITER    0  POWER           IMAX  19  POWER(MWT)         4.5000E+03  ( 100.0 %)
IBOUN    1  1/4             JMAX  19  PRESSURE(PSIA)     1.0550E+03
IRN      1  MIRROR          KMAX  25  FLOW(*10E-6LB/HR)  7.8508E+01  ( 100.0 %)
ILPA     0                  NSMAX 10  BYPASS(LB/HR)      1.1742E+07  (  15.0 %)        CONTROL ROD CONFIGURATION
IFLW     2  DETAIL          LMAX  20  ENTHALPY(BTU/LB)      512.30                      IN NOTCHES WITHDRAWN
RSTART   0  NEW             LVDCT  7  INLET TEMP(DEG F)     520.47
NEWPHY   2                  IPFTL  0  BEGINNING EXPOSURE    21105.1      1  3  5  7  9 11 13 15 17 19 21 23 25 27 29 31 33 35 75
NEXO     3  CALC.                     DELTA EXPOS.(DELTE)      0.0
RBOCA    1                  IALPRM 0  DELBRN               1000.0                                                            71
IACF     0                  IFAST  0  TOTAL NOTCHES           2176
            IPDOME  1       IAHB   0  CORE FUEL MASS    MTU:162.928     1              63                                   67
                                      CORE FUEL MASS    STU:179.596
ENERGY (MWD) (DELTE)            0.  ENERGY (MWD) (DELBRN)    179596.     3                                                   63
CYCLE ENERGY (MWD)      1616379. CYCLE EXPOSURE             9000.0
CORE AVG. POWER DENSITY   54.328033                                     5              43           18                      59
NEUTRON MULTIPLICATION  1.00039268 FINAL AVG. EXPOSURE     22105.1
DIFP   (EPS5 = 0.00200)  0.00138026 CORE AVG. NEUTRON FLUX 1.461E+14    7                                                   55
AVERAGE VOID FRACTION    0.530555 CORE AVG. GD WORTH          0.000
CORE PRESSURE DROP,PSI   8.031620 CORE AVG. GD RESIDUAL WORTH 0.000     9       43              2                           51
EXP RATIO INDEX (INER-II)  0.0000 CORE AVERAGE XENON WORTH   -0.0229
                                                                       11                                                   47
CORE HISTORY MAX. VALUES:      LOCATION: I   J   K
  NODAL EXPOSURE, MWD/T  53673.       7   7   5   METRIC     59164.    13 63           2           22                       43
  BUNDLE EXPOSURE, MWD/T 42363.      13   2       METRIC     46697.
  EXPOSURE RATIO, NEXRAT 0.0000       0   0   0                        15                                                   39
  AXIAL POWER PEAK       1.3700               5
                                                                       17       18           22                            35

                                                                       19                                                   31

                                                                       21                                                   27

                                                                       23                                                   23

                                                                       25                                                   19

                                                                       27                                                   15

                                                                       29                                                   11

                                                                       31                                                    7

                                                                       33                                                    3
```

Figure 4A-10b. Relative Axial Power at 9.9 GWd/MT Exposure

9.9 GWD/MT

Node	Axial Power
25	0.183
24	0.354
23	0.515
22	0.647
21	0.753
20	0.832
19	0.891
18	0.934
17	0.962
16	1.015
15	1.114
14	1.142
13	1.168
12	1.197
11	1.225
10	1.250
9	1.267
8	1.286
7	1.315
6	1.347
5	1.370
4	1.360
3	1.269
2	1.038
1	0.569

Figure 4A-10c. Axial Exposure at 9.9 GWd/MT Exposure

9.9GWD/MT

Node	Axial Exposure (MWD/MT)
25	5084.0
24	8778.0
23	12325.0
22	15850.3
21	18941.3
20	21498.9
19	23594.7
18	25146.1
17	26159.7
16	26950.7
15	26328.5
14	27398.9
13	28276.6
12	28877.8
11	29388.2
10	29795.0
9	29975.3
8	30200.8
7	30514.9
6	30797.1
5	30794.6
4	30024.2
3	27424.6
2	21817.4
1	11199.6
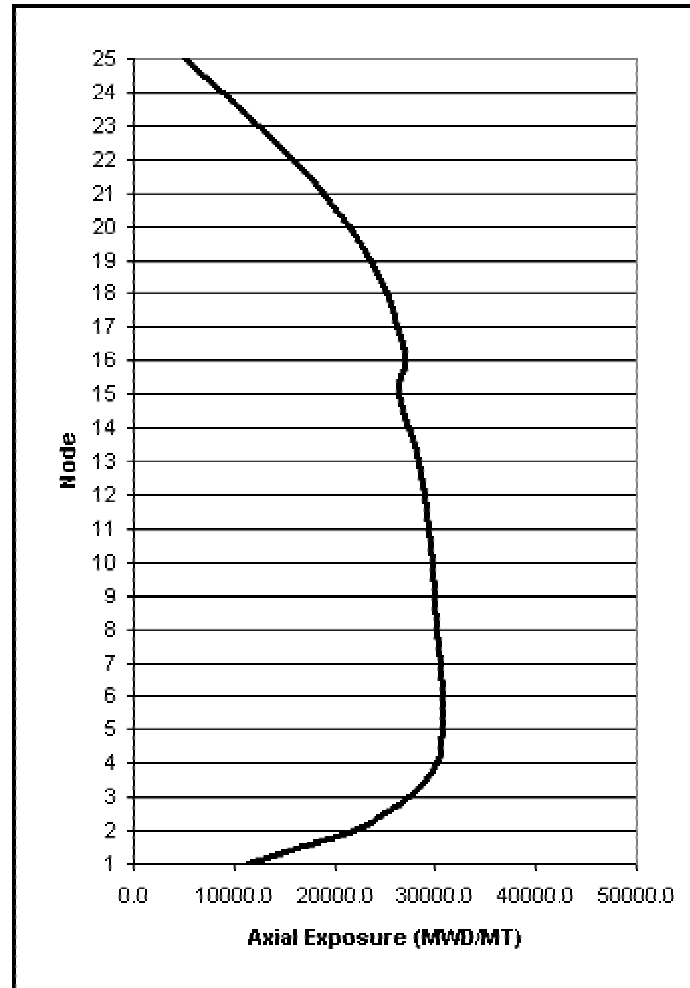
Figure 4A-10d. Relative Integrated Power Per Bundle at 9.9 GWd/MT Exposure

	1	2	3	4	5	6	7	8	9	10	11	12	13	14	15	16	17	18	19
1															0.31	0.36	0.40	0.43	0.42
2													0.35	0.45	0.50	0.66	0.72	0.74	0.73
3											0.40	0.50	0.66	0.76	0.73	0.76	0.87	0.95	0.80
4									0.38	0.49	0.68	0.82	0.92	0.97	0.85	0.90	1.06	1.07	1.05
5								0.44	0.65	0.78	0.89	0.99	1.00	1.13	1.14	1.15	0.95	1.16	1.01
6							0.43	0.67	0.85	0.92	0.98	0.97	1.18	1.08	1.24	1.08	1.21	1.03	1.12
7						0.43	0.56	0.87	0.92	1.02	0.77	0.90	1.20	1.29	1.12	1.19	1.10	1.17	0.77
8					0.44	0.67	0.87	1.00	1.10	0.99	0.93	0.86	1.26	1.24	1.28	1.25	1.29	1.06	0.79
9				0.38	0.65	0.85	0.92	1.10	1.09	1.22	1.21	1.25	1.18	1.33	1.16	1.32	1.15	1.27	1.07
10				0.49	0.78	0.92	1.02	0.99	1.22	1.11	1.28	1.15	1.32	1.13	1.24	1.23	1.29	1.15	1.29
11			0.40	0.68	0.89	0.98	0.77	0.93	1.21	1.28	1.11	1.19	1.18	1.23	0.73	0.78	1.08	1.31	1.20
12			0.50	0.82	0.99	0.97	0.90	0.86	1.25	1.15	1.19	1.18	1.30	1.22	0.77	0.77	1.23	1.30	1.22
13		0.35	0.66	0.92	1.00	1.18	1.20	1.26	1.18	1.32	1.18	1.30	1.14	1.28	1.06	1.21	1.12	1.31	1.16
14		0.45	0.76	0.97	1.13	1.08	1.29	1.24	1.33	1.13	1.23	1.22	1.28	1.12	1.27	1.13	1.30	1.14	1.22
15	0.31	0.50	0.73	0.85	1.14	1.24	1.12	1.28	1.16	1.24	0.73	0.77	1.06	1.27	1.10	1.18	1.29	1.23	0.81
16	0.36	0.66	0.76	0.90	1.15	1.08	1.19	1.25	1.32	1.23	0.78	0.77	1.21	1.13	1.18	1.18	1.29	1.09	0.84
17	0.40	0.72	0.87	1.06	0.95	1.22	1.10	1.29	1.15	1.29	1.08	1.23	1.12	1.30	1.29	1.29	1.14	1.27	1.07
18	0.43	0.74	0.95	1.07	1.16	1.03	1.17	1.06	1.27	1.15	1.31	1.30	1.31	1.14	1.23	1.09	1.27	1.13	1.28
19	0.42	0.73	0.80	1.05	1.01	1.12	0.77	0.79	1.07	1.29	1.20	1.22	1.16	1.22	0.81	0.84	1.07	1.28	1.19

Figure 4A-10e. Average Bundle Exposure at 9.9 GWd/MT Exposure

	1	2	3	4	5	6	7	8	9	10	11	12	13	14	15	16	17	18	19
1															40.45	39.57	43.32	40.45	41.45
2													46.74	42.33	42.33	26.46	25.46	24.47	6.94
3											43.43	41.78	26.46	7.72	30.09	31.42	29.21	9.15	41.01
4									42.88	42.00	24.47	7.72	8.71	9.37	32.08	30.75	10.58	10.36	24.69
5								45.53	21.27	7.50	8.49	9.48	28.66	10.58	10.80	11.13	42.22	11.35	33.40
6							42.55	22.93	8.16	8.93	9.92	31.64	11.24	33.40	11.13	34.06	11.68	34.17	11.90
7						42.55	44.42	8.27	27.67	10.25	41.67	31.31	11.35	11.57	37.15	31.53	33.40	12.24	35.27
8					45.53	22.93	8.27	9.37	10.47	32.52	28.77	41.89	11.90	25.46	26.68	27.23	12.24	33.73	35.05
9				42.88	21.27	8.16	27.67	10.47	29.43	11.24	11.35	11.79	32.96	12.46	33.62	12.24	33.73	12.35	33.62
10				42.00	7.50	8.93	10.25	32.52	11.24	33.84	11.24	32.85	12.13	34.17	12.35	12.24	12.24	33.40	11.35
11			43.43	24.47	8.49	9.92	41.67	28.77	11.35	11.24	39.46	31.42	33.18	12.24	42.00	33.84	33.84	11.24	31.42
12			41.78	7.72	9.48	31.64	31.31	41.89	11.79	32.85	31.42	32.41	11.68	12.02	33.62	34.06	12.02	11.02	30.20
13		46.63	26.46	8.71	28.66	11.24	11.35	11.90	32.96	12.13	33.18	11.68	34.50	12.13	33.73	12.13	33.84	11.57	33.07
14		42.33	7.72	9.37	10.58	33.40	11.57	25.46	12.46	34.17	12.24	12.02	12.13	34.28	11.68	33.29	11.79	33.29	11.57
15	40.45	42.33	30.09	32.08	10.80	11.13	37.15	26.68	33.62	12.35	42.00	33.62	33.73	11.68	39.57	32.08	11.24	11.79	39.90
16	39.57	26.46	31.42	30.75	11.13	34.06	31.53	27.23	12.24	12.24	33.84	34.06	12.13	33.29	32.08	32.19	11.46	32.85	34.17
17	43.32	25.46	29.21	10.58	42.22	11.68	33.40	12.24	33.73	12.24	33.84	12.02	33.84	11.79	11.24	11.46	34.06	11.90	33.84
18	40.45	24.47	9.15	10.36	11.35	34.06	12.24	33.73	12.35	33.40	11.24	11.02	11.57	33.29	11.79	32.85	11.90	34.06	11.02
19	41.45	6.94	41.01	24.69	33.40	11.90	35.27	35.05	33.62	11.35	31.42	30.20	33.07	11.57	39.90	34.17	33.84	11.02	31.31

Figure 4A-11a. Control Rod Pattern Summary at 11.0 GWd/MT Exposure

```
( ROD PATTERN DEPLETION

NITER   0  POWER         IMAX  19  POWER(MWT)          4.5000E+03  ( 100.0 %)
IBOUN   1  1/4           JMAX  19  PRESSURE(PSIA)      1.0550E+03
IRN     1  MIRROR        KMAX  25  FLOW(*10E-6LB/HR)   7.8508E+01  ( 100.0 %)
ILPA    0                NSMAX 10  BYPASS(LB/HR)       1.1742E+07  (  15.0 %)        CONTROL ROD CONFIGURATION
IFLW    2  DETAIL        LMAX  20  ENTHALPY(BTU/LB)        512.30                       IN NOTCHES WITHDRAWN
RSTART  0  NEW           LVDCT  5  INLET TEMP(DEG F)       520.47
NEWPHY  2                IPFTL  0  BEGINNING EXPOSURE     22105.1    1  3  5  7  9 11 13 15 17 19 21 23 25 27 29 31 33 35 75
NEXO    3  CALC.                   DELTA EXPOS.(DELTE)        0.0
RBOCA   1                IALPRM 0  DELBRN                  1000.0                                                        71
IACF    0                IFAST  0  TOTAL NOTCHES             2176
           IPDOME   1    IAHB   0  CORE FUEL MASS    MTU:162.928    1              63                                   67
                                   CORE FUEL MASS    STU:179.596
ENERGY (MWD) (DELTE)            0.  ENERGY (MWD) (DELBRN)   179596.  3                                                   63
CYCLE ENERGY (MWD)        1795977.  CYCLE EXPOSURE         10000.0
CORE AVG. POWER DENSITY   54.328033                                 5              43          18                       59
NEUTRON MULTIPLICATION  1.00122535  FINAL AVG. EXPOSURE    23105.1
DIFP   (EPS5 = 0.00200)  0.00131708  CORE AVG. NEUTRON FLUX 1.462E+14 7                                                 55
AVERAGE VOID FRACTION    0.530505  CORE AVG. GD WORTH        0.000
CORE PRESSURE DROP,PSI   8.042321  CORE AVG. GD RESIDUAL WORTH 0.000  9       43          2                             51
EXP RATIO INDEX (INER-II)  0.0000  CORE AVERAGE XENON WORTH  -0.0232
                                                                    11                                                 47
CORE HISTORY MAX. VALUES:       LOCATION: I   J   K
   NODAL EXPOSURE, MWD/T  54292.        7   7   5   METRIC   59847.  13 63          2          22                       43
   BUNDLE EXPOSURE, MWD/T 42715.       13   2       METRIC   47085.
   EXPOSURE RATIO, NEXRAT 0.0000        0   0   0                    15                                                 39
   AXIAL POWER PEAK       1.3741                5
                                                                    17       18          22                            35

                                                                    19                                                 31

                                                                    21                                                 27

                                                                    23                                                 23

                                                                    25                                                 19

                                                                    27                                                 15

                                                                    29                                                 11

                                                                    31                                                  7

                                                                    33                                                  3
```
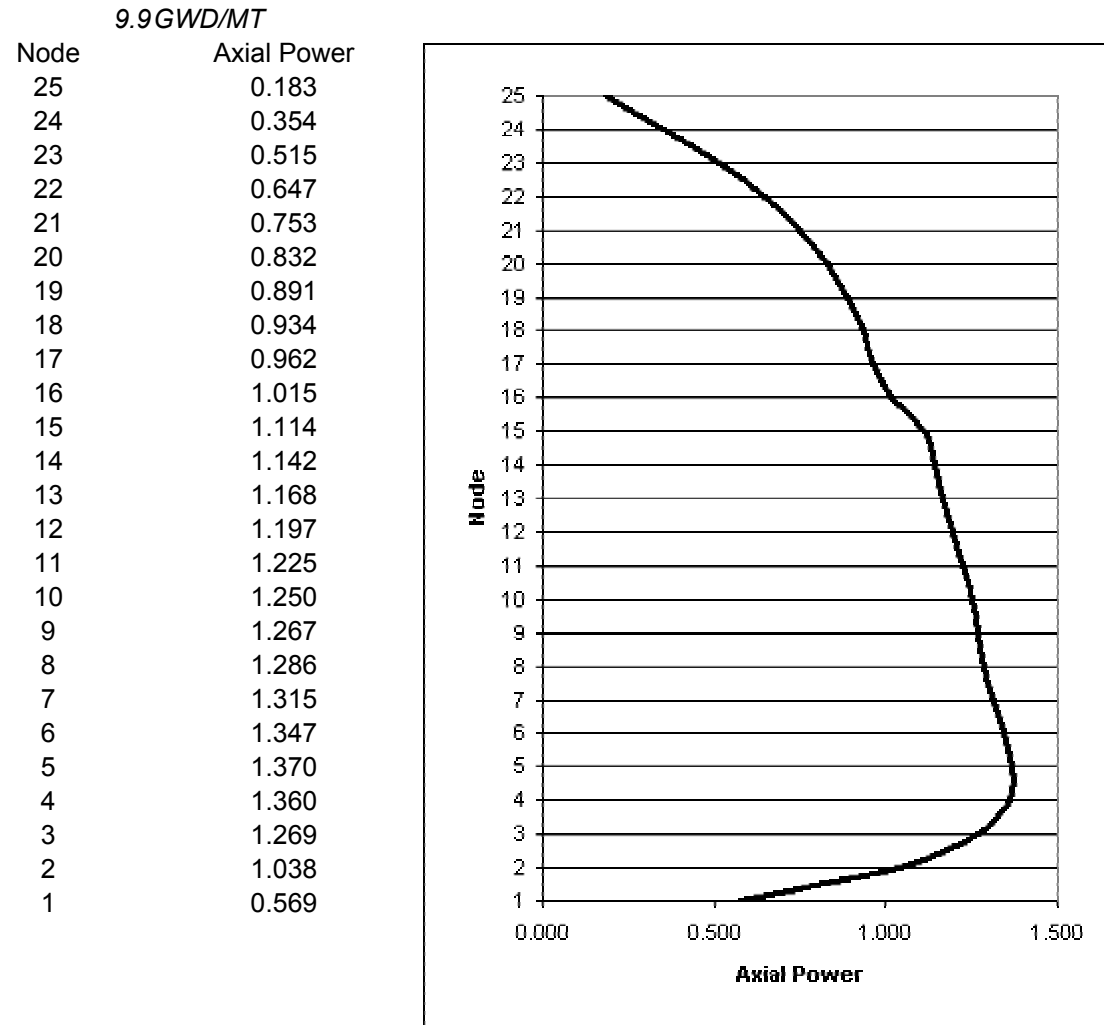
Figure 4A-11b. Relative Axial Power at 11.0 GWd/MT Exposure

11.0GWD/MT

Node	Axial Power
25	0.186
24	0.360
23	0.523
22	0.655
21	0.760
20	0.839
19	0.898
18	0.940
17	0.966
16	1.014
15	1.106
14	1.129
13	1.152
12	1.179
11	1.207
10	1.233
9	1.253
8	1.275
7	1.309
6	1.345
5	1.374
4	1.372
3	1.289
2	1.056
1	0.580
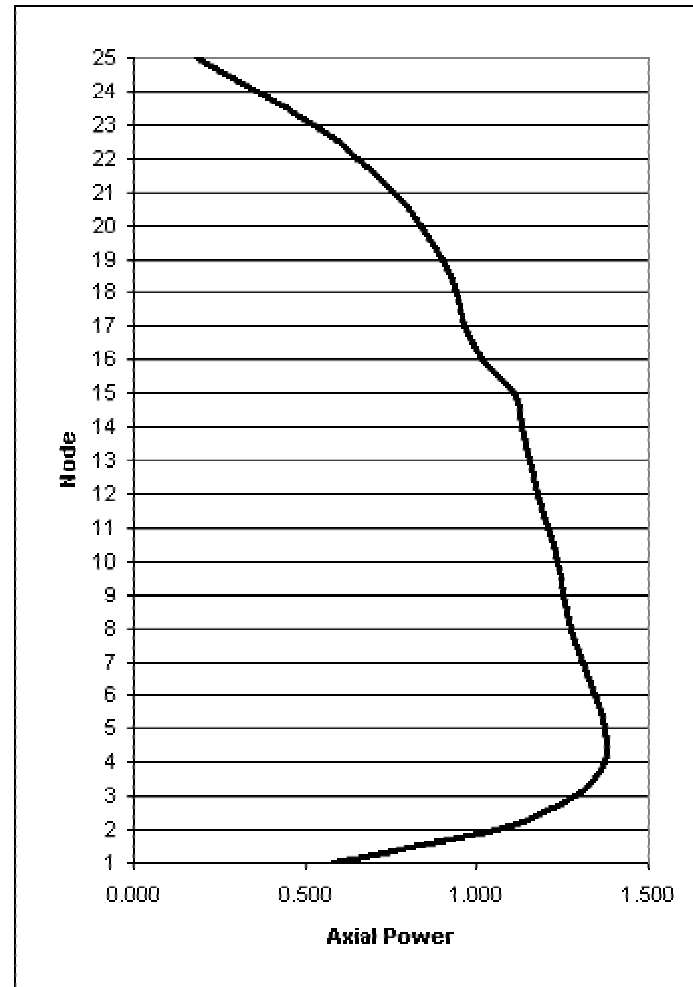
Figure 4A-11c. Axial Exposure at 11.0 GWd/MT Exposure

11.0GWD/MT

Node	Axial Exposure (MWD/MT)
25	5348.0
24	9226.0
23	12951.5
22	16636.9
21	19856.9
20	22510.8
19	24678.8
18	26282.8
17	27330.0
16	28140.5
15	27475.0
14	28574.0
13	29477.8
12	30108.8
11	30648.1
10	31080.5
9	31280.0
8	31524.7
7	31868.9
6	32183.9
5	32205.6
4	31425.3
3	28732.0
2	22886.8
1	11773.3
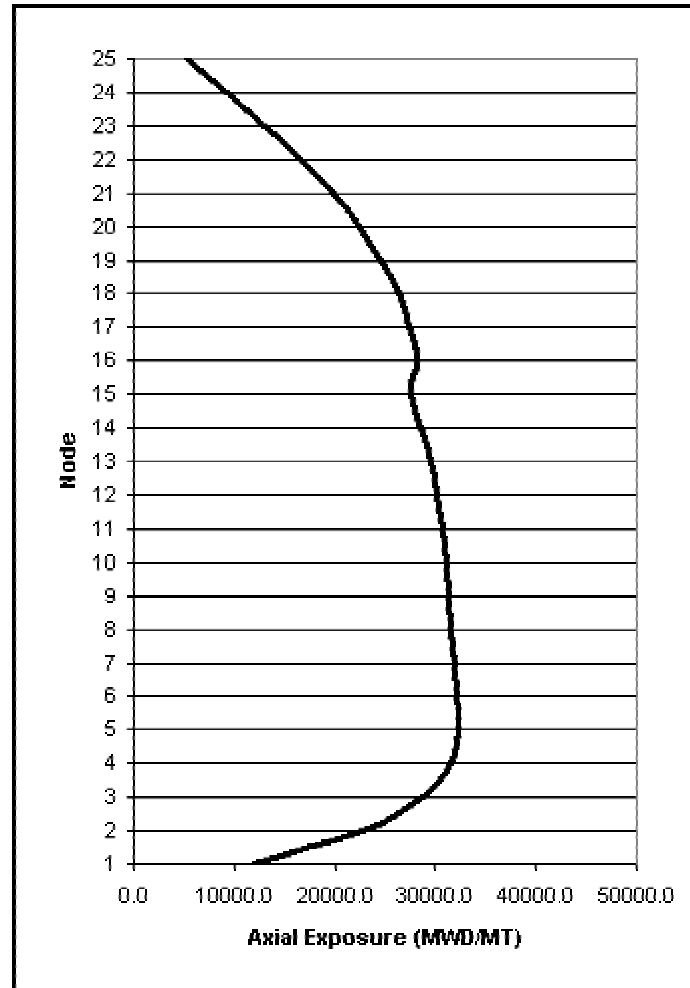
Figure 4A-11d. Relative Integrated Power Per Bundle at 11.0 GWd/MT Exposure

	1	2	3	4	5	6	7	8	9	10	11	12	13	14	15	16	17	18	19
1															0.30	0.35	0.39	0.42	0.41
2													0.35	0.44	0.49	0.64	0.70	0.72	0.73
3											0.40	0.50	0.66	0.76	0.72	0.74	0.86	0.94	0.78
4									0.37	0.49	0.68	0.82	0.93	0.98	0.84	0.89	1.06	1.07	1.03
5								0.44	0.65	0.80	0.90	1.00	1.00	1.14	1.15	1.15	0.94	1.16	1.00
6							0.43	0.67	0.86	0.94	1.00	0.97	1.19	1.07	1.24	1.07	1.22	1.02	1.12
7						0.43	0.56	0.88	0.92	1.04	0.77	0.90	1.21	1.29	1.10	1.17	1.09	1.17	0.77
8					0.44	0.67	0.88	1.01	1.12	0.99	0.93	0.86	1.27	1.22	1.26	1.23	1.29	1.04	0.78
9				0.37	0.65	0.86	0.92	1.12	1.09	1.23	1.23	1.26	1.17	1.34	1.15	1.33	1.14	1.27	1.05
10				0.49	0.80	0.94	1.04	0.99	1.23	1.11	1.30	1.14	1.32	1.13	1.25	1.25	1.30	1.14	1.30
11			0.40	0.68	0.90	1.00	0.77	0.93	1.23	1.30	1.10	1.18	1.17	1.24	0.73	0.78	1.08	1.32	1.19
12			0.50	0.82	1.00	0.97	0.90	0.86	1.26	1.14	1.18	1.17	1.32	1.24	0.77	0.77	1.24	1.32	1.21
13		0.35	0.66	0.93	1.00	1.19	1.21	1.27	1.17	1.32	1.17	1.32	1.14	1.29	1.06	1.22	1.12	1.33	1.15
14		0.44	0.76	0.98	1.14	1.07	1.29	1.22	1.34	1.13	1.24	1.24	1.29	1.12	1.29	1.13	1.32	1.14	1.24
15	0.30	0.49	0.72	0.84	1.15	1.24	1.10	1.26	1.15	1.25	0.73	0.77	1.06	1.29	1.10	1.17	1.31	1.25	0.81
16	0.35	0.64	0.74	0.89	1.15	1.07	1.17	1.23	1.33	1.25	0.78	0.77	1.22	1.13	1.17	1.17	1.31	1.09	0.83
17	0.39	0.70	0.86	1.06	0.94	1.22	1.09	1.29	1.14	1.30	1.08	1.24	1.12	1.32	1.31	1.31	1.14	1.28	1.07
18	0.42	0.72	0.94	1.07	1.16	1.02	1.17	1.04	1.27	1.14	1.32	1.32	1.33	1.14	1.25	1.09	1.28	1.13	1.30
19	0.41	0.73	0.78	1.03	1.00	1.12	0.77	0.78	1.05	1.30	1.19	1.21	1.15	1.24	0.81	0.83	1.07	1.30	1.18

Figure 4A-11e. Average Bundle Exposure at 11.0 GWd/MT Exposure

	1	2	3	4	5	6	7	8	9	10	11	12	13	14	15	16	17	18	19
1															40.79	40.01	43.76	40.90	41.89
2													47.07	42.77	42.88	27.23	26.23	25.24	7.72
3											43.87	42.33	27.23	8.60	30.86	32.30	30.20	10.25	41.89
4									43.32	42.55	25.13	8.71	9.81	10.47	32.96	31.75	11.68	11.46	25.90
5								45.97	22.05	8.38	9.48	10.58	29.76	11.79	12.02	12.46	43.21	12.68	34.50
6							42.99	23.70	9.15	10.03	11.02	32.74	12.46	34.61	12.57	35.27	13.01	35.27	13.12
7						42.99	44.97	9.15	28.66	11.46	42.55	32.30	12.68	13.01	38.36	32.85	34.61	13.56	36.05
8					45.97	23.70	9.15	10.47	11.68	33.62	29.76	42.88	13.34	26.90	28.00	28.66	13.67	34.83	35.94
9				43.32	22.05	9.15	28.66	11.68	30.64	12.68	12.68	13.12	34.28	13.89	34.94	13.67	35.05	13.78	34.83
10				42.55	8.38	10.03	11.46	33.62	12.68	35.05	12.68	34.17	13.56	35.49	13.78	13.56	13.67	34.72	12.79
11			43.87	25.13	9.48	11.02	42.55	29.76	12.68	12.68	40.68	32.74	34.50	13.56	42.77	34.72	35.05	12.79	32.74
12			42.33	8.71	10.58	32.74	32.30	42.88	13.12	34.17	32.74	33.73	13.12	13.34	34.50	34.94	13.34	12.46	31.64
13		47.07	27.23	9.81	29.76	12.46	12.68	13.34	34.28	13.56	34.50	13.12	35.71	13.56	34.94	13.45	35.16	13.01	34.39
14		42.77	8.60	10.47	11.79	34.61	13.01	26.90	13.89	35.49	13.56	13.34	13.56	35.49	13.01	34.50	13.23	34.50	13.01
15	40.79	42.88	30.86	32.96	12.02	12.57	38.36	28.00	34.94	13.78	42.77	34.50	34.94	13.01	40.79	33.40	12.68	13.12	40.79
16	40.01	27.23	32.30	31.75	12.46	35.27	32.85	28.66	13.67	13.56	34.72	34.94	13.45	34.50	33.40	33.51	12.79	34.06	35.16
17	43.76	26.23	30.20	11.68	43.32	13.01	34.61	13.67	35.05	13.67	35.05	13.34	35.16	13.23	12.68	12.79	35.38	13.23	35.05
18	40.90	25.24	10.25	11.46	12.68	35.27	13.56	34.83	13.78	34.72	12.79	12.46	13.01	34.50	13.12	34.06	13.23	35.27	12.46
19	41.89	7.72	41.89	25.79	34.50	13.12	36.05	35.83	34.83	12.79	32.74	31.64	34.39	13.01	40.79	35.16	35.05	12.46	32.63

Figure 4A-12a. Control Rod Pattern Summary at 12.1 GWd/MT Exposure

```
( ROD PATTERN DEPLETION

NITER  0  POWER       IMAX  19  POWER(MWT)        4.5000E+03  ( 100.0 %)
IBOUN  1  1/4         JMAX  19  PRESSURE(PSIA)    1.0550E+03
IRN    1  MIRROR      KMAX  25  FLOW(*10E-6LB/HR) 7.8508E+01  ( 100.0 %)
ILPA   0              NSMAX 10  BYPASS(LB/HR)     1.1742E+07  (  15.0 %)      CONTROL ROD CONFIGURATION
IFLW   2  DETAIL      LMAX  20  ENTHALPY(BTU/LB)      512.30                    IN NOTCHES WITHDRAWN
RSTART 0  NEW         LVDCT  7  INLET TEMP(DEG F)     520.47
NEWPHY 2              IPFTL  0  BEGINNING EXPOSURE    23105.1   1  3  5  7  9 11 13 15 17 19 21 23 25 27 29 31 33 35 75
NEXO   3  CALC.                 DELTA EXPOS.(DELTE)       0.0
RBOCA  1              IALPRM 0  DELBRN               1000.0                                                        71
IACF   0              IFAST  0  TOTAL NOTCHES          2220
          IPDOME  1  IAHB  0  CORE FUEL MASS   MTU:162.928     1            83                                    67
                                CORE FUEL MASS   STU:179.596
ENERGY (MWD) (DELTE)        0.  ENERGY (MWD) (DELBRN)  179596.  3                                                  63
CYCLE ENERGY (MWD)     1975574. CYCLE EXPOSURE         11000.0
CORE AVG. POWER DENSITY  54.328033                             5            28          6                          59
NEUTRON MULTIPLICATION   0.99892461 FINAL AVG. EXPOSURE 24105.1
DIFP  (EPS5 = 0.00200)   0.00093353 CORE AVG. NEUTRON FLUX 1.467E+14  7                                           55
AVERAGE VOID FRACTION    0.541182 CORE AVG. GD WORTH      0.000
CORE PRESSURE DROP,PSI   8.078023 CORE AVG. GD RESIDUAL WORTH  0.000  9        28          7                      51
EXP RATIO INDEX (INER-II)   0.0000 CORE AVERAGE XENON WORTH  -0.0235
                                                              11                                                  47
CORE HISTORY MAX. VALUES:     LOCATION: I  J  K
  NODAL EXPOSURE, MWD/T  54927.      7  7  5   METRIC  60546.  13 83         7          3                          43
  BUNDLE EXPOSURE, MWD/T 43063.     13  2      METRIC  47468.
  EXPOSURE RATIO, NEXRAT 0.0000      0  0  0                  15                                                  39
  AXIAL POWER PEAK       1.4387            4
                                                              17        6          3                              35

                                                              19                                                  31

                                                              21                                                  27

                                                              23                                                  23

                                                              25                                                  19

                                                              27                                                  15

                                                              29                                                  11

                                                              31                                                   7

                                                              33                                                   3
```

Figure 4A-12b. Relative Axial Power at 12.1 GWd/MT Exposure

12.1 GWD/MT

Node	Axial Power
25	0.182
24	0.352
23	0.505
22	0.622
21	0.721
20	0.800
19	0.863
18	0.905
17	0.919
16	0.961
15	1.049
14	1.081
13	1.119
12	1.156
11	1.194
10	1.232
9	1.272
8	1.315
7	1.361
6	1.405
5	1.438
4	1.439
3	1.362
2	1.127
1	0.621
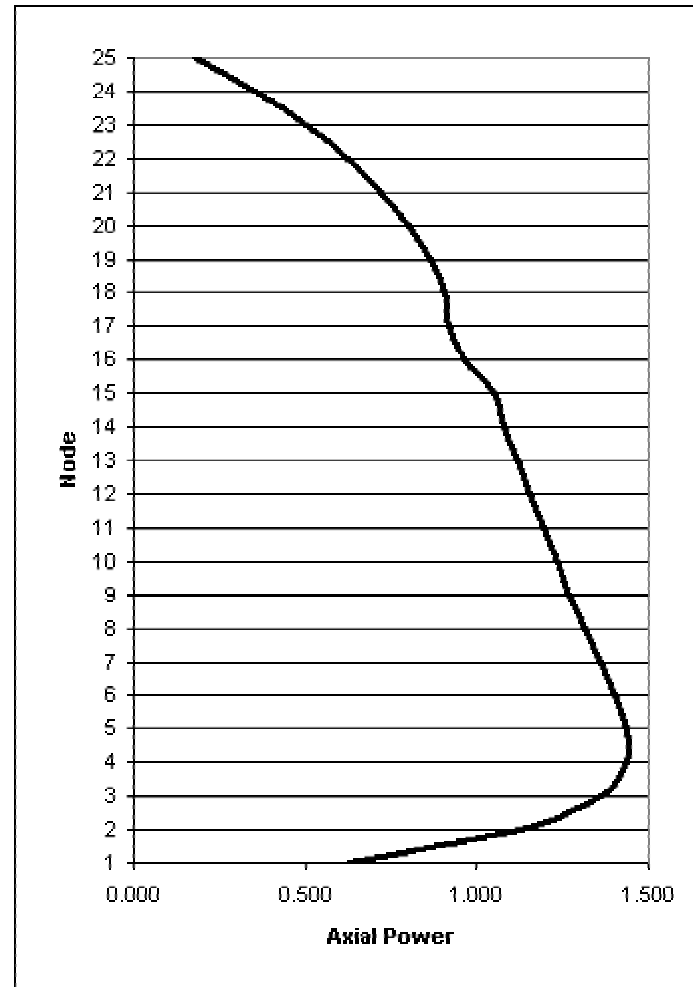
Figure 4A-12c. Axial Exposure at 12.1 GWd/MT Exposure

12.1GWD/MT

Node	Axial Exposure (MWD/MT)
25	5616.5
24	9682.4
23	13588.3
22	17433.5
21	20781.6
20	23531.3
19	25771.2
18	27427.0
17	28505.0
16	29329.3
15	28612.9
14	29735.8
13	30662.7
12	31321.9
11	31889.5
10	32348.5
9	32570.2
8	32838.3
7	33216.6
6	33569.1
5	33620.9
4	32838.8
3	30060.0
2	23974.6
1	12358.0
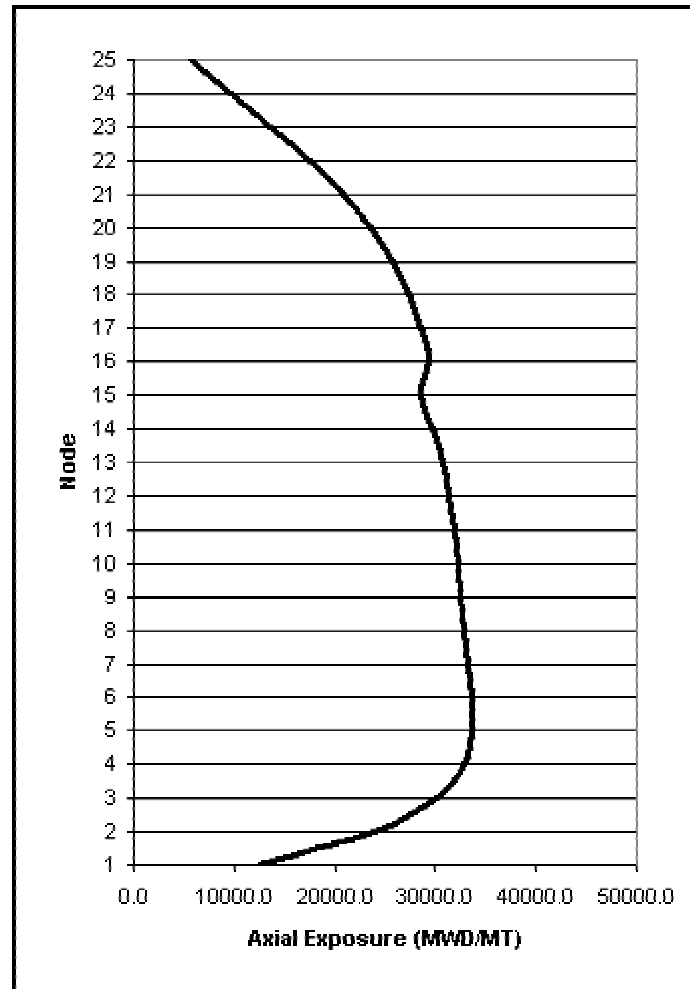
Figure 4A-12d. Relative Integrated Power Per Bundle at 12.1 GWd/MT Exposure

	1	2	3	4	5	6	7	8	9	10	11	12	13	14	15	16	17	18	19
1															0.31	0.36	0.40	0.43	0.42
2													0.36	0.46	0.51	0.66	0.72	0.74	0.74
3											0.41	0.51	0.68	0.81	0.78	0.80	0.88	0.98	0.79
4									0.38	0.49	0.69	0.85	0.97	1.03	0.92	0.96	1.11	1.11	1.04
5								0.44	0.66	0.81	0.92	1.02	1.01	1.19	1.20	1.20	0.95	1.18	0.99
6							0.43	0.67	0.87	0.95	0.99	0.95	1.20	1.08	1.27	1.07	1.23	1.02	1.12
7						0.43	0.56	0.89	0.91	1.02	0.70	0.82	1.21	1.30	1.10	1.16	1.07	1.16	0.71
8					0.44	0.67	0.89	1.02	1.11	0.96	0.85	0.78	1.25	1.20	1.24	1.21	1.29	1.02	0.73
9				0.38	0.66	0.87	0.91	1.11	1.07	1.22	1.21	1.24	1.15	1.33	1.14	1.33	1.13	1.27	1.03
10				0.49	0.81	0.95	1.02	0.96	1.22	1.09	1.29	1.12	1.32	1.12	1.26	1.26	1.31	1.13	1.31
11			0.41	0.69	0.92	0.99	0.70	0.85	1.21	1.29	1.08	1.15	1.16	1.25	0.75	0.79	1.08	1.33	1.18
12			0.51	0.85	1.02	0.95	0.82	0.78	1.24	1.12	1.15	1.15	1.33	1.25	0.79	0.78	1.26	1.33	1.19
13		0.36	0.68	0.97	1.01	1.20	1.21	1.25	1.15	1.32	1.16	1.33	1.14	1.31	1.06	1.24	1.12	1.33	1.13
14		0.46	0.81	1.03	1.19	1.08	1.30	1.20	1.33	1.12	1.25	1.25	1.31	1.12	1.30	1.12	1.33	1.12	1.23
15	0.31	0.51	0.78	0.92	1.20	1.27	1.10	1.24	1.14	1.26	0.75	0.79	1.06	1.30	1.09	1.16	1.32	1.23	0.73
16	0.36	0.66	0.80	0.96	1.20	1.07	1.16	1.21	1.33	1.26	0.79	0.78	1.24	1.12	1.16	1.15	1.31	1.05	0.74
17	0.40	0.72	0.88	1.11	0.95	1.23	1.07	1.29	1.13	1.31	1.08	1.26	1.12	1.33	1.32	1.31	1.11	1.26	1.02
18	0.43	0.74	0.98	1.11	1.18	1.02	1.16	1.02	1.27	1.14	1.33	1.33	1.33	1.12	1.23	1.05	1.26	1.10	1.28
19	0.42	0.74	0.79	1.04	0.99	1.12	0.71	0.73	1.03	1.31	1.18	1.19	1.13	1.23	0.73	0.74	1.02	1.28	1.15

Figure 4A-12e. Average Bundle Exposure at 12.1 GWd/MT Exposure

	1	2	3	4	5	6	7	8	9	10	11	12	13	14	15	16	17	18	19
1															41.12	40.34	44.20	41.34	42.44
2													47.51	43.32	43.43	27.89	27.01	26.01	8.49
3											44.31	42.88	27.89	9.37	31.75	33.07	31.09	11.24	42.77
4									43.76	43.10	25.90	9.59	10.80	11.57	33.95	32.63	12.90	12.68	27.01
5								46.41	22.71	9.26	10.47	11.68	30.86	13.12	13.34	13.67	44.31	13.89	35.60
6							43.54	24.47	10.03	11.02	12.13	33.84	13.78	35.71	13.89	36.38	14.33	36.38	14.33
7						43.54	45.64	10.14	29.76	12.57	43.32	33.29	14.00	14.44	39.57	34.17	35.83	14.88	36.93
8					46.52	24.47	10.14	11.57	12.90	34.61	30.75	43.76	14.77	28.22	29.43	29.98	15.10	36.05	36.71
9				43.76	22.71	10.03	29.76	12.90	31.86	14.00	14.00	14.55	35.49	15.32	36.16	15.21	36.27	15.21	36.05
10				43.10	9.26	11.02	12.57	34.61	14.00	36.27	14.00	35.38	14.99	36.71	15.10	14.99	15.10	35.94	14.22
11			44.31	25.90	10.47	12.13	43.32	30.75	14.00	14.00	41.89	34.06	35.83	14.88	43.65	35.60	36.27	14.22	34.06
12			42.88	9.59	11.68	33.84	33.29	43.76	14.55	35.38	34.06	34.94	14.55	14.77	35.38	35.83	14.66	13.89	32.96
13		47.40	27.89	10.80	30.86	13.78	14.00	14.77	35.49	14.99	35.83	14.55	36.93	14.99	36.16	14.77	36.38	14.55	35.60
14		43.32	9.37	11.57	13.12	35.71	14.44	28.22	15.32	36.71	14.88	14.77	14.99	36.71	14.44	35.71	14.66	35.83	14.33
15	41.12	43.43	31.75	33.95	13.34	13.89	39.57	29.43	36.16	15.10	43.65	35.38	36.16	14.44	42.00	34.72	14.11	14.44	41.67
16	40.34	27.89	33.07	32.74	13.67	36.38	34.17	29.98	15.21	14.99	35.60	35.83	14.77	35.71	34.72	34.83	14.33	35.27	36.05
17	44.20	27.01	31.09	12.90	44.31	14.33	35.83	15.10	36.27	15.10	36.27	14.66	36.38	14.66	14.11	14.33	36.60	14.66	36.16
18	41.34	26.01	11.24	12.68	13.89	36.38	14.88	36.05	15.21	35.94	14.22	13.89	14.55	35.83	14.44	35.27	14.66	36.49	13.89
19	42.44	8.49	42.77	27.01	35.60	14.33	36.93	36.71	35.94	14.22	34.06	32.96	35.60	14.33	41.67	36.05	36.16	13.89	33.95

Figure 4A-13a. Control Rod Pattern Summary at 13.2 GWd/MT Exposure

```
( ROD PATTERN DEPLETION

NITER   0  POWER        IMAX  19  POWER(MWT)         4.5000E+03  ( 100.0 %)
IBOUN   1  1/4          JMAX  19  PRESSURE(PSIA)     1.0550E+03
IRN     1  MIRROR       KMAX  25  FLOW(*10E-6LB/HR)  7.8508E+01  ( 100.0 %)          CONTROL ROD CONFIGURATION
ILPA    0               NSMAX 10  BYPASS(LB/HR)      1.1742E+07  (  15.0 %)             IN NOTCHES WITHDRAWN
IFLW    2  DETAIL       LMAX  20  ENTHALPY(BTU/LB)      512.30
RSTART  0  NEW          LVDCT  7  INLET TEMP(DEG F)     520.47
NEWPHY  2               IPFTL  0  BEGINNING EXPOSURE   24105.1    1  3  5  7  9 11 13 15 17 19 21 23 25 27 29 31 33 35 75
NEXO    3  CALC.                  DELTA EXPOS.(DELTE)      0.0
RBOCA   1               IALPRM 0  DELBRN               1000.0                                                     71
IACF    0               IFAST  0  TOTAL NOTCHES          2220
           IPDOME  1    IAHB   0  CORE FUEL MASS    MTU:162.928   1              83                               67
                                  CORE FUEL MASS    STU:179.596
ENERGY (MWD) (DELTE)            0. ENERGY (MWD) (DELBRN)  179596.   3                                             63
CYCLE ENERGY (MWD)      2155172. CYCLE EXPOSURE         12000.0
CORE AVG. POWER DENSITY   54.328033                                5           28           6                    59
NEUTRON MULTIPLICATION    0.99814361 FINAL AVG. EXPOSURE   25105.1
DIFP   (EPS5 = 0.00200)   0.00133455 CORE AVG. NEUTRON FLUX 1.468E+14  7                                         55
AVERAGE VOID FRACTION     0.529695 CORE AVG. GD WORTH       0.000
CORE PRESSURE DROP,PSI    8.065022 CORE AVG. GD RESIDUAL WORTH 0.000  9     28           7                       51
EXP RATIO INDEX (INER-II)   0.0000 CORE AVERAGE XENON WORTH  -0.0236
                                                                  11                                             47
CORE HISTORY MAX. VALUES:      LOCATION: I   J   K
  NODAL EXPOSURE, MWD/T  55610.       7   7   5   METRIC    61299.  13 83        7           3                   43
  BUNDLE EXPOSURE, MWD/T 43424.      13   2       METRIC    47867.
  EXPOSURE RATIO, NEXRAT 0.0000       0   0   0                     15                                           39
  AXIAL POWER PEAK       1.3380               5
                                                                  17        6           3                       35

                                                                  19                                             31

                                                                  21                                             27

                                                                  23                                             23

                                                                  25                                             19

                                                                  27                                             15

                                                                  29                                             11

                                                                  31                                              7

                                                                  33                                              3
```

4A-63

Figure 4A-13b. Relative Axial Power at 13.2 GWd/MT Exposure

13.2 GWD/MT

Node	Axial Power
25	0.200
24	0.389
23	0.556
22	0.682
21	0.789
20	0.873
19	0.937
18	0.976
17	0.982
16	1.017
15	1.098
14	1.117
13	1.143
12	1.168
11	1.193
10	1.217
9	1.242
8	1.270
7	1.298
6	1.323
5	1.338
4	1.327
3	1.252
2	1.041
1	0.573
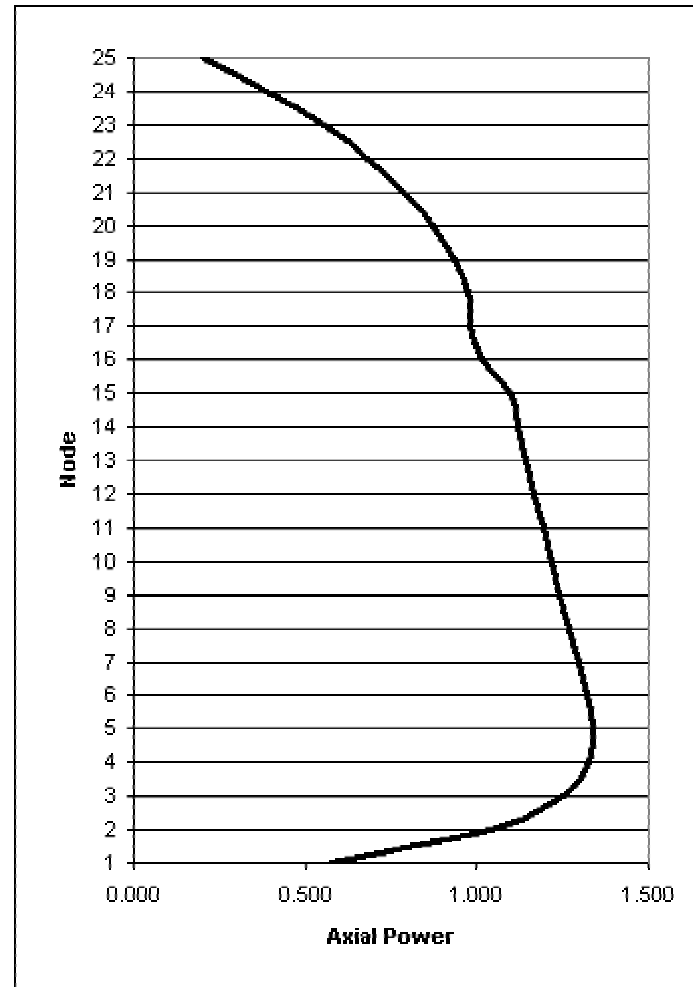
Figure 4A-13c. Axial Exposure at 13.2 GWd/MT Exposure

13.2GWD/MT

Node	Axial Exposure (MWD/MT)
25	5878.4
24	10128.0
23	14202.6
22	18190.7
21	21659.4
20	24505.2
19	26821.4
18	28527.8
17	29623.1
16	30455.8
15	29692.3
14	30847.5
13	31813.4
12	32511.5
11	33117.9
10	33616.4
9	33879.4
8	34192.9
7	34618.5
6	35015.6
5	35101.4
4	34320.6
3	31462.8
2	25135.5
1	12984.6
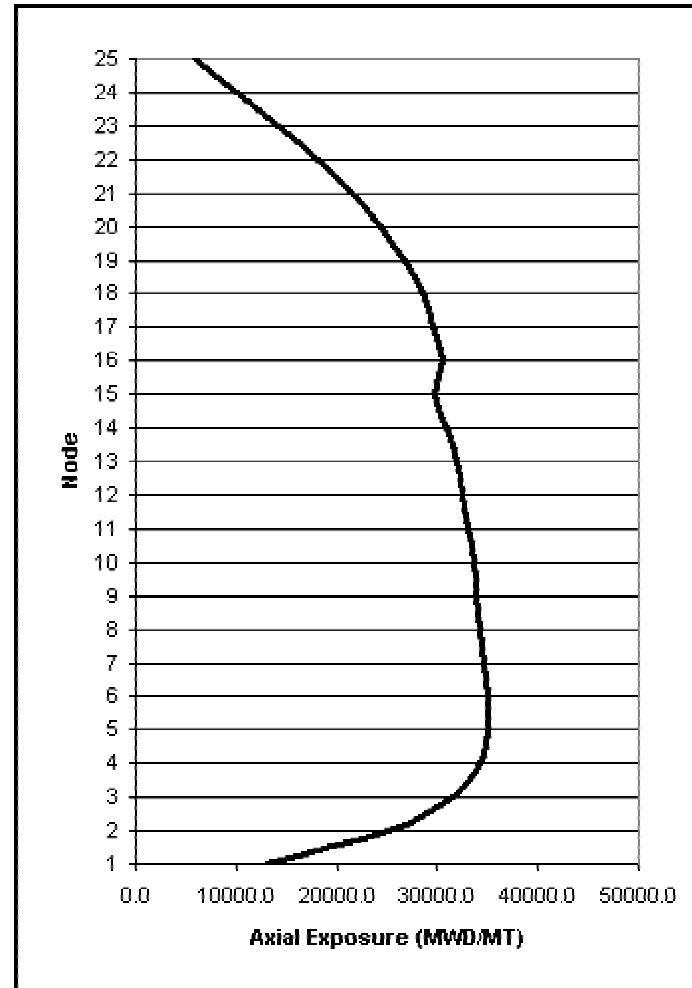
Figure 4A-13d. Relative Integrated Power Per Bundle at 13.2 GWd/MT Exposure

	1	2	3	4	5	6	7	8	9	10	11	12	13	14	15	16	17	18	19
1															0.31	0.36	0.40	0.43	0.42
2													0.37	0.46	0.51	0.66	0.72	0.74	0.75
3											0.42	0.52	0.69	0.83	0.79	0.80	0.88	0.99	0.79
4									0.39	0.51	0.71	0.88	0.99	1.06	0.92	0.96	1.12	1.12	1.03
5								0.45	0.67	0.84	0.95	1.05	1.03	1.21	1.22	1.21	0.95	1.19	0.99
6							0.44	0.69	0.90	0.98	1.03	0.97	1.22	1.08	1.28	1.06	1.23	1.01	1.12
7						0.44	0.57	0.92	0.93	1.05	0.71	0.83	1.21	1.30	1.08	1.14	1.06	1.15	0.71
8					0.45	0.69	0.92	1.05	1.14	0.97	0.86	0.79	1.25	1.19	1.21	1.19	1.27	1.00	0.72
9				0.39	0.67	0.90	0.93	1.14	1.08	1.23	1.22	1.24	1.14	1.32	1.12	1.31	1.11	1.25	1.01
10				0.51	0.84	0.98	1.05	0.97	1.23	1.09	1.29	1.11	1.31	1.10	1.24	1.25	1.30	1.12	1.29
11			0.42	0.71	0.95	1.03	0.71	0.86	1.22	1.29	1.07	1.14	1.14	1.24	0.74	0.79	1.06	1.32	1.16
12			0.52	0.88	1.05	0.97	0.83	0.79	1.24	1.11	1.14	1.14	1.32	1.25	0.78	0.78	1.25	1.33	1.17
13		0.37	0.69	0.99	1.03	1.22	1.21	1.25	1.14	1.31	1.14	1.32	1.12	1.30	1.05	1.23	1.11	1.32	1.12
14		0.46	0.83	1.06	1.21	1.08	1.30	1.19	1.32	1.10	1.24	1.25	1.30	1.11	1.29	1.11	1.32	1.11	1.22
15	0.31	0.51	0.79	0.92	1.22	1.28	1.08	1.21	1.12	1.24	0.74	0.78	1.05	1.29	1.07	1.14	1.31	1.23	0.72
16	0.36	0.66	0.80	0.96	1.21	1.06	1.14	1.19	1.31	1.25	0.79	0.78	1.23	1.11	1.14	1.14	1.30	1.04	0.73
17	0.40	0.72	0.88	1.12	0.95	1.23	1.06	1.27	1.11	1.30	1.06	1.25	1.11	1.32	1.31	1.30	1.10	1.26	1.01
18	0.43	0.74	0.99	1.12	1.19	1.01	1.15	1.00	1.25	1.12	1.32	1.33	1.32	1.11	1.23	1.04	1.26	1.09	1.28
19	0.42	0.75	0.79	1.03	0.99	1.12	0.71	0.72	1.01	1.29	1.16	1.17	1.12	1.22	0.72	0.73	1.01	1.28	1.13

Figure 4A-13e. Average Bundle Exposure at 13.2 GWd/MT Exposure

	1	2	3	4	5	6	7	8	9	10	11	12	13	14	15	16	17	18	19
1															41.45	40.79	44.64	41.78	42.88
2													47.84	43.76	43.98	28.66	27.78	26.90	9.37
3											44.75	43.43	28.66	10.25	32.63	33.95	32.08	12.35	43.65
4									44.20	43.65	26.68	10.47	11.90	12.68	34.94	33.73	14.11	13.89	28.11
5								46.96	23.48	10.14	11.57	12.79	31.97	14.44	14.66	14.99	45.30	15.21	36.71
6							43.98	25.24	11.02	12.13	13.23	34.83	15.10	36.93	15.32	37.59	15.76	37.48	15.65
7						43.98	46.30	11.13	30.75	13.67	44.09	34.17	15.32	15.87	40.79	35.38	36.93	16.09	37.70
8					46.96	25.24	11.13	12.68	14.22	35.71	31.75	44.64	16.09	29.54	30.75	31.31	16.42	37.15	37.59
9				44.20	23.48	11.02	30.75	14.22	32.96	15.32	15.32	15.87	36.82	16.87	37.48	16.64	37.48	16.53	37.15
10				43.65	10.14	12.13	13.67	35.71	15.32	37.48	15.43	36.60	16.42	37.92	16.53	16.31	16.53	37.15	15.65
11			44.75	26.68	11.57	13.23	44.09	31.75	15.32	15.43	43.10	35.27	37.04	16.31	44.42	36.49	37.37	15.65	35.38
12			43.43	10.47	12.79	34.83	34.17	44.64	15.87	36.60	35.27	36.27	16.09	16.09	36.27	36.71	16.09	15.43	34.28
13		47.84	28.66	11.90	31.97	15.10	15.32	16.09	36.82	16.42	37.04	16.09	38.25	16.42	37.26	16.20	37.59	15.98	36.93
14		43.76	10.25	12.68	14.44	36.93	15.87	29.54	16.87	37.92	16.31	16.09	16.42	38.03	15.87	37.04	16.09	37.04	15.65
15	41.45	43.98	32.63	34.94	14.66	15.32	40.79	30.75	37.48	16.53	44.42	36.27	37.26	15.87	43.21	35.94	15.54	15.87	42.55
16	40.79	28.66	33.95	33.73	14.99	37.59	35.38	31.31	16.64	16.31	36.49	36.71	16.20	37.04	35.94	36.05	15.76	36.38	36.82
17	44.64	27.78	32.08	14.11	45.30	15.76	36.93	16.53	37.48	16.64	37.37	16.09	37.59	16.09	15.54	15.76	37.81	16.09	37.37
18	41.89	26.90	12.35	13.89	15.21	37.48	16.09	37.15	16.53	37.15	15.65	15.43	15.98	37.04	15.87	36.38	16.09	37.70	15.32
19	42.88	9.37	43.65	28.11	36.71	15.65	37.70	37.59	37.15	15.65	35.38	34.28	36.93	15.65	42.55	36.82	37.37	15.32	35.16

Figure 4A-14a. Control Rod Pattern Summary at 14.3 GWd/MT Exposure

```
( ROD PATTERN DEPLETION

NITER   0  POWER         IMAX  19  POWER(MWT)            4.5000E+03  ( 100.0 %)
IBOUN   1  1/4           JMAX  19  PRESSURE(PSIA)        1.0550E+03
IRN     1  MIRROR        KMAX  25  FLOW(*10E-6LB/HR)     7.8508E+01  ( 100.0 %)
ILPA    0                NSMAX 10  BYPASS(LB/HR)         1.1742E+07  (  15.0 %)      CONTROL ROD CONFIGURATION
IFLW    2  DETAIL        LMAX  20  ENTHALPY(BTU/LB)         512.30                      IN NOTCHES WITHDRAWN
RSTART  0  NEW           LVDCT  8  INLET TEMP(DEG F)        520.47
NEWPHY  2                IPFTL  0  BEGINNING EXPOSURE     25105.1   1  3  5  7  9 11 13 15 17 19 21 23 25 27 29 31 33 35 75
NEXO    3  CALC.                   DELTA EXPOS.(DELTE)        0.0
RBOCA   1                IALPRM 0  DELBRN                  1000.0                                                           71
IACF    0                IFAST  0  TOTAL NOTCHES              2024
           IPDOME   1    IAHB   0  CORE FUEL MASS       MTU:162.928   1                                                    67
                                   CORE FUEL MASS       STU:179.596
ENERGY (MWD) (DELTE)           0.  ENERGY (MWD) (DELBRN)    179596.   3                                                    63
CYCLE ENERGY (MWD)       2334770.  CYCLE EXPOSURE          13000.0
CORE AVG. POWER DENSITY  54.328033                                   5            32            9                          59
NEUTRON MULTIPLICATION   0.99741280 FINAL AVG. EXPOSURE    26105.1
DIFP  (EPS5 = 0.00200)  0.00114751 CORE AVG. NEUTRON FLUX 1.467E+14  7                                                    55
AVERAGE VOID FRACTION    0.515586 CORE AVG. GD WORTH         0.000
CORE PRESSURE DROP,PSI   7.989758 CORE AVG. GD RESIDUAL WORTH 0.000  9       32            10                              51
EXP RATIO INDEX (INER-II)  0.0000 CORE AVERAGE XENON WORTH  -0.0237
                                                                    11                                                    47
CORE HISTORY MAX. VALUES:     LOCATION: I   J   K
  NODAL EXPOSURE, MWD/T  56294.        7   7   5   METRIC    62052.  13            10            1                         43
  BUNDLE EXPOSURE, MWD/T 43792.       13   2       METRIC    48272.
  EXPOSURE RATIO, NEXRAT 0.0000        0   0   0                     15                                                    39
  AXIAL POWER PEAK       1.2201                5
                                                                    17        9             1                             35

                                                                    19                                                    31

                                                                    21                                                    27

                                                                    23                                                    23

                                                                    25                                                    19

                                                                    27                                                    15

                                                                    29                                                    11

                                                                    31                                                     7

                                                                    33                                                     3
```

Figure 4A-14b. Relative Axial Power at 14.3 GWd/MT Exposure

14.3GWD/MT

Node	Axial Power
25	0.228
24	0.442
23	0.634
22	0.774
21	0.883
20	0.970
19	1.034
18	1.067
17	1.065
16	1.078
15	1.144
14	1.145
13	1.153
12	1.161
11	1.169
10	1.178
9	1.188
8	1.199
7	1.211
6	1.218
5	1.220
4	1.206
3	1.143
2	0.960
1	0.531
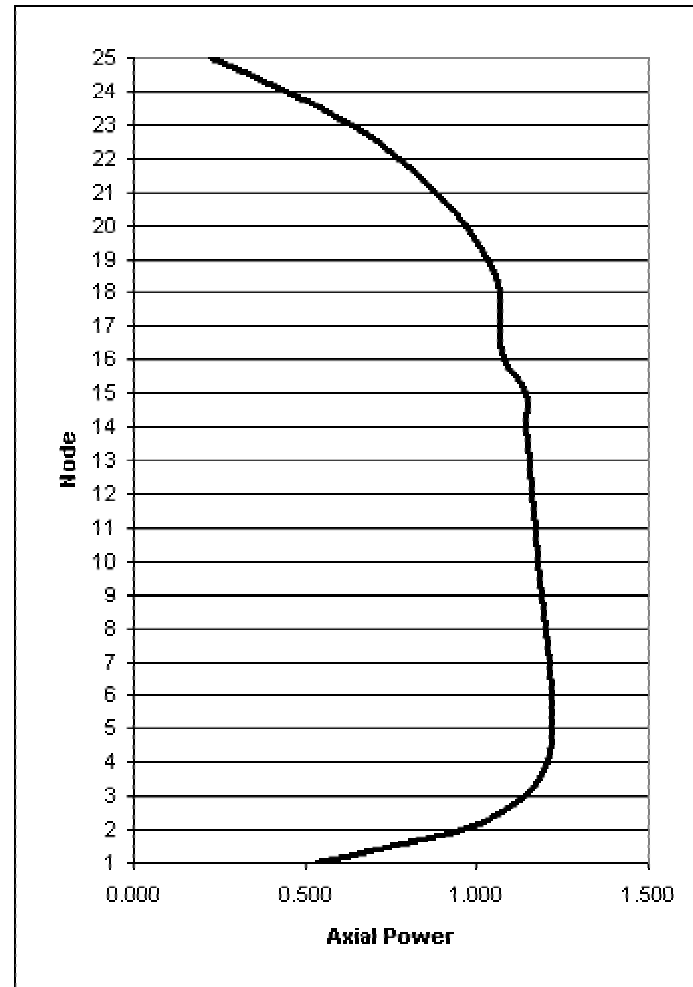
Figure 4A-14c. Axial Exposure at 14.3 GWd/MT Exposure

14.3GWD/MT

Node	Axial Exposure (MWD/MT)
25	6167.4
24	10620.3
23	14878.8
22	19020.9
21	22619.0
20	25566.9
19	27962.0
18	29715.4
17	30818.5
16	31647.5
15	30821.6
14	31996.8
13	32989.4
12	33713.3
11	34344.8
10	34868.5
9	35158.4
8	35501.1
7	35955.5
6	36378.0
5	36479.5
4	35687.1
3	32752.3
2	26207.5
1	13562.6
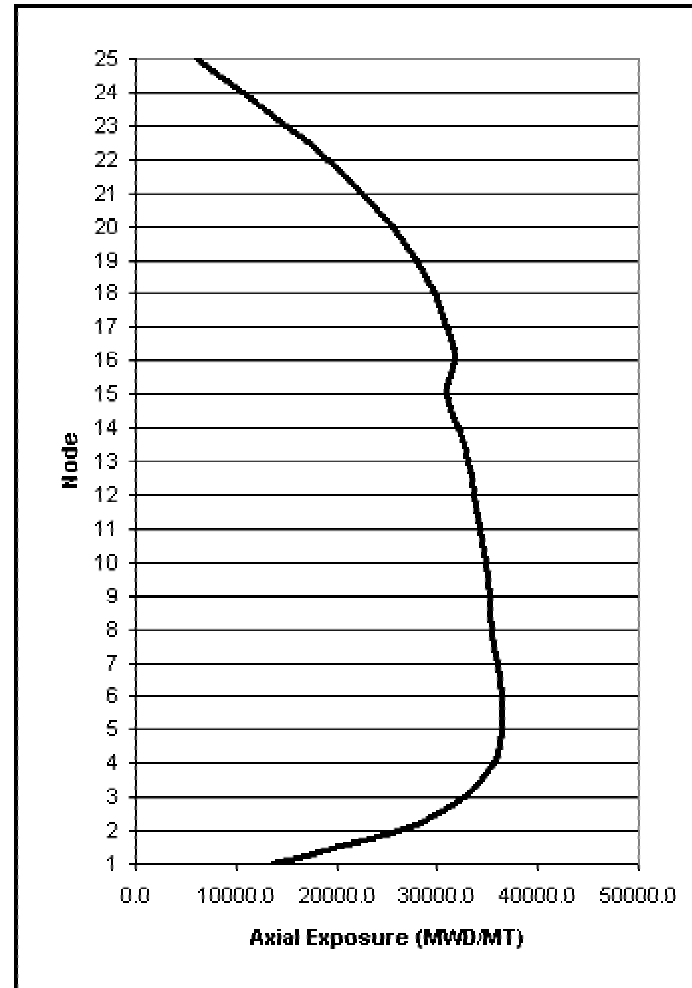
Figure 4A-14d. Relative Integrated Power Per Bundle at 14.3 GWd/MT Exposure

	1	2	3	4	5	6	7	8	9	10	11	12	13	14	15	16	17	18	19
1															0.32	0.36	0.40	0.43	0.42
2													0.38	0.47	0.52	0.67	0.72	0.74	0.76
3											0.43	0.54	0.71	0.85	0.81	0.82	0.89	1.00	0.79
4									0.40	0.53	0.73	0.91	1.02	1.08	0.95	0.99	1.13	1.13	1.03
5								0.47	0.69	0.87	0.98	1.08	1.04	1.22	1.23	1.22	0.96	1.19	0.98
6							0.46	0.71	0.93	1.02	1.06	0.99	1.23	1.08	1.28	1.06	1.22	1.00	1.12
7						0.46	0.59	0.95	0.96	1.09	0.75	0.87	1.23	1.30	1.07	1.12	1.04	1.14	0.72
8					0.47	0.71	0.95	1.08	1.17	0.99	0.90	0.82	1.25	1.17	1.19	1.17	1.25	0.99	0.72
9				0.40	0.69	0.93	0.96	1.17	1.10	1.25	1.24	1.25	1.14	1.30	1.10	1.29	1.09	1.23	1.00
10				0.53	0.87	1.02	1.09	0.99	1.25	1.10	1.29	1.11	1.30	1.09	1.23	1.23	1.28	1.10	1.27
11			0.43	0.73	0.98	1.06	0.75	0.90	1.24	1.29	1.07	1.12	1.13	1.23	0.75	0.79	1.05	1.30	1.13
12			0.54	0.91	1.08	0.99	0.87	0.82	1.25	1.11	1.12	1.12	1.30	1.23	0.79	0.78	1.23	1.30	1.14
13		0.38	0.71	1.02	1.04	1.23	1.23	1.25	1.14	1.30	1.13	1.30	1.11	1.28	1.03	1.21	1.09	1.30	1.09
14		0.48	0.85	1.08	1.22	1.08	1.30	1.17	1.30	1.09	1.23	1.23	1.28	1.09	1.27	1.09	1.29	1.08	1.20
15	0.32	0.52	0.81	0.95	1.23	1.28	1.07	1.19	1.10	1.23	0.75	0.79	1.03	1.27	1.05	1.11	1.28	1.20	0.71
16	0.36	0.67	0.82	0.99	1.22	1.06	1.12	1.17	1.29	1.23	0.79	0.78	1.21	1.09	1.11	1.11	1.28	1.01	0.71
17	0.40	0.72	0.89	1.13	0.96	1.22	1.04	1.25	1.09	1.28	1.05	1.23	1.09	1.29	1.28	1.28	1.08	1.23	0.98
18	0.43	0.74	1.00	1.13	1.19	1.00	1.14	0.99	1.23	1.10	1.30	1.30	1.30	1.08	1.20	1.01	1.23	1.06	1.25
19	0.42	0.76	0.79	1.03	0.98	1.12	0.72	0.72	1.00	1.27	1.13	1.14	1.09	1.20	0.71	0.71	0.98	1.25	1.10

Figure 4A-14e. Average Bundle Exposure at 14.3 GWd/MT Exposure

	1	2	3	4	5	6	7	8	9	10	11	12	13	14	15	16	17	18	19
1															41.78	41.23	45.08	42.33	43.32
2													48.28	44.31	44.53	29.43	28.55	27.67	10.14
3											45.19	43.98	29.43	11.13	33.40	34.83	33.07	13.45	44.53
4									44.53	44.20	27.45	11.46	13.01	13.89	35.94	34.83	15.32	15.10	29.32
5								47.40	24.14	11.02	12.57	14.00	33.18	15.76	15.98	16.31	46.41	16.53	37.70
6							44.53	25.90	12.02	13.12	14.33	35.94	16.42	38.14	16.76	38.80	17.09	38.58	16.87
7						44.53	46.85	12.13	31.75	14.88	44.86	35.05	16.76	17.31	42.00	36.71	38.14	17.42	38.47
8					47.40	25.90	12.13	13.89	15.43	36.82	32.63	45.53	17.53	30.86	32.19	32.63	17.86	38.25	38.36
9				44.64	24.14	12.02	31.75	15.43	34.17	16.64	16.64	17.20	38.03	18.30	38.69	18.08	38.80	17.97	38.25
10				44.20	11.02	13.12	14.88	36.82	16.64	38.69	16.87	37.92	17.86	39.13	17.86	17.75	17.97	38.47	17.09
11			45.19	27.45	12.57	14.33	44.97	32.63	16.64	16.87	44.20	36.60	38.36	17.64	45.19	37.37	38.58	17.09	36.60
12			43.98	11.46	14.00	35.94	35.05	45.53	17.20	37.92	36.60	37.48	17.53	17.53	37.15	37.48	17.42	16.87	35.49
13		48.28	29.43	13.01	33.18	16.42	16.76	17.53	38.03	17.86	38.36	17.53	39.46	17.86	38.47	17.53	38.80	17.42	38.14
14		44.31	11.13	13.89	15.76	38.14	17.31	30.86	18.30	39.13	17.64	17.53	17.86	39.24	17.31	38.25	17.53	38.25	17.09
15	41.78	44.53	33.40	35.94	15.98	16.76	42.00	32.19	38.69	17.86	45.30	37.15	38.47	17.31	44.31	37.15	16.98	17.20	43.32
16	41.23	29.43	34.83	34.83	16.31	38.80	36.71	32.63	18.08	17.75	37.37	37.48	17.53	38.25	37.15	37.37	17.20	37.59	37.70
17	45.08	28.55	33.07	15.32	46.41	17.09	38.14	17.86	38.80	17.97	38.58	17.42	38.80	17.53	16.98	17.20	39.02	17.42	38.47
18	42.33	27.67	13.45	15.10	16.53	38.58	17.42	38.25	17.97	38.47	17.09	16.87	17.42	38.25	17.20	37.59	17.42	38.91	16.76
19	43.32	10.14	44.53	29.32	37.70	16.87	38.47	38.36	38.25	17.09	36.60	35.49	38.14	17.09	43.32	37.70	38.47	16.76	36.49

Figure 4A-15a. Control Rod Pattern Summary at 15.4 GWd/MT Exposure

```
(  ROD PATTERN DEPLETION

NITER   0   POWER          IMAX  19   POWER(MWT)          4.5000E+03  ( 100.0 %)
IBOUN   1   1/4            JMAX  19   PRESSURE(PSIA)      1.0550E+03
IRN     1   MIRROR         KMAX  25   FLOW(*10E-6LB/HR)   7.8508E+01  ( 100.0 %)
ILPA    0                  NSMAX 10   BYPASS(LB/HR)       1.1742E+07  (  15.0 %)       CONTROL ROD CONFIGURATION
IFLW    2   DETAIL         LMAX  20   ENTHALPY(BTU/LB)       512.30                       IN NOTCHES WITHDRAWN
RSTART  0   NEW            LVDCT  8   INLET TEMP(DEG F)      520.47
NEWPHY  2                  IPFTL  0   BEGINNING EXPOSURE    26105.1     1  3  5  7  9 11 13 15 17 19 21 23 25 27 29 31 33 35 75
NEXO    3   CALC.                     DELTA EXPOS.(DELTE)       0.0
RBOCA   1                  IALPRM 0   DELBRN                 1000.0                                                           71
IACF    0                  IFAST  0   TOTAL NOTCHES            1788
            IPDOME   1     IAHB   0   CORE FUEL MASS     MTU:162.928   1                                                     67
                                      CORE FUEL MASS     STU:179.596
ENERGY (MWD) (DELTE)           0.  ENERGY (MWD) (DELBRN)     179596.   3                                                     63
CYCLE ENERGY (MWD)       2514367.  CYCLE EXPOSURE            14000.0
CORE AVG. POWER DENSITY    54.328033                                   5                    30                               59
NEUTRON MULTIPLICATION   0.99675137 FINAL AVG. EXPOSURE      27105.1
DIFP   (EPS5 = 0.00200)  0.00143063 CORE AVG. NEUTRON FLUX 1.464E+14   7                                                     55
AVERAGE VOID FRACTION      0.498509 CORE AVG. GD WORTH        0.000
CORE PRESSURE DROP,PSI     7.903303 CORE AVG. GD RESIDUAL WORTH  0.000 9               13             1                       51
EXP RATIO INDEX (INER-II)   0.0000 CORE AVERAGE XENON WORTH  -0.0239
                                                                      11                                                     47
CORE HISTORY MAX. VALUES:        LOCATION:  I    J    K
  NODAL EXPOSURE, MWD/T   56955.          7    7    5    METRIC    62782. 13        30             4                          43
  BUNDLE EXPOSURE, MWD/T  44168.         13    2         METRIC    48687.
  EXPOSURE RATIO, NEXRAT  0.0000          0    0    0                  15                                                     39
  AXIAL POWER PEAK        1.1887               15
                                                                      17             1              0                        35

                                                                      19                                                     31

                                                                      21                                                     27

                                                                      23                                                     23

                                                                      25                                                     19

                                                                      27                                                     15

                                                                      29                                                     11

                                                                      31                                                      7

                                                                      33                                                      3
```

Figure 4A-15b. Relative Axial Power at 15.4 GWd/MT Exposure

15.4GWD/MT

Node	Axial Power
25	0.254
24	0.494
23	0.705
22	0.866
21	0.988
20	1.075
19	1.131
18	1.147
17	1.123
16	1.127
15	1.189
14	1.178
13	1.175
12	1.171
11	1.165
10	1.160
9	1.154
8	1.148
7	1.139
6	1.124
5	1.103
4	1.071
3	1.003
2	0.844
1	0.469
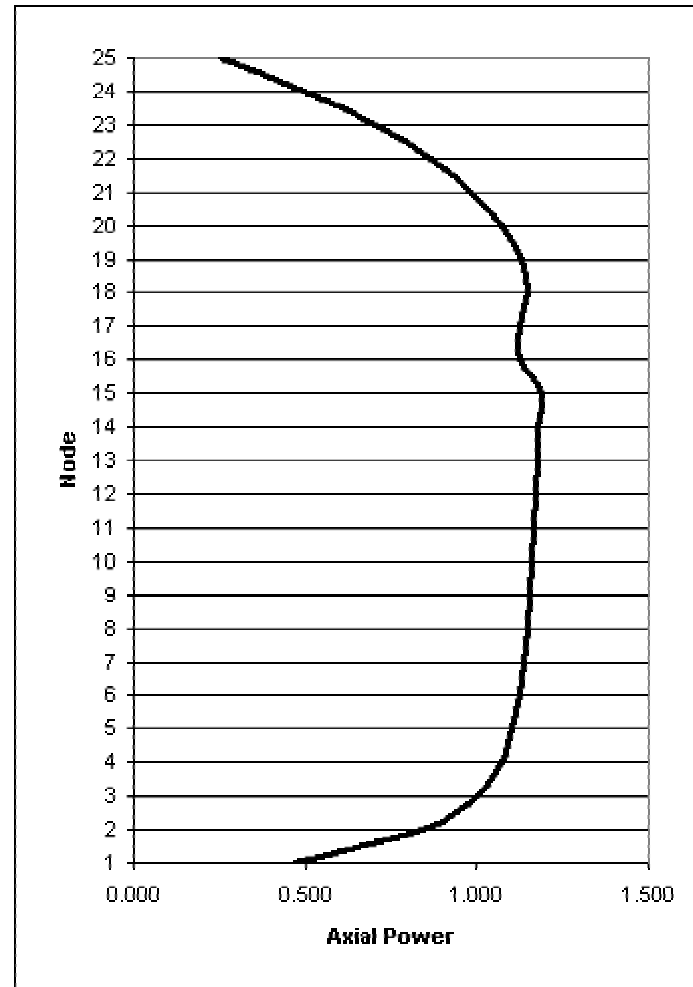
Figure 4A-15c. Axial Exposure at 15.4 GWd/MT Exposure

15.4GWD/MT

Node	Axial Exposure (MWD/MT)
25	6495.8
24	11180.5
23	15650.3
22	19962.1
21	23693.6
20	26747.2
19	29219.8
18	31013.2
17	32114.6
16	32910.9
15	31998.8
14	33174.9
13	34175.7
12	34907.6
11	35547.2
10	36080.1
9	36381.2
8	36736.5
7	37202.3
6	37633.0
5	37736.3
4	36929.0
3	33929.3
2	27196.3
1	14098.5
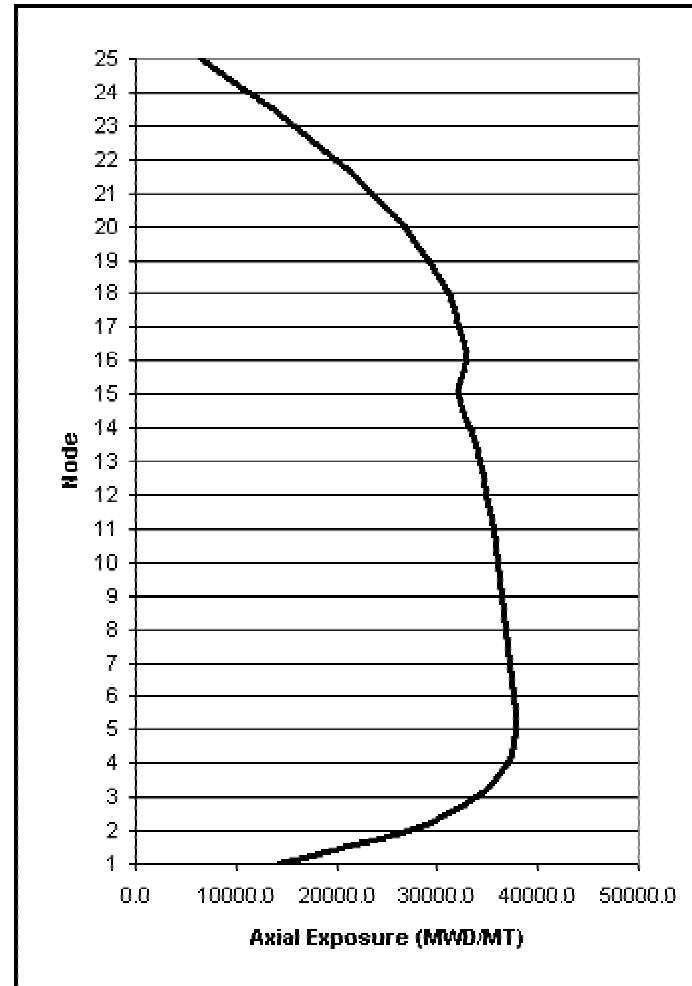
Figure 4A-15d. Relative Integrated Power Per Bundle at 15.4 GWd/MT Exposure

	1	2	3	4	5	6	7	8	9	10	11	12	13	14	15	16	17	18	19
1															0.32	0.36	0.40	0.44	0.43
2													0.38	0.48	0.52	0.67	0.72	0.75	0.78
3											0.45	0.56	0.72	0.86	0.81	0.82	0.89	1.02	0.80
4									0.43	0.57	0.77	0.95	1.05	1.09	0.94	0.98	1.14	1.15	1.05
5								0.51	0.75	0.95	1.07	1.15	1.06	1.22	1.20	1.19	0.96	1.22	1.03
6							0.49	0.76	1.01	1.12	1.19	1.07	1.27	1.06	1.19	0.99	1.20	1.04	1.23
7						0.49	0.63	1.02	1.03	1.22	0.99	1.12	1.27	1.23	0.85	0.88	1.01	1.22	1.05
8					0.51	0.76	1.02	1.16	1.25	1.07	1.15	1.03	1.28	1.12	0.94	0.93	1.19	1.05	1.03
9				0.43	0.75	1.01	1.03	1.25	1.14	1.29	1.28	1.27	1.13	1.27	1.06	1.23	1.07	1.23	1.03
10				0.57	0.95	1.12	1.22	1.07	1.29	1.08	1.21	1.03	1.25	1.09	1.28	1.28	1.27	1.05	1.16
11			0.45	0.77	1.07	1.19	0.99	1.15	1.28	1.21	0.75	0.78	1.05	1.27	1.05	1.10	1.07	1.19	0.74
12			0.56	0.95	1.15	1.07	1.12	1.03	1.27	1.03	0.78	0.78	1.20	1.27	1.09	1.08	1.25	1.18	0.74
13		0.38	0.72	1.05	1.06	1.27	1.27	1.28	1.13	1.25	1.05	1.20	1.06	1.26	1.05	1.23	1.06	1.22	0.98
14		0.48	0.86	1.09	1.22	1.06	1.23	1.12	1.27	1.09	1.27	1.27	1.26	1.04	1.15	0.98	1.22	1.05	1.21
15	0.32	0.52	0.81	0.94	1.20	1.19	0.85	0.94	1.06	1.28	1.05	1.09	1.05	1.15	0.69	0.72	1.16	1.21	1.00
16	0.36	0.67	0.82	0.98	1.19	0.99	0.88	0.93	1.23	1.28	1.10	1.08	1.23	0.98	0.72	0.72	1.14	1.01	1.00
17	0.40	0.72	0.89	1.14	0.96	1.20	1.01	1.19	1.07	1.27	1.07	1.25	1.06	1.22	1.16	1.14	1.00	1.18	0.98
18	0.44	0.75	1.02	1.15	1.22	1.04	1.22	1.05	1.23	1.05	1.19	1.18	1.22	1.05	1.21	1.01	1.18	0.98	1.10
19	0.43	0.78	0.80	1.05	1.03	1.23	1.05	1.04	1.03	1.16	0.74	0.74	0.98	1.21	1.00	1.00	0.98	1.10	0.69

Figure 4A-15e. Average Bundle Exposure at 15.4 GWd/MT Exposure

	1	2	3	4	5	6	7	8	9	10	11	12	13	14	15	16	17	18	19
1															42.11	41.56	45.53	42.77	43.76
2													48.72	44.86	45.08	30.09	29.32	28.44	11.02
3											45.64	44.53	30.20	12.13	34.39	35.83	34.06	14.55	45.30
4									44.97	44.75	28.22	12.46	14.11	14.99	37.04	35.94	16.53	16.42	30.42
5								47.95	24.91	12.02	13.67	15.21	34.28	17.09	17.42	17.75	47.51	17.86	38.80
6							44.97	26.79	13.01	14.33	15.54	37.04	17.86	39.35	18.08	39.90	18.41	39.68	18.08
7						44.97	47.51	13.23	32.85	16.09	45.75	36.05	18.08	18.74	43.21	37.92	39.24	18.63	39.35
8					47.95	26.79	13.23	15.10	16.76	37.92	33.62	46.41	18.85	32.19	33.51	33.95	19.29	39.35	39.13
9				45.08	24.91	13.01	32.85	16.76	35.38	18.08	18.08	18.63	39.35	19.73	39.90	19.51	39.90	19.29	39.35
10				44.75	12.02	14.33	16.09	37.92	18.08	39.90	18.30	39.13	19.29	40.34	19.18	19.07	19.40	39.68	18.52
11			45.64	28.22	13.67	15.54	45.75	33.62	18.08	18.30	45.42	37.81	39.57	18.96	46.08	38.25	39.68	18.52	37.92
12			44.64	12.46	15.21	37.04	36.05	46.41	18.63	39.13	37.81	38.69	18.96	18.85	37.92	38.36	18.85	18.30	36.82
13		48.61	30.20	14.11	34.28	17.86	18.08	18.85	39.35	19.29	39.57	18.96	40.68	19.29	39.57	18.85	40.01	18.85	39.35
14		44.86	12.13	14.99	17.09	39.35	18.74	32.19	19.73	40.34	18.96	18.85	19.29	40.45	18.74	39.46	18.96	39.46	18.30
15	42.11	45.08	34.39	37.04	17.42	18.08	43.21	33.40	39.90	19.18	46.08	37.92	39.57	18.74	45.53	38.47	18.41	18.52	44.09
16	41.56	30.09	35.83	35.94	17.75	39.90	37.92	33.95	19.51	19.07	38.25	38.36	18.85	39.46	38.47	38.58	18.63	38.69	38.47
17	45.53	29.32	34.06	16.64	47.51	18.41	39.24	19.29	39.90	19.40	39.68	18.85	40.01	18.96	18.41	18.63	40.23	18.85	39.57
18	42.77	28.44	14.55	16.42	17.86	39.68	18.63	39.35	19.29	39.68	18.52	18.30	18.85	39.46	18.52	38.69	18.85	40.12	18.08
19	43.76	11.02	45.42	30.42	38.80	18.08	39.35	39.13	39.35	18.52	37.92	36.82	39.35	18.30	44.09	38.47	39.57	18.08	37.70

Figure 4A-16a. Control Rod Pattern Summary at 16.5 GWd/MT Exposure

```
( ROD PATTERN DEPLETION

NITER   0  POWER          IMAX  19  POWER(MWT)          4.5000E+03  ( 100.0 %)
IBOUN   1  1/4            JMAX  19  PRESSURE(PSIA)      1.0550E+03
IRN     1  MIRROR         KMAX  25  FLOW(*10E-6LB/HR)   7.8508E+01  ( 100.0 %)
ILPA    0                 NSMAX 10  BYPASS(LB/HR)       1.1742E+07  (  15.0 %)       CONTROL ROD CONFIGURATION
IFLW    2  DETAIL         LMAX  20  ENTHALPY(BTU/LB)       512.30                      IN NOTCHES WITHDRAWN
RSTART  0  NEW            LVDCT  6  INLET TEMP(DEG F)      520.47
NEWPHY  2                 IPFTL  0  BEGINNING EXPOSURE    27105.2      1  3  5  7  9 11 13 15 17 19 21 23 25 27 29 31 33 35 75
NEXO    3  CALC.                    DELTA EXPOS.(DELTE)       0.0
RBOCA   1                 IALPRM 0  DELBRN                 1000.0                                                           71
IACF    0                 IFAST  0  TOTAL NOTCHES            1224
           IPDOME  1      IAHB   0  CORE FUEL MASS   MTU:162.928      1                                                    67
                                    CORE FUEL MASS   STU:179.596
ENERGY (MWD) (DELTE)         0.  ENERGY (MWD) (DELBRN)    179596.     3                                                    63
CYCLE ENERGY (MWD)      2693965. CYCLE EXPOSURE          15000.0
CORE AVG. POWER DENSITY   54.328033                                  5                    98                               59
NEUTRON MULTIPLICATION  0.99618649 FINAL AVG. EXPOSURE     28105.2
DIFP   (EPS5 = 0.00200) 0.00142032 CORE AVG. NEUTRON FLUX  1.466E+14 7                                                    55
AVERAGE VOID FRACTION    0.493528 CORE AVG. GD WORTH        0.000
CORE PRESSURE DROP,PSI   7.918104 CORE AVG. GD RESIDUAL WORTH 0.000   9               12           0                       51
EXP RATIO INDEX (INER-II)  0.0000 CORE AVERAGE XENON WORTH  -0.0240
                                                                    11                                                    47
CORE HISTORY MAX. VALUES:      LOCATION: I   J   K
  NODAL EXPOSURE, MWD/T  57658.        7   7   5   METRIC   63557.   13         98          11                             43
  BUNDLE EXPOSURE, MWD/T 44551.       13   2       METRIC   49109.
  EXPOSURE RATIO, NEXRAT 0.0000        0   0   0                     15                                                    39
  AXIAL POWER PEAK       1.2120               15
                                                                    17               0           0                        35

                                                                    19                                                    31

                                                                    21                                                    27

                                                                    23                                                    23

                                                                    25                                                    19

                                                                    27                                                    15

                                                                    29                                                    11

                                                                    31                                                     7

                                                                    33                                                     3
```

Figure 4A-16b. Relative Axial Power at 16.5 GWd/MT Exposure

16.5GWD/MT

Node	Axial Power
25	0.262
24	0.512
23	0.730
22	0.889
21	1.002
20	1.082
19	1.129
18	1.142
17	1.126
16	1.141
15	1.212
14	1.204
13	1.200
12	1.193
11	1.183
10	1.171
9	1.158
8	1.142
7	1.120
6	1.092
5	1.060
4	1.022
3	0.958
2	0.815
1	0.457
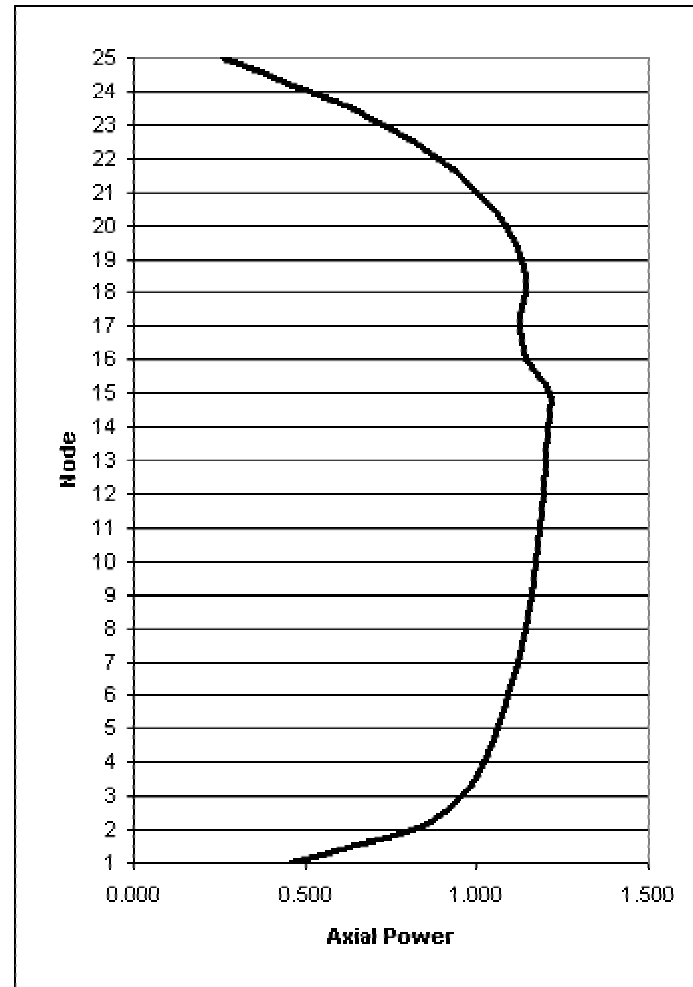
Figure 4A-16c. Axial Exposure at 16.5 GWd/MT Exposure

16.5GWD/MT

Node	Axial Exposure (MWD/MT)
25	6861.7
24	11805.7
23	16507.8
22	21015.3
21	24895.3
20	28055.7
19	30596.0
18	32408.9
17	33480.7
16	34231.8
15	33221.7
14	34387.1
13	35384.3
12	36111.8
11	36746.1
10	37273.5
9	37569.8
8	37919.0
7	38374.9
6	38790.3
5	38872.2
4	38031.7
3	34962.3
2	28065.5
1	14571.4
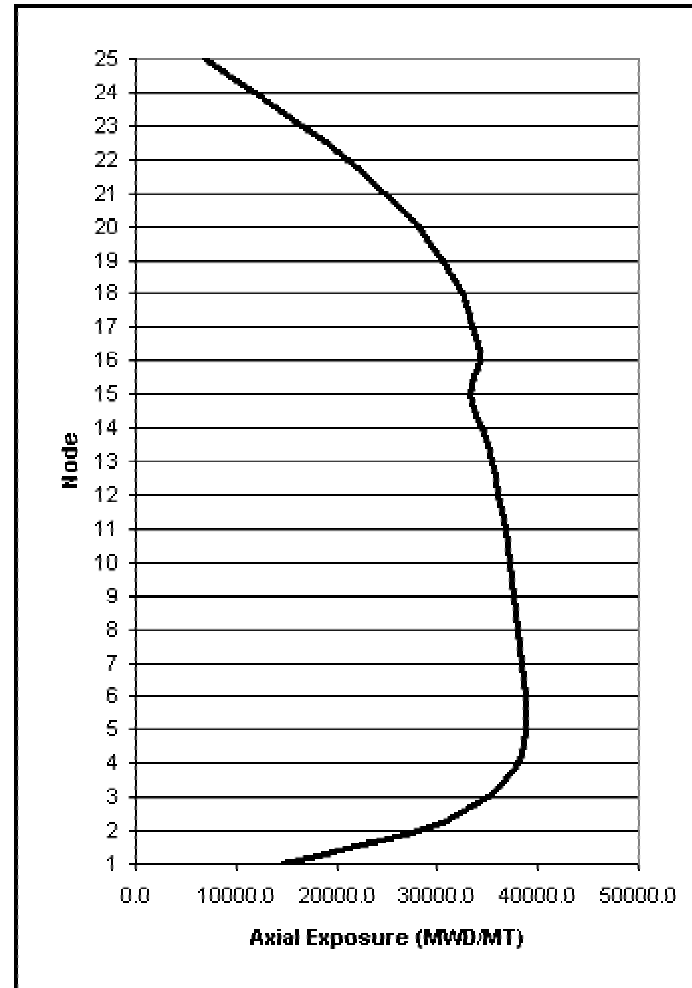
Figure 4A-16d. Relative Integrated Power Per Bundle at 16.5 GWd/MT Exposure

	1	2	3	4	5	6	7	8	9	10	11	12	13	14	15	16	17	18	19
1															0.32	0.36	0.40	0.43	0.43
2													0.39	0.48	0.52	0.66	0.72	0.75	0.79
3											0.46	0.56	0.73	0.88	0.81	0.81	0.89	1.02	0.80
4									0.43	0.57	0.77	0.97	1.07	1.12	0.95	0.99	1.15	1.16	1.04
5								0.50	0.74	0.96	1.08	1.16	1.07	1.25	1.25	1.23	0.97	1.23	1.02
6							0.49	0.75	1.01	1.13	1.20	1.07	1.29	1.09	1.28	1.05	1.24	1.05	1.23
7						0.49	0.63	1.02	1.01	1.21	0.98	1.11	1.29	1.31	1.07	1.12	1.06	1.24	1.04
8					0.50	0.75	1.02	1.15	1.23	1.05	1.13	1.02	1.30	1.17	1.18	1.16	1.26	1.05	1.02
9				0.43	0.74	1.01	1.01	1.23	1.12	1.26	1.25	1.25	1.12	1.29	1.10	1.29	1.08	1.23	1.02
10				0.57	0.96	1.13	1.21	1.05	1.26	1.05	1.18	1.00	1.23	1.08	1.28	1.28	1.26	1.03	1.14
11			0.46	0.77	1.08	1.20	0.98	1.13	1.25	1.18	0.73	0.76	1.02	1.23	1.02	1.08	1.04	1.15	0.71
12			0.56	0.97	1.16	1.07	1.11	1.02	1.25	1.00	0.76	0.76	1.16	1.22	1.06	1.05	1.21	1.14	0.71
13		0.39	0.73	1.07	1.07	1.29	1.29	1.30	1.12	1.23	1.02	1.16	1.02	1.21	1.01	1.18	1.02	1.17	0.94
14		0.48	0.88	1.12	1.25	1.09	1.31	1.17	1.29	1.08	1.23	1.22	1.21	1.00	1.11	0.95	1.17	1.01	1.16
15	0.32	0.52	0.81	0.95	1.25	1.28	1.07	1.18	1.10	1.28	1.02	1.06	1.01	1.11	0.70	0.73	1.12	1.16	0.95
16	0.36	0.66	0.81	0.99	1.23	1.05	1.12	1.16	1.29	1.28	1.08	1.05	1.18	0.95	0.73	0.72	1.10	0.97	0.96
17	0.40	0.72	0.89	1.15	0.97	1.24	1.06	1.26	1.08	1.26	1.04	1.21	1.02	1.17	1.12	1.10	0.96	1.12	0.94
18	0.43	0.75	1.02	1.16	1.23	1.05	1.24	1.05	1.23	1.03	1.15	1.14	1.17	1.01	1.16	0.97	1.12	0.94	1.05
19	0.43	0.79	0.80	1.04	1.02	1.23	1.04	1.02	1.02	1.14	0.71	0.71	0.94	1.16	0.95	0.96	0.94	1.05	0.66

Figure 4A-16e. Average Bundle Exposure at 16.5 GWd/MT Exposure

	1	2	3	4	5	6	7	8	9	10	11	12	13	14	15	16	17	18	19
1															42.55	42.00	45.97	43.21	44.20
2													49.16	45.42	45.75	30.86	30.20	29.32	11.90
3											46.19	45.19	30.97	13.12	35.27	36.71	35.05	15.65	46.30
4									45.53	45.42	29.10	13.56	15.21	16.20	38.03	36.93	17.86	17.64	31.53
5								48.50	25.79	13.01	14.88	16.42	35.49	18.41	18.74	19.07	48.50	19.18	40.01
6							45.53	27.56	14.11	15.54	16.87	38.25	19.29	40.45	19.40	41.01	19.73	40.90	19.40
7						45.53	48.28	14.33	33.95	17.42	46.85	37.26	19.40	20.06	44.09	38.91	40.34	19.95	40.45
8					48.50	27.56	14.33	16.31	18.08	39.02	34.94	47.62	20.28	33.40	34.50	34.94	20.61	40.45	40.23
9				45.53	25.79	14.11	33.95	18.08	36.71	19.51	19.40	20.06	40.57	21.16	41.01	20.83	41.12	20.72	40.45
10				45.42	13.01	15.54	17.42	39.02	19.51	41.12	19.62	40.23	20.72	41.56	20.61	20.50	20.83	40.79	19.73
11			46.19	29.10	14.88	16.87	46.85	34.94	19.40	19.62	46.30	38.69	40.79	20.39	47.29	39.46	40.90	19.84	38.69
12			45.19	13.56	16.42	38.25	37.26	47.62	20.06	40.23	38.69	39.57	20.28	20.28	39.13	39.57	20.17	19.62	37.59
13		49.05	30.97	15.21	35.49	19.29	19.40	20.28	40.57	20.72	40.79	20.28	41.89	20.61	40.68	20.17	41.23	20.17	40.45
14		45.42	13.12	16.20	18.41	40.45	20.06	33.40	21.16	41.56	20.39	20.28	20.61	41.56	19.95	40.45	20.39	40.57	19.73
15	42.55	45.75	35.27	38.03	18.74	19.40	44.09	34.50	41.01	20.61	47.29	39.13	40.68	19.95	46.30	39.24	19.73	19.84	45.19
16	42.00	30.86	36.71	36.93	19.07	41.01	38.91	34.94	20.83	20.50	39.46	39.57	20.17	40.45	39.24	39.35	19.84	39.79	39.57
17	45.97	30.20	35.05	17.86	48.50	19.73	40.34	20.61	41.12	20.83	40.90	20.17	41.23	20.39	19.73	19.84	41.34	20.06	40.57
18	43.21	29.32	15.65	17.64	19.18	40.90	19.95	40.45	20.72	40.79	19.84	19.62	20.17	40.57	19.84	39.79	20.06	41.23	19.29
19	44.20	11.90	46.30	31.53	39.90	19.40	40.45	40.23	40.45	19.73	38.69	37.59	40.45	19.73	45.19	39.57	40.57	19.29	38.47

Figure 4A-17a. Control Rod Pattern Summary at 17.6 GWd/MT Exposure

```
      ( ROD PATTERN DEPLETION

NITER   0  POWER          IMAX  19  POWER(MWT)          4.5000E+03  ( 100.0 %)
IBOUN   1  1/4            JMAX  19  PRESSURE(PSIA)      1.0550E+03
IRN     1  MIRROR         KMAX  25  FLOW(*10E-6LB/HR)   7.8508E+01  ( 100.0 %)
ILPA    0                 NSMAX 10  BYPASS(LB/HR)       1.1742E+07  (  15.0 %)      CONTROL ROD CONFIGURATION
IFLW    2  DETAIL         LMAX  20  ENTHALPY(BTU/LB)       512.30                     IN NOTCHES WITHDRAWN
RSTART  0  NEW            LVDCT  8  INLET TEMP(DEG F)      520.47
NEWPHY  2                 IPFTL  0  BEGINNING EXPOSURE    28105.2    1  3  5  7  9 11 13 15 17 19 21 23 25 27 29 31 33 35 75
NEXO    3  CALC.                    DELTA EXPOS.(DELTE)       0.0
RBOCA   1                 IALPRM 0  DELBRN                 1200.0                                                       71
IACF    0                 IFAST  0  TOTAL NOTCHES            483    1                                                   67
           IPDOME  1      IAHB   0  CORE FUEL MASS    MTU:162.928
                                    CORE FUEL MASS    STU:179.596
ENERGY (MWD) (DELTE)             0. ENERGY (MWD) (DELBRN)   215515.   3                                                   63
CYCLE ENERGY (MWD)         2909482. CYCLE EXPOSURE         16200.0
CORE AVG. POWER DENSITY   54.328033                                   5                                                   59
NEUTRON MULTIPLICATION    0.99613714 FINAL AVG. EXPOSURE    29305.2
DIFP   (EPS5 = 0.00200)   0.00120324 CORE AVG. NEUTRON FLUX  1.467E+14  7                                                 55
AVERAGE VOID FRACTION       0.474275 CORE AVG. GD WORTH        0.000
CORE PRESSURE DROP,PSI      7.838252 CORE AVG. GD RESIDUAL WORTH  0.000  9                                               51
EXP RATIO INDEX (INER-II)    0.0000 CORE AVERAGE XENON WORTH  -0.0242
                                                                        11                                              47
CORE HISTORY MAX. VALUES:      LOCATION: I   J   K
  NODAL EXPOSURE, MWD/T  58431.        7   7   5   METRIC     64409.    13                    4                          43
  BUNDLE EXPOSURE, MWD/T 45179.        5  17       METRIC     49801.
  EXPOSURE RATIO, NEXRAT 0.0000        0   0   0                        15                                              39
  AXIAL POWER PEAK       1.2529               15
                                                                        17                          1                   35

                                                                        19                                              31

                                                                        21                                              27

                                                                        23                                              23

                                                                        25                                              19

                                                                        27                                              15

                                                                        29                                              11

                                                                        31                                               7

                                                                        33                                               3
```

Figure 4A-17b. Relative Axial Power at 17.6 GWd/MT Exposure

17.6GWD/MT

Node	Axial Power
25	0.291
24	0.572
23	0.808
22	0.982
21	1.108
20	1.181
19	1.216
18	1.214
17	1.182
16	1.187
15	1.253
14	1.233
13	1.218
12	1.200
11	1.178
10	1.152
9	1.124
8	1.091
7	1.050
6	1.002
5	0.949
4	0.892
3	0.822
2	0.698
1	0.395
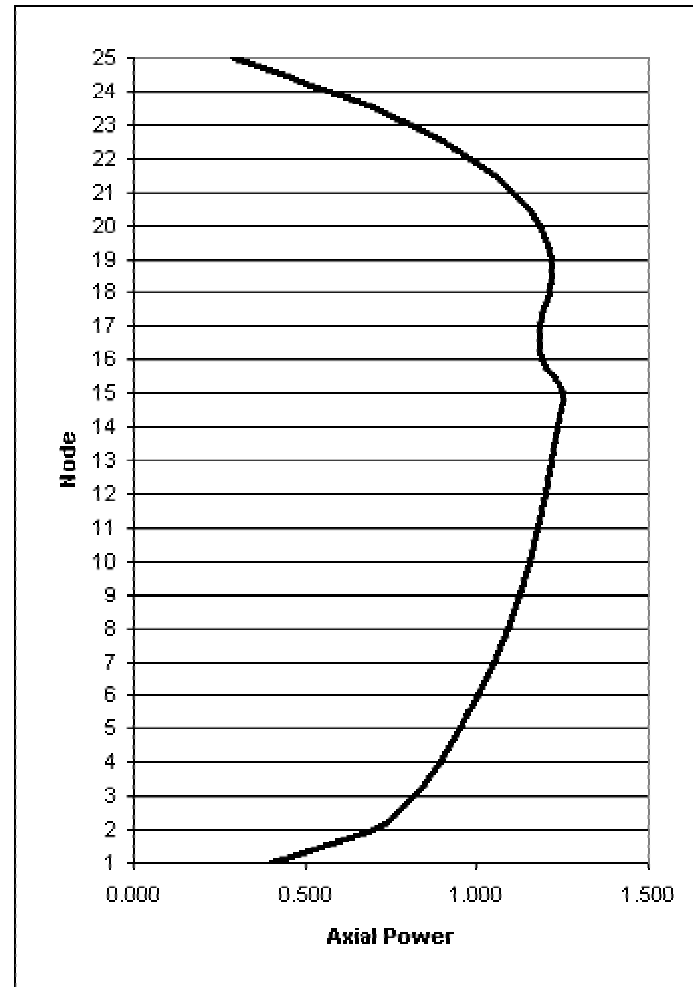
Figure 4A-17c. Axial Exposure at 17.6 GWd/MT Exposure

17.6GWD/MT

Node	Axial Exposure (MWD/MT)
25	7315.1
24	12583.6
23	17573.1
22	22313.0
21	26358.8
20	29635.7
19	32244.4
18	34076.4
17	35124.6
16	35837.0
15	34718.0
14	35873.1
13	36865.5
12	37584.3
11	38206.4
10	38719.2
9	39000.4
8	39330.1
7	39759.0
6	40140.0
5	40182.3
4	39294.3
3	36146.2
2	29072.7
1	15125.0
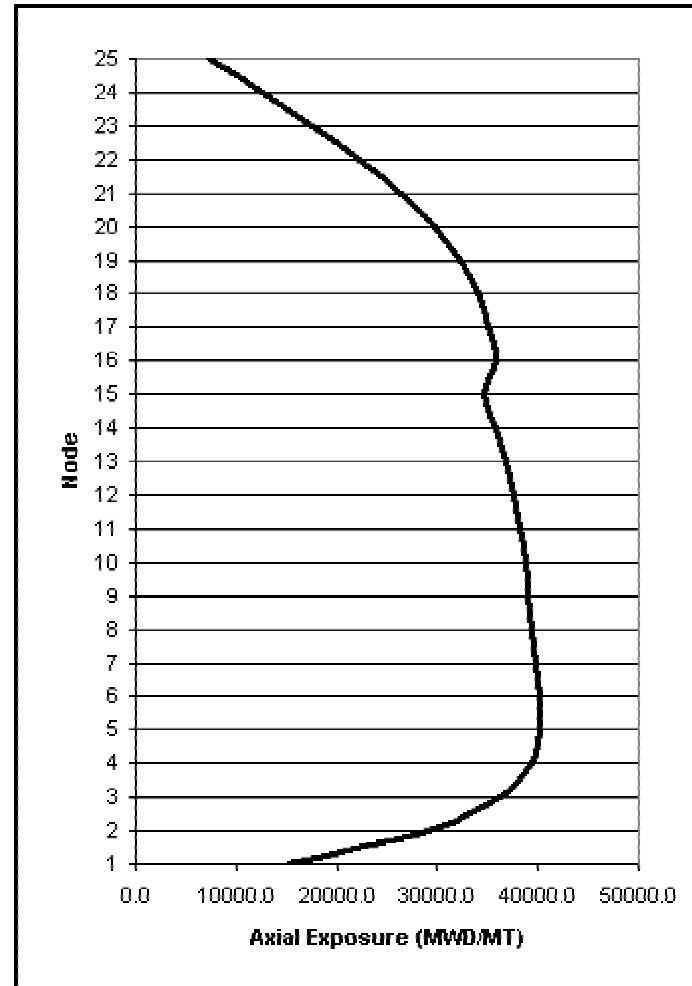
Figure 4A-17d. Relative Integrated Power Per Bundle at 17.6 GWd/MT Exposure

	1	2	3	4	5	6	7	8	9	10	11	12	13	14	15	16	17	18	19
1															0.30	0.34	0.38	0.42	0.42
2													0.37	0.47	0.50	0.63	0.69	0.72	0.77
3											0.45	0.55	0.71	0.86	0.78	0.78	0.85	0.99	0.77
4									0.43	0.57	0.76	0.95	1.04	1.08	0.91	0.94	1.10	1.11	0.99
5								0.50	0.74	0.96	1.07	1.14	1.04	1.21	1.20	1.18	0.93	1.17	0.97
6							0.49	0.75	1.01	1.12	1.18	1.05	1.25	1.05	1.22	1.01	1.18	1.00	1.17
7						0.49	0.63	1.02	1.01	1.20	0.97	1.09	1.26	1.26	1.03	1.07	1.02	1.19	1.00
8					0.50	0.75	1.02	1.15	1.23	1.05	1.13	1.01	1.27	1.13	1.14	1.12	1.22	1.03	1.01
9				0.43	0.74	1.01	1.01	1.23	1.13	1.28	1.28	1.27	1.12	1.27	1.08	1.26	1.07	1.23	1.04
10				0.57	0.96	1.12	1.20	1.05	1.28	1.09	1.28	1.08	1.27	1.08	1.27	1.27	1.27	1.08	1.26
11			0.45	0.76	1.07	1.18	0.97	1.13	1.28	1.28	1.05	1.09	1.11	1.26	1.03	1.08	1.08	1.28	1.11
12			0.55	0.95	1.14	1.05	1.09	1.01	1.27	1.08	1.09	1.09	1.27	1.26	1.06	1.05	1.25	1.27	1.11
13		0.37	0.71	1.04	1.04	1.25	1.26	1.27	1.12	1.27	1.11	1.27	1.07	1.22	1.01	1.18	1.04	1.24	1.05
14		0.47	0.86	1.08	1.21	1.05	1.26	1.13	1.27	1.08	1.26	1.26	1.22	0.99	1.09	0.93	1.16	1.02	1.19
15	0.30	0.50	0.78	0.91	1.20	1.22	1.03	1.14	1.08	1.27	1.03	1.06	1.01	1.09	0.66	0.68	1.08	1.13	0.94
16	0.34	0.63	0.78	0.94	1.18	1.01	1.07	1.12	1.26	1.27	1.08	1.05	1.18	0.93	0.68	0.67	1.05	0.92	0.91
17	0.38	0.69	0.85	1.10	0.93	1.18	1.02	1.22	1.07	1.27	1.08	1.25	1.04	1.16	1.08	1.05	0.91	1.06	0.88
18	0.42	0.72	0.99	1.11	1.17	1.00	1.19	1.03	1.23	1.08	1.28	1.27	1.24	1.02	1.13	0.92	1.06	0.88	0.99
19	0.42	0.77	0.77	0.99	0.97	1.17	1.00	1.01	1.04	1.26	1.11	1.11	1.05	1.19	0.94	0.91	0.88	0.99	0.63

Figure 4A-17e. Average Bundle Exposure at 17.6 GWd/MT Exposure

	1	2	3	4	5	6	7	8	9	10	11	12	13	14	15	16	17	18	19
1															42.88	42.44	46.41	43.87	44.86
2													49.60	45.97	46.41	31.75	31.09	30.31	12.90
3											46.74	45.97	31.97	14.22	36.27	37.81	36.16	17.09	47.29
4									46.08	46.19	30.09	14.77	16.64	17.75	39.24	38.25	19.40	19.18	32.96
5								49.16	26.79	14.33	16.31	17.97	36.82	20.06	20.39	20.61	49.82	20.83	41.34
6							46.19	28.55	15.54	16.98	18.41	39.68	20.94	41.89	21.16	42.44	21.38	42.22	21.05
7						46.19	49.05	15.65	35.27	18.96	48.17	38.69	21.16	21.83	45.53	40.34	41.78	21.61	41.89
8					49.16	28.55	15.65	17.86	19.73	40.45	36.38	48.94	21.94	34.94	36.05	36.49	22.27	41.89	41.67
9				46.08	26.79	15.54	35.27	19.73	38.14	21.16	21.05	21.72	42.00	22.82	42.55	22.60	42.55	22.27	41.78
10				46.19	14.33	16.98	18.96	40.45	21.16	42.44	21.16	41.56	22.38	42.99	22.38	22.16	22.49	42.11	21.27
11			46.74	30.09	16.31	18.41	48.17	36.38	21.05	21.16	47.18	39.68	42.11	22.05	48.61	40.90	42.33	21.38	39.57
12			45.97	14.77	17.97	39.68	38.69	48.94	21.72	41.56	39.68	40.57	21.83	21.83	40.57	41.01	21.83	21.16	38.58
13		49.60	31.97	16.64	36.82	20.94	21.16	21.94	42.00	22.38	42.11	21.83	43.21	22.27	42.11	21.83	42.55	21.72	41.67
14		45.97	14.22	17.75	20.06	41.89	21.83	34.94	22.82	42.99	22.05	21.83	22.27	42.88	21.50	41.78	21.94	41.89	21.16
15	42.88	46.41	36.27	39.24	20.39	21.16	45.53	36.05	42.55	22.38	48.61	40.57	42.00	21.50	47.18	40.23	21.16	21.38	46.52
16	42.44	31.75	37.81	38.25	20.61	42.44	40.34	36.49	22.60	22.16	40.90	41.01	21.83	41.78	40.12	40.34	21.27	41.01	40.79
17	46.41	31.09	36.16	19.40	49.82	21.38	41.78	22.27	42.55	22.49	42.33	21.83	42.55	21.94	21.16	21.27	42.55	21.61	41.89
18	43.87	30.31	17.09	19.18	20.83	42.22	21.61	41.89	22.27	42.11	21.38	21.16	21.72	41.89	21.38	41.01	21.61	42.44	20.72
19	44.86	12.90	47.29	32.96	41.34	21.05	41.78	41.67	41.78	21.27	39.57	38.58	41.67	21.16	46.41	40.79	41.89	20.72	39.35

Figure 4A-18a. Control Rod Pattern Summary at 18.5 GWd/MT Exposure

```
( ROD PATTERN DEPLETION

NITER   0  POWER          IMAX  19  POWER(MWT)          4.5000E+03  ( 100.0 %)
IBOUN   1  1/4            JMAX  19  PRESSURE(PSIA)      1.0550E+03
IRN     1  MIRROR         KMAX  25  FLOW(*10E-6LB/HR)   7.8508E+01  ( 100.0 %)       CONTROL ROD CONFIGURATION
ILPA    0                 NSMAX 10  BYPASS(LB/HR)       1.1742E+07  (  15.0 %)          IN NOTCHES WITHDRAWN
IFLW    2  DETAIL         LMAX  20  ENTHALPY(BTU/LB)        512.30
RSTART  0  NEW            LVDCT  7  INLET TEMP(DEG F)       520.47
NEWPHY  2                 IPFTL  0  BEGINNING EXPOSURE     29305.1    1  3  5  7  9 11 13 15 17 19 21 23 25 27 29 31 33 35 75
NEXO    3  CALC.                    DELTA EXPOS.(DELTE)        0.0
RBOCA   1                 IALPRM 0  DELBRN                  571.7                                                        71
IACF    0                 IFAST  0  TOTAL NOTCHES               0
           IPDOME   1  IAHB  0  CORE FUEL MASS      MTU:162.928    1                                                    67
                                   CORE FUEL MASS      STU:179.596
ENERGY (MWD) (DELTE)            0.  ENERGY (MWD) (DELBRN)    102666.   3                                                 63
CYCLE ENERGY (MWD)        3012149. CYCLE EXPOSURE          16771.7
CORE AVG. POWER DENSITY   54.328033                                   5                                                 59
NEUTRON MULTIPLICATION    0.99644101 FINAL AVG. EXPOSURE    29876.8
DIFP   (EPS5 = 0.00200)   0.00122070 CORE AVG. NEUTRON FLUX 1.467E+14  7                                                55
AVERAGE VOID FRACTION     0.465628 CORE AVG. GD WORTH         0.000
CORE PRESSURE DROP,PSI    7.820543 CORE AVG. GD RESIDUAL WORTH 0.000   9                                                51
EXP RATIO INDEX (INER-II)   0.0000 CORE AVERAGE XENON WORTH  -0.0243
                                                                     11                                                47
CORE HISTORY MAX. VALUES:     LOCATION: I   J   K
  NODAL EXPOSURE, MWD/T   58746.        7   7   5   METRIC    64756.  13                                                43
  BUNDLE EXPOSURE, MWD/T  45709.        5  17       METRIC    50385.
  EXPOSURE RATIO, NEXRAT  0.0000        0   0   0                     15                                                39
  AXIAL POWER PEAK        1.2624               15
                                                                     17                                                35

                                                                     19                                                31

                                                                     21                                                27

                                                                     23                                                23

                                                                     25                                                19

                                                                     27                                                15

                                                                     29                                                11

                                                                     31                                                 7

                                                                     33                                                 3
```

Figure 4A-18b. Relative Axial Power at 18.5 GWd/MT Exposure

18.5GWD/MT

Node	Axial Power
25	0.309
24	0.607
23	0.859
22	1.039
21	1.162
20	1.227
19	1.253
18	1.241
17	1.201
16	1.200
15	1.262
14	1.238
13	1.218
12	1.195
11	1.168
10	1.138
9	1.105
8	1.066
7	1.019
6	0.964
5	0.903
4	0.840
3	0.766
2	0.651
1	0.370
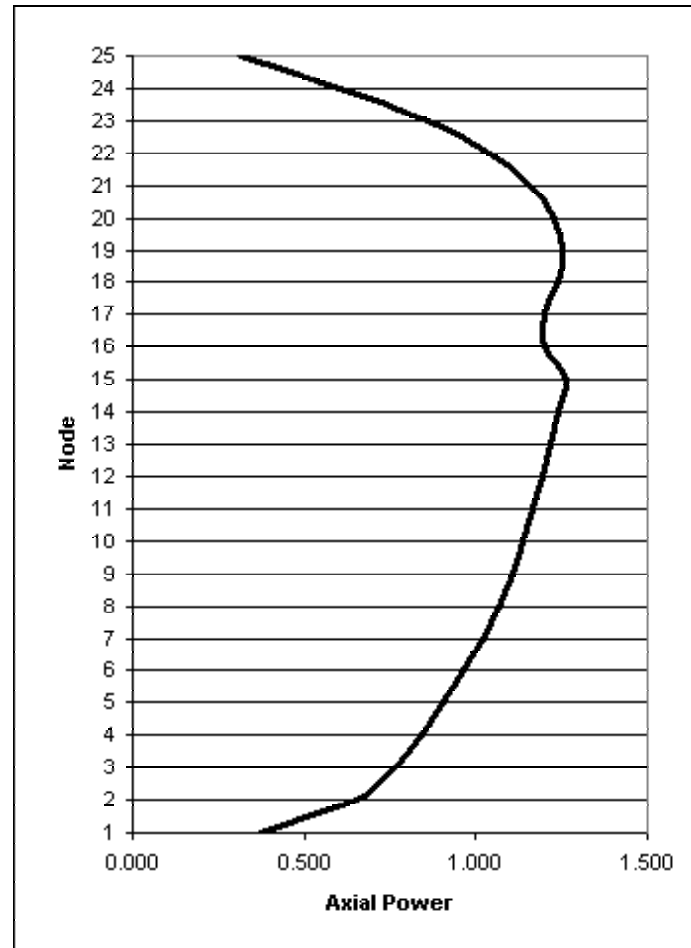
Figure 4A-18c. Axial Exposure at 18.5 GWd/MT Exposure

18.5GWD/MT

Node	Axial Exposure (MWD/MT)
25	7555.3
24	12997.8
23	18134.9
22	22996.1
21	27129.3
20	30457.4
19	33090.2
18	34921.0
17	35947.0
16	36632.4
15	35454.8
14	36598.3
13	37581.9
12	38289.7
11	38898.9
10	39396.9
9	39662.2
8	39972.7
7	40377.5
6	40729.9
5	40741.0
4	39819.7
3	36630.0
2	29483.8
1	15353.0
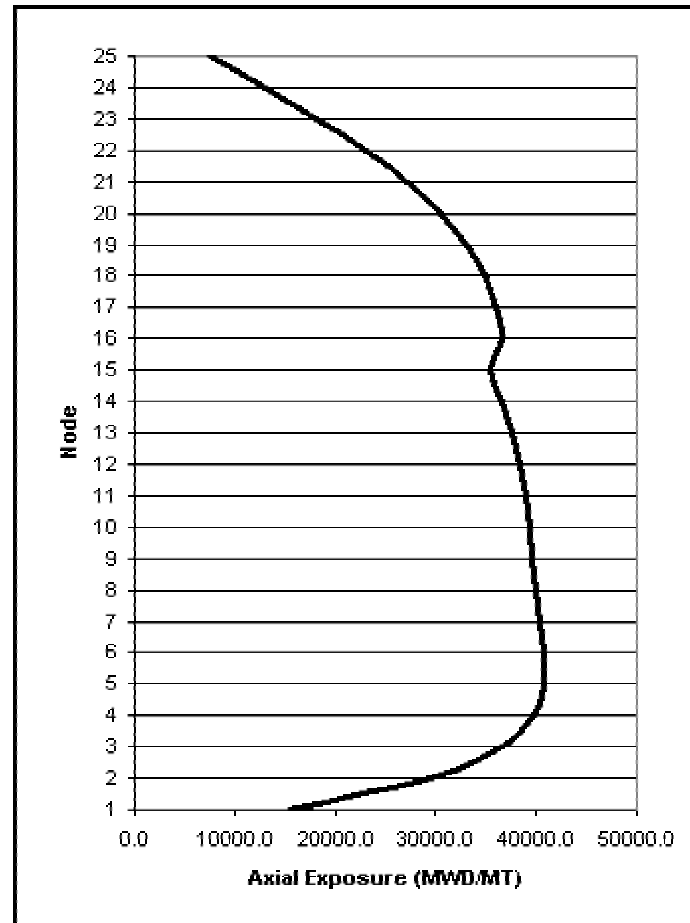
Figure 4A-18d. Relative Integrated Power Per Bundle at 18.5 GWd/MT Exposure

	1	2	3	4	5	6	7	8	9	10	11	12	13	14	15	16	17	18	19
1															0.29	0.33	0.37	0.40	0.40
2													0.36	0.45	0.48	0.61	0.66	0.70	0.75
3											0.43	0.53	0.69	0.84	0.75	0.75	0.82	0.96	0.74
4									0.42	0.55	0.74	0.93	1.02	1.05	0.88	0.91	1.06	1.07	0.95
5								0.48	0.72	0.93	1.04	1.11	1.01	1.17	1.15	1.13	0.89	1.12	0.93
6							0.47	0.73	0.99	1.09	1.15	1.01	1.21	1.01	1.17	0.97	1.13	0.96	1.12
7						0.47	0.61	0.99	0.98	1.17	0.94	1.05	1.21	1.21	0.99	1.02	0.98	1.14	0.96
8					0.48	0.73	0.99	1.12	1.19	1.02	1.08	0.97	1.22	1.09	1.09	1.08	1.17	0.99	0.97
9				0.42	0.72	0.99	0.98	1.19	1.09	1.23	1.23	1.22	1.08	1.22	1.04	1.22	1.03	1.19	1.01
10				0.55	0.93	1.09	1.17	1.02	1.23	1.05	1.24	1.05	1.22	1.05	1.23	1.24	1.24	1.06	1.23
11			0.43	0.74	1.04	1.15	0.94	1.08	1.23	1.24	1.01	1.05	1.08	1.24	1.01	1.07	1.07	1.27	1.09
12			0.53	0.93	1.11	1.01	1.05	0.97	1.22	1.05	1.05	1.06	1.25	1.25	1.07	1.07	1.27	1.28	1.11
13		0.36	0.69	1.02	1.01	1.21	1.21	1.22	1.08	1.22	1.08	1.25	1.07	1.26	1.06	1.25	1.08	1.28	1.08
14		0.45	0.84	1.05	1.17	1.01	1.21	1.09	1.22	1.05	1.24	1.25	1.26	1.06	1.24	1.07	1.28	1.09	1.25
15	0.29	0.48	0.75	0.88	1.15	1.17	0.99	1.09	1.04	1.23	1.01	1.07	1.06	1.24	1.04	1.09	1.28	1.26	1.03
16	0.33	0.61	0.75	0.91	1.13	0.97	1.02	1.08	1.22	1.24	1.07	1.07	1.25	1.07	1.09	1.09	1.27	1.06	1.04
17	0.37	0.66	0.82	1.06	0.89	1.13	0.98	1.17	1.03	1.24	1.07	1.27	1.08	1.28	1.28	1.27	1.07	1.24	1.04
18	0.40	0.70	0.96	1.07	1.12	0.96	1.14	0.99	1.19	1.06	1.27	1.28	1.28	1.09	1.26	1.06	1.24	1.06	1.25
19	0.40	0.75	0.74	0.95	0.93	1.12	0.96	0.97	1.01	1.23	1.09	1.11	1.08	1.25	1.03	1.04	1.04	1.25	1.10

Figure 4A-18e. Average Bundle Exposure at 18.5 GWd/MT Exposure

	1	2	3	4	5	6	7	8	9	10	11	12	13	14	15	16	17	18	19
1															43.10	42.66	46.74	44.09	45.08
2													49.82	46.30	46.74	32.19	31.53	30.75	13.45
3											47.07	46.30	32.41	14.77	36.82	38.25	36.71	17.64	47.73
4									46.30	46.52	30.64	15.43	17.31	18.41	39.90	38.91	20.06	19.84	33.51
5								49.49	27.23	14.88	16.98	18.74	37.48	20.83	21.05	21.38	50.38	21.61	41.89
6							46.52	29.10	16.09	17.75	19.18	40.34	21.72	42.55	21.94	42.99	22.16	42.88	21.83
7						46.52	49.49	16.31	35.94	19.73	48.72	39.46	21.94	22.60	46.19	41.01	42.44	22.38	42.44
8					49.49	29.10	16.31	18.63	20.50	41.12	37.15	49.60	22.82	35.60	36.82	37.15	23.04	42.55	42.22
9				46.41	27.23	16.09	35.94	20.50	38.91	21.94	21.94	22.49	42.77	23.59	43.21	23.37	43.21	23.04	42.44
10				46.52	14.88	17.75	19.73	41.12	21.94	43.10	22.05	42.22	23.15	43.65	23.15	23.04	23.26	42.88	22.05
11			47.07	30.64	16.98	19.18	48.72	37.15	21.94	22.05	47.84	40.34	42.77	22.82	49.27	41.56	42.99	22.16	40.34
12			46.30	15.43	18.74	40.34	39.46	49.60	22.49	42.22	40.34	41.23	22.60	22.60	41.23	41.67	22.60	21.94	39.24
13		49.82	32.41	17.31	37.48	21.72	21.94	22.82	42.77	23.15	42.77	22.60	43.87	23.04	42.66	22.49	43.21	22.49	42.33
14		46.30	14.77	18.41	20.83	42.55	22.60	35.60	23.59	43.65	22.82	22.60	23.04	43.54	22.16	42.33	22.60	42.55	21.94
15	43.10	46.74	36.82	39.90	21.05	21.94	46.19	36.82	43.21	23.15	49.27	41.23	42.66	22.16	47.62	40.57	21.83	22.16	47.07
16	42.66	32.08	38.25	38.91	21.38	42.99	41.01	37.15	23.37	23.04	41.56	41.67	22.49	42.33	40.57	40.68	21.94	41.67	41.45
17	46.74	31.53	36.71	20.06	50.38	22.16	42.44	23.04	43.21	23.26	42.99	22.60	43.21	22.60	21.83	21.94	43.21	22.27	42.44
18	44.09	30.75	17.64	19.84	21.61	42.88	22.38	42.55	23.04	42.88	22.16	21.94	22.60	42.55	22.16	41.67	22.27	42.99	21.27
19	45.08	13.45	47.84	33.51	41.89	21.83	42.44	42.22	42.44	22.05	40.34	39.24	42.33	21.94	47.07	41.45	42.44	21.27	39.68

Figure 4A-19. Minimum Critical Power Ratio (MCPR) as a Function of Exposure

Exposure (MWD/MT)	MCPR
0	1.4998
1102	1.5074
2205	1.4956
3307	1.5041
4409	1.5108
5512	1.5083
6614	1.5030
7716	1.5518
8818	1.5419
9921	1.4863
11023	1.4872
12125	1.4962
13228	1.5060
14330	1.5279
15432	1.5363
16535	1.5065
17637	1.5152
18487	1.5130
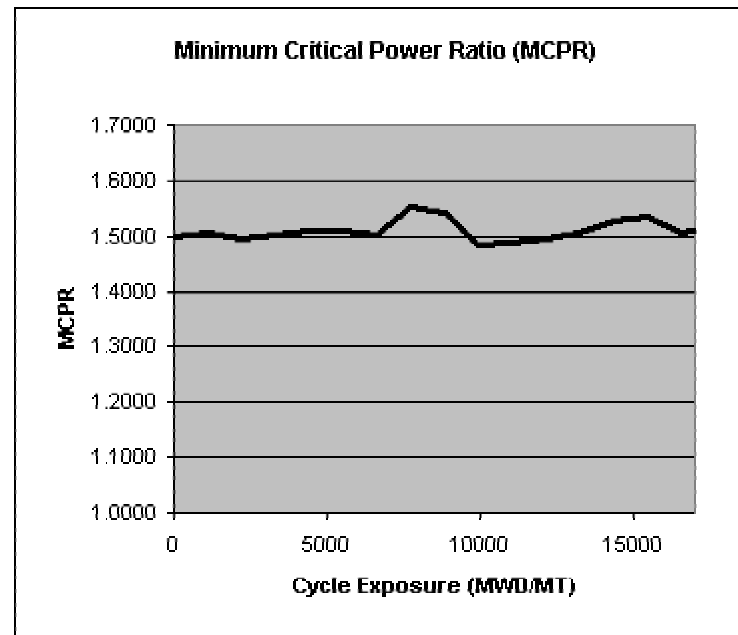
4B. FUEL LICENSING ACCEPTANCE CRITERIA

A set of fuel licensing acceptance criteria has been established for evaluating fuel designs and for determining the applicability of generic analyses to these designs. Fuel design compliance with the fuel licensing acceptance criteria constitutes NRC acceptance and approval of the fuel design for initial core and reload applications without specific NRC review. The fuel licensing acceptance criteria are presented in the following subsections.

4B.1 GENERAL CRITERIA

NRC-approved analytical models and analysis procedures are applied. Consistent with current practice, NRC-approved procedures and methods are used to evaluate new fuel designs.

New design features are included in lead use assemblies (LUAs). GE's "test before use" fuel design philosophy includes irradiation experience with new fuel design features in full-scale fuel assemblies, called LUAs, in operating reactors prior to standard reload application.

The generic post-irradiation fuel examination program approved by the NRC is maintained. Section 4.2.II.D.3 of the Standard Review Plan (SRP) requires each plant to implement a post-irradiation fuel surveillance program to detect anomalies or to confirm expected fuel performance. The NRC has found that the fuel surveillance program described in Reference 4B 1 is an acceptable means for licensees to satisfy the post-irradiation surveillance requirement of the SRP. This program includes examination of LUAs and selected discharged bundles with the results reported to the NRC in a yearly operating experience report.

4B.2 THERMAL-MECHANICAL

The fuel design thermal-mechanical analyses are performed for the following conditions:

- Either worst tolerance assumptions are applied or probabilistic analyses are performed to determine statistically bounding results (i.e., upper 95% confidence).

- Operating conditions are taken to bound the conditions anticipated during normal steady-state operation and anticipated operational occurrences (AOOs).

- The fuel design evaluations are performed against the following criteria:

- The fuel rod and fuel assembly component stresses, strains, and fatigue life usage do not exceed the material ultimate stress or strain and the thermal fatigue capability.

- The fuel rod and assembly components are evaluated to ensure that the fuel does not fail due to stresses or strains exceeding the fuel assembly component mechanical capability. The limit is patterned after ANSI/ANS-57.5. The figure of merit employed is the design ratio, which is defined as a ratio of effective stress and stress limit, or of effective strain and strain limit.

- The material capability limit is taken as the material ultimate stress or strain. The limit used is that the design ratio must be less than or equal to one (design ratio < 1.0). Fatigue is addressed in a similar manner where the calculated fatigue duty must be less than or equal to the material fatigue capability (fatigue life usage < 1.0).

- Mechanical testing is performed to ensure that loss of fuel rod and assembly component mechanical integrity does not occur due to fretting wear.

- Evaluations of the fuel assembly for fretting wear are based on mechanical testing and extensive reactor operating experience.

- The fuel rod and assembly component evaluations include consideration of metal thinning and any associated temperature increase due to oxidation and the buildup of corrosion products to the extent that these influence the material properties and structural strength of the components.

- The effects of cladding oxidation and corrosion product buildup on the fuel rod surface (i.e., increased calculated temperatures, material property changes and cladding thinning) are explicitly included in the evaluations performed.

- The fuel rod internal hydrogen content is controlled during manufacture of the fuel rod consistent with ASTM standards C776-83 and C934-85 to ensure that loss of fuel rod mechanical integrity does not occur due to internal cladding hydriding.

- Internal cladding hydriding is controlled during fuel manufacture by restricting the level of moisture and other hydrogenous impurities within limits consistent with SRP 4.2. Extensive operating experience with fuel designs manufactured to the hydrogen content limits specified in the SRP demonstrates that hydriding is not an active failure mechanism for normal operation or AOOs.

- The fuel rod is evaluated to ensure that fuel rod or channel bowing does not result in loss of fuel rod mechanical integrity due to boiling transition.

- As part of the fuel surveillance program and other inspections, the peripheral row of fuel rods is visually inspected to determine the extent of fuel rod to fuel rod gap closure due to rod bowing caused by fuel rod growth. Observations of gap closure greater than 50% are reported to the NRC. Any change to the 50% closure requirement is based on thermal-hydraulic testing to assure that the criterion is satisfied.

- The effect of potential channel bow on fuel rod/bundle performance, if any, is accounted for by adjusting minimum critical power ratio (MCPR) limits as determined by analyses and/or by the evaluation of channel bow measurements.

- Loss of fuel rod mechanical integrity does not occur due to excessive cladding pressure loading. To achieve this objective, the fuel rod internal pressure is conservatively limited so that the cladding creepout rate due to internal gas pressure during normal steady-state operation does not exceed the instantaneous fuel pellet irradiation swelling rate.

- The fuel assembly (including channel box), control rod and control rod drive are evaluated to assure that control rods can be inserted, when required. These evaluations are performed in accordance with NUREG-0800 (Appendix A to SRP Section 4.2) where the effect of combined safe shutdown earthquake (SSE) and loss-of-coolant accident (LOCA) loads (which conservatively bound the worst case hydraulic loads possible during normal conditions) are evaluated to assure that component deformation is not severe enough to prevent control rod insertion and vertical lift-off forces does not unseat

the lower tie plate such that the resulting loss of lateral fuel bundle positioning would prevent control rod insertion.

- Loss of fuel rod mechanical integrity does not occur due to cladding collapse into a fuel column axial gap. To achieve this objective, the fuel rod is evaluated to ensure that fuel melting during normal operation and core-wide AOOs does not occur. For local AOOs such as rod withdrawal error, a small amount of calculated fuel pellet center melting may occur, but is limited by the 1% cladding circumferential plastic strain criterion.

- Loss of fuel rod mechanical integrity does not occur due to pellet-cladding mechanical interaction. To achieve this objective, the fuel rod is evaluated to ensure that the calculated cladding circumferential plastic strain due to pellet-cladding mechanical interaction does not exceed 1% during AOOs.

- When GNF fuel is loaded into a core with other vendor fuel, other vendor thermal analyses are assumed to be applicable for that vendor's fuel in the core. When GNF fuel is loaded into a core containing other vendor fuel, the operating limits established by the other vendor based on thermal-mechanical considerations continue to be applied to the other vendor fuel.

4B.3 NUCLEAR

A negative Doppler reactivity coefficient is maintained for any operating condition. The Doppler reactivity coefficient is of high importance in reactor safety. The Doppler coefficient of the core is a measure of the reactivity change associated with an increase in the absorption of resonance-energy neutrons caused by a change in the temperature of the material and is a function of the average of the bundle Doppler coefficients. A negative Doppler coefficient provides instantaneous negative reactivity feedback to any rise in fuel temperature, on a gross or local basis and thus assures the tendency of self-control for the ESBWR.

A negative core moderator void reactivity coefficient resulting from boiling in the active flow channels is maintained for any operating conditions. The core moderator void coefficient resulting from boiling in the active flow channels is maintained negative over the complete range of ESBWR operation. This flattens the radial power distribution and provides ease of reactor control due to the negative void feedback mechanism.

A negative moderator temperature reactivity coefficient is maintained above hot standby. The moderator temperature coefficient is associated with a change in the moderating capability of the water. Once the reactor reaches the power producing range, boiling begins and the moderator temperature remains essentially constant. The moderator temperature reactivity coefficient is negative during power operation.

To prevent a super prompt critical reactivity insertion accident originating from any operating condition, the net prompt reactivity feedback due to prompt heating of the moderator and fuel is negative. The mechanical and nuclear designs of the fuel are such that the prompt reactivity feedback (requiring no conductive or convective heat transfer and no operator action) provides an automatic shutdown mechanism in the event of a super prompt reactivity incident. This characteristic ensures rapid termination of super prompt critical accidents, with additional long-term shutdown capability due to negative void coefficient, for those cases where conductive heat transfer from the fuel to the water results in boiling in the active channel region.

A negative power reactivity coefficient (as determined by calculating the reactivity change due to an incremental power change) from a steady-state base power level is maintained for all operating power levels above hot standby. A negative power coefficient provides an inherent negative feedback mechanism to provide more reliable control of the plant as the operator performs power maneuvers. It is particularly effective in preventing xenon initiated power oscillations in the core. The power coefficient is effectively the combination of Doppler, void and moderator temperature reactivity coefficients. For fast system transients, these three individual reactivity components are explicitly considered to determine the core transient response.

The plant meets the cold shutdown margin requirement. The core is capable of being made subcritical with margin in the most reactive condition throughout an operating cycle with the most reactive control rod in its full-out position and all other rods fully inserted. This parameter is dependent upon the core loading and is calculated for each plant cycle prior to plant operation of that cycle.

The effective multiplication factor for fuel designs stored under normal and abnormal conditions is shown to meet fuel storage limits by demonstrating that the peak uncontrolled lattice k-infinity calculated in a normal reactor core configuration meets the limits for GE designed regular or high density storage racks. The basic criterion associated with the storage of both irradiated and new fuel is that the effective multiplication factor of fuel stored under normal conditions is less than or equal to 0.90 for regular density racks and less than or equal to 0.95 for high density racks. Abnormal storage conditions are limited to a keff of less than or equal to 0.95 for both high and regular density designs. For GE designed fuel storage racks, these storage criteria are satisfied for all GNF fuel designs.

When GNF fuel is loaded into a core with other vendor fuel, nuclear libraries are calculated for other vendor fuel. When GNF fuel is placed into a core containing other vendor fuel, complete exposure and void dependent nuclear libraries are calculated for the other vendor fuel to assure integration in the core nuclear analyses with the GNF bundles.

4B.4 HYDRAULIC

Flow pressure drop characteristics are included in the calculation of the operating limit minimum critical power ratio (MCPR).

Because of the channeled configuration of ESBWR fuel assemblies, there is no bundle-to-bundle cross flow inside the core, and the only issue of hydraulic compatibility of various bundle types in a core is the bundle inlet flow rate variation and its effect on margin to thermal limits [i.e., MCPR and maximum linear heat generation rate (MLHGR)]. The coupled thermal-hydraulic-nuclear analyses performed to determine fuel bundle flow and power distribution use the various bundle pressure loss coefficients to determine the flow distribution required to maintain a total core pressure drop boundary condition to be applied to all fuel bundles. The margin to the thermal limits of each fuel bundle is determined using this consistent set of calculated bundle flow and power.

A major contribution to the acceptability of core operation with varying fuel bundle pressure drop characteristics is the fact that the nature of the ESBWR tends to self-correct any inherent differences in these characteristics. The flow variation tends to self-correct by virtue of the fact

that a fuel bundle with high loss coefficient tends to get less flow; however, this lower flow rate tends to reduce the bundle power, which, in turn, tends to increase the bundle flow rate to that bundle. The margin to the MCPR limit also tends to self-correct by virtue of the fact that a reduction in bundle flow rate tends to reduce bundle critical power capability; however, this bundle flow rate reduction would reduce the power of that bundle, depending on the power level of the neighboring fuel bundles, thus tending to mitigate the effect on margin to thermal limits.

Therefore, although the effect of different characteristics tends to be self-mitigating, these characteristics are explicitly modeled in the analyses process.

4B.5 OPERATING LIMIT MCPR

The plant Operating Limit MCPR (OLMCPR) is established by considering the limiting anticipated operational occurrences (AOOs) for each operating cycle. The OLMCPR is determined such that 99.9% of the rods avoid boiling transition (BT) during the transient of the limiting analyzed AOO. These limiting events are established based on sensitivity studies of bundle and plant parameters. Because the OLMCPR is dependent upon the core loading patterns, this limit is cycle dependent and is calculated just prior to operation of the cycle.

The OLMCPR calculations consider the following:

- The analysis is performed for the specific plant.

- The analysis is performed for the specific core loading and the specific bundle design.

- Core radial power distributions are selected to reasonably bound the number of bundles at or near thermal limits.

- The local power distribution is selected such that the largest anticipated number of rods is near boiling transition. Local fuel pin power distribution is based on the specific bundle design.

- 99.9% of the rods in the core must be expected to avoid boiling transition for core-wide incidents of moderate frequency (anticipated operational occurrences).

- The analysis accounts for the uncertainty ranges of manufacturing tolerances, uncertainties in measurement of core operating parameters, calculation uncertainties, and statistical uncertainty associated with critical power correlations and transient analysis model uncertainties.

When GNF fuel is loaded into a core with other vendor fuel, mixed core effects are included in the calculation of the limit. When GNF fuel is placed in a core with other vendor fuel, GE-NE/GNF performs transient analyses of the mixed core to determine the OLMCPR for each cycle. The calculation of nuclear libraries with GE-NE/GNF methods for other vendor fuel and use if the fuel design parameters assure that the transient analysis of other vendor fuel in the core is accurately performed.

4B.6 CRITICAL POWER CORRELATION

The currently approved critical power correlations will be confirmed or a new correlation is established when there is a change in wetted parameters of the flow geometry; this specifically includes fuel and water rod diameter, channel sizing and spacer design.

The coefficients for the critical power correlation of a fuel design are determined based on the criteria documented in Reference 4B-4. The fuel design parameters given in these criteria are those that have the primary effect on determining the need for a new critical power correlation when there is a change in the fuel design.

A new correlation may be established if significant new data exists for a fuel design(s). When significant new data have been taken for a fuel design, a better fit to the data may be achieved by adjusting the coefficients in the critical power correlation. The resulting new critical power correlation would be a more accurate representation of actual plant operation. These coefficients are documented in the fuel design information report.

The criteria for establishing the new correlation are as follows:

·   The new correlation shall be based on full-scale prototypical test assemblies.

·   Tests shall be performed on assemblies with typical rod-to-rod peaking factors.

·   The functional form of the currently approved correlations shall be maintained.

·   Correlation fit to data shall be best fit.

·   One or more additional assemblies must be tested to verify correlation accuracy (i.e., test data not used to determine the new correlation coefficients).

·   Coefficients in the correlation shall be determined as described in Reference 4B-2 or Reference 4B-3.

·   The uncertainty of the resulting correlation shall be determined by:

$$\sigma = \sqrt{\frac{1}{N-1}\sum_{i=1}^{N}(\mu - ECPR_i)^2}$$

Where:

σ =   Standard deviation

μ =   Mean

N =   Total number of data in both the data set used to determine the coefficients and the set used for verification.

ECPR =   Calculated bundle critical power divided by experimentally determined bundle critical power.

The criteria for establishing a new correlation are those that were used in establishing the correlations approved by the NRC. The basis of the correlation is a best fit of data taken of prototypical test assemblies with typical rod-to-rod peaking factors. To ensure that no safety concern exists, the NRC prior to use shall approve the functional form of the current correlation's form. The correlation coefficients and uncertainties are determined in the same manner as approved by the NRC for the current correlations.

When GNF fuel is placed in core containing other vendor fuel, GE-NE/GNF simulates the critical power correlation used by the other vendor to assure that the other vendor's fuel is properly calculated. This is done by determining the CPR predicted by the other vendor correlation as a function of variations in flow, inlet subcooling, peaking, and pressure.

4B.7 STABILITY

The requirements set forth in 10 CFR 50 Appendix A, GDC 12, are met. The stability compliance criteria consider potential limit cycle response within the limits of safety system and/or operator intervention and assure that the GE fuel design during this operating mode does not result in the specified acceptable fuel design limits being exceeded. The stability compliance of GNF fuel designs is demonstrated in Appendix 4D on a generic basis and a specific analysis for each cycle is not required.

For each fuel design, no region of the power/flow operating map needs to be excluded and the plant operates in the entire region. Characteristics of a new fuel design that could change the operation through the entire power/flow map are the fuel time constant, the void coefficient and the in-core pressure drop. Each new fuel design must satisfy either of the following criteria:

- The stability behavior, as indicated by core and limiting channel decay ratios, must be equal to or better than a previously approved GNF BWR design.

- If the core and limiting channel decay ratios are not equal to or better than a previously approved GNF fuel design, it must be demonstrated that there is no change to the entire region of operation.

When loading GNF fuel into a core with other vendor fuel, GE-NE/GNF uses the nuclear libraries calculated for the other vendor fuel and the actual fuel bundle parameters of the other vendor fuel to calculate the core decay ratio.

4B.8 OVERPRESSURE PROTECTION ANALYSIS

Adherence to the ASME overpressure protection criteria is demonstrated by plant/cycle-specific analysis. The demonstration of the adequacy of the plant overpressure protection system is dependent upon the plant core-loading pattern and must be demonstrated for each cycle. This cycle-specific analysis is performed prior to operation of that core.

When GNF fuel is loaded into a core with other vendor fuel, mixed core effects are included in the calculation. When loading GNF fuel into a core with other vendor fuel, GENE uses the nuclear libraries calculated from the other vendor fuel and the actual fuel bundle parameters of the other vendor fuel in a mixed core analysis to demonstrate the adequacy of the plant overpressure system.

4B.9 REFUELING ACCIDENT ANALYSIS

The consequences of refueling accidents are confirmed as bounding or a new analysis shall be performed and documented when a new fuel design is introduced.

The consequences of the refueling accident are primarily dependent upon the number of fuel rods in a bundle. When the number of fuel rods changes, the effect on the refueling accident must be determined based on the fuel design information report.

4B.10 ANTICIPATED TRANSIENT WITHOUT SCRAM

The fuel must meet either of the following criteria:

- A negative core moderator void reactivity coefficient, consistent with the analyzed range of void coefficients provided in Subsection 15.5.4, shall be maintained for any operating conditions above the startup critical condition.

- If the criterion above is not satisfied, the limiting events (as described in Subsection 15.5.4) are evaluated to demonstrate that the plant response in within the ATWS criteria specified in Subsection 15.5.4.

4B.11 COL INFORMATION

None.

4B.12 REFERENCES

4B-1   USNRC Letter, from L. S. Rubenstein (NRC) to R. L. Gridley (GE), "Acceptance of GE Proposed Fuel Surveillance Program," June 27, 1984.

4B-2   General Electric Company, "General Electric BWR Thermal Analysis Basis (GETAB): Data Correlation and Design Application," NEDE-10958-PA, Class III (proprietary), and NEDO-10958-A, Class I (non-proprietary), January 1977.

4B-3   GE Nuclear Energy Letter, from J. S. Charnley (GE) to C. O. Thomas (NRC), "Amendment 15 to General Electric Licensing Topical Report NEDO-24011-A," January 25, 1986.

4B-4   Global Nuclear Fuel, "General Electric Standard Application for Reactor Fuel (GESTAR II)" NEDE-24011-P-A-14, Class III (proprietary), June 2000, and NEDO-24011-A-14, Class I (non-proprietary), July 2000.

4C. CONTROL ROD LICENSING ACCEPTANCE CRITERIA

A set of acceptance criteria has been established for evaluating new control rod designs. Control rod compliance with these criteria constitutes the basis for NRC acceptance and approval of the design without specific NRC review. The control rod licensing acceptance criteria and their bases are provided below. Any change to these criteria must have prior NRC review and approval.

4C.1 GENERAL CRITERIA

Control rod designs meeting the following acceptance criteria are considered to be approved and do not require specific NRC review:

- The control rod stresses, strains, and cumulative fatigue shall be evaluated to not exceed the ultimate stress or strain limit of the material.

- The control rod shall be evaluated to be capable of insertion into the core during all modes of plant operation within the limits assumed in the plant analyses.

- The material of the control rod shall be shown to be compatible with the reactor environment.

- The reactivity worth of the control rod shall be included in the plant core analyses.

- Prior to use of new design features on a production basis, lead surveillance control rods may be used.

4C.2 BASIS FOR ACCEPTANCE CRITERIA

The following licensing bases is provided for the acceptance criteria given in Section 4C.1:

Stress, Strain and Fatigue

The control rod is evaluated to assure that it does not fail because of loads due to shipping, handling, normal operation, including the effects of anticipated operational occurrences (AOOs), infrequent incidents and accidents. To ensure that the control rod does not fail, these loads must not exceed the ultimate stress and strain limit of the material. Fatigue must not exceed a fatigue usage factor of 1.0.

The loads evaluated include those due to normal operational transients (scram and jogging), pressure differentials, thermal gradients, flow and system induced vibration, and irradiation growth in addition to the lateral and vertical loads expected for each condition. Fatigue usage is based upon the cumulative effect of the cyclic loadings. The analyses include corrosion and crud deposition as a function of time, as appropriate.

Conservatism is included in the analyses by including margin to the limit or by assuming loads greater than expected for each condition. Higher loads can be incorporated into the analyses by increasing the load itself or by statistically considering the uncertainties in the value of the load.

Control Rod Insertion

The control rod is evaluated to be sure that it can be inserted during normal operations including the effects of anticipated operational occurrences (AOOs), infrequent incidents and accidents.

These evaluations include a combination of analyses of the geometrical clearance and actual testing. The analyses consider the effects of manufacturing tolerances, swelling and irradiation growth. Tests may be performed to demonstrate control rod insertion capability for conditions such as control rod or fuel channel deformation and vibrations due to safe shutdown earthquakes.

Control Rod Material

The external control rod materials must be capable of withstanding the reactor coolant environment for the life of the control rod. Effects of crudding, crevices, stress corrosion and irradiation upon the material must be included in the control rod and core evaluations. Irradiation effects to be considered include material hardening and absorber depletion and swelling.

Reactivity

The reactivity worth of the control rod is determined by the initial amount and type of absorber material and irradiation depletion. Scram time insertion performance must also be included in the plant core analyses including normal operations, including the effects of anticipated operational occurrences (AOOs), and accidents.

Surveillance

Visual inspection of the lead depletion control rod design possessing the new design feature and three additional control rods of such design that are within 15% of the estimated fast fluence of the lead control rod shall be performed. If fewer than three control rods are within 15% of the estimated fast fluence of the lead control rod, only those within 15% shall be inspected. If a control rod with the new design feature reaches analytical end of life, and is visually inspected with no significant issues, the new design feature surveillance program ends. Should evidence of a problem arise, the inspection program is expanded to additional control rods to the extent necessary to identify the root cause of the problem.

4C.3 COL INFORMATION

None.

4D. STABILITY EVALUATION

The stability licensing criterion for all nuclear power plants is set forth in 10 CFR 50 Appendix A, General Design Criterion 12 (GDC-12). As discussed in Section 4B.8, this requires assurance that power oscillations, which can result in conditions exceeding specified acceptable fuel design limits, are either not possible or can be reliably detected and suppressed. Because the most limiting stability condition in the ESBWR normal operating region is at the rated power/flow condition, the ESBWR is designed so that power oscillations are not possible (i.e., remains stable) throughout the whole operating region, including plant startup. In addition, the ESBWR is designed to be stable during anticipated operational occurrences (AOOs). As a backup, the ESBWR will implement a Detect and Suppress solution as a defense-in-depth system. The details of the solution will be developed during the ESBWR Construction and Operating License (COL) phase.

This appendix summarizes the stability evaluation of the ESBWR design. Section 4D.1 presents the stability performance during power operation and Section 4D.2 presents the stability performance during plant startup.

4D.1 STABILITY PERFORMANCE DURING POWER OPERATION

4D.1.1 Stability Criteria

Compliance with General Design Criterion 12 is assured by implementing design criteria for the decay ratio. GE uses a stability criteria map of core decay ratio vs. channel decay ratio to establish margins to stability. Stability acceptance criteria for BWRs are established on this map at core decay ratio = 0.8 and limiting channel decay ratio = 0.8, with an allowance for regional mode oscillations in the top right corner of the defined rectangle. These boundaries were established considering model uncertainties of the order of 0.2 in the core and channel decay ratio in the GE analysis methods (FABLE and ODYSY). There is also margin in the regional boundary, which is drawn below available plant regional oscillation data, though the amount of conservatism has not been quantified. The NRC has approved application of ODYSY to the E1A Long Term Stability Solution [4D-1, 4D-2].

The ESBWR stability design criteria are shown in this map in Figure 4D-1. The ESBWR core size of 1132 bundles is significantly larger than the largest operating BWR (ABWR with 872 bundles). The sub-criticality of the azimuth harmonic, which is relevant for regional oscillations, decreases with core size. The regional stability boundary is expected to move inwards in the Core Decay ratio vs. Channel Decay Ratio plane as the sub-criticality decreases. Figure 4D-1 shows the approximate effect of the larger core size on the calculated regional stability boundary. The calculated values of higher harmonic sub-criticality for the ESBWR core vary between $0.76 and $0.95. These values are bounded by the estimated boundary for a sub-criticality of $0.70. In order to account for regional stability for the ESBWR, the acceptance criteria for the limiting channel decay ratio is constrained to be less than 0.5. This conservatively adjusts the operating plant criteria for the larger ESBWR core.

The design goal is for the nominal values of the core and channel decay ratios at rated power and flow to be less than 0.4 and 0.3 respectively, or about half the BWR acceptance criteria (where the channel decay ratio was reduced to approximately 0.6 to accommodate the regional stability

boundary). Figure 4D-1 shows that the design goal maintains a large margin to the onset of instability even with the reduction of the stable region on the stability map to account for the larger core size.

The design requirement is for the core and channel decay ratios to be less than the acceptance criteria of 0.8 and 0.5 at the 2σ level of uncertainty. Because the ESBWR is a new plant and there are no plant data, the uncertainties includes operating state and model uncertainties, even though there is already an explicit allowance for model uncertainty in the acceptance criteria.

4D.1.2 Analysis Methods

The TRACG computer code is used for the analysis of ESBWR stability margins. TRACG is a General Electric (GE) proprietary version of the Transient Reactor Analysis Code (TRAC). TRACG uses advanced one-dimensional and three-dimensional methods to model the phenomena that are important in evaluating the operation of BWRs. The NRC has approved TRACG for ESBWR LOCA (ECCS and containment) analysis. [4D-3]. The application of TRACG for Anticipated Operational Occurrences (AOOs) and for ATWS overpressure calculations for operating BWRs has also been approved by the NRC [4D-4, 4D-5].

TRACG has a multi-dimensional, two-fluid model for the reactor thermal hydraulics and a three-dimensional reactor kinetics model. The models can be used to accurately simulate a large variety of test and reactor configurations. These features allow for realistic simulation of a wide range of BWR phenomena, and are described in detail in the TRACG Model Description Licensing Topical Report [4D-6].

TRACG has been extensively qualified against separate effects tests, component performance data, integral system effects tests and operating BWR plant data. The details are presented in the TRACG Qualification Licensing Topical Report [4D-7]. Specific qualification studies for tests simulating passive BWR design features are reported in References 4D-8 and 4D-9.

The stability analysis statistically accounts for the uncertainties and biases in the models and plant parameters using a Monte Carlo method for the Normal Distribution One-Sided Upper Tolerance Limit (ND-OSUTL) if the output distribution is normal, or the Order Statistics method if it is not. Conservative values are used in place of probability distributions for some plant parameters for convenience. The uncertainties and biases considered include the following:

- Model uncertainties
- Experimental uncertainties and any uncertainties related to test scale-up
- Plant uncertainties
- Process measurement errors
- Manufacturing tolerances

The overall analysis approach followed is consistent with the Code Scaling Applicability and Uncertainty (CSAU) analysis methodology [4D-10].

The application methodology is described in Reference 4D-11, Licensing Topical Report, NEDE-33083P, Supplement 1, "TRACG Application for ESBWR Stability Analysis".

4D.1.3 Steady State Stability Performance

4D.1.3.1 Baseline Analysis

A baseline analysis was performed for the ESBWR at rated conditions, which are the most limiting from the perspective of stability due to the highest power/flow ratio [4D-11]. Analysis was conducted for equilibrium GE14 core at various points in the cycle: Beginning of Cycle (BOC), Middle of Cycle (MOC) near the peak reactivity state, and End of Cycle (EOC). The initial conditions are tabulated in Table 4D-1. The core average axial power shapes for the three exposure points are shown in Figure 4D-2.

Channel Stability

Channel stability is evaluated for the highest power channels by perturbing the inlet flow velocity while maintaining constant channel power.

Super Bundle Stability

A super bundle is defined as a group of 16 bundles below a common chimney cell. The hydrodynamic stability of the highest power super bundle was analyzed by perturbing the inlet flow to the group of 16 bundles while maintaining constant power. The calculation was performed at BOC conditions because this is the most limiting for channel hydrodynamic stability.

Core wide Stability

Core stability was evaluated at BOC, MOC and EOC conditions. The calculations were made with the 3-D kinetics model interacting with the thermal hydraulics parameters. The response to a pressure perturbation in the steam line was analyzed to obtain the decay ratio.

Regional Stability

Regional stability is covered in the stability map through the combination of the core and channel decay ratios. As a reference point, the 'nominal' decay ratio for out-of-phase regional oscillations was specifically calculated by perturbing the core in the out-of-phase mode about the line of symmetry for the azimuth and harmonic mode.

The initial conditions were the same as for the channel and core stability cases. The decay ratio calculations were made at BOC conditions because of the lowest value of the sub-criticality and highest bottom peaking at these conditions. The channel decay ratio is also the highest at BOC because of the bottom peaked axial flux shape. The decay ratio and oscillation frequency were extracted from the responses for the individual channel groups.

Results

The results for channel, super bundle, core and regional stability are tabulated in Table 4D-2. The channel decay ratio was the highest at BOC because of the bottom peaked axial power shape. The channel decay ratios meet the design goal of 0.3. The oscillation time period is approximately twice the transit time for the void propagation through the channel. The transit time through the chimney does not contribute to the oscillation time period. There is pressure equalization at the top of the bypass region, which reduces the importance of the chimney. Moreover, there are insignificant frictional losses in the chimney and the static head does not affect the stability performance.

The super bundle decay ratio was lower than that for the single high power bundle, because of the lower average power for the group of 16 bundles. Again, the transit time through the chimney does not contribute to the oscillation time period. The slightly larger time period relative to the hot bundle is also due to the lower average power level.

The core decay ratio was the highest at MOC conditions due to the combination of axial power shape and void coefficient. The oscillation time period corresponds to twice the vapor transit time through the core region. The core decay ratios meet the design goal of 0.4.

The regional decay ratio for the limiting channel group is in line with the core decay ratio and channel decay ratio at BOC conditions.

4D.1.4 Statistical Analysis of ESBWR Stability

4D.1.4.1 Channel Decay Ratio Statistical Analysis

A Monte Carlo analysis of channel stability was performed at rated power and flow and BOC conditions that were determined to be limiting. A total of 59 trials were made. In each trial, random draws are made for each of the parameters determined to be important for stability. Some of these parameters are not important for channel stability per se, but the same set of parameters was perturbed for both channel and core stability. These parameters and their individual probability distributions are listed in Reference 4D-11. The value for each of these parameters is drawn from the individual probability distribution for that parameter. A TRACG calculation is made with this perturbed set of parameters to obtain a new steady state. The channel decay ratio for the highest power channel is then calculated by applying a perturbation in inlet velocity. This constitutes one trial in the Monte Carlo process. A One-Sided Upper Tolerance Limit with 95% content and 95% confidence level (OSUTL95/95) is calculated from the Monte Carlo distribution. Table 4D-3 shows the value of the OSUTL95/95 for the channel decay ratio.

4D.1.4.2 Core Wide Decay Ratio Statistical Analysis

The Monte Carlo analysis of core stability was performed at rated power and flow and MOC conditions that were determined to be limiting. As for channel stability, a total of 59 trials were made. In each trial, random draws are made for each of the parameters determined to be important for stability. A TRACG calculation is made with this perturbed set of parameters to obtain a new steady state. The core decay ratio is then calculated by applying a pressure perturbation in turbine inlet pressure. This constitutes one trial in the Monte Carlo process. An OSUTL95/95 is calculated from the Monte Carlo distribution. Table 4D-3 shows the value of the OSUTL95/95 for the core decay ratio.

4D.1.4.3 Comparison with Design Limits

Figure 4D-3 shows the stability map with the design criteria. The baseline results for core and channel decay ratios are compared against the design goal. The OSUTL95/95 values for core and channel decay ratios are compared against the design criteria. Note that these values are calculated at different times in the cycle and represent the highest individual values. The combination of these decay ratios at the same time is not possible. Nevertheless, the limiting channel and core decay ratios (OSUTL95/95) are simultaneously compared against the design

limits. Figure 4D-3 shows that both the design goals and design limits are satisfied for the ESBWR core.

4D.1.5 Stability Performance During AOOs

In general, the stability margin reduces when the reactor power increases and/or core flow reduces. Because the ESBWR design relies on natural circulation for core flow circulation, the core flow during full power operation is only dependent upon the vessel water level. Higher water level means higher core flow, and vice versa. During normal operation, the water level is tightly controlled within a pre-set range (between Level 4 and Level 7 setpoints) through the feedwater and level control system. During AOOs, a reactor scram is initiated when the water level is too high (higher than Level 8 setpoint) or too low (below Level 3 setpoint). In addition, high neutron flux scram and high-simulated thermal power scram are initiated to prevent the reactor from operating at high power. Therefore, the stability during AOOs is assured by the scram protection.

Two limiting AOOs were identified based on the above discussion: Loss-of Feedwater Heater (LOFWH), which results in increased power; and Loss of Feedwater Flow (LOFW), which results in a lower flow. The trajectories of the transients in the power – flow map are shown in Figure 4D-4. The curve A-A corresponds to operation with a reduced level in the downcomer. The lower level leads to a reduction in flow. Different points on A – A correspond to changes in control reactivity or changes in core inlet subcooling.

LOFWH is a slow transient, in which the power increases slowly as the feedwater temperature drops. If the operator takes no action, the power would increase until a high thermal power scram occurs at 115% of rated power. The worst operating point would be one where the drop in feedwater temperature is such that the power increases to just below the setpoint (115%) and levels off at that value.

Stability analysis was performed at the pre-scram conditions due to the loss of the feedwater heating at MOC conditions. Decreasing the feedwater temperature simulated the transient. The power increased to approximately 116% (slightly above the scram conditions of 115%) due to the feedwater temperature reduction. The circulation flow increased slightly and the average core void fraction stayed almost constant.

Stability analysis was performed at new power/flow/feedwater conditions after a steady state was achieved (Table 4D-4). Under these conditions the feedwater temperature had dropped from 488 to 447°K and reactor power had increased from 4500 to 5221 MWt. The transient response to a pressure perturbation was analyzed to determine the decay ratio. The core decay ratio and channel decay ratio at the pre-scram conditions are shown in Table 4D-4, and are well below the stability design criteria.

Analysis of the LOFW transient turned out to be more complex. The transient is rapid and unless the feedwater flow is restored, will scram in a few seconds on a trip at L3. In this period, the flow, power and subcooling are dropping and pressure is responding to the pressure controller. Rather than imposing a pressure perturbation on top of the transient response to evaluate the decay ratio, the following approach was adopted. When the level had fallen below L3, the feedwater flow was restored to maintain a reduced level. This eventually led to a new steady state where the circulation flow was reduced slightly and the power stabilized close to the

initial value with a reduced core inlet temperature. This operating point is more severe than the rated condition as the flow is reduced at the same power level. It provides a conservative evaluation of the LOFW transient, as the power is higher than would occur during a LOFW.

Results of stability analysis for the reduced level case are shown in Table 4D-4. The results from these studies show that adequate margin is maintained to the stability design criteria even for these more severe operating states.

4D.1.6 Stability Performance During Anticipated Transients Without Scram

The Anticipated Transients Without Scram (ATWS) mitigation design for the ESBWR is summarized in Section 15.5.4. This includes automatic feedwater runback and automatic boron injection. The TRACG analysis results presented in Section 15.5.4 confirm the conclusion that there are no stability issues during the ATWS transient.

4D.2 STABILITY PERFORMANCE DURING PLANT STARTUP

In contrast to operating BWRs, the ESBWR plant starts up without recirculation pumps. At low pressure, the initiation of voiding in the core and chimney causes perceptible changes in the driving head because of the large difference between liquid and vapor densities. Consequently, startup procedures are developed to assure smooth ascension in pressure and power.

Tests in experimental natural circulation loops [4D-12, 4D-13, 4D-14] have identified two mechanisms for potential flow oscillations at low pressure. First, at very low flows, a periodic "geysering" flow oscillation was found to occur due to condensation of core exit vapor in the subcooled chimney region. Condensation–induced oscillations may occur under these conditions. The chimney subcooling and the rate of vapor production in the core determine the condensation rate. Oscillations of this kind are unlikely given the ESBWR startup procedures, which are similar to those of the natural circulation Dodewaard reactor. Dodewaard experienced no "geysering" oscillation in its 22 refuel cycles of operation. Second, initiation of vapor production in the chimney region leads to a reduction in hydrostatic head in the chimney and a resultant core flow increase. This, in turn, could cause voids to collapse in the chimney, leading to a reduction in flow. Oscillations of this second kind (known in the literature as Type 1 instability [4D-15], (Figure 4D-5) had also never been seen at Dodewaard. In the final cycle of its operation, a special startup test was performed to probe the low-pressure portion of the startup trajectory. Though no oscillations were detectable on the APRMs, it was possible to infer the presence of small oscillations in core velocity from the auto correlation function of the APRM signal (Figure 4D-6) [4D-16]. These were small oscillations superposed on the core velocity with little, if any, reactivity impact, as the core flow is single phase in this phase of the startup transient.

In this section, the mechanism of the hydrostatic oscillations is examined and startup trajectories are analyzed with TRACG. The results show that large margins to boiling transition are maintained throughout the startup scenario.

4D.2.1 Phenomena Governing Oscillations during Startup

During startup, the water in the ESBWR vessel is initially heated to about 85°C by decay heat supplemented by auxiliary heaters. Following de-aeration, control rods are pulled to criticality and nuclear heatup begins at a low core power. As the water circulates through the core and

downcomer by natural circulation, it is gradually heated up. The RWCU system removes a portion of the heat by draining water from the downcomer and lower plenum, cooling it in heat exchangers and returning it through the feedwater sparger. Because of the large height of the ESBWR vessel, the pressure at the water level (near the top of the separators) is lower than the core pressure by about 1 bar. Figure 4D-7 shows a schematic of the vessel and the axial pressure profile. At low pressures corresponding to startup conditions, the pressure gradient gives rise to a significant difference in the saturation temperature between the core exit and the top of the separators. The saturation temperature profile is shown on the right side of the figure. As the circulating water is slowly heated up, saturation temperature is first reached at the top of the separators. Vapor generation at the top of the separators results in a reduction in the density head in the separators, and the voids propagate downwards. The formation of voids also results in a larger driving head for natural circulation flow. The increase in natural circulation flow reduces the core exit temperature and leads to a collapse of the voids. This completes one cycle of the hydrostatic head oscillation. The sequence of events for one cycle is illustrated in the right hand portion of Figure 4D-7. These oscillations persist until the inlet temperature to the core increases and a steady void fraction is established in the separators. Small oscillations in the flow rate are harmless when the flow in the core is single phase and consequently there is a very large margin to thermal limits. This type of oscillation is termed Type 1 instability in the literature.

Figure 4D-5 is a schematic of a generalized stability map in the plane of Subcooling Number vs. Zuber Number. (The figure does not represent a quantitative stability map specifically for the ESBWR and is used primarily for illustrative purposes.) Two different boundaries are shown for core-wide (in-phase) and regional (out-of-phase) oscillations that have been covered earlier in this report. These are driven by density wave oscillations and are known as Type 2 oscillations. The region above the lower (out-of-phase) stability boundary curve is unstable; the region under the curve is stable. The Type 1 oscillations appear at the onset of voiding and occupy a narrow region next to the line that demarcates the single-phase region from the two-phase region. At normal conditions the ESBWR is very stable as shown in the figure, with significant margin to the stability boundary. During startup, the Type 1 instability region is reached to obtain rated pressure and power. It is best to cross the Type 1 instability region at low power before boiling starts in the core to maintain a large margin to thermal limits. Once steady voiding is established in the separators and chimney, the core power can be raised along a trajectory to full power.

The parameters that control Type 1 instability are the Zuber Number and Subcooling Number. The Froude Number is a parameter that is relevant in determining the relationship between the riser buoyancy and the circulation flow. This is important in establishing a scaling basis for tests facility design, but not for loop stability once the scaled flow characteristics are known. Another group that is important for tall columns of liquid at low system pressure is the Flashing Number. These dimensionless numbers are defined below:

$$N_{Zu} = \frac{\rho_l}{\rho_{gsd}} \frac{Q}{W_c h_{fg}}$$

$$N_{sub} = \frac{\rho_l}{\rho_{gsd}} \frac{(h_{fsd} - h_{in})}{h_{fg}}$$

$$N_{Fr} = \frac{V_c^2}{g H_{dc}}$$ (4D.1)

$$N_{fl} = \frac{\rho_l}{\rho_{gsd}} \frac{(h_{fin} - h_{fsd})}{h_{fg}}$$

where

ρ =density (kg/m3)

V_c = core average inlet velocity (m/s)

Q =core thermal power (kW)

W_c =core flow (kg/s)

h = enthalpy (kJ/kg)

h_f = saturated liquid enthalpy (kJ/kg)

h_{fg} =latent heat of evaporation at steam dome pressure (kJ/kg)

H_{dc} = downcomer height (m)

sd denotes properties at the steam dome pressure and in denotes properties at the inlet to the core.

The significance of these quantities is discussed below with the aid of Figure 4D-8.

The Zuber Number is a measure of the enthalpy increase in the core. As there is no increase in the enthalpy in the chimney, the Zuber number is also a measure of the total enthalpy increase in the core and chimney regions. The Flashing Number has special relevance for tall columns of liquid at low pressure. It is a measure of the enthalpy margin to flashing at the core exit (see Figure 4D-8) when the flow just reaches saturation at the top of the chimney. The Subcooling Number is a measure of the enthalpy margin to saturation at the core inlet. At low system pressures, the definition of the Subcooling Number must be considered carefully because of the difference in pressure at different elevations. In Equation 4D.1, it is defined with respect to the saturated enthalpy at the steam dome pressure.

With the above definitions, when saturated conditions are reached at the top of the riser (Path A in Figure 4D-8), an energy balance leads to:

   $NZu = Nsub$ (4D.2)

For Type 1 oscillations that occur when voiding begins at the top of the riser, Nsub is the relevant parameter to be used in the stability map of Figure 4D-5.

For a rapid heatup rate corresponding to Path C in Figure 4D-8, saturated conditions may be reached at the top of the core (i.e. at a pressure close to core inlet pressure) with a subcooled chimney. In the extreme case when the entire chimney is still subcooled:

$$NZu = Nsub + Nfl \qquad (4D.3)$$

These heatup rates can lead to condensation-induced oscillations. A large flashing number requires a correspondingly higher Zuber number (enthalpy increase in the core) to trigger such oscillations and thus provides a buffer to the occurrence of this phenomenon.

At intermediate conditions, as the void initiation location moves down into the chimney,

$$Nsub < NZu < (Nsub + Nfl)$$

This corresponds to Path B in Figure 4D-8.

For the ESBWR at 0.2 MPa, the Zuber Number is of the order of 22, the subcooling number is 22 and the flashing number is 25 and the trajectory corresponding to Path A is followed during the heatup.

4D.2.2 TRACG Analysis of Typical Startup Trajectories

4D.2.2.1 ESBWR Plant Startup

Detailed startup procedures for the ESBWR are developed at a later stage. The startup process is expected to generally follow the established procedure from the Dodewaard plant. The Dodewaard plant started up for 22 cycles of operation without any problems related to flow or power oscillations.

Figure 4D-9 shows the stages of the startup process. In the De-aeration Period, the reactor coolant is de-aerated by drawing a vacuum on the main condenser and reactor vessel using mechanical vacuum pumps with the steam drain lines open. The reactor coolant is heated up to between 80 and 90°C with the Reactor Water Cleanup/Shutdown Cooling System (RWCU/SDC) auxiliary heater and decay heat. The reactor pressure is reduced to about 50 to 60 kPa. Following de-aeration, the Main Steam Isolation Valves (MSIVs) are closed to initiate the Startup Period. Control rods are withdrawn to criticality. Fission power is used to heat the reactor water, while maintaining the water level close to the top of the separators but well below the steam lines. Steaming at the free surface starts to pressurize the reactor vessel. The core region remains subcooled due to the large static head in the chimney and separators.

As the reactor heats up and pressurizes, the RWCU/SDC system heat exchangers are used to control the downcomer temperature, enhance coolant flow and reduce lower plenum stratification. The MSIVs are reopened at the end of the Startup Period, when the pressure reaches 6.3 MPa. Subsequently, the turbine bypass valves are used to control pressure. The RPV power is increased and preparations made to roll the turbine.

4D.2.2.2 TRACG calculations for Simulated Startup Scenarios

The startup transient for the ESBWR was simulated with TRACG. These TRACG calculations were performed with imposed core power, without activating the kinetics model. This is valid as long as there are no feedbacks from oscillations in the core void fraction during the startup transient. This assumption is validated as part of the calculation. The calculation was initiated at the end of the de-aeration period with the steam dome pressure at 0.52 bar and RPV water at 82°C. The water level was maintained near the top of the separators. The MSIVs were closed to isolate the RPV. To simplify comparisons, the power level was maintained constant until the

ESBWR

pressure reached 6.3MPa. Subsequently, the MSIVs were opened and the power level was increased in steps to achieve rated pressure at 300 MW (6.67% of rated power).

Three heatup rates were considered. The lowest power level of 50 MW corresponds to a heatup rate of 30°C/hour and is likely to be close to the actual value for startup. The median power level of 85 MW yields a heatup rate of 55°C/hour, which is the highest allowable to comply with reactor vessel thermal stress requirements. The highest power level of 125 MW heats up the reactor vessel water at 82°C/hour which is above allowable limits, and is only included as a sensitivity study. The three power trajectories are shown in Figure 4D-10.

Figure 4D-11 shows the pressure response for the three cases. The circulating water heats up because of the core power. The heat exchangers in the RWCU/SDC system are enabled to remove a part of the energy and control the core inlet subcooling. Steam generation begins at the water surface and starts to pressurize the vessel.

Figure 4D-12 shows the variation in core inlet subcooling as a function of time. The local inlet subcooling drops from an initial value around 40°K to less than 10°K as the system pressurizes to 6.3MPa. The core flow transient response is shown in Figure 4D-13. For the lowest heatup rate, the flow trace shows a minor oscillation (noise) between 3000 to 5500 s. The cause of this noise can be traced to the beginning of voiding at the top of the separators (Figure 4D-14). The flow noise is terminated when a steady void fraction is established at the top of the separators. This is the symptom of a Type 1 oscillation at the onset of voiding in the riser. At a power level of 85 MW, the noise is spread over two periods: early on there is some void initiation in the separators (500 to 3000 s) followed by a more sustained period of void generation beginning around 9000 s (Figure 4D-15). At the highest heatup rate (125 MW), the flow becomes noisier. The highest oscillation amplitude occurs between 500 to 1500 s and again between 3500 to 5000 s. The void fractions in the separator are shown in Figure 4D-16.

Further insight into the core flow response is obtained by examining the core void fractions, specifically in the highest power bundles. Figure 4D-17 shows the void fractions for the 50 MW case in the high power bundle at the exit and at cell 30, which is close to the top of the bundle. Voids are not produced even in the high power bundles until 13000 s, well after the noisy flow period is over and the system has pressurized to above 15 bar. Figure 4D-18 shows that for the 85 MW case, vapor generation begins at the top of the high power bundles at 5000s, after the initial flow noise has subsided. At this time the pressure is about 8 bar. Voids propagate to cell 30 at about 8000 s, by which time the system pressure is above 25 bar. The high power level (125 MW) leads to extreme conditions during the heatup. Vapor generation in the core begins early. Figure 4D-19 shows that the high power bundle has an exit void fraction of 15% at 4000 s. Rapid heating of the core leads to conditions that favor condensation-induced oscillations because vapor is generated in the core while the chimney is not yet at saturated conditions. These are the extreme conditions examined in the tests by Aritomi [4D-12] and Kuran, et al [4D-14]. The situation is further illustrated by looking at the flows in individual bundles. The exit flows in the high power and the low power peripheral bundles were examined. Figure 4D-20 depicts the exit flows in the high power bundle for the three cases. These traces follow the core average flow response shown in Figure 4D-13. The exit flows in the peripheral bundles (Figure 4D-21) show a more dramatic distribution. In the two lower power cases, the peripheral bundles are in upflow throughout the transient, despite the noise imposed on the

average flow rate. However, at 125 MW, large condensation induced oscillations lead to flow reversals between 3500 to 4000 s.

Margins to thermal limits (CPR) were calculated for the three startup scenarios. The thermal margin for the high power bundles is shown in Figure 4D-22. Large margins are maintained throughout. Figure 4D-23 is the corresponding plot for the peripheral bundles. Again, large margins are maintained throughout the transient. This is true even for the extreme case with 125 MW. Despite the flow reversals, the heat fluxes are low enough that critical heat flux conditions are not approached.

Subsequent to this analysis, a coupled nuclear-thermal hydraulic analysis of the ESBWR startup has been performed [4D-18]. In this calculation, control rods were withdrawn to maintain a core power level of approximately 85MW. The results confirm that the conclusions in the preceding paragraphs are valid and that the startup proceeds smoothly without any significant oscillations in core flow or power.

4D.3 COL INFORMATION

The COL applicant shall verify that the stability of the final core design is at least as stable as the GE14 core design used in the analysis in this section. If the nominal decay ratios are higher than the calculated values, the statistical analysis of decay ratios shall be performed and the results checked versus the design criteria.

The COL applicant shall confirm that an NRC approved detect and suppress stability solution is implemented that will scram or reduce power if an instability occurs.

The COL startup procedures shall be verified to limit core and bundle power to the values used in the 4D.2 analysis.

4D.4 REFERENCES

4D-1   GE Nuclear Energy, J. S. Post and A. K. Chung, "ODYSY Application for Stability Licensing Calculations," NEDC-32992P-A, July 2001.

4D-2   GE Nuclear Energy, "BWR Owners' Group Long-Term Stability Solutions Licensing Methodology," NEDO-31960-A, November 1995.

4D-3   GE Nuclear Energy, B. S. Shiralkar and Y. K. Cheung, "TRACG Application to ESBWR," NEDC-33083P-A, March 2005.

4D-4   GE Nuclear Energy, J. G. M. Andersen, et al., "TRACG Application for Anticipated Operational Occurrences Transient Analysis," NEDE-32906P-A, Revision 1, April 2003.

4D-5   GE Nuclear Energy, F. T. Bolger and M. A. Holmes, "TRACG Application for ATWS Overpressure Transient Analysis," NEDE-32906P, Supplement 1-A, November 2003.

4D-6   GE Nuclear Energy, J. G. M. Andersen, et al., "TRACG Model Description," NEDE-32176P, Revision 2, December 1999.

4D-7   GE Nuclear Energy, J. G. M. Andersen, et al., "TRACG Qualification," NEDE-32177P, Revision 2, January 2000.

4D-8   GE Nuclear Energy, J. R. Fitch, et al., "TRACG Qualification for SBWR," NEDC-32725P, Revision 1, Vol.1 and 2, August 2002.

4D-9   GE Nuclear Energy, J. R. Fitch, et al., "TRACG Qualification for ESBWR," NEDC-33080P, Revision 1, May 2005.

4D-10   USNRC, "Quantifying Reactor Safety Margins: Application of Code Scaling, Applicability, and Uncertainty Evaluation Methodology to a Large-Break, Loss-of-Coolant Accident," NUREG/CR-5249, December 1989.

4D-11   GE Nuclear Energy, B.S.Shiralkar, et al, "TRACG Application for ESBWR Stability Analysis," NEDE-33083P, Supplement 1, December 2004.

4D-12   M. Aritomi, J. H. Chiang. M. Mori, "Fundamental Studies on Safety-Related Thermal-Hydraulics of Natural Circulation Boiling Parallel Channel Flow System under Startup Conditions (Mechanism of Geysering in Parallel Channels)," Nuclear Safety, Vol. 33, No.2, pp. 170-182, 1992.

4D-13   F. Inada, Y. Yasuo, "The Boiling Flow Instability of a Natural Circulation BWR with a Chimney at Low Pressure Startup," Proc. International Conference on the Design and Safety of Advanced Nuclear Power Plants (ANP '92), Tokyo, Japan, Paper 25.3, October 25-29, 1992.

4D-14   S. Kuran, M. Ishii, X. Sun, L. Cheng, Y. Xu, H. Yoon, S.T. Revankar, "Nuclear Coupled Flow Instability Study for Natural Circulation BWR Startup Transient," Paper N6P002, 6th International Conference on Nuclear Thermal Hydraulics, Operation and Safety (NUTHOS-6), Nara, Japan, October 2004.

4D-15   D.D.B. van Bragt and T.H.J.J. van der Hagen, "Stability Of Natural Circulation Boiling Water Reactors: Part II - Parametric Study Of Coupled Neutronic-Thermohydraulic Stability," Nuclear Technology 121 (1998), 52-62.

4D-16   T.H.J.J. van der Hagen, F.J. van der Kaa, J. Karuza, W.H.M. Nissen, A.J.C. Stekelenburg, J.A.A. Wouters, "Startup of the Dodewaard Natural Circulation Boiling Water Reactor," GKN Report 92-017/FY/R, 1992.

4D-17   A. Manera and T.H.J.J. van der Hagen, "Stability Of Natural-Circulation-Cooled Boiling Water Reactors During Start-Up: Experimental Results," Nuclear Technology, 143 (2003), 77-88.

4D-18   Letter from K. Sedney, GE to A. Cubbage, USNRC, "GE Responses to NRC RAIs on NEDE-33083P, Supplement 1, TRACG Application for ESBWR Stability Analysis," MFN 05-52, June 2, 2005.

Table 4D-1

Initial Conditions for Channel and Core Stability Analysis

Parameter	Value		
	BOC	MOC	EOC
Core Thermal Power (MW)	4500	4500	4500
Core Flow (kg/s)*	9,925	10,003	10,153
Feedwater temperature (K)	488	488	488
Narrow range water level (m)	21.0	21.0	21.0
Feedwater flow (kg/s)*	2421	2421	2421
Core inlet subcooling* (K)	16.6	16.3	16.2
Steam dome pressure (MPa)	7.05	7.05	7.05
ICPR*	1.40	1.46	1.38
Hot Bundle Power (MW)*	5.10	4.94	5.09
Hot Bundle flow (kg/s)*	8.6	8.7	8.8

*Calculated parameter

Table 4D-2

Baseline Stability Analysis Results

Mode	BOC		MOC		EOC	
	Decay Ratio	Frequency (Hz)	Decay Ratio	Frequency (Hz)	Decay Ratio	Frequency (Hz)
Channel	0.23	0.80	0.09	~0.75	0.05	~0.7
Superbundle	0.14	0.74				
Core	0.26	0.74	0.33	0.74	0.29	0.66
Regional	0.37	0.82				

Table 4D-3

Statistical Stability Analysis Results

	Decay Ratio – One Sided Upper Tolerance Limit (95/95)	Decay Ratio - Design Criteria
Core	0.51	0.8
Channel	0.36	0.5

Table 4D-4

Limiting AOO Event Results

AOO	Power (% of Rated)	Flow (% of Rated)	Core Decay Ratio	Hot Channel Decay Ratio
LOFWH	116	101	0.47	0.18
LOFW	100	96.6	0.36	0.14
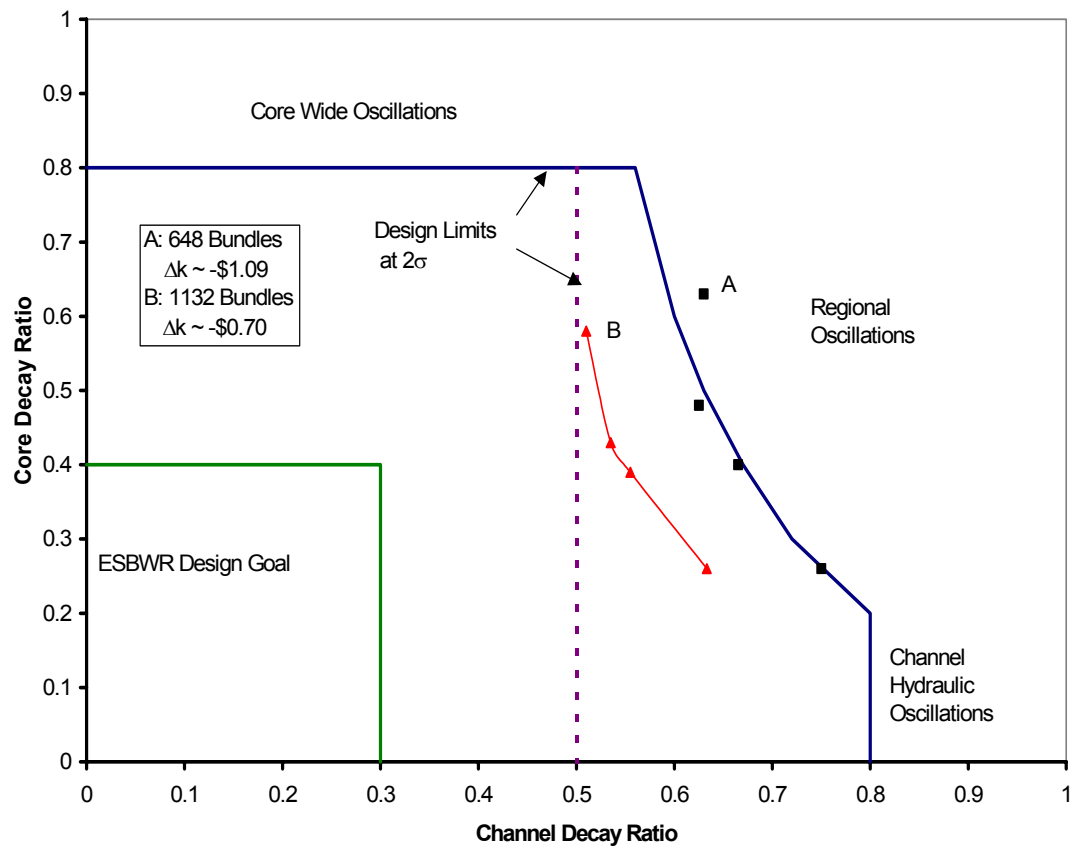
Figure 4D-1. Proposed Stability Map for ESBWR

ESBWR-1132 Core Average Axial Power Shape
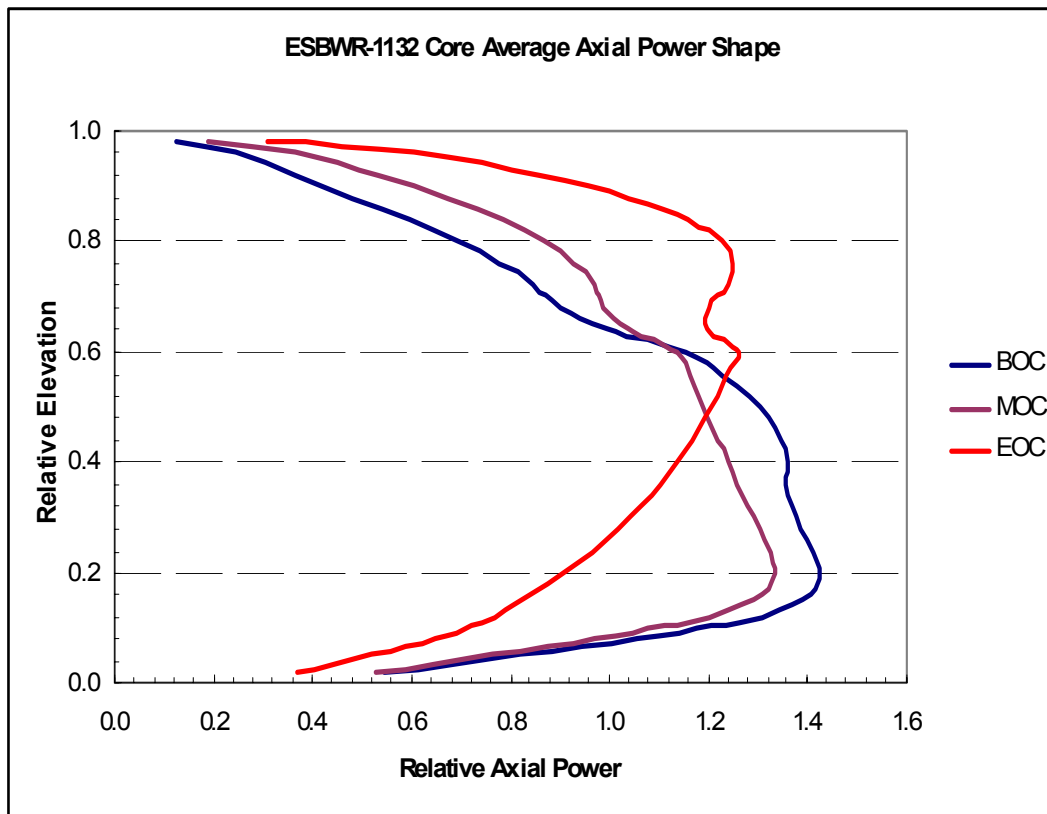
Figure 4D-2. Core Average Axial Power Shape at Different Exposures
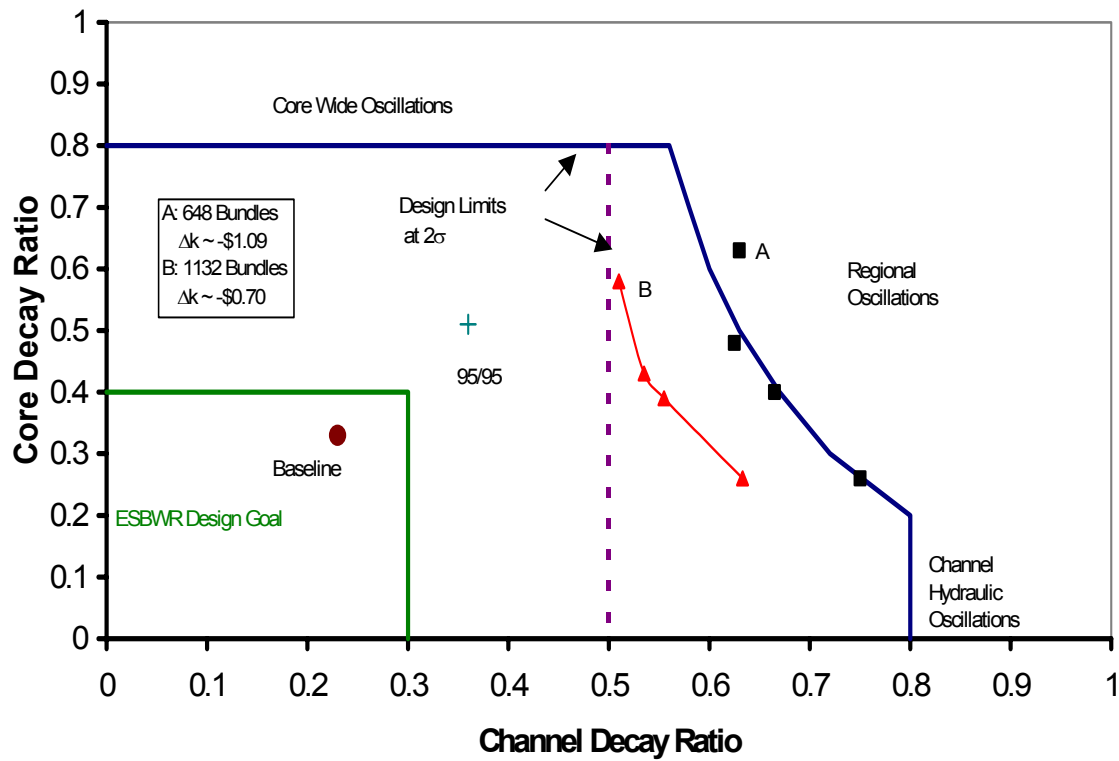
Figure 4D-3. Decay Ratio Results Compared to Design Criteria
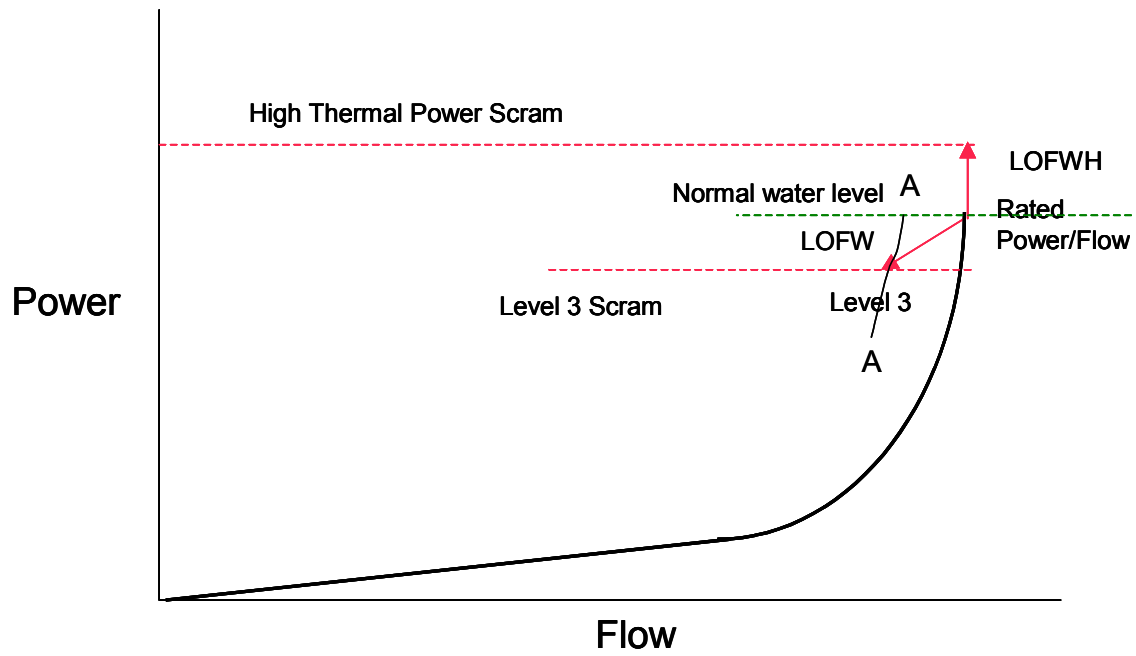
Figure 4D-4. Stability in Expanded Operating Map
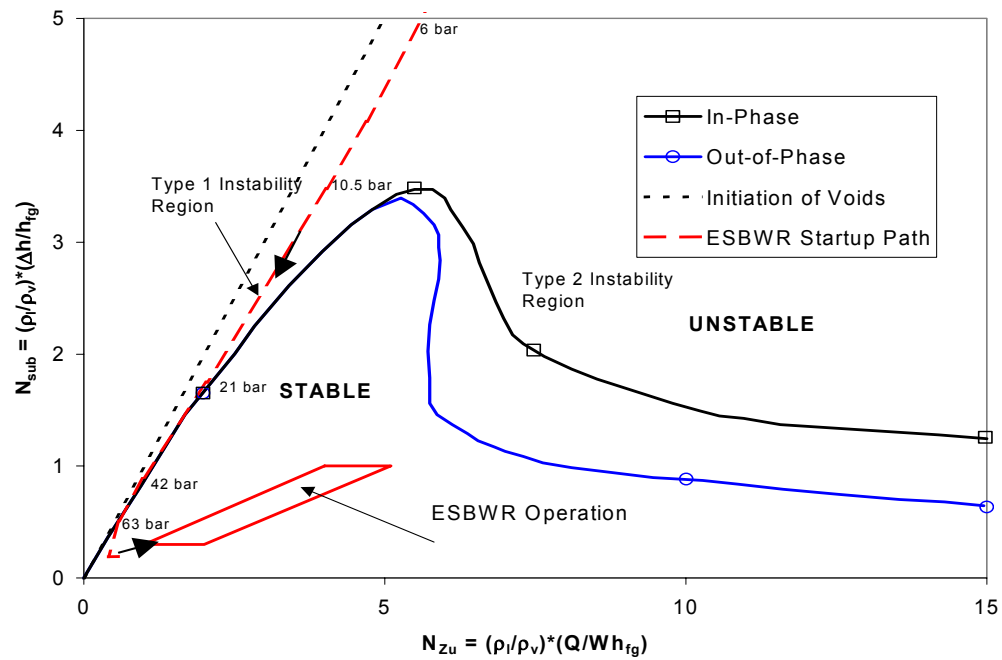
Figure 4D-5. Generalized Stability Map showing Type 1 and Type 2 Instability
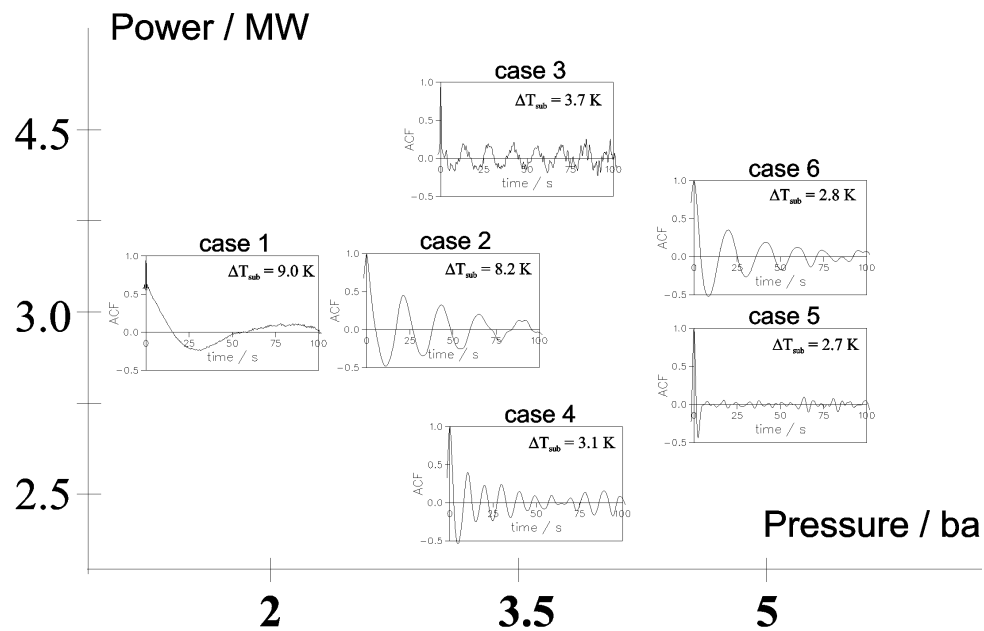
Figure 4D-6. Indications of Periodic Behavior during Dodewaard Startup
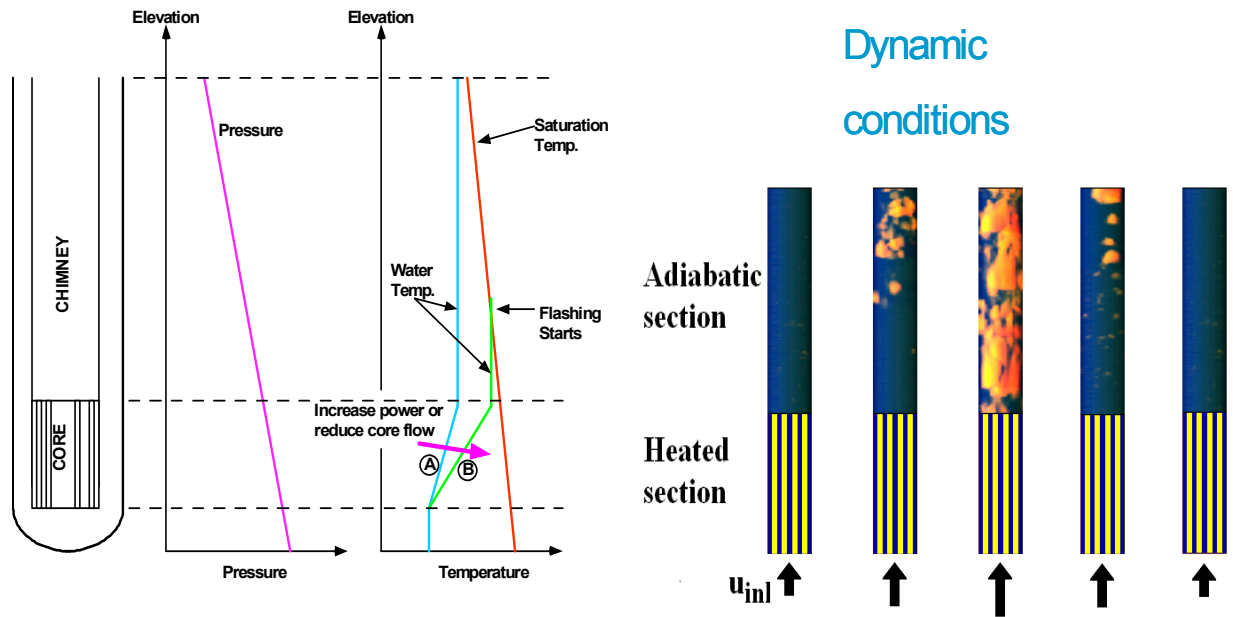
Figure 4D-7. Thermal – Hydraulic Conditions during Startup [4D-17]
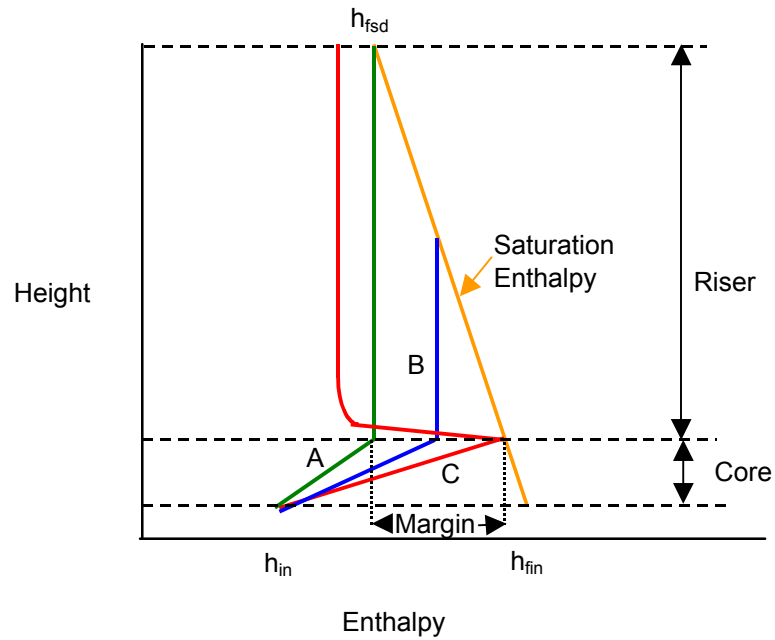
Figure 4D-8. Enthalpy Profiles for Different Heatup Rates
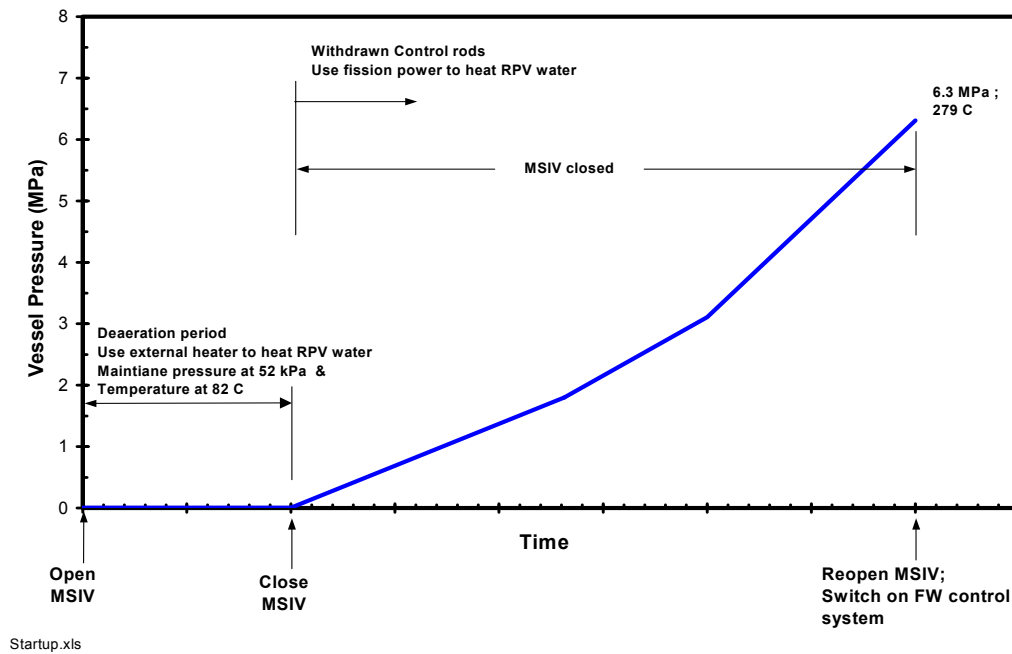
Figure 4D-9. ESBWR Startup Trajectory
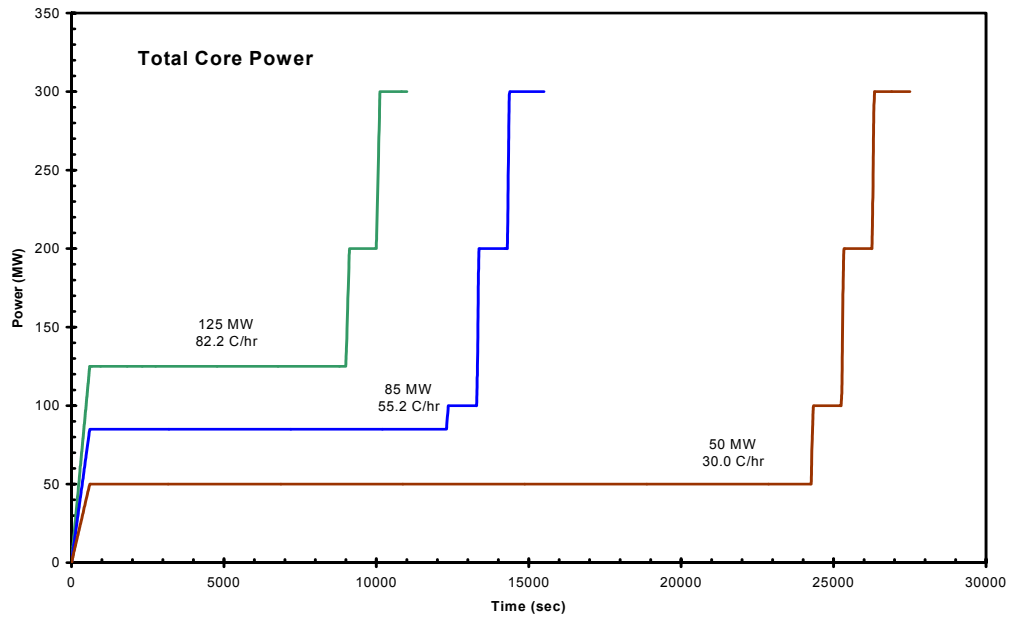
Figure 4D-10. TRACG Startup Simulation: Reactor Power Trajectories
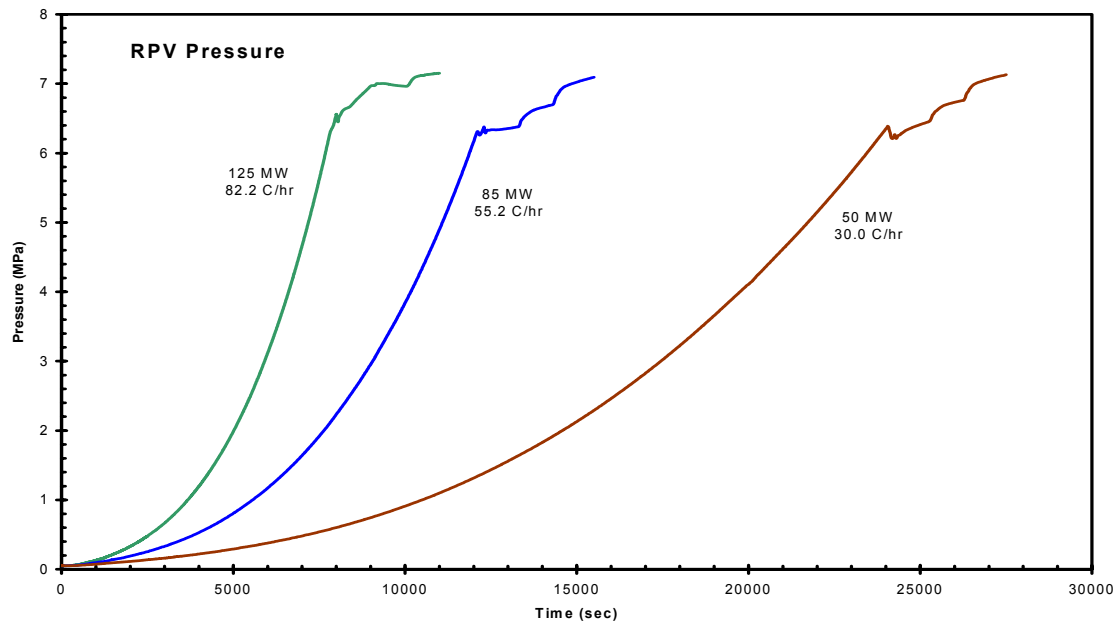
Figure 4D-11. TRACG Startup Simulation: Pressure Response
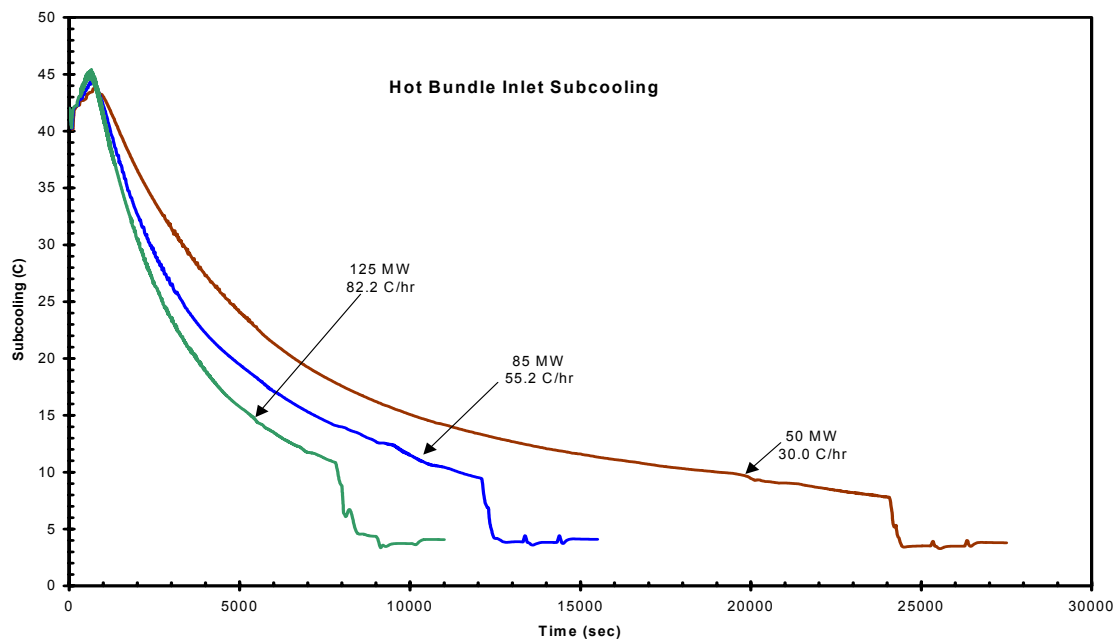
Figure 4D-12. TRACG Startup Simulation – Core Inlet Subcooling
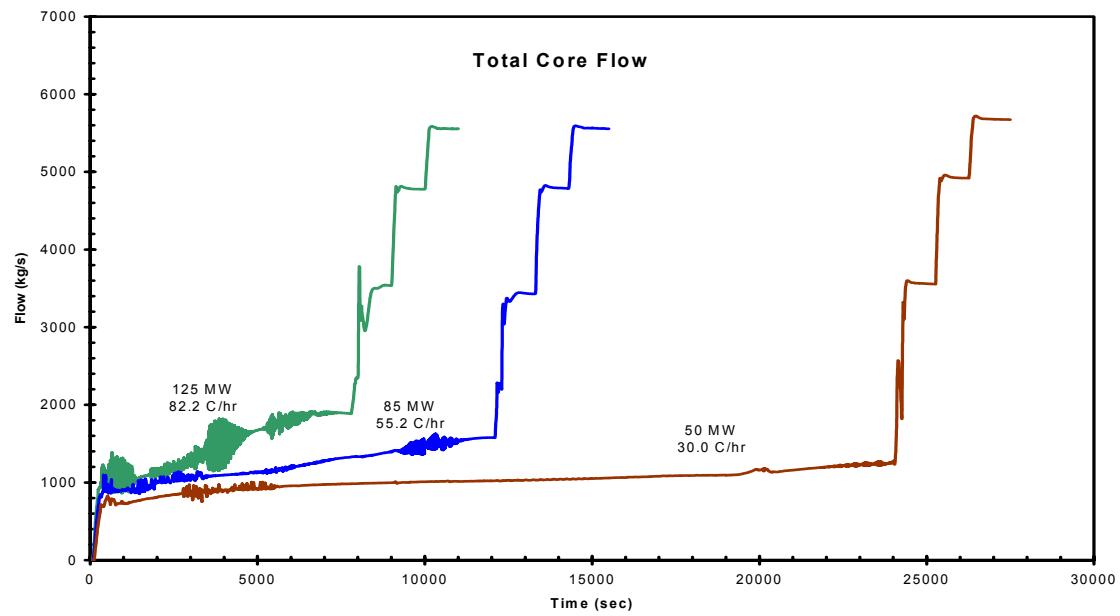
Figure 4D-13. TRACG Startup Simulation – Core Inlet Flow
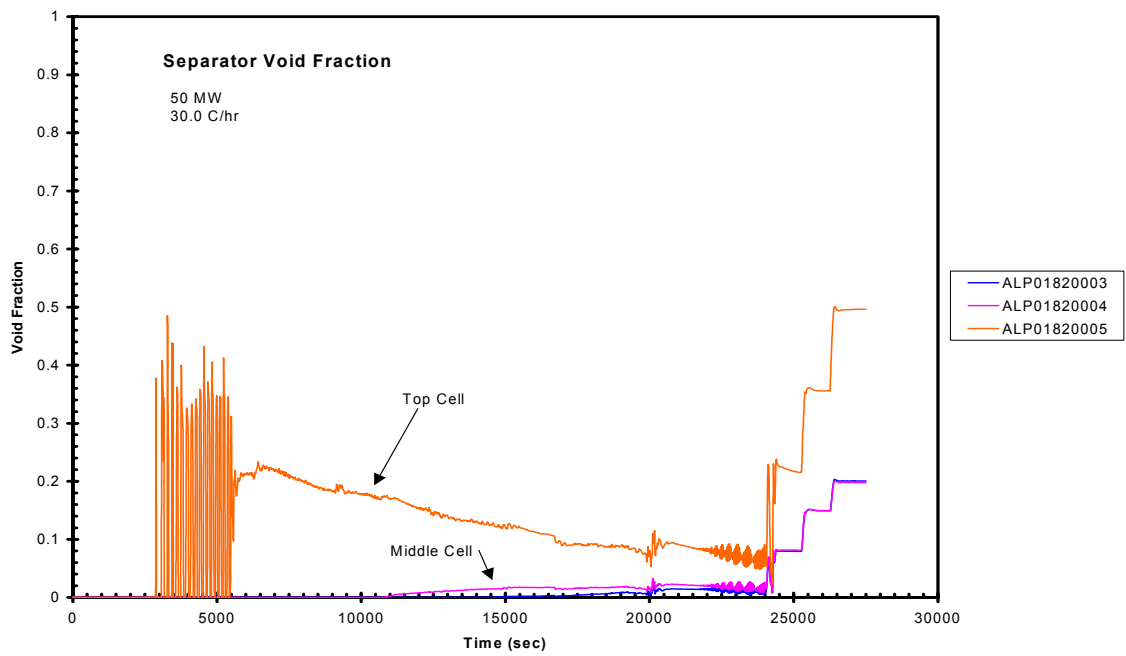
Figure 4D-14. Separator Void Fraction (50 MW heatup)
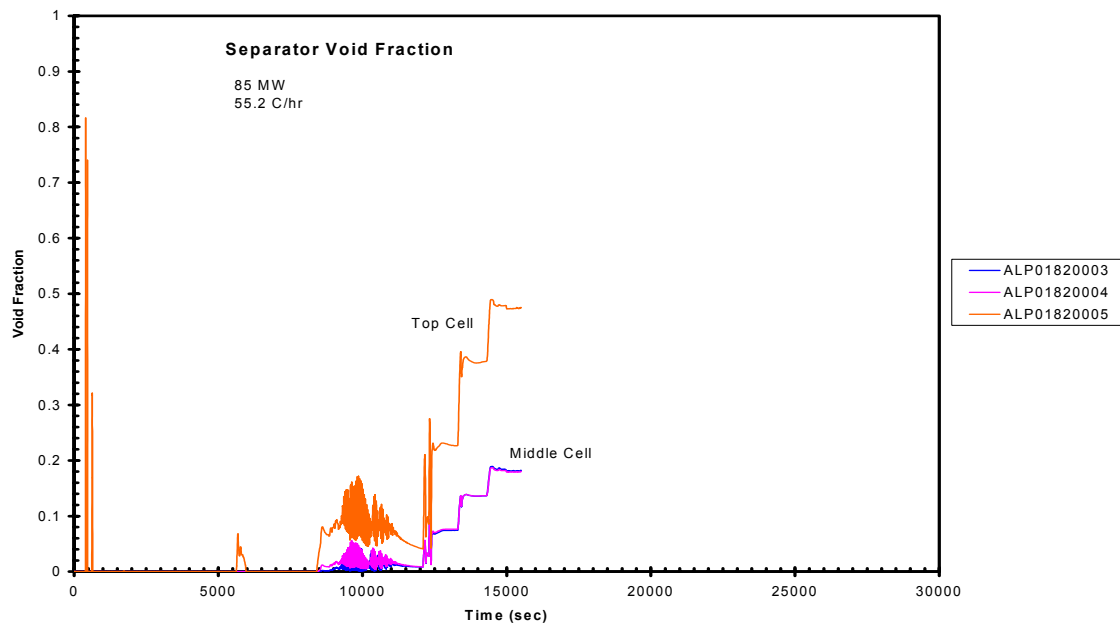
Figure 4D-15. Separator Void Fraction (85MW heatup)
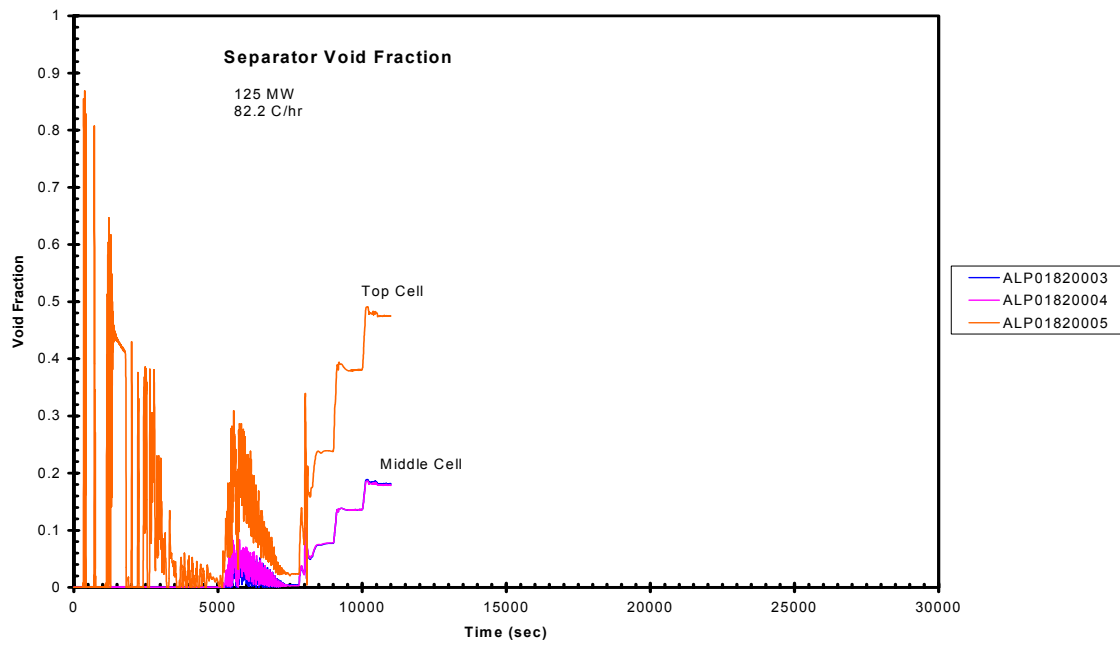
Figure 4D-16. Separator Void Fraction (125 MW heatup)
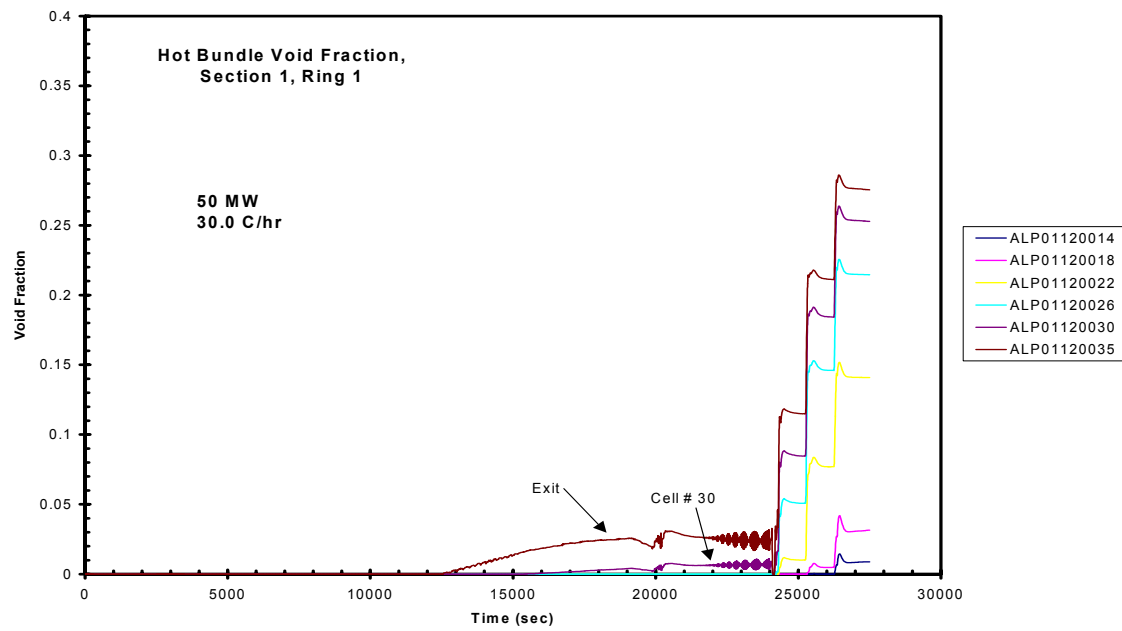
Figure 4D-17. Hot Bundle Void Fraction (50 MW heatup)
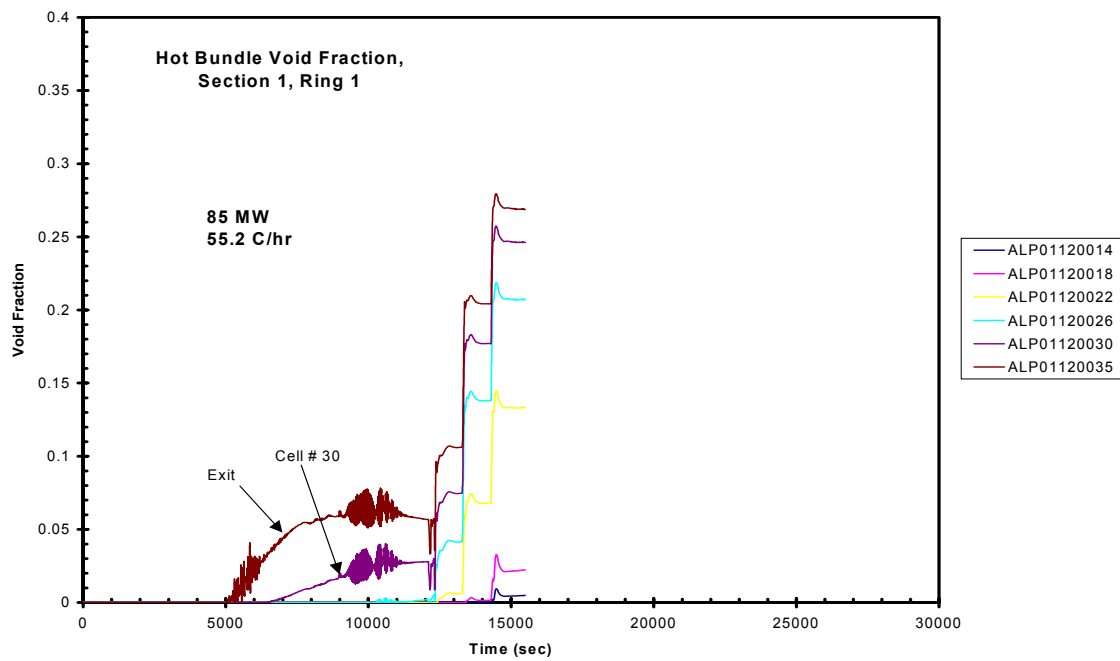
Figure 4D-18. Hot Bundle Void Fraction (85 MW heatup)
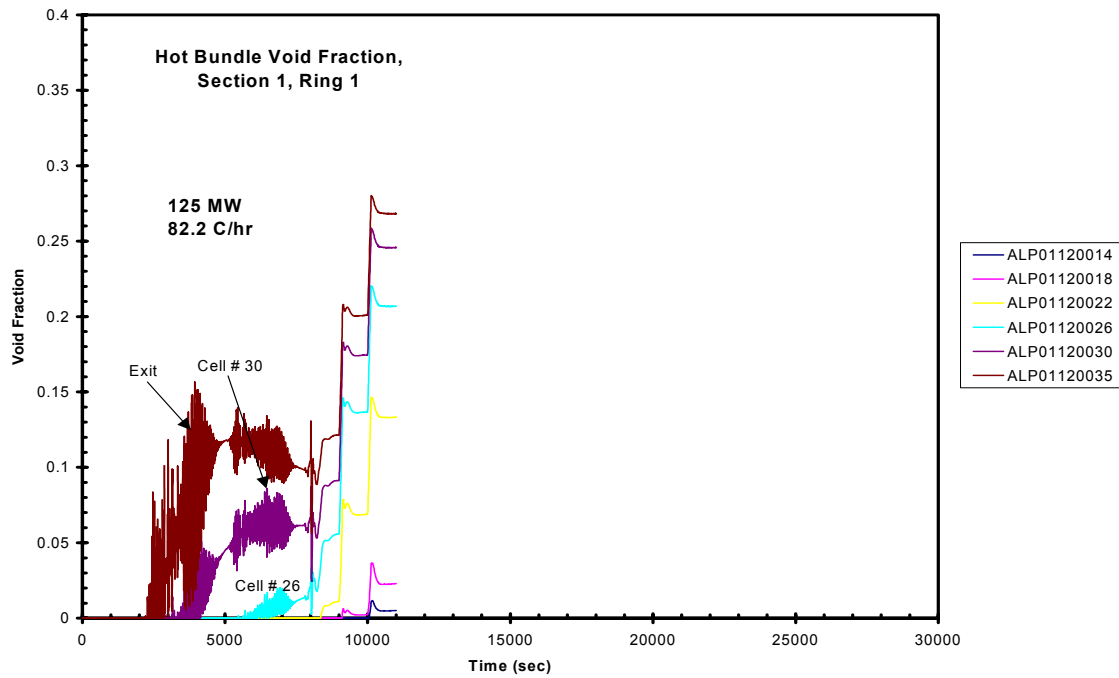
Figure 4D-19. Hot Bundle Void Fraction (125 MW heatup)
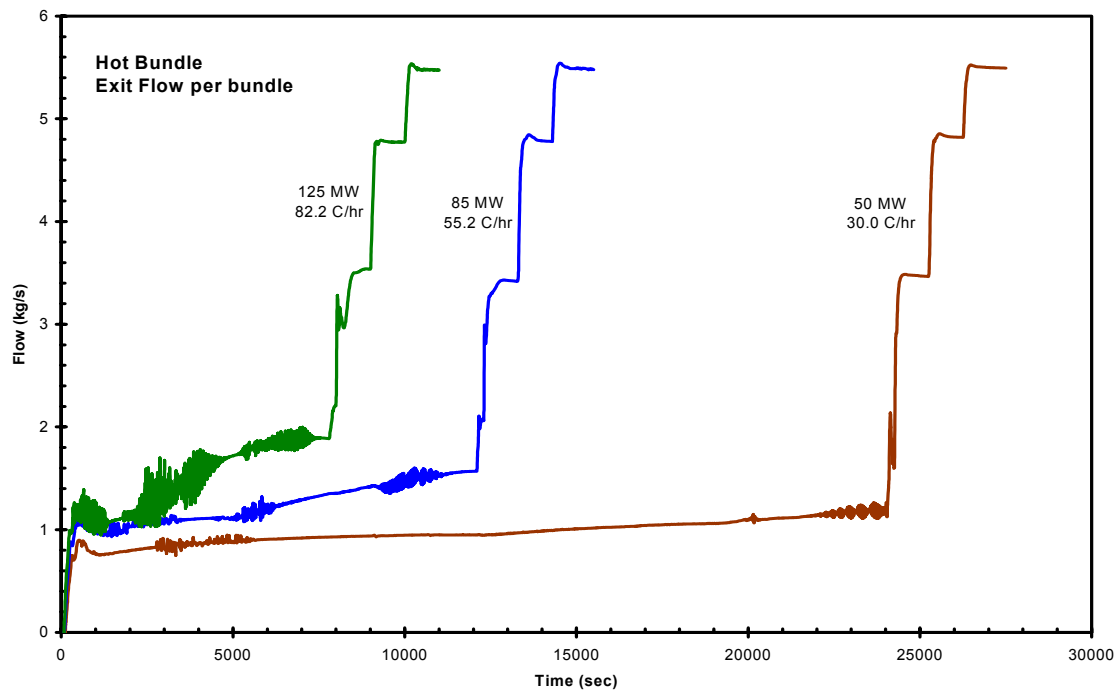
Figure 4D-20. Hot Bundle Exit Flow
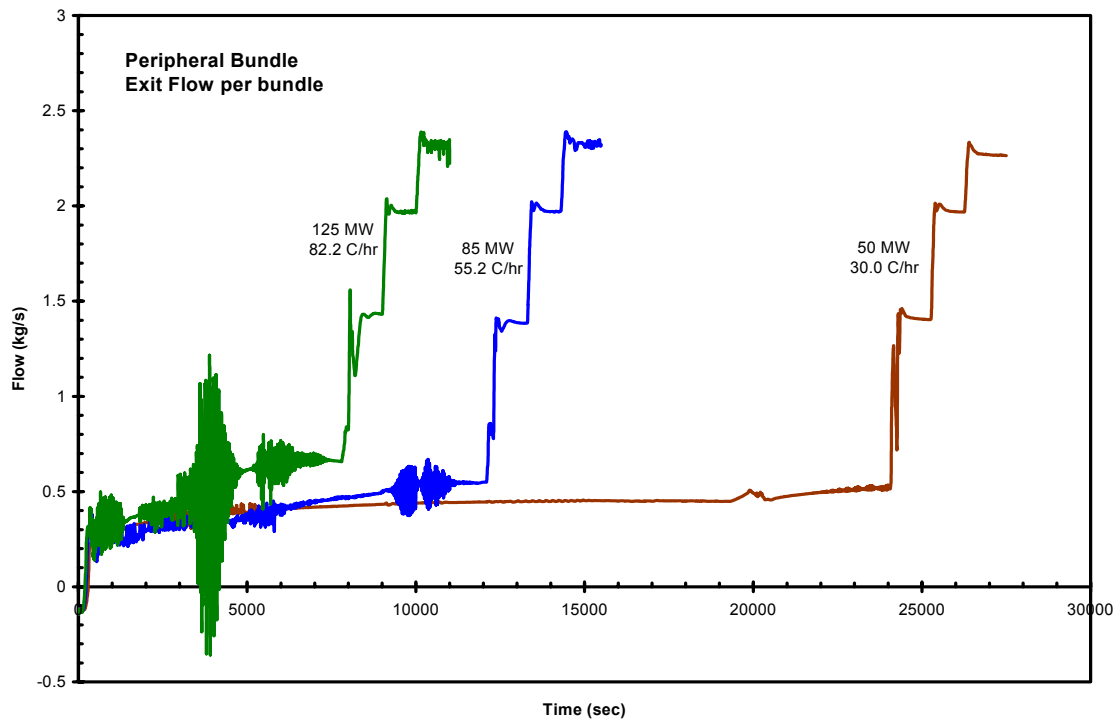
Figure 4D-21. Peripheral Bundle Exit Flow

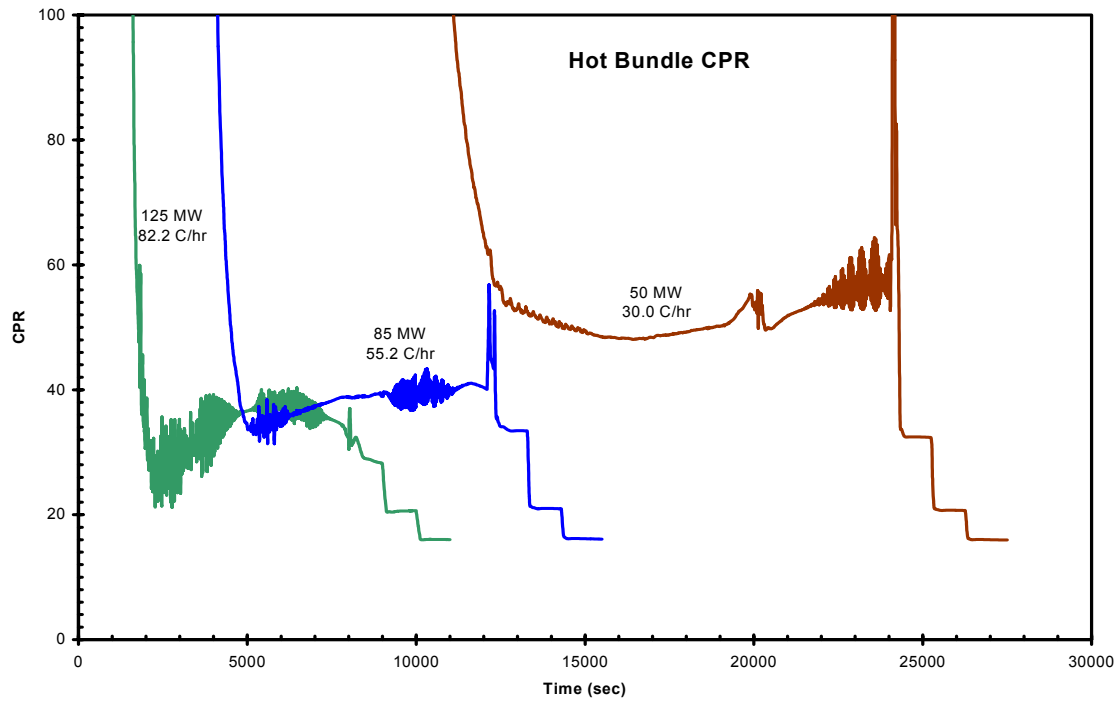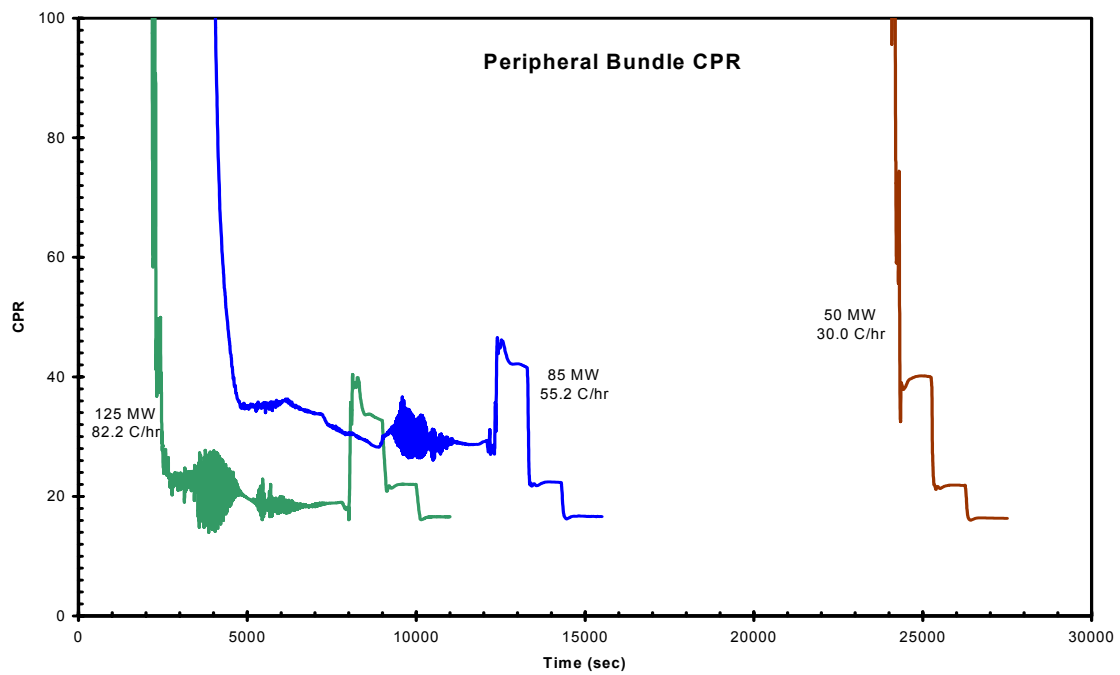**Figure 4D-22. Hot Bundle CPR**

Figure 4D-23. Peripheral Bundle CPR